BRNO UNIVERSITY OF TECHNOLOGY

VYSOKÉ UČENÍ TECHNICKÉ V BRNĚ

FACULTY OF MECHANICAL ENGINEERING

FAKULTA STROJNÍHO INŽENÝRSTVÍ

INSTITUTE OF PROCESS ENGINEERING

ÚSTAV PROCESNÍHO INŽENÝRSTVÍ

INTEGRATED APPROACH OF INTELLIGENT ASSET MAINTENANCE AND RESOURCE CONSERVATION FOR CIRCULAR ECONOMY

INTEGRATED APPROACH OF INTELLIGENT ASSET MAINTENANCE AND RESOURCE CONSERVATION FOR CIRCULAR ECONOMY

DOCTORAL THESIS

DIZERTAČNÍ PRÁCE

AUTHOR — MEng. Hon Huin Chin

AUTOR PRÁCE

SUPERVISOR — prof. Ing. Jiří Klemeš, DrSc., dr. h. c.

ŠKOLITEL

CO-SUPERVISORS — Doc. Dr-Habil. Ing. Petar Sabev Varbanov, PhD

Prof. DDr. Hon Loong Lam

BRNO 2021

KEYWORDS

Resource Conservation Network, Eco-Industrial Park, Industrial Symbiosis, Water Integration, Pinch Analysis, Asset Maintenance

KLÍČOVÁ SLOVA

Síť na ochranu zdrojů, ekologický průmyslový park, průmyslová symbióza, integrace vody, analýza stisku, údržba majetku

CITATION

CHIN, Hon Huin. *Integrated Approach of Intelligent Asset Maintenance and Resource Conservation for Circular Economy* [online]. Brno, 2021 [cit. 2021-05-05]. Available from: https://www.vutbr.cz/studenti/zav-prace/detail/133084. Doctoral Thesis. Vysoké učení technické v Brně, Fakulta strojního inženýrství, Institute of Process Engineering. Supervisor Jiří Klemeš

Declaration

I declare that I am the author of this doctoral thesis. It has been prepared under the guidance of my supervisors. The reported results are original research that developed based on my knowledge gained during PhD study and consultation with experts. I have quoted all the sources, including my own publications. The related references are provided at the end of this thesis

Brno, 2021 Ing Hon Huin CHIN

Abstract

The rapid global industrialisation and urbanisation have placed heavy burdens on natural material resources consumption. For example, water scarcity and water pollution have been affecting human lives and economic developments for a long time, and resorting to clean fresh water has been becoming an important issue. The increasing irregular water supply and water pollution issues require more advanced water resources assessment methodologies to guide practical water use and management. Another well-known issue is the plastic waste accumulation in the option, which raises an alarming concern in achieving the optimal resources conservation network, striving towards the goal of Circular Economy. The Circular Economy concept not only focuses on resources conservation but also highlights the importance of maintaining and preserving the assets' lifetime. This thesis is focused on developing advanced approaches for resources conservation and asset maintenance

This thesis presents the extended analysis of Pinch-based methods in conserving the material resources for an industrial site. The major extensions involve the conceptual analysis on the resource conservation network that involves multiple qualities constraints, headers targeting and synthesis, and Total Site material conservation network synthesis. These methods serve as the graphical user interface for the users to select the preferable design options while ensuring the fresh resources consumptions are minimal. The study also extends the incorporation of different types of resources, such as heat and water, into the conservation network. The management issues such as resources management, subsidies and cost allocations are also studied for the eco-industrial site.

Considering the asset's lifetime prolongation, the long-term planning of a process or industrial site is incorporated in this study covering the assets' age, depreciation and reliability. Process Integration tools are proposed to plan for the maintenance cost for a time period and workforce scheduling. The study is also extended to more analysis involving standby units and technologies investment for any process. Combining asset performance with resources conservation, the fault diagnosis and prognosis framework is applied to the Total Site/Eco-industrial park asset maintenance planning.

Abstrakt

Rychlá globální industrializace a urbanizace kladla velkou zátěž na spotřebu přírodních zdrojů. Například nedostatek vody a znečištění vody již dlouhou dobu ovlivňují lidské životy a hospodářský rozvoj a uchýlení se k čisté sladké vodě se stává důležitým problémem. Rostoucí problémy s nepravidelným zásobováním vodou a znečištěním vody vyžadují pokročilejší metodiky hodnocení vodních zdrojů, které by vedly k praktickému využívání vody a hospodaření s ní. Dalším známým problémem je akumulace plastového odpadu v této možnosti, což vyvolává znepokojivé obavy ohledně dosažení optimální sítě pro zachování zdrojů, směřující k cíli oběhového hospodářství. Koncept cirkulární ekonomiky se zaměřuje nejen na ochranu zdrojů, ale také zdůrazňuje důležitost zachování a zachování životnosti aktiv. Tato práce je zaměřena na vývoj pokročilých přístupů k ochraně zdrojů a údržbě majetku

Tato práce představuje rozšířenou analýzu metod založených na Pinch při zachování materiálových zdrojů pro průmyslové místo. Hlavní rozšíření zahrnují koncepční analýzu sítě pro zachování zdrojů, která zahrnuje omezení několika kvalit, cílení a syntézu záhlaví a syntézu sítě pro zachování materiálu v rámci celého webu. Tyto metody slouží uživatelům jako grafické uživatelské rozhraní k výběru preferovaných možností návrhu a zároveň zajišťují minimální spotřebu čerstvých zdrojů. Studie také rozšiřuje začlenění různých typů zdrojů, jako je teplo a voda, do ochranné sítě. Otázky řízení, jako je řízení zdrojů, dotace a rozdělování nákladů, jsou rovněž studovány pro ekologický průmysl.

S ohledem na prodloužení životnosti aktiva je do této studie začleněno dlouhodobé plánování procesu nebo průmyslového areálu pokrývajícího věk majetku, odpisy a spolehlivost. Nástroje pro integraci procesů jsou navrženy tak, aby plánovaly náklady na údržbu na časové období a plánování pracovní síly. Studie je také rozšířena o další analýzu zahrnující investice do pohotovostních jednotek a technologií pro jakýkoli proces. Kombinace výkonu aktiv s ochranou zdrojů, rámce diagnostiky chyb a prognózy se aplikuje na plánování údržby majetku Total Site/Eco-industrial park.

Acknowledgement

This thesis is a milestone of my study and research in the three years of work in the SPIL group. Throughout this journey, my passion has been focused on investigating novel tools to provide solutions for industrial site planning. This thesis presents the lessons and knowledge learned in developing the assessment tools and also the results of many experiences I have encountered from those remarkable individuals whom I wish to acknowledge.

First and foremost, I wish to thank Prof Jiří Jaromír Klemeš and Dr Petar Varbanov for being my major supervisors. Prof Klemeš and Dr Varbanov have been more than supportive in my studies and life since the days I began working and studying in the group. Prof Klemeš has always been encouraging me to focus on my field and broaden my mind in research, and his passion and active performance in scientific research have been such an encouragement for me to keep the passion in seeking solutions for practical environmental issues. I have been given unique opportunities and experience to participate in and organise conferences, work as a Guest Editor and reviewer for several international journals. He has been supportive not only in scientific research but also in helping me to fit in the local life. Dr Petar Varbanov has always been encouraging me to explore critical thinking through many fruitful discussions. There have been many collaborations and suggestions that contributed to the improvement of my research. His dedication to research and guidance have ensured the progress of my study and the development of this thesis. I would also like to thank my co-supervisor, Prof Lam Hon Loong, who has always been reachable and supportive with insightful suggestions to uplift my work.

It has been my appreacited duty to gratefully appreciate the financial support from the EU supported project Sustainable Process Integration Laboratory – SPIL (funded as project No. CZ.02.1.01/0.0/0.0/15_003/0000456, by Czech Republic Operational Programme Research and Development, Education), the project LTACH19033 “Transmission Enhancement and Energy Optimised Integration of Heat Exchangers in Petrochemical Industry Waste Heat Utilisation”, under the bilateral collaboration of the Czech Republic and the People's Republic of China (partners Xi'an Jiaotong University and Sinopec Research Institute Shanghai; SPIL VUT, Brno University of Technology and EVECO sro, Brno), programme INTER-EXCELLENCE, INTER-ACTION of the Czech Ministry of Education, Youth and Sports; and by National Key Research and Development Program of China (2018YFE0108900), as well as the doctoral scholarship and extraordinary scholarship by VUT.

A big thank you to Dr Šárka Zemanová, SPIL colleagues, and specialy Prof Stehlík, for supporting me throughout all this journey with all the communication, administrative work and help in many ways.

I would also like to say a heartfelt thank you to my families in Malaysia for always believing in me physically or mentally and encouraging me to follow my dreams. Their love and supports are the main motivations for me to continue my research journey.

Poděkování

Tato práce je milníkem mého studia a výzkumu za tři roky práce ve skupině SPIL. Během této cesty se moje vášeň soustředila na zkoumání nových nástrojů pro poskytování řešení pro plánování průmyslových areálů. Tato práce představuje ponaučení a znalosti získané při vývoji hodnotících nástrojů a také výsledky mnoha zkušeností, se kterými jsem se setkal od těch pozoruhodných osobností, které bych rád ocenil.

V první řadě chci poděkovat prof. Jiřímu Jaromírovi Klemešovi a doktoru Petaru Varbanovovi za to, že byli mými hlavními supervizory. Profesor Klemeš a doktor Varbanov mě od doby, kdy jsem začal pracovat a studovat ve skupině, ve studiu i v životě více než podporovali. Prof. Klemeš mě vždy povzbuzoval, abych se zaměřil na svůj obor a rozšířil svou mysl ve výzkumu, a jeho vášeň a aktivní výkon ve vědeckém výzkumu pro mě byly takovým povzbuzením, abych si udržel vášeň při hledání řešení praktických environmentálních problémů. Dostal jsem jedinečné příležitosti a zkušenosti účastnit se a organizovat konference, pracovat jako hostující redaktor a recenzent pro několik mezinárodních časopisů. Podporoval mě nejen ve vědeckém výzkumu, ale také mi pomáhal zapadnout do místního života. Doktor Petar Varbanov mě vždy povzbuzoval k prozkoumání kritického myšlení prostřednictvím mnoha plodných diskusí. Došlo k mnoha spolupracím a návrhům, které přispěly ke zlepšení mého výzkumu. Jeho oddanost výzkumu a vedení zajistila postup mé studie a vypracování této práce. Chtěl bych také poděkovat svému spoluzakladateli, profesoru Lamu Honovi Loongovi, který byl vždy dosažitelný a podporující moudré návrhy na povznesení mé práce.

Bylo mojí uznanou povinností vděčně ocenit finanční podporu z projektu EU podporovaného projektu Laboratoře integrace udržitelného procesu - SPIL (financovaný jako projekt č. CZ.02.1.01/0,0/0,0/15_003/0000456, Operačním programem Česká republika Výzkum a Development, Education), projekt LTACH19033 „Vylepšení přenosu a energeticky optimalizovaná integrace výměníků tepla v petrochemickém průmyslu Využití odpadního tepla“, v rámci dvoustranné spolupráce České republiky a Čínské lidové republiky (partneři Univerzity Xi'an Jiaotong a Sinopec Research Institute Shanghai; SPIL VUT, Vysoké učení technické v Brně a EVECO sro, Brno), program INTER-EXCELLENCE, INTER-ACTION Ministerstva školství, mládeže a tělovýchovy ČR; a Národním klíčovým programem výzkumu a vývoje v Číně (2018YFE0108900), stejně jako doktorské stipendium a mimořádné stipendium VUT.

Velké poděkování patří doktorce Šárce Zemanové, kolegům ze SPIL a zejména profesoru Stehlíkovi, že mě po celou tuto cestu podporoval veškerou komunikací, administrativní prací a pomocí v mnoha ohledech.

Chtěl bych také srdečně poděkovat svým rodinám v Malajsii za to, že mi vždy věřili fyzicky nebo duševně a povzbuzovali mě, abych šel za svými sny. Jejich láska a podpora jsou pro mě hlavní motivací pokračovat ve své výzkumné cestě

Contributing Research Work Presented in Peer-Reviewed Publications

This thesis has been developed based on my publications in several distinguished international journals. **Chapter 1** introduces the research scope of the thesis, summarise the research gaps, and presents the research aims and objectives. **Chapter 2** presents a thorough literature review of resource conservation with Pinch Analysis tools, Total Site/eco-industrial park synthesis, Game Theory in resources allocation, as well as fault diagnosis and monitoring in a chemical process system. The primary research work and achievements for resources conservation are introduced with three chapters (Chapter 3, 4 and 5). **Chapter 3** introduces the extension of Pinch Analysis tools for material resources targeting multiple constraints/contaminants. **Chapter 4** introduces the Material Headers/Mains targeting framework with a graphical user interface based on the Pinch framework for both single and multiple contaminants. **Chapter 5** presents the Game Theory analyses in deriving a balanced economy policy to realise the Circular Economy in a material exchange eco-industrial park, which includes distribution of subsidies/incentives, taxation policy and price negotiation on wastes recycling. The rest of the two chapters (Chapter 6 and 7) denote the proposed approaches in asset management. **Chapter 6** introduces the Pinch framework applied in opportunistic maintenance framework and short term maintenance tasks targeting. **Chapter 7** presents the maintenance decision-making framework for a chemical process system, as well as for an eco-industrial park. **Chapter 8** concludes all the research works and proposing the direction of future works.

Main Publications:

- **Chin HH**, Varbanov PS, Liew PY, Klemeš JJ, 2021. Pinch-based targeting methodology for multi-contaminant material recycle/reuse. Chemical Engineering Science, 230, 116129 **(Citations = 12) [IF = 4.311] [CiteScore = 7.3]**
- **Chin HH**, Varbanov PS, Liew PY, Klemeš JJ, 2021. Extension of Pinch Analysis to Targeting and Synthesis of Multi-Contaminant Material Recycle and Reuse Networks. Chemical Engineering Science **(R2 Under Review) [IF = 4.311] [CiteScore = 7.3]**
- **Chin HH**, Varbanov PS, Liew PY, Klemeš JJ, 2021. Enhanced Cascade Table Analysis to target and design multi-constraint resource conservation networks. Computers & Chemical Engineering, 148, 107262. **[IF = 3.845] [CiteScore = 7.0]**
- **Chin HH**, Xuexiu Jia, Varbanov PS, Klemeš JJ, Liu Z-Y, 2021. Internal and Total Site Water Networks Design with Water Mains Using Pinch-Based and Optimisation Approaches. ACS Sustainable Chemistry & Engineering, 9(19), 6639-6658. **[IF = 8.198] [CiteScore = 12]**
- **Chin HH**, Varbanov PS, Klemeš JJ, Wan-Alwi SR, 2021. Total Site Material Recycling Network Design and Headers Targeting Framework with Minimal Cross-Plant Source Transfer. Computers & Chemical Engineering, 151, 107364. **[IF = 3.845] [CiteScore = 7.0]**
- **Chin HH**, Varbanov PS, Klemeš JJ, Wan-Alwi SR**,** 2021. Industrial Site Water Exchange Network Synthesis Considering Multiple Qualities and Water Headers. Journal of Cleaner Production **(Under Review) [IF = 9.297] [CiteScore = 13.1]**

- **Chin HH**, Varbanov PS, Klemeš JJ, Bandyopadhyay S, 2021. Subsidised Water Symbiosis of Eco-Industrial Parks: A Multi-Stage Cooperative Game Theory Approach. Computers & Chemical Engineering **(R1 Under Review) [IF = 3.845] [CiteScore = 7.0]**
- **Chin HH**, Varbanov PS, Klemeš JJ, Tan R.R., Benjamin MFD, 2020. Asset Maintenance Optimisation Approaches in the Chemical and Process Industries - A Review. Chemical Engineering Research and Design, 164, 162-194. **(Citations = 4) [IF = 3.739] [CiteScore = 6.3]**
- **Chin HH,** Wang B, Varbanov PS, Klemeš JJ, Zeng M, Wang QW, 2020. Long-term Investment and Maintenance Planning for Heat Exchanger Network Retrofit. Applied Energy, 279, 115713. **(Citations = 4) [IF = 9.746] [CiteScore = 17.6]**

Journal articles-with CiteScore in SCOPUS:

- **Chin HH**, Varbanov PS, Liew PY, Klemeš JJ, 2020. Pinch Approach for Targeting in Multi-Contaminant Material Recycle/Reuse Network. Chemical Engineering Transactions, 81, 145-150 **(Citations = 1) [CiteScore = 1.5]**
- **Chin HH**, Xuexiu Jia, Varbanov PS, Klemeš JJ, Wan-Alwi SR, 2021. Targeting Flowrates and Concentrations in Internal or Total Site Water Mains for Single Contaminant. Chemical Engineering Transactions, 86, 895-900 **[CiteScore = 1.5]**
- **Chin HH**, Varbanov PS, Klemeš JJ, Lam HL, 2019. Application of pinch analysis to opportunistic maintenance management. Chemical Engineering Transactions, 76, 535-540 **(Citations = 3) [CiteScore: 1.5]**
- **Chin HH**, Varbanov PS, Klemeš JJ, 2020. Short Term Maintenance Tasks Scheduling with Pinch Methodology. Chemical Engineering Transactions, 78, 499-504. **(Citations = 1) [CiteScore = 1.5]**
- **Chin HH,** Wang B, Varbanov PS, Klemeš JJ, 2021. Markov Decision Process on Asset Investment and Maintenance Planning for Chemical Process Systems. Computer-Aided Chemical Engineering, 50, 1853-1858 **[CiteScore = 0.9]**

Table of Contents

CHAPTER 1 **INTRODUCTION**

1.1 Resources recycling for Circular Economy

Circular economy was introduced as an economic or business model for the transition of linear to circular systems. It has risen in popularity in recent years as a conceptual model to guide better use of natural resources and management of waste (Murray et al., 2017). The utilisation of recycled resources can scale down the demand for the extraction of new resources and avert the impacts created along the processing chain. This is critical to support the transition from a linear to a circular economy. The circular system can be achieved by avoiding the material flow to the end of the life cycle (reducing) or by regenerating the material through reusing, recycling and recovering. The full framework for Circular Economy proposed by MacArthur (2013) is shown in Figure 1-1 below.

According to the definition from Tura et al. (2019), a circular economy is a system developed by minimising the use of energy, natural resources and waste generation. It can be achieved by mitigating, closing and narrowing loops of utilities and materials flows. Based on a conducted systematic analysis, most scholarly see the circular economy as an avenue for economic prosperity (Kirchher et al., 2017) and a material or energy flow balance.

The current indicators of the circular economy are more specific on the material flow accounting system, which is usually derived based on European Union material flow and Japanese material flow indicator system (Geng et al., 2012). Sustainability is not within the concern of such accounting. The other material flow accounting derived indicators based on regional nuances and policy are a) energy and material efficiency indicator in Korea and b) decoupling of material flow intensity in the United States. In China, the circular economy evaluation system covers a more extensive range of considerations include resources output and consumption rate, integrated resource utilisation rate, waste disposal and pollutant emission. Haupt et al. (2017) apply recycling rates as an indicator to measure the degree of circularity of the Swiss waste management system. Nakamura and Kondo (2018) developed a dynamic waste input-output model. A circular material use rate is proposed by Eurostat (2018) to measure the share of material recovered and fed back into the economy. A set of indicators comprise of a) scale indicators (t) (In-and output flows, consumption-based perspective, interim flows), and b) circularity rate (%) (socioeconomic cycling, ecological cycling potential, non-circularity) has been proposed by Mayer et al. (2019) to identify the circularity of EU. As shown in Figure 1-2, only 0.71 Gt of the processed materials are from secondary materials. This suggested that not all the reprocessed secondary material is utilised in the domestic economy.

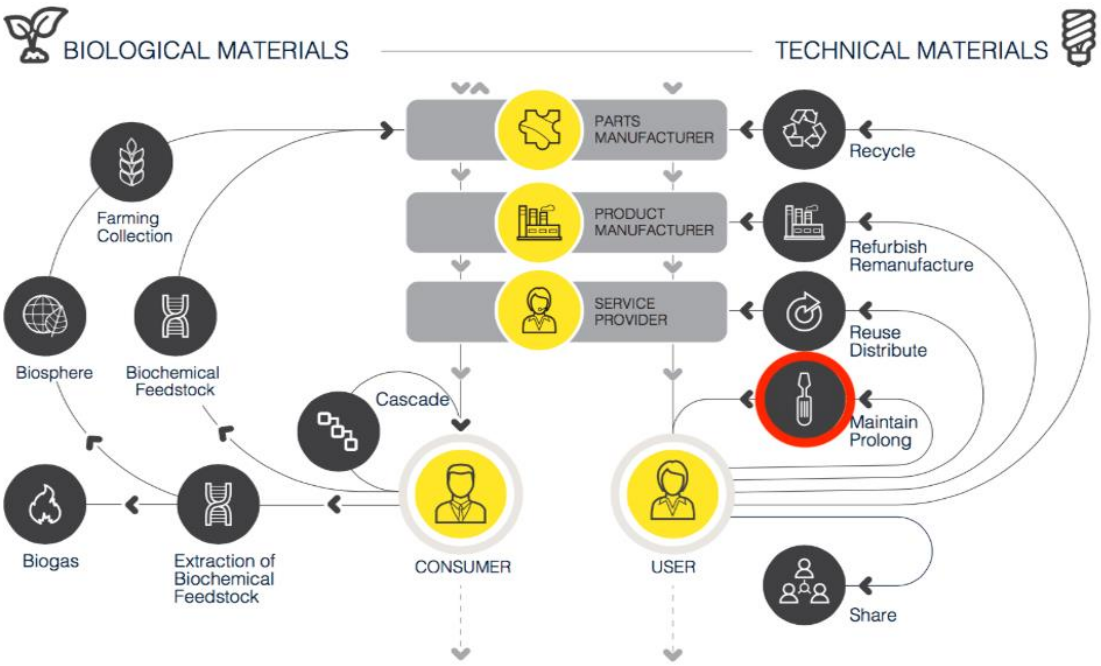

Figure 1-1: The framework for Circular Economy, adapted from MacArthur (2013)

This study highlights the roles of internal sources recovery in a circular economy and the need for systematic resource conservation planning to reduce the reliance on virgin raw materials. The proposed indicators are relatively comprehensive; however, they only serve as a monitoring framework (assessment instead of scientific analysis) and tells very little on the constraints/bottlenecks for the material recycle/reuse. The results inform the circularity situation, but the optimal recycling strategy is unknown. Process Integration tools, such as Pinch Analysis, provide scientific analysis on the problem using thermodynamic knowledge to derive the optimal resource recycling strategy. However, this is limited to only a single criterion/constraint problem (e.g. Water Pinch Analysis). Not many developments on the Pinch-based tools considering multiple constraints. For practical application, the consideration of multiple constraints in the internal resources is crucial to derive optimal recycling steps. Pinch-based tools could provide insights on how materials should be recycled to achieve minimum use of the virgin raw materials, striving towards more quality and informative Circular Economy. Not only that, it is also crucial to target for the minimum inter-transfer of the resources between stakeholders. This is to reduce the additional cost to build the facilities to transfer the resources. The intermediate storage of the resources should be targeted with the parameters such as flowrates, qualities of the resources or number of storages for the resources. A Pinch-based tool provides a good graphical interface for the users to target the intermediate storage through the mixing of the waste resources.

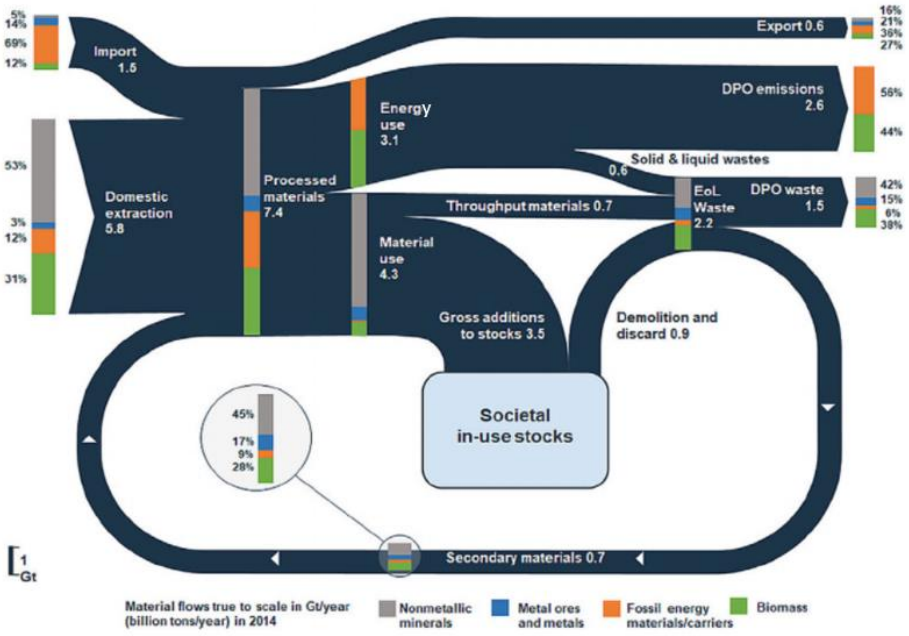

Figure 1-2: Material flows through the EU28 economy, amended from Mayer et al. (2019). (Domestic processed outputs=DPO. EoL= End of life)

1.2 Asset management for Circular Economy

Asset management (AM) is defined as a coordinated activity to realise value from the assets by the organisation (ISO 55000, 2014). It aims at ensuring the longevity of the assets and optimising the business impacts of the assets in terms of cost, performance and risk exposures. The values of the asset are realised through operation, maintenance and investment activities (Komonen, 2008). The goals of the AM are congruent with the goals of the Circular Economy. The term Circular Economy (CE) is defined as a system that creates value by minimising waste generation, energy and natural resources utilisation (Geissdoerfer et al., 2017). The solution to creating a CE is too slow, close and narrow the loops of material and energy usage. One of the solutions includes long-lasting product design or design for easy disassembly and maintainability. The main concept is to provide 'product as a service' for the end-users instead of mainly rely on the use of virgin resources and creates an abundance of unnecessary by-products and wastes. Maintenance actions such as repair, refurbishing, reuse, remanufacturing and recycling are in line with the concept of CE to preserve the condition of assets for long-lasting usage. Figure 1-3 below shows the analogous connection between AM and CE.

The keywords for achieving CE presented in Figure 1-1 include 'repair', 'reuse', 'maintain' or 'extend'. This shows that asset maintenance plays an active role in this strategic concept. As Kalmykova et al. (2018) mentioned, the CE strategies overlap with the terminologies such as 'green supply chain management', 'industrial symbiosis', 'cradle-to-cradle or 'closed-loop economy'. Potting et al. (2017) summarised the strategies for CE and structured them into three groups: a) useful application of materials, b) extend the lifespan of products and their parts and

c) smarter product manufacturing and use. These groups stem from the 10R framework, as shown in Figure 1-4

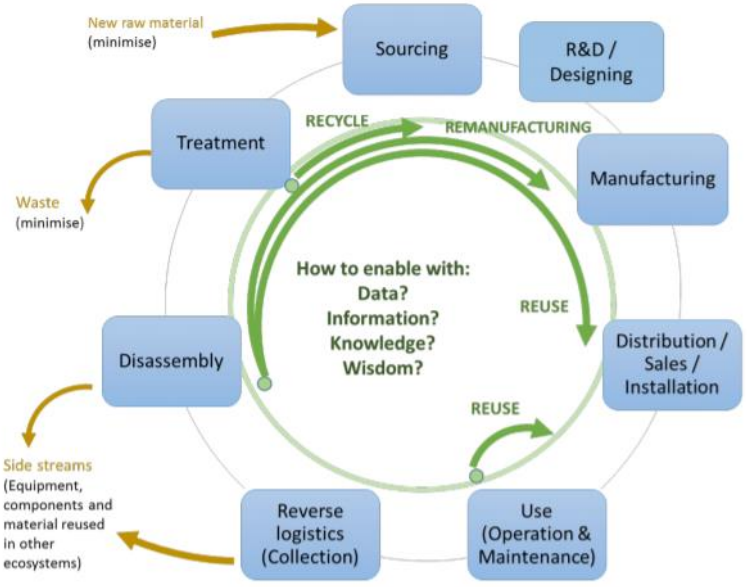

Figure 1-3: Asset Maintenance and Circular Economy, adapted from Valkokari et al. (2017)

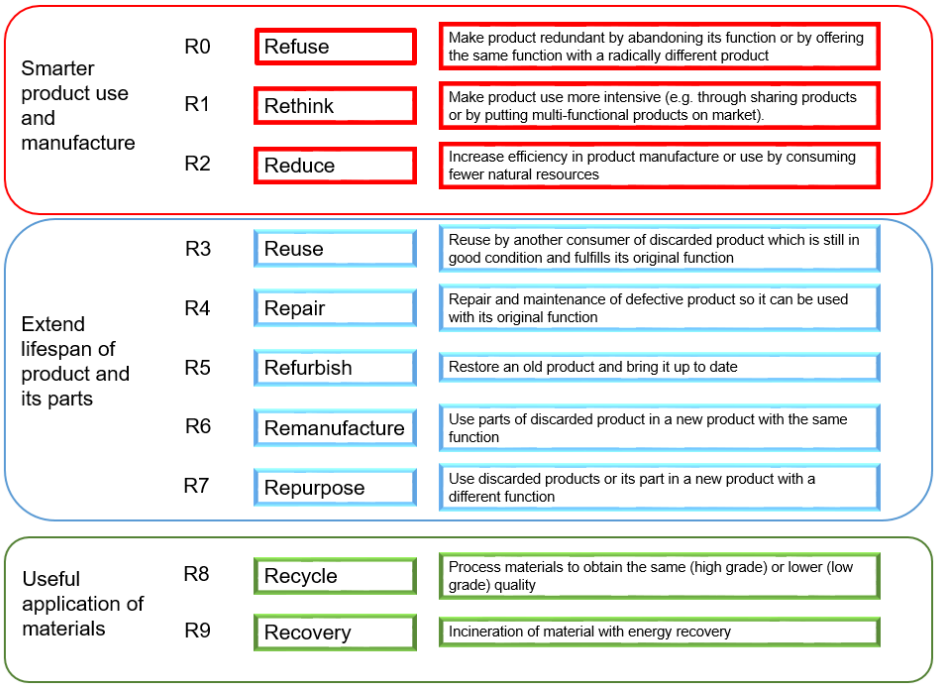

Figure 1-4: Circular Economy strategy: 10R framework, adapted from Potting et al. (2017) and Klemeš et al. (2020)

The strategy in the group 'Extend the lifespan of the product and its parts' (R3-R7) emphasises retaining finished parts or products longer while maintaining or improving their value (Morseletto, 2020). Maintenance is defined as the actions for keeping equipment/parts/products

in good condition for prolonging the durability. According to MacArthur (2013), asset maintenance is not a part of the CE strategy, but rather it is a set of strategic actions that resemblance with the CE strategies: Repair (R4), Refurbish (R5) and Remanufacture (R6). Morseletto (2020) has interpreted maintenance as a form of soft Repair as maintenance is congruent with the 10R framework. In fact, corrective/reactive maintenance is identical to the Repair (R4) strategy (den Hollander et al., 2017). Equipment upgrading can be considered as a life extension strategy, but also as the remedial actions in the forms of Refurbish/Remanufacture. The equipment lifetime extension is also beneficial in tightening the material circulating loop efficiency, for which material recycling can be costly or energy-intensive. Raising resource prices could potentially make the circulating loop more attractive, but a possible increase in operating and maintenance cost or efficiency gains due to rapid product innovation can make the circulating power obsolete (MacArthur, 2013). In some cases, extending the lifespan of the product can slow down innovation or prevent the development of new products (Bressanelli et al., 2018). However, proper planning of the maintenance strategies is also required to prevent the waste of valuable resources – labour/time/spares.

Reuse (R3) is also a part of a maintenance strategy in which the products/parts are used within the inner circulation loop (MacArthur, 2013). For example, pallets or containers could be reused to carry a variety of goods or properly maintained tube bundles could be reused in a heat exchanger. Reuse strategy could prevent the rapid consumption of goods as making new spare parts is often unavailable or prohibitively costly. However, in certain cases, repairing can be expensive as well, owing to the technical difficulties and the associated time/labour (Milios, 2018). Reduce (R2) strategy should also be widely applied in the field of asset management to reduce the scraps generation from equipment decommissioning. Globally, Allwood (2014) shows that 25 % of steel and 50 % of aluminium are converted into scraps in the industries. Careful maintenance could potentially enhance the service life of the equipment, but the warranty life of the equipment is inevitably declining annually. Enforcing rules on consequent material savings from plant decommissioning projects could reduce the generation of scraps. Eliminating these obstacles is the key to make the economy more circular.

Other than the resource conservation framework, this study also highlights the roles of asset maintenance and management in striving towards the goals of CE. The research on the impact of asset maintenance and management in the system of CE is scarce (Morseletto, 2020). Asset optimisation is now widely adopted in the chemical industries to drive more business profits. This study considers the asset investment and maintenance optimisation in the processing system to determine the effectiveness of asset planning in driving business profit, especially in a plant retrofit project. A Pinch-based tool is also developed to account for the cost targeting in opportunistic maintenance management. A short term Pinch Methodology for manpower planning for delegation of maintenance tasks is also derived from showcasing the advantages of the methodology in resource planning and bottlenecks determination.

1.3 Research Aim and Objectives

The central research aim of this thesis is to develop and extend the current decision support models and tools in realising the goals of Circular Economy, emphasising the resource recycling or reuse and the assets maintenance or management approaches. The main research questions targeted from this work include:

(i) The fundamental understanding of material recycling or reuse network problems with a single quality that led to the development of the traditional Material Pinch method has to be extended to multi-quality problems. This enables decision-makers to solve the real problems without the need for artificial simplification to single-quality formulations, reflecting a more realistic Circular Economy system.

(ii) An insightful resources targeting tool with intermediate storage systems is needed for a Circular Economy system in an eco-industrial park. This allows the users to explore different solutions of resources mixing and allocation while ensuring the fresh resources requirements are minimal, and the cross-plant transfer is minimal.

(iii) A balanced economic policy between stakeholders and the government or authorities to facilitate the Circular Economy system is required. Scientific analysis on the subsidies/incentives distribution scheme to sponsor the infrastructure building cost. Proper setting of the tax rates or price negotiations of waste selling is needed as stimulants for recycling activities while acting as a source of income.

(iv) An integrated framework on asset and process optimisation in the chemical industry to incorporate the reliability issues, the service life of equipment and depreciation of the units is needed. This is crucial for long-term development and footprint minimisation to achieve the goals of the Circular Economy through equipment upgrading or lifetime extension as well as resource conservation.

(v) A scientific analytical framework to provide insights on the mathematical optimisation model is needed to determine the bottlenecks in a Circular Economy system. A Pinch-based framework is not only useful for multiple constraints material recycling or reusing network, but also can be applied for asset planning- maintenance tasks planning and scheduling to maximise the usage of resources.

1.4 Thesis Outline

Chapter 1 introduces the research scope of the thesis, summarise the research gaps, and presents the research aims and objectives. **Chapter 2** presents a thorough literature review of resource conservation with Pinch Analysis tools, Total Site/eco-industrial park synthesis, Game Theory in resources allocation, as well as asset maintenance and investment planning. The primary research work and achievements for resources conservation are introduced with three chapters (Chapter 3, 4 and 5). **Chapter 3** introduces the extension of Pinch Analysis

tools for material resources targeting multiple constraints/contaminants. **Chapter 4** introduces the Material Headers/Mains targeting framework with a graphical user interface based on the Pinch framework for both single and multiple contaminants. **Chapter 5** presents the Game Theory analyses in deriving a balanced economy policy to realise the Circular Economy in a material exchange eco-industrial park, which includes distribution of subsidies/incentives and taxation policy. The rest of the two chapters (Chapter 6 and 7) denote the proposed approaches in asset management considering various risks. **Chapter 6** introduces the Pinch framework applied in opportunistic maintenance framework and short term maintenance tasks targeting. **Chapter 7** presents the maintenance decision-making framework for a chemical process system, as well as for an eco-industrial park. **Chapter 8** concludes all the research works and proposing the direction of future works.

Following are the publications for each chapter:

Chapter 3: Extension of Pinch Analysis tools in resources targeting for multiple constraints resource conservation network problem

- **Chin HH**, Varbanov PS, Liew PY, Klemeš JJ, 2021. Pinch-based targeting methodology for multi-contaminant material recycle/reuse. Chemical Engineering Science, 230, 116129 **(Citations = 12) [IF = 4.311] [CiteScore = 7.3]**
- **Chin HH**, Varbanov PS, Liew PY, Klemeš JJ, 2021. Extension of Pinch Analysis to Targeting and Synthesis of Multi-Contaminant Material Recycle and Reuse Networks. Chemical Engineering Science **(R2 Under Review) [IF = 4.311] [CiteScore = 7.3]**
- **Chin HH**, Varbanov PS, Liew PY, Klemeš JJ, 2021. Enhanced Cascade Table Analysis to target and design multi-constraint resource conservation networks. Computers & Chemical Engineering, 148, 107262. **[IF = 3.845] [CiteScore = 7.0]**
- **Chin HH**, Varbanov PS, Liew PY, Klemeš JJ, 2020. Pinch Approach for Targeting in Multi-Contaminant Material Recycle/Reuse Network. Chemical Engineering Transaction, 81, 145-150 **(Citations = 1) [CiteScore = 1.5]**

Chapter 4: Total Site Materials Headers/Mains targeting framework using Pinch framework and Optimisation

- **Chin HH**, Xuexiu Jia, Varbanov PS, Klemeš JJ, Liu Z-Y, 2021. Internal and Total Site Water Networks Design with Water Mains Using Pinch-Based and Optimisation Approaches. ACS Sustainable Chemistry & Engineering, 9(19), 6639-6658. **[IF = 8.198] [CiteScore = 12]**
- **Chin HH**, Varbanov PS, Klemeš JJ, Wan-Alwi SR, 2021. Total Site Material Recycling Network Design and Headers Targeting Framework with Minimal Cross-Plant Source

Transfer. Computers & Chemical Engineering, 151, 107364. **[IF = 3.845] [CiteScore = 7.0]**

- **Chin HH**, Xuexiu Jia, Varbanov PS, Klemeš JJ, Wan-Alwi SR, 2021. Targeting Flowrates and Concentrations in Internal or Total Site Water Mains for Single Contaminant. Chemical Engineering Transaction, 86, 895-900 **[CiteScore = 1.5]**
- **Chin HH**, Varbanov PS, Klemeš JJ, Wan-Alwi SR**,** 2021. Industrial Site Water Exchange Network Synthesis Considering Multiple Qualities and Water Headers. Journal of Cleaner Production **(Under Review) [IF = 9.297] [CiteScore = 13.1]**

Chapter 5: Game Theory approaches in deriving a balanced economic policy of waste recycling in Total Site/Eco-Industrial park

- **Chin HH**, Varbanov PS, Klemeš JJ, Bandyopadhyay S, 2021. Subsidised Water Symbiosis of Eco-Industrial Parks: A Multi-Stage Cooperative Game Theory Approach. Computers & Chemical Engineering **(R1 Under Review) [IF = 3.845] [CiteScore = 7.0]**

Chapter 6: Application of Pinch framework in opportunistic maintenance management and tasks allocation

- **Chin HH**, Varbanov PS, Klemeš JJ, Lam HL, 2019. Application of Pinch aAnalysis to Opportunistic Maintenance Management. Chemical Engineering Transactions, 76, 535-540 **(Citations = 3) [CiteScore: 1.5]**
- **Chin HH**, Varbanov PS, Klemeš JJ, 2020. Short Term Maintenance Tasks Scheduling with Pinch Methodology. Chemical Engineering Transactions, 78, 499-504. **(Citations = 1) [CiteScore = 1.5]**

Chapter 7: Maintenance decision-making framework for process system

- **Chin HH**, Varbanov PS, Klemeš JJ, Tan R.R., Benjamin MFD, 2020. Asset Maintenance Optimisation Approaches in the Chemical and Process Industries - A Review. Chemical Engineering Research and Design, 164, 162-194. **(Citations = 4) [IF = 3.739] [CiteScore = 6.3]**
- **Chin HH,** Wang B, Varbanov PS, Klemeš JJ, Zeng M, Wang QW, 2020. Long-term Investment and Maintenance Planning for Heat Exchanger Network Retrofit. Applied Energy, 279, 115713. **(Citations = 4) [IF = 9.746] [CiteScore = 17.6]**
- **Chin HH,** Wang B, Varbanov PS, Klemeš JJ, 2021. Markov Decision Process on Asset Investment and Maintenance Planning for Chemical Process Systems. Computers Aided Chemical Engineering, 50, 1853-1858 **[CiteScore = 0.9]**.

CHAPTER 2 LITERATURE REVIEW

2.1 Process Integration tools for material resource conservation

An important invention of Mass Exchange Networks (MENs) was introduced in 1994 by Wang and Smith (1994). They proposed a graphical approach to target the minimum freshwater consumption and wastewater discharged by the transfer of contaminants from process streams to water streams. El-Halwagi (2006) introduced the problem of synthesising for mass transfer operations. They showed that it is possible to target the minimum usage of external lean streams using systematic representations such as Composite Curves. El-Halwagi et al. (2003) later provided a single-stage targeting method to identify minimum resources for a single contaminant water network, with the solution strategy identified through rigorous analysis. Both methods apply to mass exchange processes, and they rely on the basic principle of concentration driving force. A new simpler design procedure was introduced by Olesen and Polley (1997), continuing the work of Wang and Smith (1994) for single contaminant problems. This new methodology results in better constructions for regeneration reuse and recycles designs. Hallale (2002) introduced a new graphical targeting method for water minimisation. Gomes et al. (2007) presented a heuristic algorithmic procedure, water source diagram procedure (WSD), to synthesise water mass exchange networks

A comprehensive review of the historical development of Pinch Analysis in the water network has been done by Foo (2009). Klemeš et al. (2018) have conducted a comprehensive overview of various extensions of PA in Mass Integration, including water and hydrogen integration. The water PA has been successfully applied to water system optimisation in various industries, including the ethanol industry (Liu et al., 2019), starch industry (Dakwala et al., 2009), oil refineries (Mohammadnejad et al., 2011), brick manufacturing industry (Skouteris et al., 2018) and the steel industry (Tian et al., 2008). Govindarajan (2018) provided a recent review dedicated to Water Pinch Analysis from 2008 to 2018. This proves the central importance of using simplified and accurate graphical tools in addressing complex water design problems. The detailed development until 2013 was covered by the first edition of the PI Handbook (Klemeš, 2013a), which proves the success of PA as a tool for handling a single contaminant water network target and design.

Mann and Liu (1999) have found that, when considering water regeneration recycling, some systems had a different Pinch Point, termed Regeneration Pinch, which is located higher than the process Pinch obtained without regeneration. They also introduced a graphical approach to determine the minimum water flow rate in the case of multi contaminant systems. Dakwala et al. (2009) used graphical strategies and demonstrated a case study of a multi-contaminant system for starch industries based on fixed flow rate operations. They presented a graphical strategy, namely concentration interval diagram (CID), Concentration Composite Curve and water supply line primarily to determine the key contaminants for each operation. This procedure involves shifting the inlet and/or outlet concentration of specific contaminants to maintain the feasibility of water reuse. However, the concentration shifting requires tedious

analysis on both inlets and outlets for each operation. Alva-Argaez and Smith (2007) combine PA and mathematical approaches to identify design water-using systems for petroleum refineries. An iterative procedure is proposed to handle the multi-contaminants in the nonlinear superstructure model. Fan et al. (2019) proposed an iterative approach to design the water network, including regeneration, recycle/reuse and wastewater treatment. However, multiple impurity problems using the PA approach frequently only locate the approximate freshwater flowrates rather than the fully optimum figures due to multidimensional problems to be solved, e.g. in Tan et al. (2007).

Various other strategies have been proposed to tackle multi-contaminant problems. Alva-Argaez et al. (1999) developed Mixed-Integer Linear Programming (MILP) based multi-contaminant transhipment model used for targeting, particular for mass exchange networks and wastewater minimisation problems. Their model could tackle the general problem of mass exchange networks, but it could not evaluate the mixing effect of multi-contaminant problems. By using MP, the calculation in designing multiple contaminant water networks can be fast. However, it is often difficult to understand how the optimal solutions are obtained and determine the process bottlenecks from these models. To address this problem, Liu et al. (2009) proposed methodology concepts of concentration potential. The concepts are presented based on the overall allocating possibility of source streams to demand streams. The concept is analogous to the single contaminant water network as it identifies the concentration order of the streams. Fan et al. (2012) extended the concepts of concentration potential to the fixed flowrate operations. Li et al. (2017) provide a review on this approach with their extension and applicability, and Zhao et al. (2019) utilised the concept in designing heat-integrated water networks.

Other attempts include the work of Castano and Higuita (2016), who used the property of turbidity (which sums a number of contaminants) in the design of water networks. The authors regarded turbidity as the key measured parameter, and linear correlations of it were made with the concentration of the suspended solids. To this date, there is limited research in the context of Pinch based techniques on procedures that determine optimal regenerator performance prior to the water network design. Mabitla and Majozi (2019) presented a hybrid of graphical and mathematical approaches in solving multi-contaminant water and regeneration networks. The graphical approach involves the pre-processing steps to identify the minimum water target and optimal regenerator removal ratios. The multi-contaminant problem is simplified using the reference contaminants approach proposed by Calixto et al. (2015). The detailed design of the reverse osmosis unit is then identified by formulating a mathematical model that optimises the water and energy use of the unit. However, their approach could only account for at most two contaminants.

The aforementioned design procedures for the multi-contaminant recycle/reuse problem have significant advantages, but none of them presents a systematic targeting procedure. Nemati-Amirkolaii et al. (2019) mentioned that in the case of three or more contaminants available

in the water network system, they declared that a multidimensional mathematical model remains the best option. They highlighted that in the food industry, it is almost impossible to include all the components, such as the microbiological aspect and the quality of the food product. In some food processing sectors, it is common to select representative contamination indicators. The development of PA is an essential step for industrial application because it reveals the inherent system limitations – targets of the resource supply and the internal bottlenecks. These targets are then used in the detailed design model setting the optimisation strategy and providing bounds on the key variables. This is the logic that has led to the Process Integration strategy to identify the target for minimum usage of fresh resources ahead of detailed design.

2.2 Asset investment planning in the chemical process industry

Optimisation of capacity planning for processes is a problem that is widely studied by various researchers. The core concept of this field is to optimise future investment in expanding the units' sizes. More substantial investments at the same time are often more beneficial due to the time value of money. Manne (1967) was one of the pioneers that developed a solution for capacity planning with linear growth of demand analytically within an infinity planning horizon. Sahinidis et al. (1989) investigated a network of existing and new chemical processes based on the capacity expansion potential with several optimisation strategies. In each period, the decisions to be made are the amount of chemical to be produced, the capacity expansion and shut-down actions, aiming to optimise the Net Present Value (NPV). Sahinidis and Grossmann (1991) then extended for more flexible processes by considering continuous and batch operation modes. Wiesner et al. (2008) formulated a MILP, which constitutes a step-wise approach in capacity expansion planning for chemical plants.

Investment planning is also widely applied in energy system planning. The location, timing, technologies and sizes of new plant additions are the central core of the problem. Bakirtzis et al. (2012) developed a MILP model for the Greek power system in monthly intervals. The monthly decisions for unit maintenance scheduling, reservoir management and investment decisions are formulated in a single optimisation problem. The emission allowance cost is also included to reflect the environmental effect on the units. Pereira et al. (2017) studied long-term planning coupled with short-term decision making in expansion planning for electricity generation with renewable energies. The long-term investment planning with 10 years horizon, with the short term hourly impact, was done to investigate the sensitivity of the system to renewables. The resources of seasonal availability have a significant impact on the function of the system. Zhang et al. (2015) studied the transmission system to optimise the energy hub operations, considering the investment options for transmission lines, furnaces, generating units and combined heat and power (CHP) units.

Investment planning on a global supply chain is vital to ensure global competitiveness. Liu and Papageorgiou (2013) proposed a MILP-based multi-objective optimisation framework that addresses capacity and production planning for the global supply chain. The various

capacity expansion strategies are also taken into account to optimise the total cost, also the total flow time and total lost sales. The strategic investment planning on the bioethanol supply chain is studied by Dal-Mas et al. (2011). A MILP model is developed to assess the economic and investment risks under the uncertainty of product selling price and biomass production.

For process facilities, Wickart and Madlener (2007) developed a framework to aid in decision-making whether to invest in a CHP unit or an industrial boiler for utility system. The uncertainty of electricity and fuel prices were considered. They concluded that capital investment is less preferred if the operational risks are high. Redlarski et al. (2017) applied several evolutionary algorithms in the investment planning of a bioethanol plant. The decision on the investment includes the selection of equipment from the market as well as the location of the plant itself. Yazdi et al. (2019) developed the Fuzzy Analytic Hierarchy Process to allow investment planning on offshore process facilities with uncertain data. Knowledge of experts from various domains is collected to identify the potential risks and rank the factors affecting the investment. A bi-objective nonlinear optimisation model is then formulated to minimise the accident risk and safety investments. Baaqeel and El-Halwagi (2018) formulated a multi-scale capacity planning model for seawater desalination system, considering the emerging technologies such as membrane distillation or alternative options such as multi-effect distillation. Their aim is to simultaneously optimise the sizing of the desalination units over a planning horizon by maximising economic return.

Lambert et al. (2016) proposed multistage stochastic programming for optimal planning of district heating networks. The pipe diameters are first identified by minimising the capital cost. The solutions then serve as the parameters for the long-term deployment model of a district heating network. Bütün et al. (2019) employed a long-term investment model, coupled with the Process Integration approach to clusters of district heating networks. The investment model includes the units' depreciation and the units' lifetime, so the decision to invest and sell the units is made every year. The objectives studied are NPV and CO_2 emissions.

Past works on investment planning have addressed a wide range of problems, but they were directed mostly towards capacity expansions. Not many of the proposed methods are fully applicable to industrial problems. In most cases, the issue that the current equipment on plants has a limited lifetime is usually ignored. The capital expenditure would eventually be needed if the equipment's life has ended. Since the capital investment is inevitable, the money could be spent on purchasing a more efficient and bigger unit or implementing the Best Available Techniques (BAT) while utilising units with sizes similar to the old unit. The investments in improvements in energy efficiency have better advantages than just replacing aged or obsolete equipment for a long time horizon. This, however, increases the computation burdens to the modelling framework. The option is now not just "what to invest in", but also "when to invest" to achieve higher profit. Not only the service life of the units has to be considered, the remaining life before the failure of the units, which associates with the reliability of the units, have to be evaluated as well. This issue is crucial because the units'

failure could drastically affect the system and cause process interruption.

2.3 Asset maintenance planning in the chemical process industry

Tseng et al. (2015) did a comprehensive review of the maintenance management models in various industries. Most of the studied areas focus on power plants, manufacturing facilities and oil refineries. Various published works from 1995 to 2011 that utilise preventive and predictive maintenance strategies, e.g. time-based maintenance (TBM) and condition-based maintenance (CBM), are reviewed. Alrabghi and Tiwari (2015) conducted a state-of-the-art review of simulation-based approaches for maintenance systems in various industries. The majority of the reported works used discrete event simulation and genetic algorithm (GA) as an optimisation tool. They suggest that a well-developed framework to guide the maintenance planning process is needed in real case studies, especially in the context of CBM. Carlo and Arleo (2017) conducted reviews on the applications of 'perfect' maintenance into real practises in the industry and provided guidelines to select the proper 'imperfect' maintenance model. Jonge and Scarf (2019) presented a comprehensive review of different mathematical approaches used by researchers in generic systems up until 2018 in maintenance planning

Ahmed et al. (2015) devised a maintenance scheduling problem for a complex gas absorption system in a hydrocarbon processing facility. Considering the constraints of equipment risk, maintenance cost, system reliability and availability, the proper scheduling involving inspection, maintenance and replacement is determined. In their model, they assumed different actions could alter the original failure characteristics over time. However, accurate failure analysis of the equipment is needed, which heavily depends on historical data, fault diagnostics, and prognostic information.

Megow et al. (2010) consider turnaround scheduling in the chemical industry, specifically in continuous plants. The task is to minimise the cost of maintenance with respect to the resources used, which are manpower and maintenance equipment. This minimisation is subject to pre-set precedence rules for maintenance tasks and resource scheduling constraints that involve shift calendars for maintenance workers. The assignment constraint, which assigns maintenance resources to jobs in each time period, gives the detailed maintenance schedule. The interesting trade-off is the time-cost trade-off, where more expensive external resources can be utilised in order to perform a certain task in reduced time.

Aguirre and Papageorgiou (2017) formulated a continuous-time MILP model to determine the optimum production and maintenance schedule for a multiproduct batch process. The tasks are scheduled by using the travelling salesman problem (TSP)/precedence-based concepts, which are different from the previously applied principle of first-in-first-out (FIFO) (Dedopoulos and Shah, 1995). Their model also incorporated the production resources constraint and unit performance decay that reflect the reality of a chemical batch process. The performance decay is modelled as a statistical distribution. It provides some numerical guidelines to engineers to determine the optimal maintenance actions considering the

deterioration model. However, the representation of performance decay without any data as evidence is hardly convincing. Another published work on integrating process and maintenance scheduling can be found in Idris (2016). The study is conducted on a Mexican oil chemical company. The authors proposed a mixed-integer nonlinear programming (MINLP) model to optimise the product processing time and overall profit. The PM actions are translated into maintenance demands, and they are considered as products constraints with specific time windows and goals. By using historical production data from the company, they applied the Monte Carlo approach to generate several production instances and significant improvement of profit is obtained using the proposed model. However, the practicality of the model is questionable since a longer time horizon of maintenance planning enlarges the problem significantly.

The need to have the right spare parts at the right place and at the right time inevitably requires the joint optimisation of maintenance schedules and logistics of maintenance resources. The joint decision-making problem becomes particularly challenging if one considers multiple options for PM operations and multiple delivery methods for the necessary spare parts. Wang and Djurdjanovic (2018) presented an integrated decision-making policy for simultaneous PM scheduling, spare parts inventory management and transportation planning in a system of geographically dispersed multi-part degrading assets and maintenance. This integrated decision-making policy considers both perfect and imperfect maintenance options, as well as multiple shipping methods for spare part deliveries. The problem investigated here is only a theoretical example, but the framework can be extended and applied to large-scale practical problems in chemical process plants with real data. The allocation of human resources also deserves to be researched to execute maintenance activities.

Most of the methods mentioned are mainly mathematical optimisation models. It is often difficult to understand how the optimal solutions are obtained and determine the process bottlenecks from these models. Strong programming background is required for the users to understand the model. As such, this study proposes a graphical approach named Pinch Analysis to identify the opportunistic maintenance activities grouping created by the failure events. This method has been widely applied in different fields and is famous for its easily understandable methodology. Linnhoff et al. (1982) first developed the Heat Recovery Pinch Analysis in solving the Heat Integration problem. Tan et al. (2016) extended the method to select the optimal industrial risks and pollution reduction measures based on available budgets. Klemeš et al. (2018) had conducted a comprehensive overview of various extensions of Pinch Analysis, including water integration, regional resources planning, power system planning and hydrogen network synthesis. The capability of Pinch Analysis to target the resources and identify bottlenecks through visualisation provides added merits for its applicability.

CHAPTER 3 EXTENSION OF PINCH ANALYSIS TOOLS IN RESOURCES TARGETING FOR MULTIPLE CONSTRAINTS RESOURCE CONSERVATION NETWORK PROBLEM

This chapter presents an analysis for extension of the Pinch-based framework in material resources targeting in the domain of multiple qualities Mass Integration problem, more specifically a resource conservation network synthesis. Section 3.1 presents a problem analysis of the problem analysis and derivation of the insights (i.e. source arrangement sequence)- see the published paper by the same authors (Chin et al., 2021c). Section 3.2 explains the optimal recycling strategy for the sources in different scenarios (conflicting or non-conflicting sources. Section 3.3 explains the Pinch-based targeting and network synthesis framework using Composite Curves) - see the published paper in (Chin et al., 2021c), and Section 3.4 explains the Cascade Table representation of the multiple qualities problem (Chin et al., 2021a).

3.1 Problem analysis

The typical source-sink allocation model of the water network presented in Figure 3-1 gives rise to four governing equations – Eqs (3-1)-(3-4). The problem maps to an optimisation formulation. Its objective function is expressed in Eq (3-1), which stipulates the minimisation of the total required freshwater, which is the freshwater target.

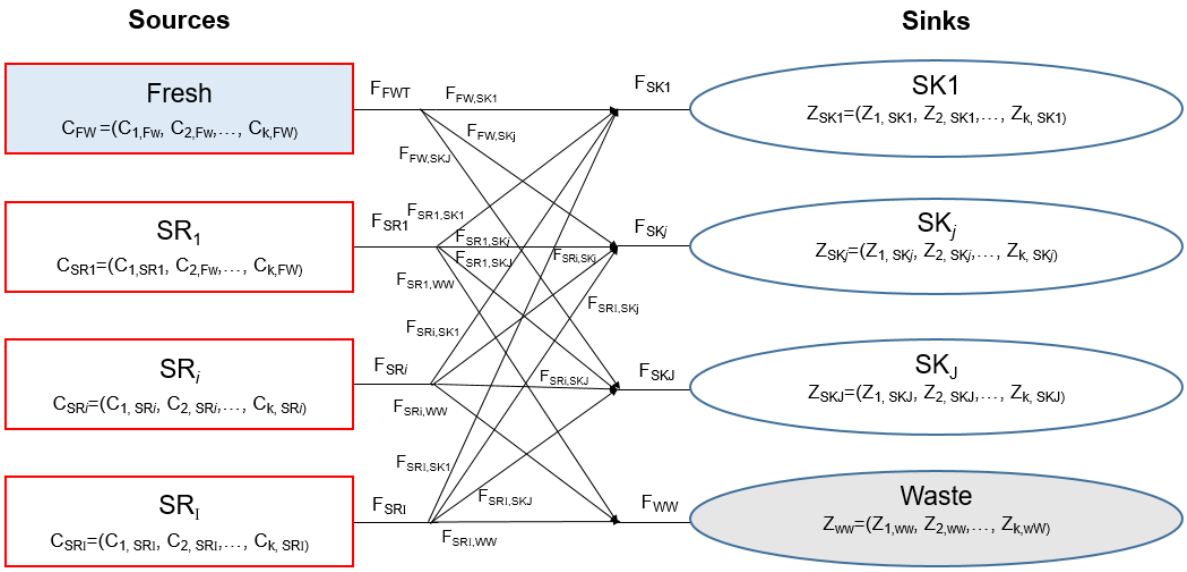

Figure 3-1: Source-to-sink allocation model demonstration

Eqs (3-2) and (3-3) express the mass balances for sources and sinks, while Eq (3-4) represent the contaminant constraints for individual sinks. Note that as proven by El-Halwagi et al. (2003), the composition of the sink should represent the maximum contaminant concentration to minimise the

use of a fresh resource. These equations are crucial for understanding the model characteristics to derive the proper procedures for obtaining the optimal freshwater target. The main characteristics are explained in sections 3.1.1 to 3.1.2.

$$Min\ F_{FWT} = \sum_j F_{Fw,SKj} \tag{3-1}$$

$$F_{SRi} = \sum_j F_{SRi,SKj} + F_{SRi,WW} \quad \forall \text{ i} \tag{3-2}$$

$$F_{SKj} = \sum_i F_{SRi,SKj} + F_{Fw,SKj} \quad \forall \text{ j} \tag{3-3}$$

$$\sum_i F_{SRi,SKj} C_{k,SRi} + F_{Fw,SKj} C_{k,Fw} \leq F_{SKj} Z_{k,SKj} \quad \forall \text{ j } \forall \text{ k} \tag{3-4}$$

where F_{FWT} represents the total freshwater flowrate, $F_{Fw,SKj}$ is freshwater to sink 'j' flowrate, F_{SRi} is source 'i' flowrate, $F_{SRi,SKj}$ is source 'i' to sink 'j' flowrate, $F_{SRi,\,WW}$ is source 'i' to waste flowrate, F_{SKj} is the sink 'j' flowrate, $C_{k,\,SRi}$ is the concentration of contaminant 'k' in source 'i', $C_{k,Fw}$ is the concentration of contaminant 'k' in freshwater, and $Z_{k,SKj}$ is the concentration of contaminant 'k' in sink 'j'.

The mass-based Pinch Analysis (PA) relies on the ranking or prioritisation of sources/sinks to determine the fresh resource target. The sinks with lower concentrations are prioritised because they are harder to be fulfilled, and they should be fulfilled first with better quality/lower concentration sources. This follows the traditional Process Integration principle to resolve the most constrained part of the problem first. For multi-contaminant problems, the sources and sinks are not constrained by a single contaminant anymore. Each sink is controlled by the most limiting contaminants. The identification of the limiting contaminant thus plays an important role in determining the source prioritisation pattern. The following sub-sections are devoted to utilising Eqs (3-1)-(3-4) for understanding the multi-contaminant problem and deriving certain heuristics for fresh resource targeting purposes.

3.1.1 Identify the limiting contaminants for each source-sink pair

Limiting contaminants are those whose constraints the sink the most and determine the real freshwater flowrate required, based on the available sources. Let's consider two contaminants problems (contaminant 'k1' and 'k2') with one source (SR1) and one sink (SK1). Using Eq (3-3) and Eq (3-4), the mass balance for the sink and its contaminant constraints are:

$$F_{SK1} = F_{SR1,SK1} + F_{FW,SK1} \tag{3-5}$$

$$F_{Fw,SK1} C_{k1,Fw} + F_{SR1,SK1} C_{k1,SR1} \leq F_{SK1} Z_{k1,SK1} \quad \forall k \tag{3-6}$$

Eqs (3-5) and (3-6) can be rearranged to find the expression of the minimum freshwater target. To eliminate the unknown variables $F_{SR1,SK1}$, express $F_{SR1,SK1}$ in terms of F_{SK1} and F_{FW1} in Eq (3-5), and substitute into Eq (3-6) and move F_{FW1} to the left-hand side, the minimum freshwater requirement for both contaminants are formulated- see Eq (3-7).

$$F_{Fw,SK1} \geq \left(F_{SK1}\left[1-\left(\frac{Z_{k1,SK1}-C_{k1,FW}}{C_{k1,SR1}-C_{k1,FW}}\right)\right]\right) \quad , \text{ for Contaminant k1} \tag{3-7a}$$

$$F_{Fw,SK1} \geq \left(F_{SK1}\left[1-\left(\frac{Z_{k2,SK1}-C_{k2,FW}}{C_{k2,SR1}-C_{k2,FW}}\right)\right]\right) \quad \text{, for Contaminant k2} \tag{3-7b}$$

The freshwater requirement is equal to the maximum value among the requirements across all of the contaminants- expression (3-7c). The maximum value is used as one contaminant may require more dilution than another and becomes limiting. For example, if contaminant 'k1' requires 1,000 t/h of freshwater to dilute the sources to fulfil sink constraints, but contaminant 'k2' requires 2,000 t/h of freshwater to dilute, then the freshwater flowrate is 2,000 t/h of freshwater (maximum amount).

$$\begin{aligned} F_{Fw,SK1} &\geq \max_k\left(F_{SK1}\left[1-\left(\frac{Z_{k,SK1}-C_{k,FW}}{C_{k,SR1}-C_{k,FW}}\right)\right]\right) \\ &= F_{SK1}\left[1-\min_k\left(\frac{Z_{k,SK1}-C_{k,FW}}{C_{k,SR1}-C_{k,FW}}\right)\right] \\ &= F_{SK1}\left[1-\min_k\left(\frac{Z^*_{k,SK1}}{C^*_{k,SR1}}\right)\right] \end{aligned} \tag{3-7c}$$

Where $Z^*_{k,SKj}$ ($Z^*_{k,SKj} = Z_{k,SKj} - C_{k,FW}$) is the shifted sink concentration and $C^*_{k,SRi}$ ($C^*_{k,SRi} = C_{k,SRi} - C_{k,FW}$) is the shifted source concentration. The role of the shifting is to account for the freshwater source with certain contaminant content.

Based on expression (3-7c), the maximum value of the bracketed term represents the real minimum water target if only a single source is used. As the flowrate of sink SK1 (F_{SK1}) is a constant, the minimum value of the concentration ratio of the sink to the source corresponds to the maximum amount of the term, indicating more fresh resource is needed. This also means that if contaminant 'k' corresponds to the minimum value of the ratio, then the sink is limited by contaminant 'k'. The method agrees with the concentration potential concept proposed by Liu et al. (2009). This concentration ratio also means how much of SR1 can be used to fulfil one unit of SK1, as shown in expression (3-7d).

$$F_{SR1,SK1} = F_{SK1}\left[\min_{k}\left(\frac{Z_{k,SK1} - C_{k,FW}}{C_{k,SR1} - C_{k,FW}}\right)\right] \quad (3\text{-}7d)$$

The following steps can be performed to identify the limiting contaminants for a sink-source pair:

(a) For each contaminant 'k', subtract the concentration of the contaminants for all sinks ($Z_{k,SKj}$) and sources ($C_{k,SRi}$) with the contaminant concentration of the fresh external resources ($C_{k,FW}$). This yields both shifted sink concentration ($Z^*_{k,SKj}$,) and shifted source concentration ($C^*_{k,SRi}$).

(b) The ratio of the shifted sink concentration ($Z^*_{k,SKj}$,) to the shifted source concentration ($C^*_{k,SRi}$) can be computed for each source-sink pair.

(c) If contaminant 'k' corresponds to the minimum value of the ratio, then the sink is limited by contaminant 'k' for the specific source 'i'.

For a problem with 'k' contaminants with 'N' internal sources, the real freshwater target is shown in expression (3-8) – see derivation in Appendix A. To identify the preferred source ranking for the specific sink, the ratio of sink concentration to the source concentration play an important role. In expression (3-8), it is proposed that the maximum source concentration is used because it also shows exactly the prioritisation of sources if more than two sources are used. For example, if the coefficient of $F_{SR1,SK1}$ is more negative than $F_{SR2,SK1,}$ then SR1 should be prioritised.

$$\begin{aligned} F_{Fw,SK1} \geq \max_{k}\Bigg(& F_{SR1,SK1}\left[\frac{C_{k,SR1} - C_{k,FW}}{C_{k,SR\_\max} - C_{k,FW}} - 1\right] + \cdots \\ & + F_{SRN,SK1}\left[\frac{C_{k,SRN} - C_{k,FW}}{C_{k,SR\_\max} - C_{k,FW}} - 1\right] + F_{SK1}\left[1 \right. \\ & \left. - \left(\frac{Z_{k,SK1} - C_{k,FW}}{C_{k,SR\_\max} - C_{k,FW}}\right)\right]\Bigg) \end{aligned} \quad (3\text{-}8)$$

The proposed ratio ($Z^*_{k,sk}/C^*_{k,SR\_max}$) helps to identify the source prioritisation as this ratio constitutes the constant term in expression (3-8). If the ratio is minimum for contaminant 'k', then the constant term: $F_{SK1}\left[1 - \left(\frac{Z_{k,SK1} - C_{k,FW}}{C_{k,SR\_\max} - C_{k,FW}}\right)\right]$ has a maximum value which means the source allocation is more likely to follow the prioritisation sequence for contaminant 'k'. The optimal source allocation is done to minimise this term. However, this does not mean that the sink should follow exactly the source prioritisation sequence for contaminant 'k' because different sources are traded-off by other contaminants. The proposed concentration ratio is just to show which source prioritisation order is likely to be followed to achieve the minimum fresh resource target for the specific sink. Section 3.2 details the explanation of the source allocation characteristics for a multi-contaminant problem.

For a more general problem with more than one source, the following heuristics are presented to identify the most likely limiting contaminant for a sink but also to identify the assignment of the sinks to the proper cascade:

(a) The ratio of the shifted sink concentration to the shifted maximum of source concentration ($Z^*_{k,sk}/C^*_{k,sr\_max}$) for each contaminant 'k' are evaluated, where $Z^*_{k,SKj} = Z_{k,SKj} - C_{k,FW}$ and $C^*_{k,SR\_max} = C_{k,SR\_max} - C_{k,FW}$. The lower value of the ratio corresponds to tighter limitations of the contaminant on the current sink.

(b) If contaminant 'k' corresponds to the minimum value of the ratio, then the sink is limited by contaminant 'k' for the specific source 'i'. It is to be noted that the limiting contaminant identified here is the most likely limiting contaminant, but not all. This is because a sink can be limited by several contaminants.

3.2 Optimal recycle strategy for sources

The concentration ratio (Z*k,sk/C*k,SR_max) shows which contaminant's source prioritisation order is likely to be followed for the specific sink. However, the source prioritisation cannot be fully followed as other sources might trade-off other contaminants as well. The following sub-sections explain the source allocation characteristics for a multi-contaminant problem and infer the source allocation steps to be followed to achieve the minimum freshwater target.

3.2.1 Conflicting sources

The sources that are conflicting are defined as sources that have different sequences when considering different contaminants. By referring to the numerical example in Table 1, if only contaminant 'A' is considered, SR1 is cleaner than SR2, while for contaminant 'B', SR2 is cleaner than SR1. The prioritisation sequence of the sources is not obvious in this case. Considering the problem as a whole requires computing the ratio ($Z^*_{k,sk}/C^*_{k,sr\_max}$). For the example in Table 4, for sink SK1, it is obtained $Z_{A,SK1}/C_{A,SRmax} = 100/500=0.2$ and $Z_{B,SK1}/C_{B,SRmax} = 100/200=0.5$. Since $Z_{A,SK1}/C_{A,SRmax} < Z_{B,SK1}/C_{B,SRmax}$, the source prioritisation sequence based on contaminant 'A' should be used because contaminant A is the limiting contaminant to fulfil SK1. This means that SR2 is preferred before SR1.

Table 3-1: Example: two-contaminant problem with both examples of conflicting and non-conflicting sources

SR	F_{sr} (t/h)	$C_{A,sr}$ (ppm)		$C_{B,sr}$ (ppm)	
		Example a: Conflicting	Example b: Non-conflicting	Example a: Conflicting	Example b: Non-conflicting: Non-conflicting
1	23	500	500	30	500
2	123	50	50	200	200
Fw	-	0	0	0	0
SK	F_{sk} (t/h)	$Z_{A,sk}$ (ppm)		$Z_{B,sk}$ (ppm)	
1	50	100	100	100	100

Reusing Eqs (3-8) by expressing $F_{SR1,SK1}$ as the variable, the minimum freshwater targets for both contaminants 'A' and 'B' are shown in Eqs (3-9a-b). These inequalities are plotted in Figure 3-2.

$$F_{Fw} \geq \left(F_{SR1,SK1}\left[\frac{500}{50}-1\right]+50\left[1-\left(\frac{100}{50}\right)\right]\right), \text{ for contaminant 'A'} \quad (3\text{-}9a)$$

$$F_{Fw} \geq \left(F_{SR1,SK1}\left[\frac{30}{200}-1\right]+50\left[1-\left(\frac{100}{200}\right)\right]\right), \text{ for contaminant 'B'} \quad (3\text{-}9b)$$

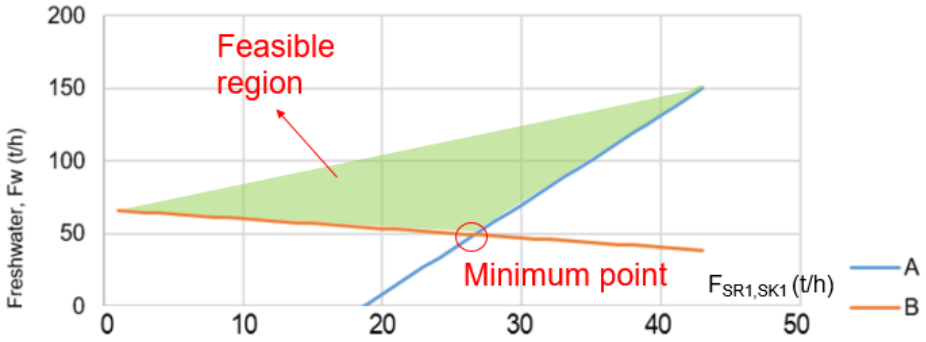

Figure 3-2: Relationship between freshwater requirement (Fw) vs flowrate of SR1 for numerical example 2, for conflicting SR1 and SR2.

Figure 3-2 shows the plot of the relationship between the freshwater target for SK1 and the flowrate of SR1 supplied to SK1, for both contaminants. Note that the flowrate of SR2 ($F_{SR2,SK1}$) is dependent on SR1 and $F_{w,}$ so its flowrate can be computed by performing mass balance around SK1 ($F_{SR2,SK1} = F_{SK1} - F_{FW,SK1} - F_{SR1,SK1}$). The shaded region represents the feasible region of the

freshwater requirement. By observing Figure 3-2, it is apparent that the minimum freshwater always falls into the boundaries of the feasible region, i.e. one of the impurity constraints would always be active. The interesting point is where both the boundary lines intercept, which represents both impurity constraints, are active. As SR1 and SR2 are conflicting sources in both contaminants' A' and 'B', the boundary lines are linear with the respective negative and positive gradients. Assuming no limitation on SR1 and SR2 flowrates, the minimum freshwater point is always at the point where all impurity constraints are active. If one of the sources have a limited flowrate, the minimum point cannot be achieved, then any points along the lowest boundary line are resorted to. In this example, since SR1 has only 23 t/h, all SR1 is used up first and then SR2.

3.2.2 Non-conflicting sources

The previous part explains how the sources with conflicting sequences should be allocated. Using the same example in Table 4, it is apparent that SR1 and SR2 are not conflicting anymore as $C_{A,SR1} > C_{A,SR2,}$ and $C_{B,SR1} > C_{B,SR2.}$ Similarly, the minimum boundary lines for the freshwater target showing the relationship between freshwater and SR1 flowrate are plotted, illustrated in Figure 3-3. The freshwater target of SK1 varies monotonically with the variation of the flowrate of SR1 supplied to SK1. As a result, the freshwater target is minimal with the minimum use of SR1.

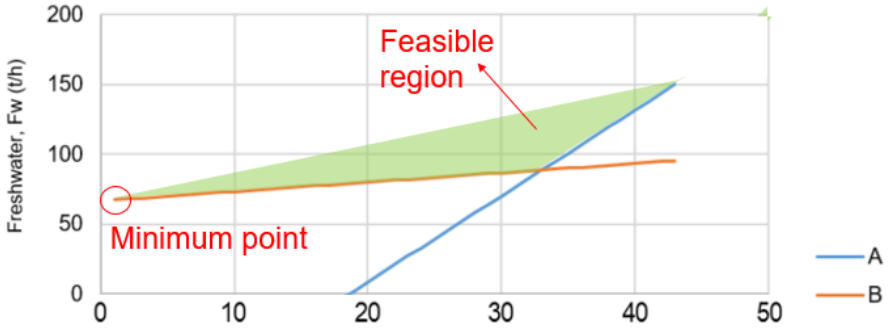

Figure 3-3: Relationship between freshwater requirement (Fw) vs flowrate of SR1, for non-conflicting SR1 and SR2.

In this case, the intersection point between the boundary lines is no longer the minimum point because both lines are with a positive gradient. To reduce the freshwater target, the usage of SR1 should be minimised, which means SR2 should be maximised. SR2 should be fully used up first before SR1 is used. The source prioritisation becomes similar to the single contaminant case. As $C_{A,SR1} > C_{A,SR2,}$ and $C_{B,SR1} > C_{B,SR2}$, the source prioritisation sequence for both contaminants are SR2->SR1. The following inference can be made: for 'k' contaminants problem, if the source prioritisation sequence is consistent among all the 'k' contaminants, then the sources with lower concentrations should be used up first.

3.3 Pinch-based graphical interface for resource targeting

3.3.1 Polygons rule for sources mixing

Yang et al. (2014) presented a triangle rule in the graphical method for hydrogen Pinch Analysis, accounting for the purification process. In their work, they proposed the purification of the hydrogen feed stream into purified products and tail gas. The mass of the contaminants is conserved around the purification unit. Figure 3-4a shows the presented 'polygon' (triangle) rule. The feed stream that has a certain flowrate and quality load is plotted on a load vs flowrate diagram. The horizontal distance of line AC represents the flowrate of the feed stream, while the vertical distance is the contaminant load of the stream. The gradient of the line represents the contaminant concentration of the feed stream. The feed stream is balanced by lines 'AB' and 'BC', which represent the load and flowrate contributions of the purified product and the tail gas. This concept can be applied to streams mixing as well, but the process direction is reverse. A dirtier stream (line 'AB') can be mixed with a cleaner stream (line 'BC') to form a stream 'AC'. It doesn't matter which path to go from point 'A' to point 'C', as long as the final point 'C' is reached. The direction of the process has to be denoted separately, as the diagram represents only the balance.

The 'triangle' rule can be generalised into a 'Polygon' rule, as presented in Figure 3-4b. The feed stream AC can be balanced by more than two streams such as AB, BD, DE and EC.

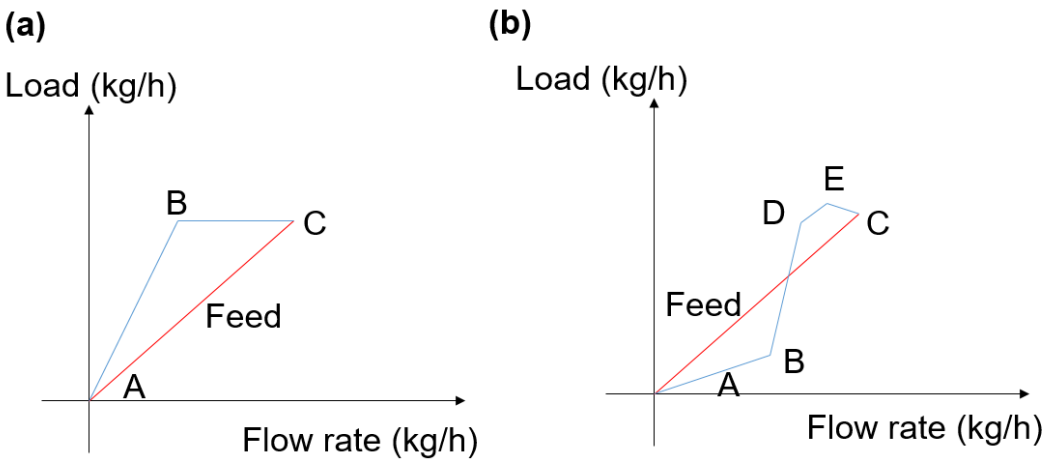

Figure 3-4: Demonstration of 'polygon' rule, adapted from Yang et al. (2014)

The concept of the 'Polygon' rule can be applied to the streams mixing as well. Considering a mass balance of sinks that are fulfilled by various sources (for a single contaminant)- Eqs(3-3) and (3-4)

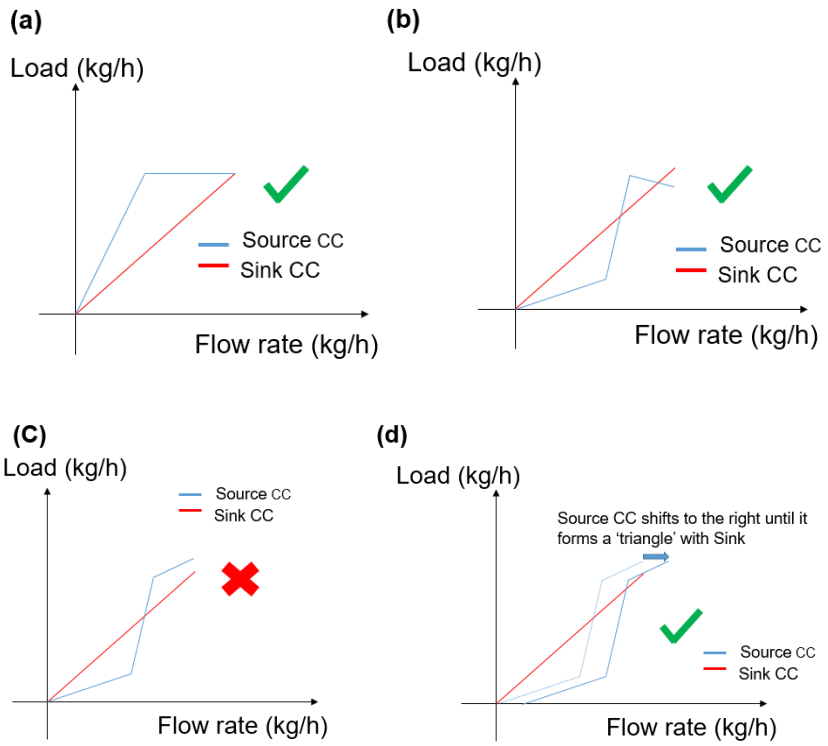

Figure 3-5: Different sources of mixing scenarios

Figures 3-5a-b show examples of feasible source mixing. As long as the final cumulative load of the source Composite Curve (CC) touches or is below the endpoint (final cumulative load) of the sink CC, the maximum quality limit of the sink is still fulfilled (Eq 2). This is in-line with the concept of stream mixing. A dirtier source (higher gradient line) can be mixed with a cleaner source (lower gradient line) to fulfil the concentration or quality limit of the sink demand- Figure 3-5a. The cumulative load of sources is located below a load of sink CC means that the total allocated source streams have a lower concentration than the maximum limit of the sink's concentration- Figure 3-5b. Figure 3-5c is the example of infeasible source mixing as the cumulative load of the sources is above the sink's requirement. In this scenario, more freshwater is needed by shifting the source CC to the right.

3.3.2 Targeting framework for each sink and contaminant cascades

An efficient graphical targeting or design method for the single contaminant material recycle/reuse problem is the cumulative load vs cumulative flowrate diagram [9]. This strategy is equivalent to sequential, fulfilling each sink with internal resources, which are prioritised with contaminant concentrations. Each segment of the line represents each sink/source, with a horizontal length of the line represents the flowrate and a vertical length represents the contaminant load. The figures are usually plotted by compositing each sink/source line based on the ascending order of the contaminants' concentration.

In the case of a single contaminant, the recycle strategy first starts with the cleanest (highest quality) sink with the use of the cleanest source. The source line is moved horizontally (pure fresh resource) until it touches the sink line, and the source is located below the sink line – see Figure 3-6. The overlapped flow rate represents how many sources can be used for the sink. The remaining flow of the sink can only be fulfilled by fresh resources. The remaining flowrate of the source is transferred to the next sink – Figure 3-6. For the third sink, it can be fully fulfilled by the mix of the remainder of the second source and third source, without the use of fresh resources – Figure 3-6. Adding together the fresh resource flow, Figure 3-6 shows the typical representation of the Composite Curves in the Load vs Flow diagram. The total freshwater target is so ($F_1 + F_2$), which is the fresh resource requirement.

In fact, the water network design with source allocation can already be determined from Figures 3-6a-c. For example, Figure 3-6a shows only part of source 1 can be allocated to sink 1. Figure 3-6b shows the allocation of sources 1 and 2 to sink 2. The benefits of determining the freshwater target for each sink sequentially allows for that sink the source allocation to be determined simultaneously.

If a similar strategy is applied in the multi-contaminant problem, a slight adjustment on the Source CC has to be done. For illustrative purposes, Figure 3-7 shows that for the first sink, the limit for contaminant A is reached. There is still room for contaminant B for the first sink as its limit is

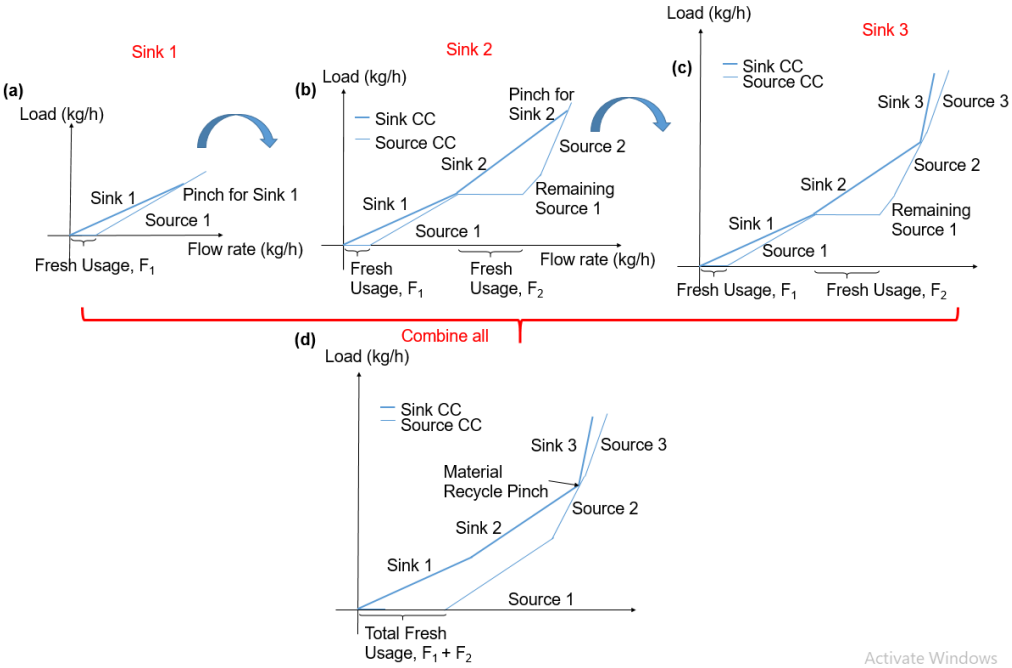

Figure 3-6: Sequential source allocation with Pinch-based methodology with graphical representation, adapted from El-Halwagi et al. (2003)

not reached (a triangle is formed). This also means the limiting contaminant for the first sink is A (which is dependent on the source sequence). Moving on to the second sink, the starting point for the source CC (for contaminant B) after the first sink should be shifted vertically upwards to account for the unfulfilled concentration limit for the first sink – Figure 3-7b. Note that the 'triangle' formed in Figure 3-7a around Sink CC (contaminant B) is still feasible, as explained in section 2.1. For the second sink, the limit for contaminant B is reached, so the source CC for contaminant A after the second sink should be shifted vertically downwards when the remaining is transferred to the third sink – Figure 3-7c.

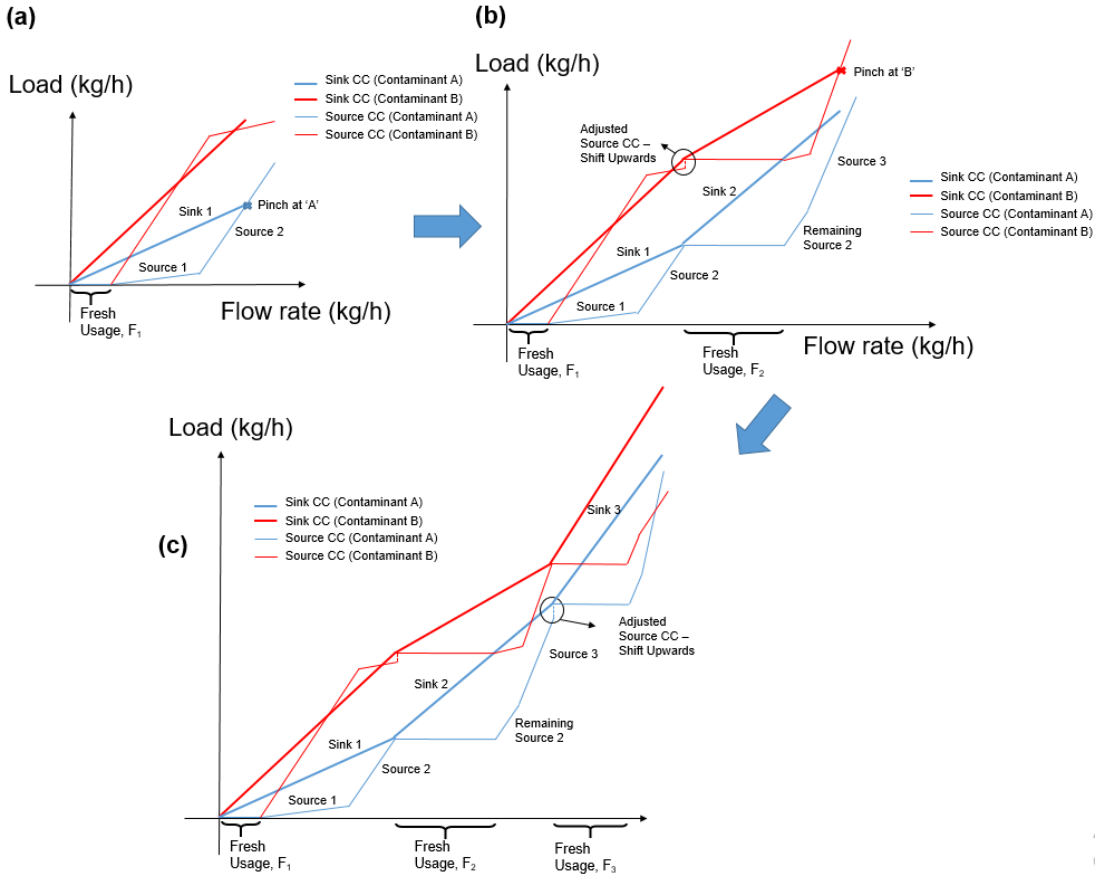

Figure 3-7: Sequential source allocation with a developed methodology for multiple contaminants

However, the optimal source allocation strategy in a multi-contaminant water network is not straightforward. The prioritisation of the cleaner source is no longer applicable for the multi-contaminant case as the ranking of the sources is not obvious. This is demonstrated in Figure 3-8.

Figure 3-8a shows the demonstration plot of the sink and source CC for a single sink and two sources. Source 1 and Source 2 are conflicting. The sources are arranged based on the ascending order of contaminant 'A' concentration. In this example, the Pinch point occurs at the contaminant 'B' if Source 1 is prioritised over Source 2, while for contaminant 'A' Pinch is not reached. However,

there is room for freshwater reduction by reducing the Source 1 flowrate allocated to sink 1. This is because Source 1 has a higher concentration in Contaminant B than Source 2. Reducing the use of Source 1 helps to reduce the load for Contaminant B. As presented in the previous section for the case of conflicting sources, the optimal freshwater requirement occurs when all contaminant limits are reached. To achieve this, Source 1 can be reduced until the distances from the endpoint of both sink CCs to both of the source CCs are identical (see Figure 3-8b), i.e. Pinch Points occur for all the contaminants. The source CCs can be shifted to the left until both Pinch points are reached (Figure 3-8c). This is the optimal source allocation strategy for the specific sink. Similar steps can be repeated for the subsequent sinks.

The determination of the sources flowrates by manually adjusting the curves can be time-consuming, especially when there are plenty of sources available. This issue can be solved by using Eqs(3-10-11). To determine the reduced flowrates of the sources, one can set the following condition from Eq(3-10):

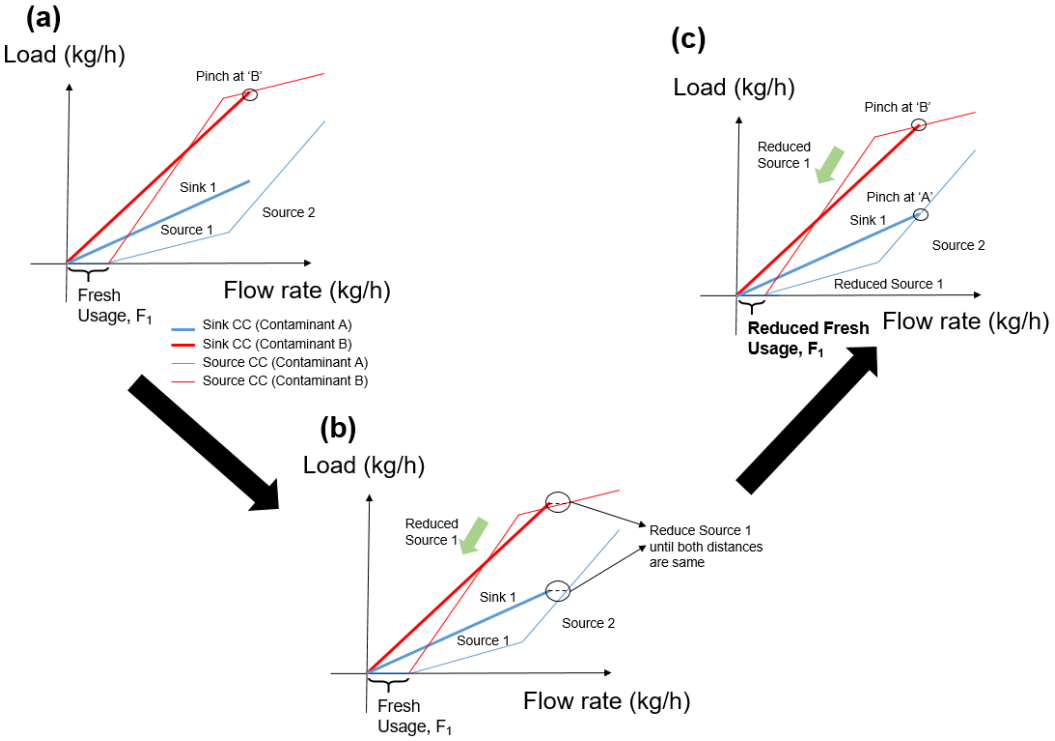

Figure 3-8: Source allocation strategy for a single sink

$$F_{Fw,SK1}\ for\ contaminant\ A = F_{Fw,SK1}\ for\ contaminant\ B \tag{3-10}$$

$$F_{Fw,SK1} = \sum_{i=1}^{I} F_{SRi,SKj}\left[\frac{(C_{k,SRi} - C_{k,Fw})}{(C_{k,SRi_s} - C_{k,Fw})} - 1\right] + F_{SKj}\left[1 - \frac{(Z_{k,SKj} - C_{k,Fw})}{(C_{k,SRi_s} - C_{k,Fw})}\right] \tag{3-11}$$

Where C_{k,SR_ref} is the concentration of a reference source. In the example above, the reference source should be source 2 when the flowrate for source 1 is to be determined. Otherwise, if the flowrate of source 2 should be determined, then source 1 should be used as the reference source.

The freshwater reduction by reducing the flowrates of the sources is only possible when the Pinch Point occurs at the non-limiting contaminants. For example, if the Pinch Point occurs at the contaminant 'A' after shifting the source CC in Figure 3-7a, the freshwater requirement is already at the optimum level. There is no room for further reduction. The ratio with the concentration of sink to the maximum concentration of source can be used as the indicator to determine the limiting contaminant for the specific sink.

For a more general 'k' contaminants case and many sources available, the source allocation is dependent on the number of contaminants. The following step is presented to identify the optimal source flowrates for a specific sink:

(i) For a specific sink, check whether the Pinch Point occurs at the CCs that correspond to the main limiting contaminant. The main limiting contaminant is the one producing the smallest concentration ratio of- see Eq (3-9). If the Pinch is at the limiting contaminant, go to step (vi), else continue to step (ii).

(ii) For a sink, if there are 'k' contaminants, then pair with 'k' sources that are arranged in the order based on the contaminant cascade that the sink is assigned to.

- For example, if SK1 is assigned to contaminant cascade 'A', then pair with the first 'k' sources that are arranged with ascending order of concentration 'A'. This is explained in the next point.

(iii) Set $F_{Fw,SK1}$ for contaminant 'k1' = $F_{Fw,SK1}$ for contaminant 'k2' for each binary contaminant pair minus 1 (${}^{k}C_{2} - 1$). Determine the flowrates of the first 'k' sources using Eq(3-9) by using one of the sources as a reference source.

- For example, if there are 3 contaminants, i.e. k={A, B, C}, then set a condition $F_{Fw,SK1} = F_{Fw,SK1}$ for each binary pair, i.e. A-C, A-B, B-C. By setting $F_{Fw,SK1}$ for A = $F_{Fw,SK1}$ for B and $F_{Fw,SK1}$ for B = $F_{Fw,SK1}$ for C, this means the freshwater requirement for A is set to equal to for C as well. Setting the freshwater conditions is sufficient for 2 of the pairs (${}^{3}C_{2} - 1$).
- For 3 contaminants case, solve the system of equations with Eq(3-11) for both A-B and B-C pairs. If SR1, SR2 and SR3 are the first 3 sources in the cascade, determine the flowrate of SR1 and SR2 by setting SR3 as a reference source. This is to achieve the limits for 3 contaminants. As there are 3 equations (1 sink mass balance equation and 2 Eqs(3-11) for two of the contaminant pairs) for 3 contaminants, to ensure zero degrees of freedom, 3 sources are needed.

- Repeat this by setting each source as the reference source until all the flowrates have been identified.

(iv) If one of the source flowrates is determined as negative, this means the scenario where all contaminants have Pinch Points does not exist. If this is the case, repeat the procedures (i) to (iv) for 'k-1' contaminants. If not, go to step (vi)

(v) Check if the sources flowrates are sufficient for the sink. If one of the sources has insufficient flowrates, the source should be fully utilised. The procedures (i) to (iv) are repeated with the next 'k' sources.

- For example, for the 3 contaminants example, if the optimal flowrates of SR1 exceed the available SR1, fully use up SR1 for the sink. Repeat similar procedures using the next three sources, i.e. SR2, SR3 and SR4.

(vi) Repeat procedures (i) to (v) until all sinks are fulfilled

3.3.3 Overall Targeting framework

Based on these observations, the following overall design procedures using graphical methodology with Pinch concept are presented in Figure 3-9:

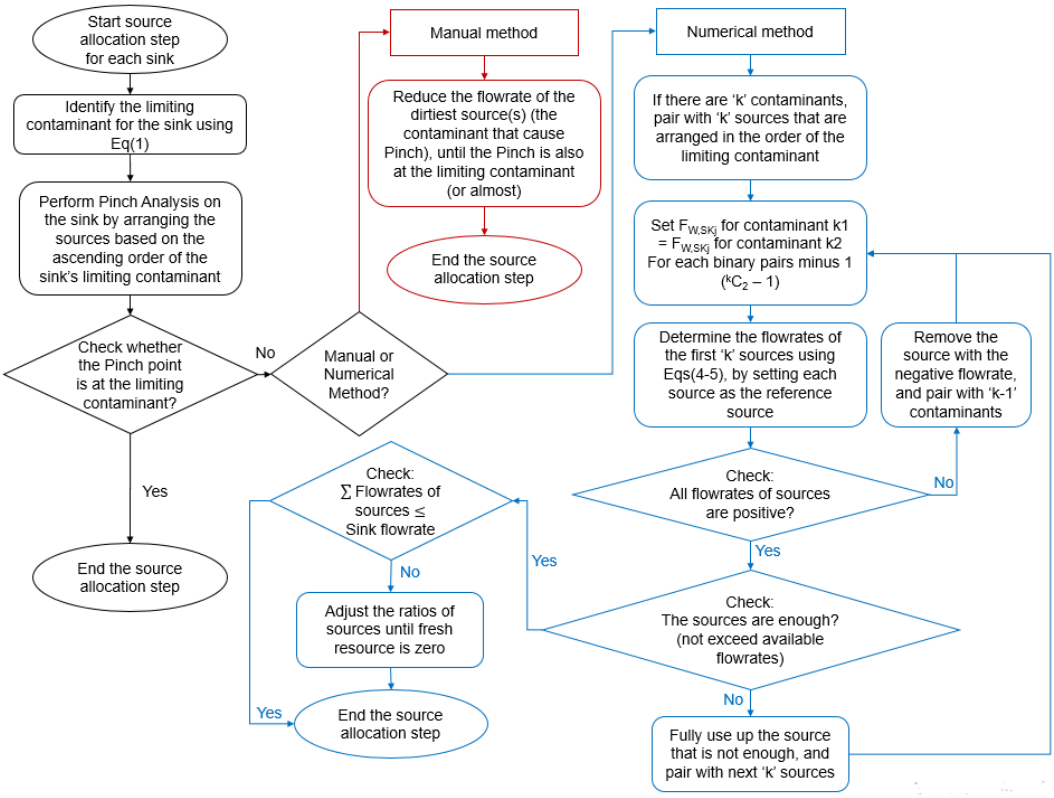

Figure 3-9: Proposed source allocation heuristics for a specific sink, adapted from Chin et al. (2021a).

3.3.4 Case Study and discussion of results

The proposed methodology is demonstrated in several case studies. The first case study contains four sources/sinks with two contaminants as the constraints from Teles et al. (2008). For this case, several scenarios are studies by changing the source sequence through adjusting their concentrations. The scenario where there is a sink that should be Above the Pinch is also explored. For other case studies demonstrations, the readers could refer to the paper Chin et al. (2021c)

For this study, the concentration or flowrate of sources is adjusted to study different scenarios with the proposed methodology.

3.3.4.1 Scenario 1: Complete conflicting sources

The concentrations of the sources are shuffled so that the sources are complete conflicting, In this scenario, the source arrangement for contaminant 'B' is manipulated so that it is opposite with the sequence for contaminant 'A'. Table 3-2 shows the source and sink data:

Table 3-2: Data for case study 1: scenario 1

SR	**F_{sr} (kg/h)**	**$C_{A,SR}$ (ppm)**	**$C_{B,SR}$ (ppm)**	**SK**	F_{sk} (kg/h)	$Z_{A,Sk}$ (ppm)	$Z_{B,SK}$ (ppm)
1	23	50	300	1	23	20	60
2	47	100	120	2	47	50	20
3	123	150	100	3	123	100	150
4	60	250	80	4	70	200	80
Fw	-	0	0				

The concentration ratio for each contaminant 'k' ($Z_{k,sk}/C_{k,sr\_max}$) is first determined for all the sinks. The results are presented in Table 3-3. Judging based on the smallest value of the ratio, SK1 and SK3 should be assigned to cascade 'A' as they are limited by contaminant 'A'. The SK2 and SK4 are assigned to cascade 'B' for the identical reason.

The next step is to check whether the sinks are located Below or Above Pinch regions. Based on the results from Table 3-3, it can be deduced that all sinks are impossible to be fulfilled based solely on the sources. This also can be checked by computing the concentration ratios for each sink/source pair- see Table 3-4. As each ratio is less than or equal to 1, this suggests that the sinks requirements are higher quality than the sources. The sinks cannot be fully satisfied with just the available sources without the fresh resources.

Table 3-3: Concentration ratio results, using maximum source concentration as denominators for Case study 1 scenario 1

	$Z_{A,SK}/C_{A,SRmax}$ $C_{A,SRmax}$ = 250	$Z_{B,SK}/C_{B,SRmax}$ $C_{B,SRmax}$ = 300	Minimum ratio	Cascade
SK1	**0.08**	0.20	0.08	A
SK2	0.20	**0.07**	0.07	B
SK3	**0.40**	0.50	0.40	A
SK4	0.8	**0.27**	0.27	B

Table 3-4: Concentration ratios for each sink-to-source pair. The highlighted in bold represent the smallest values

	Contaminant A (Z_{sk}/C_{SR})					Contaminant B (Z_{sk}/C_{SR})			
	SK1	SK2	SK3	SK4		SK1	SK2	SK3	SK4
SR1	0.40	1	2	4	SR1	**0.20**	**0.067**	**0.50**	**0.27**
SR2	**0.20**	0.50	**1**	2	SR2	0.50	**0.17**	1.25	**0.67**
SR3	**0.13**	0.33	**0.67**	1.33	SR3	0.60	**0.20**	1.50	**0.80**
SR4	**0.08**	**0.20**	**0.40**	**0.80**	SR4	0.80	0.25	1.875	1.00

After the sink classification is done, Pinch Analysis can be initiated for each sink. As the total flowrates of sinks in contaminant cascade 'A' (SK1+SK3) has the greatest flowrate, they should be 'Pinched' first as they require more resources. The design methodology starts with SK1 first as it has a lower concentration. The source ranking order based on contaminant 'A' is SR1->SR2->SR3->SR4. Figure 7a first presents the source and sink CCs specifically for SK1. Notice that the Pinch occurs at contaminant 'B', with required freshwater as 18.4 t/h.

According to the proposed source allocation methodology in Section 3.3.4, since the Pinch does not occur at the sink's main limiting contaminant 'A' - step (i), as well as SR1 and SR2 are conflicting sources, there is still room for freshwater reduction. SR1 allocated to SK1 can be reduced. Using the graphical strategy presented in Section 3.3.2, SR1 can be reduced until the distance of sink CC to source CC for both contaminants are identical. The source CC is then shifted to the left. Figure 7b shows the source and sink CCs with reduced SR1. Otherwise, using the

procedure from Section 3.3.3, step (ii) from the source allocation step can be performed. Since this involves two contaminants, pair with two sources from the arranged source, i.e. SR1 and SR2. In step (iii), use Eqs(3-10 to 11) to determine the flowrates of SR2 and SR1 to be allocated to SK1. As this is only two contaminants, setting the freshwater requirement- Eq(3-10) for A to be equal to B is enough. In step (iv), the flowrates of SR2 and SR1 that can be allocated to SK1 needs to be checked. The determined flowrates are found as: SR1=3.45 t/h and SR2=2.875 t/h. As both flowrates are not negative and are less than the available flowrates, the step for SK1 is completed. The procedure is then repeated for SK3 – step (vi). It can be noticed that the freshwater requirement is reduced to 16.675 t/h, with only 3.45 t/h of SR1 to be allocated to SK1- see Figures 3-10.

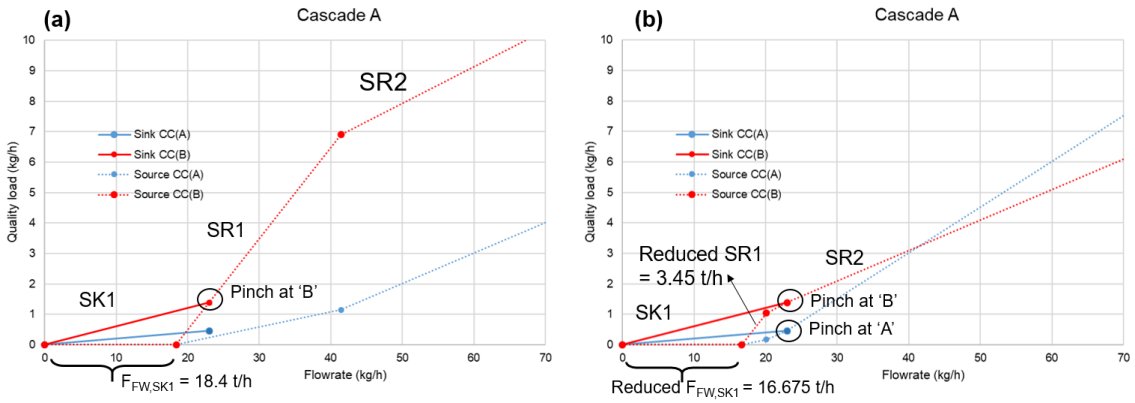

Figure 3-10: Source and sink CC for SK1 (a) Follow the source ranking order (b) Further freshwater reduction

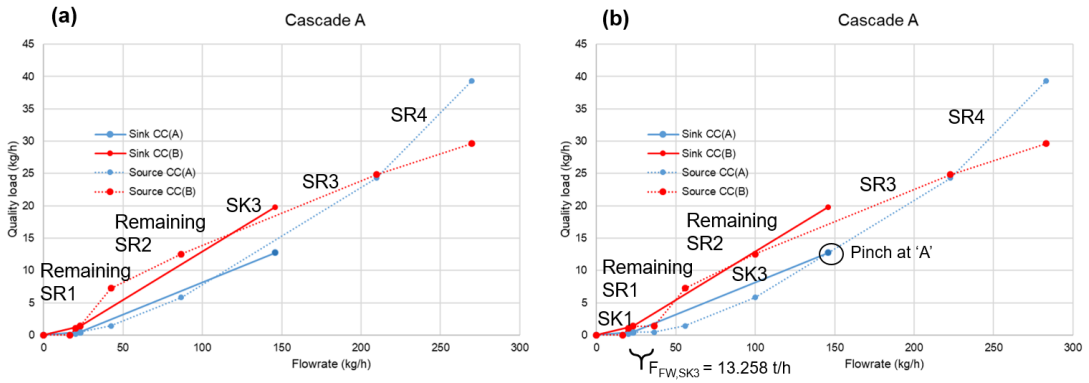

Figure 3-11: Source and sink CC for SK1+SK3 in contaminant cascade 'A' (a) Before shifting source CC for SK3 (b) After shifting source CC for SK3

The design methodology is repeated for SK3, and the Composite Curves are stacked above SK1. Figure 3-11a first presents the source and sink CCs before identifying the freshwater target for SK3. It is worth to be noted that contaminant 'B' is not constraining for SK3. After shifting the source CC to the right, the Pinch occurs at the sink's main limiting contaminant 'A', see Figure 3-11b. As the Pinch occurs at the main limiting contaminant, there is no room to further reduce the

freshwater target. In this case, the total freshwater target for both SK1 and SK3 is 16.675 + 13.258 = 29.933 t/h.

The step is repeated again for the sinks that are in contaminant cascade 'B'. The source ranking order based on contaminant 'B' is SR4->SR3->SR2->SR1. The design first starts with SK2. If the sources are allocated based solely on the prioritisation of SR4, the Pinch occurs at contaminant 'A' (see Figure 3-12a). This is not optimal as SR3 can still be allocated due to the limit for contaminant 'B' is not reached. The flowrate of SR4 is then reduced, and SR3 is used until both contaminants have Pinches (see Figure 3-12b). An identical scenario is observed for SK4 (Figures 3-12c and d). Notice that in Figure 3-12d, a triangle is formed around the source and sink CC for contaminant 'A'. This is feasible as the final load of contaminant 'A' for SK4 is still satisfied.

The Composite Curves show exactly the sources to be allocated for each sink. This is because the freshwater target and the Pinch are determined sequentially for each sink. By doing this, the simultaneous target and source allocation for each sink can be obtained. The allocation of sources is directly connected to the network design as well. The detailed illustration of the source allocation to the sinks is shown in Figure 3-13. More applications of case study can be found in Chin et al. (2021f).

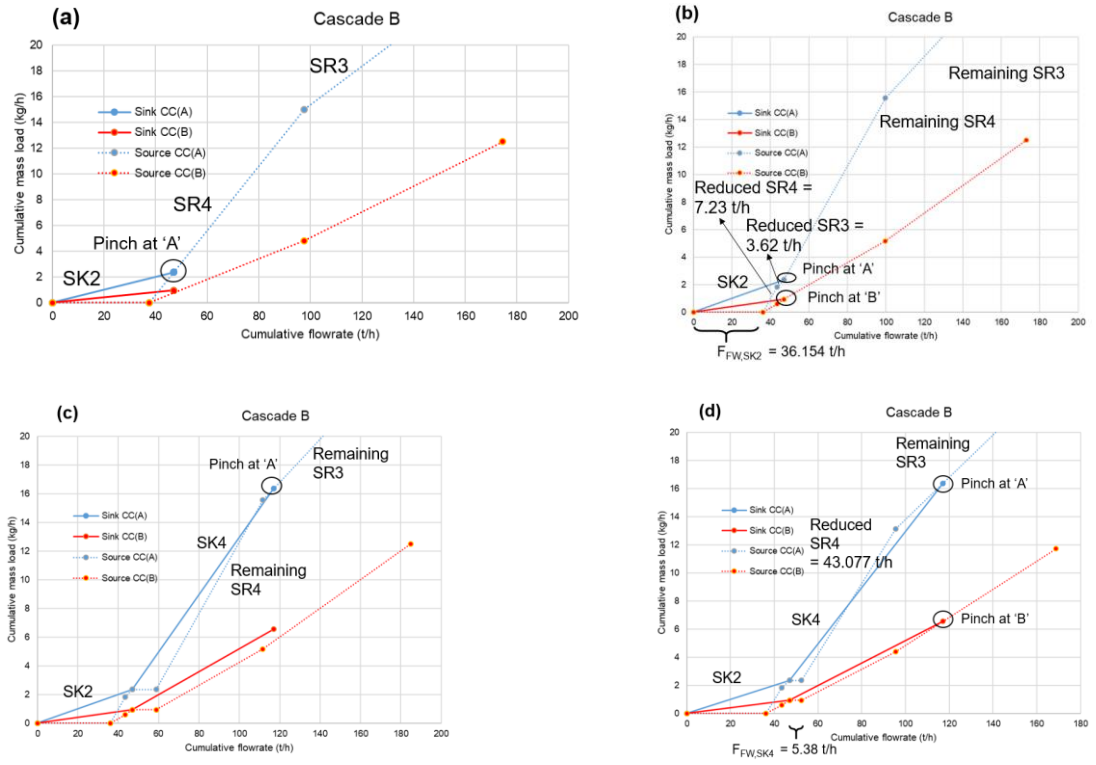

Figure 3-12: Source and sink CC for scenario 1 case study 1 (a) SK2 (b) SK2 with the reduced freshwater target (c)SK4 (d) SK4 with reduced freshwater target

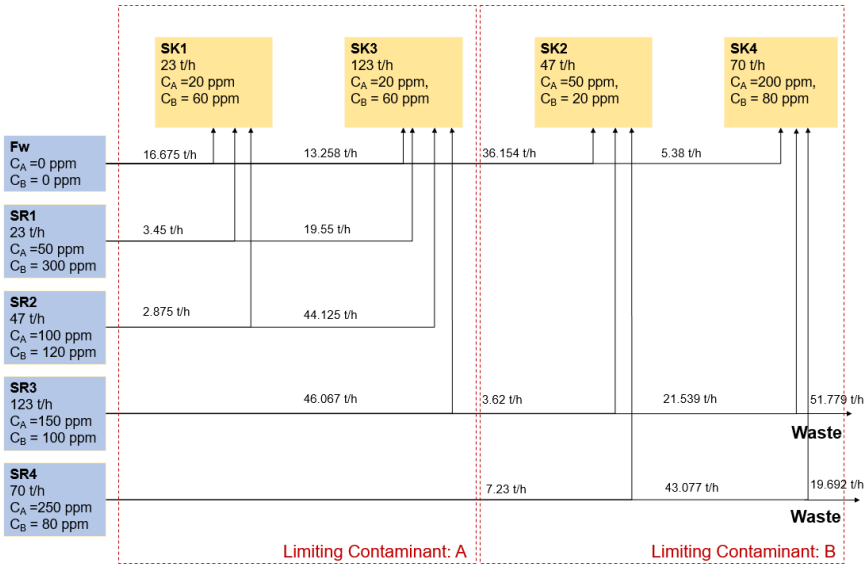

Figure 3-13: Detailed network design for case study 1

3.3.5 Conclusions

This work has formulated a Pinch-Based methodology for targeting and synthesis of material recycle-reuse networks with multiple contaminants, on the example of water networks. It involves the methods to determine the sink classification to proper contaminant cascade and to Below/Above Pinch. This step determines the main source prioritisation for each sink which is based on the limiting contaminant of the sinks. The procedure to determine the reduced flowrate of the sources to satisfy the contaminant constraints is proposed as well. The cascade containing the largest total flowrates of sinks should be 'Pinched' first. In this work, it is proposed that the Pinch Analysis should be conducted for each sink sequentially. If the Pinch Point occurs at the non-limiting contaminant of the sink, a source reduction can be performed to further reduce the freshwater target for that sink. As the method involves targeting the freshwater for each sink, this enables the exact source allocation to be directly identified.

Note that the freshwater requirements determined in this work represent the resource requirement ignoring the interaction between the sinks and sources. The data used in this work are the maximum flowrates and concentrations of the sources and sinks. Certain sink's maximum concentration limit might not be reached, and this could affect the concentration of the sources from the same operation of the sink. If fixed contaminant load is assumed for each unit operation, the concentration of the source might be reduced as well, and the overall fresh requirement can be reduced. For fixed load operation, the flowrates of the sink and source can be reduced as long as the fixed mass load is guaranteed. This could lead to a reduction in the fresh resource.

3.4 Enhanced Cascade Table Analysis on multiple constraints resources targeting

3.4.1 Introduction

The objective of this part is to extend the Cascade Table Analysis for simultaneous targeting and design of material conservation networks with multiple constraints, demonstrated with a multi-contaminant water recycling network. The graphical plots using the load vs flowrate diagram are added for visualisation of the numerical approach. Both representations can show the Pinch Point(s) for different contaminants, maximum mass recovery, source allocation and minimum external resource targets for individual sinks simultaneously. The results can then be directly translated into a source allocation network with the optimal design without the need to perform calculations to check for mass transfer feasibility.

3.4.2 Methodology

This section explains the method of using Cascade Table Analysis, based on Manan et al. (2004), to target and design for water recycle/reuse network. The method is first demonstrated using the single contaminant problem, and it is shown how it could be used for network design as well. The extension of the Cascade Table to multiple contaminants is then explained.

3.4.2.1 Cascade table analysis-targeting for single contaminant problem

For a single contaminant problem, the Water Cascade Analysis (WCA) developed by Manan et al. (2004) is aimed to determine the minimum freshwater target for a process based on the possibility of using the available water sources. The table is used to determine the net water source or water demand at each purity level. To demonstrate the construction of the Water Cascade Table, the case study from Manan et al. (2004) is used, with data represented in Table 3-5.

Table 3-5: Water source and sink data for example 1

SR	**F_{sr} (kg/h)**	**$C_{A,SR}$ (ppm)**	**SK**	**F_{sk} (kg/h)**	**$Z_{A,Sk}$ (ppm)**
1	20	100	1	20	0
2	100	100	2	100	50
3	40	800	3	40	50
4	10	800	4	10	400
Fw	TBC	0			

Table 3-6:Generic Cascade Table representation for a single contaminant

n	**Conc., C_n (ppm)**	**$\Delta C_n = C_n - C_{n-1}$ (ppm)**	**$\sum_i F_{SRi}$ (kg/h)**	**$\sum_j F_{SKj}$ (kg/h)**	**$F_{net,n} = \sum_i F_{SRi,Cn} - \sum_j F_{SKj,Cn}$ (kg/h)**	**$F_{cum,n} = F_{cum,n-1} + F_{net,n}$ (kg/h)**	**$\Delta load_n = F_{cum,n} * \Delta C_n$ (kg/h)**	**$CumLoad_n = CumLoad_{n-1} + \Delta load_{n-1}$ (kg/h)**	**$CumFresh_n = CumLoad_n / (C_n - C_{FW})$ (kg/h)**
						$F_{cum,0} = \max \lvert CumFresh_n \rvert$			
1	C_1		$\sum_i F_{SRi,C1}$	$\sum_j F_{SKj,C1}$	$F_{net,1}$			0	0
		$\Delta C_1 = C_2 - C_1$				$F_{cum,1} = F_{cum,0} + F_{net,1}$	$\Delta load_1 = F_{cum,1} * \Delta C_1$		
2	C_2		$\sum_i F_{SRi,C2}$	$\sum_j F_{SKj,C2}$	$F_{net,2}$			$CumLoad_2$	$CumFresh_2$
		$\Delta C_2 = C_3 - C_2$				$F_{cum,2} = F_{cum,1} + F_{net,2}$	$\Delta load_2 = F_{cum,2} * \Delta C_2$		
3	C_3		$\sum_i F_{SRi,C3}$	$\sum_j F_{SKj,C3}$	$F_{net,3}$			$CumLoad_3$	$CumFresh_3$
		$\Delta C_3 = C_4 - C_3$				$F_{cum,3} = F_{cum,2} + F_{net,3}$	$\Delta load_3 = F_{cum,3} * \Delta C_3$		
n	C_n		$\sum_i F_{SRi,Cn}$	$\sum_j F_{SKj,Cn}$	$F_{net,n}$			$CumLoad_n$	$CumFresh_n$
		ΔC_n				$F_{cum,n} = F_{cum,n-1} + F_{net,n}$	$\Delta load_n = F_{cum,n} * \Delta C_n$		
n+1	C_{n+1}		$\sum_i F_{SRi,C(n+1)}$	$\sum_j F_{SKj,C(n+1)}$	$F_{net,n+1}$			$CumLoad_{n+1}$	$CumFresh_{n+1}$

The generic Cascade Table for a single contaminant is shown in Table 3-6 that shows the calculation procedure. The first two columns in Table 3-6 shows the concentration levels of the streams, arranged in ascending order (or descending order of the qualities). Column 3 calculates the differences in concentrations between two consecutive levels. Columns 4 and 5 denote the total flowrates of the sources and sinks in each concentration level. Column 6 shows the difference between the flowrates of sources and sinks, and Column 7 calculates the cumulated flowrates differences. Column 8 computes the contaminant loads in each level, and Column 9 calculates the cumulated load. Column 10 calculates the freshwater requirement for each level. The highest absolute value among the levels represents the required total freshwater flowrate, as indicated in the first row of Column 7.

Table 3-7 shows the construction of the Water Cascade Table for the example. The first column consists of the contaminant concentration levels arranged in ascending order or descending order of water quality. This is because the cascade analysis is done from the highest quality/cleanest to the lowest quality/dirtiest. The value in the last row represents the maximum value of the concentration (1,000,000 ppm). Column 2 represents the concentration differences between the current concentration level and the next concentration (ΔC). For example, at the first concentration level (0 ppm), the concentration difference is the next concentration level minus current concentration (50 – 0 = 50 ppm). Column 3 contains the flowrates of the water sources for each concentration level, while Column 4 is the flowrates of the water sinks/demands for each concentration level. Column 5 is the difference between Column 3 and 4, which shows whether it is water deficit and surplus for each concentration level. If the value is negative, then it is a water deficit; else, if the value is positive, then it is a water surplus.

The net water deficit of 20 kg/h at the first concentration level is cascaded to the second level to meet the demand for the second concentration level: 140 kg/s, yielding a cumulative net water deficit (F_{cum}) of 160 kg/h (20+140). This net water deficit is then cascaded to the subsequent concentration level. This is represented in Column 6, assuming the freshwater resource is zero. Column 7 represents the product of the cumulative water source/demand (F_{cum}) in Column 6 and the concentration difference across the concentration level (ΔC) in Column 2- Eq(3-12). Column 8 is the cumulative load difference from Column 7. Column 9 is the cumulative pure water deficit or surplus, calculated from Eq(3-13). For example, at concentration level 3 (100 ppm), the cumulative pure water deficit is calculated as -9,000/(100-0) = -90 kg/h. The most negative value is the total freshwater target required for this process. In this representation, the pure water surplus (positive values) means that water is not required for this concentration level, and the water sources which are higher purity are enough to fulfil the water deficit for this level. The negative pure water surplus or pure water deficit means that water of higher purity than this level is required. Negative pure water surplus indicates the cascade is the infeasible cascade. Adding the absolute value of the

most negative value in Column 9 to Column 6 gives the feasible cascade- see Table 3-7a. For this example, the total freshwater target is 90 kg/h, and the Pinch is at 100 ppm (SR1+SR2).

$$\Delta C = C_N - C_{N+1} \qquad \text{where } N = concentration\ level \tag{3-12}$$

$$Cum.\ Fresh\ resource_N = \frac{Cum.\Delta\ load_{N-1}}{C_N - C_{FW}} \qquad \text{where } N = concentration\ level \tag{3-13}$$

Table 3-7: Water Cascade Table for example 1- infeasible

Concentration,C (ppm)	**ΔC (ppm)**	**$\sum_i F_{SRi}$ (kg/h)**	**$\sum_j F_{SKj}$ (kg/h)**	**$\sum_i F_{SRi} - \sum_j F_{SKj}$ (kg/h)**	**F_{cum} (kg/h)**	**Δload (kg/h)**	**Cum Δload (kg/h)**	**Cum Fresh (kg/h)**
					0			
0		-	20	-20				
	50				-20	-1,000		
50		-	140	-140			-1,000	-20
	50				-160	-8,000		
100		120	-	120			-9,000	-90
	300				-40	-12,000		
400		-	10	-10			-21,000	-52.5
	400				-50	-20,000		
800		50	-	50			-41,000	-51.25
	999,200				0			
1,000,000							-41,000	-0.041

As mentioned by El-Halwagi et al. (2003), the Pinch Point is always located at one of the source stream using a load vs flowrate diagram, in which the source is labelled as the Pinch-causing source - see Figure 3-14. Figure 3-14 also shows the relationship between the graphical plots and the Water Cascade Table. Based on the figure, it shows that the Pinch should always be at the source stream equal to or higher than the concentration of sinks that are Below the Pinch. In this case, the Pinch is at 100 ppm, larger than the last sink Below the Pinch with a concentration of 50 ppm. This point is the bottleneck of the sources recycling in this specific process, as this source has higher impurity than all the other sinks Below Pinch, and the other lower impurity sources are used up in

the process. The concentration limit for SK4 is 400 ppm, for which SR1 and SR2 are enough to fulfil.

Table 3-7a: Water Cascade Table for example 1- feasible

C (ppm)	ΔC (ppm)	$\sum_i F_{SRi}$ (kg/h)	$\sum_j F_{SKj}$ (kg/h)	$\sum_i F_{SRi} - \sum_j F_{SKj}$ (kg/h)	F_{cum} (kg/h)	Δload (kg/h)	Cum Δload (kg/h)	Cum Fresh (kg/h)
					90 (Fresh)			
0		-	20	-20				
	50				70	3,500		
50		-	140	-140			3,500	70
	50				-70	-3,500		
100		120	-	120			0	0 (Pinch)
	300				50	15,000		
400		-	10	-10			15,000	37.5
	400				40	16,000		
800		50	-	50			31,000	38.75
	999,200				90 (Waste)	8,993k		
1M							89,959k	89.959

Notice that the Pinch-causing source divides the graph into two regions: high quality (Below the Pinch in the plot) and low quality (Above the Pinch in the plot) regions. The sources Below the Pinch are of higher quality, and in this case, they are cleaner than both SK2 and SK3. The sources can be fully used. The Pinch-causing source (SR2) has lower quality (higher concentration) than the sinks Below the Pinch. By observing the Water Cascade Table in Figure 3-14, it can be deduced that the Pinch point is always of lower quality (higher concentration) than the sinks Below the Pinch. Part of the Pinch-causing source is used up for the sinks at the high-quality region (Below the Pinch in the plot), denoted as F_{HQR} = 70 kg/h. The remaining is used for the low-quality region (Above the Pinch in the plot), denoted as F_{LQR} = 50 kg/h.

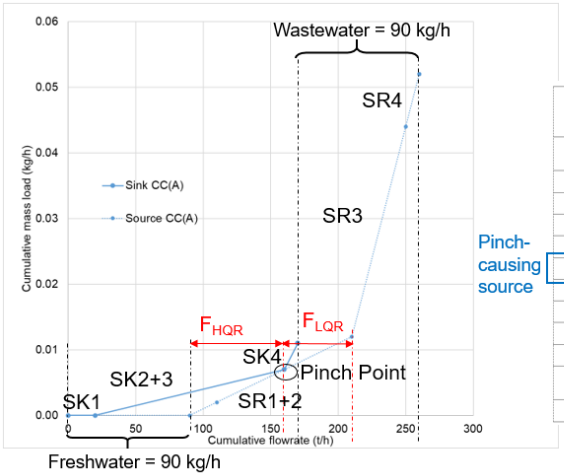

Concentration, C (ppm)	ΔC (ppm)	$\sum_i F_{SRi}$ (kg/h)	$\sum_j F_{SKj}$ (kg/h)	$\sum_i F_{SRi} - \sum_j F_{SKj}$ (kg/h)	F_{cum} (kg/h)	Δload (kg/h)	Cum Δload (kg/h)	Cum Fresh (kg/h)
					90 (Fresh)			
0		-	20	-20				
	50				70	3,500		
50		-	140	-140			3,500	70
	50		F_{HQR} = 70 kg/h		-70	-3,500		
100		120	-	120			0	0 (Pinch)
	300		F_{LQR} = 50 kg/h		50	15,000		
400		-	10	-10			15,000	37.5
	400				40	16,000		
800		50	-	50			31,000	38.75
	999,200				90 (Waste)	8,993k		
1,000,000							89,959k	89.959

Pinch-causing source

Figure 3-14: Cumulative load vs flowrate diagram and the Water Cascade Table used for targeting

3.4.2.2 Cascade table analysis-targeting and design for single contaminant problem

The above algorithm explains the targeting for total freshwater resources in a specific process. According to Chin et al. (2021a), performing Pinch Analysis for each sink sequentially enables the freshwater target and the source allocation to be determined accordingly, inspired by the idea of the Material Recovery Pinch Diagram by El-Halwagi et al.(2003)– see Figure 3-6.

A similar example is used to showcase how the Water Cascade Table can be used to target and perform source allocation for each sink. The explanation is aided with the graphical representation using load vs flowrate diagram – see Figure 3-15. Based on example 1, SK1 is the demand for pure water, so no other sources can be allocated to it. The freshwater required for SK1 is 20 kg/h. Moving on to the next cleanest SK2 and SK3 since they have the same impurity constraints, part of SR2 is recycled to both of the sinks (70 kg/h). The Pinch-causing source for the sinks is SR2 (100 ppm), and the freshwater required for SK2+3 is 70 kg/h. The remaining SR2 (120-70 = 50 kg/h) is transferred to SK4. Similar steps are repeated, and it shows that SK4 does not require fresh resources.

However, let us consider a scenario when SR2 is not enough. The flowrate of SR2 is now reduced to 20 kg/h. SR1 and SR2 are clearly not enough now, and SR3 has to be used for SK2+3. In this case, SR3 becomes the Pinch-causing source – see Figure 3-16.

The typical arrangement is to sort the streams with ascending order of their concentrations. However, there is another possible arrangement for Water Cascade. In fact, the sources or streams above the sinks can be considered as the sources at the high-quality region (Below the Pinch) and should be fully used up. The source right next to the sink should be the Pinch-causing source, and the Pinch Point should always be located at the source just below the sink. Figure 3-17 shows the alternative arrangement of the streams, and it shows the results are identical.

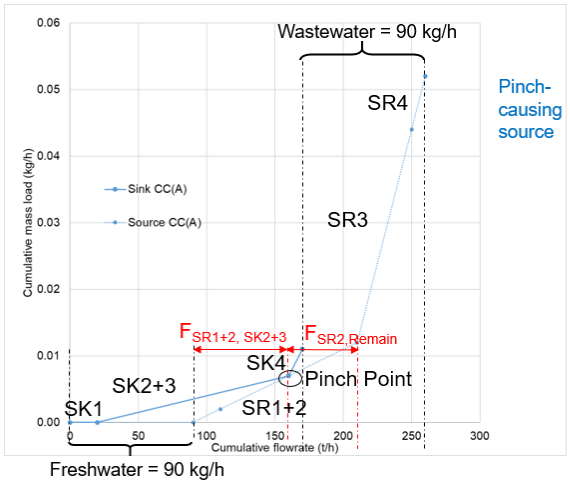

For SK2+3:

Concentration, C (ppm)	ΔC (ppm)	$\sum_i F_{SRi}$ (kg/h)	$\sum_j F_{SKj}$ (kg/h)	$\sum_i F_{SRi} - \sum_j F_{SKj}$ (kg/h)	F_{cum} (kg/h)	Δload (kg/h)	Cum Δload (kg/h)	Cum Fresh (kg/h)
					70 → Freshwater for SK2+3			
0		-	-	0				
	50				70	3,500		
50		-	140	-140			3,500	70
	50	$F_{SR1+2,SK2+3}$ = 70 kg/h			-70	-3,500.		
100		120	-	120			0	0
	700	$F_{SR2,Remain}$ = 50 kg/h			50	35,000	Pinch for SK2+3	
800		50	-	50			35,000	43.75
	999.2k				100	999.2k		
1,000,000				0.00			999.6k	99.96

For SK4:

Concentration, C (ppm)	ΔC (ppm)	$\sum_i F_{SRi}$ (kg/h)	$\sum_j F_{SKj}$ (kg/h)	$\sum_i F_{SRi} - \sum_j F_{SKj}$ (kg/h)	F_{cum} (kg/h)	Δload (kg/h)	Cum Δload (kg/h)	Cum Fresh (kg/h)
					0			
0		-	-	0				
	100				0	0		
100		50	-	50			0	0.00
	300				50	15,000		
400		-	10	-10			15,000	37.50
	400				40	16,000		
800		50	-	50			31,000	38.75
	999,200				90	89,928k		
1,000,000							89,959k	89.96

Figure 3-15: Sequential sink targeting with graphical representation and Water Cascade Table for example 1

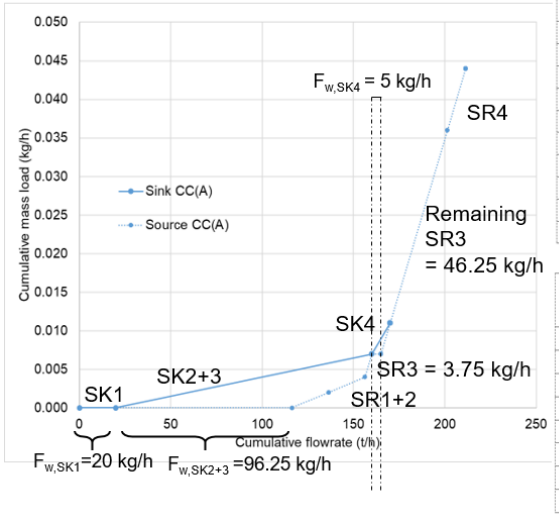

SK2+3:

Concentration, C (ppm)	ΔC (ppm)	$\sum_i F_{SRi}$ (kg/h)	$\sum_j F_{SKj}$ (kg/h)	$\sum_i F_{SRi} - \sum_j F_{SKj}$ (kg/h)	F_{cum} (kg/h)	Δload (kg/h)	Cum Δload (kg/h)	Cum Fresh (kg/h)
					96.25 → Freshwater for SK2+3			
0		-	-	0				
	50				96.25	4,812.50		
50		-	140	-140			4,812.50	96.25
	50				-43.75	-2,187.50		
100		40	-	40			2,625.00	26.25
	700	$F_{SR3,SK2+3}$ = 3.75 kg/h			-3.75	-2,625		
800		50	-	50			0.00	0.00
	999.2k	$F_{SR3,Remain}$ = 46.25 kg/h			46.25	46,213k	Pinch for SK2+3	
1,000,000				0			46,213k	46.21

SK4:

Concentration, C (ppm)	ΔC (ppm)	$\sum_i F_{SRi}$ (kg/h)	$\sum_j F_{SKj}$ (kg/h)	$\sum_i F_{SRi} - \sum_j F_{SKj}$ (kg/h)	F_{cum} (kg/h)	Δload (kg/h)	Cum Δload (kg/h)	Cum Fresh (kg/h)
					5 → Freshwater for SK4			
0		-	-	0				
	400				5	2,000		
400		-	10	-10			2,000	5
	400	$F_{SR3,SK4}$ = 5 kg/h			-5	-2,000		
800		46.25	-	46.25			0	0
	999,200	$F_{SR3,Waste}$ = 41.25 kg/h			41.25	41,217k	Pinch for SK4	
1,000,000							41,217k	41.22

Figure 3-16: Sequential sink targeting with Composite Curves graphical representation and Water Cascade Table for example 1 (Scenario where F_{SR2} = 20 kg/h)

(a)

Concentration, C (ppm)	ΔC (ppm)	$\sum_i F_{SRi}$ (kg/h)	$\sum_j F_{SKj}$ (kg/h)	$\sum_i F_{SRi} - \sum_j F_{SKj}$ (kg/h)	F_{cum} (kg/h)	ΔLoad (kg/h)	Cum ΔLoad (kg/h)	Cum Fresh (kg/h)
					96.25 → Freshwater for SK2+3			
0		-	-	0				
	50				96.25	4,812.50		
50		-	140	-140			4,812.50	96.25
	50				-43.75	-2,187.50		
100		40	-	40			2,625.00	26.25
	700	$F_{SR3,SK2+3}$ = 3.75 kg/h			-3.75	-2,625		
800		50	-	50			0.00	0.00
	999.2k	$F_{SR3,Remain}$ = 46.25 kg/h			46.25	46,213k	Pinch for SK2+3	
1,000,000				0			46,213k	46.21

(b)

Concentration, C (ppm)	ΔC (ppm)	$\sum_i F_{SRi}$ (kg/h)	$\sum_j F_{SKj}$ (kg/h)	$\sum_i F_{SRi} - \sum_j F_{SKj}$ (kg/h)	F_{cum} (kg/h)	ΔLoad (kg/h)	Cum ΔLoad (kg/h)	Cum Fresh (kg/h)
					96.25 → Freshwater for SK2+3			
0		-	-	0				
	100				96.25	9,625		
100		40	-	40			9,625.00	96.25
	-50				136.25	-6,812.50		
50		-	140	-140			2,812.50	56.25 ← Sink
	750	$F_{SR3,SK2+3}$ = 3.75 kg/h			-3.75	-2,812.50		
800		50	-	50			0	0
	999,200	$F_{SR3,Remain}$ = 46.25 kg/h			46.25	46,213k	Pinch for SK2+3	
1,000,000							46,213k	46.21

Sources in high quality region (Below Pinch)

Pinch-causing source

Figure 3-17: Water Cascade Table for SK2+3 in example 1 scenario 2 with different stream arrangement (a) ascending order of concentration (b) grouping the 'high quality' sources above the sink

This alternative arrangement may not be useful for a single contaminant case, but it is crucial for multiple contaminants cases. This is because the arrangement sequence of the streams based on different contaminants can be varied. For example, SR1 may have the lowest concentration on A, but it might have a very high amount of contaminant B. The cascades for both contaminants A and B can be very different. In this case, the concentration difference in Column 2 can become negative, and the cumulative load is negative. This will cause the calculated cumulative pure water deficit at a certain concentration level to be negative - see Eq(3-13), but perhaps this concentration level is actually pure water surplus. This will be explained in Section 3.4.2.3.

3.4.2.3 Cascade table analysis-targeting and design for multiple contaminant problem

A similar procedure as the single contaminant case can be used to construct the Water Cascade Table for multiple contaminants, but with slight modification on the arrangement sequence of the sources. As stated in Section 3.2, the arrangement sequence of the streams based on different contaminants can be varied. The sources may have different contaminants concentrations, and the cascades for each contaminant are very different. In this case, it is easier to arrange the stream in an alternative way, as shown in Figure 3-17, i.e. group all the 'high quality' sources above the sink stream and the Pinch-causing source below the sink.

It is imperative to first determine for each sink, which contaminant cascade it will fall into, and the arrangement of the sources. The sources that should be in the high-quality region (Below Pinch) and the Pinch-causing source has to be identified prior to performing the cascade analysis. The following heuristic is proposed to identify the sources that should be in the high-quality region (Below Pinch), and the Pinch is causing source.

i. Determine the limiting contaminant for the specific sink using Eq(3-14).
ii. Arrange the available sources in ascending order based on the limiting contaminant of sinks.
iii. Add up the flowrates of each source (F_{SRi}) and its contaminant loads ($F_{SRi}C_{k,SRi}$ for any k). For source 'i', if the cumulative flowrates of sources after adding F_{SRi} exceed or equal to sink's flowrate (F_{SKj}) OR cumulative loads after adding $F_{SRi}C_{k,SRi}$ exceed or equal to sink's load $F_{SKj}Z_{k,SKj}$, then source 'i' is the Pinch-causing source. All sources before source 'i' are considered 'high quality' sources.

Figure 3-9 is the recommended source allocation strategy for a specific sink. This is based on the analysis from Chin et al. (2021) that concluded that the optimal source allocation for a sink is to fulfil all the contaminants loads limits as much as possible. The readers can refer to Chin et al. (2021) for a detailed explanation of the strategy.

Table 3-8: Source and sink data for example 2

SR	**F_{sr} (t/h)**	**$C_{A,SR}$ (ppm)**	**$C_{B,SR}$ (ppm)**	**SK**	**F_{sk} (t/h)**	**$Z_{A,Sk}$ (ppm)**	**$Z_{B,SK}$ (ppm)**
1	23	50	120	**1**	23	20	60
2	47	100	80	**2**	47	50	20
3	123	150	300	**3**	123	100	150
4	60	250	100	**4**	70	200	80
Fw	-	0	0				

The similar two contaminant problem from Teles et al. (2008) is used to showcase the proposed full Water Cascade Table analysis. Table 3-8 shows the source-sink data. The contaminant cascades for each sink has to be identified first, which can be identified using Eq (3)- see Section 3.1.1. Table 3-9 presents the results. Judging based on the smallest value of the ratio, SK1 and SK3 are limited to contaminant ‘A’, and they are assigned to contaminant cascade 'A', while SK2 and SK4 are assigned to contaminant cascade ‘B’ for the identical reason.

Table 3-9: Sink-to-source concentration for Example 2, with maximum source concentration as the denominator

	$Z_{A,SK}/C_{A,SRmax}$ $C_{A,SRmax}$ = 250 ppm	$Z_{B,SK}/C_{B,SRmax}$ $C_{B,SRmax}$ = 300 ppm	Minimum ratio	Cascade
SK1	**0.08**	0.4	0.08	A
SK2	0.4	**0.27**	0.07	B
SK3	**0.40**	0.50	0.40	A
SK4	0.8	**0.27**	0.27	B

The contaminant cascade with the highest sinks' flowrates should be 'Pinched' first as they are demanding more water, so allocating the sources to them first could reduce the fresh resource requirement (Chin et al., 2021). As the total sink flowrates (SK1+SK3) in contaminant cascade 'A' has the highest flowrate, the design methodology is performed on contaminant cascade 'A' first. The design methodology starts with SK1 first. The source ranking order based on contaminant 'A' is SR1->SR2->SR3->SR4. The previous heuristic can be used to determine the Pinch-causing source. Since in this case, the flowrate of SR1 (23 t/h) is equal to the flowrate of sink 1 (23 t/h) or the load of contaminant A (23 x 50) exceeds the load of the sink (23 x 20), SR1 is the Pinch-causing source. In Figure 3-18a, the Source CC is shifted to the right until it touches the endpoint of SK1 line. It should be noted that the Pinch occurs at contaminant 'A'. Since SK1 is determined as limited by contaminant 'A', there is no room for fresh resource reduction for SK1. The cascade table in Figure 3-18b also shows exactly how much of SR1 is allocated to SK1, which is 9.2 t/h. The remaining SR1 (13.8 t/h) is used for the subsequent sinks.

Notice the feasible cascade in Figure 3-18b, and there are several concentration levels that contain still negative pure water surplus, which should mean that they have a pure water deficit. However, they are not actually deficit due to the concentration difference at the previous level is negative. This is due to the arrangement of sources that are not based on the ascending order any more. If arranging the sources and sinks solely based on ascending order of the concentration level, the results might become misleading, and so the fresh resource might be wrongly identified. Determining the Pinch-causing source and the 'high quality' sources are crucial for multiple contaminants cases.

After SK1 is satisfied, the next sink to be fulfilled is SK3. Figure 3-19 shows the plot of the CC with SK3 is stacked above SK1. SR3 is the Pinch-causing source, and SR1+2 are the high-quality sources due to the cumulative load of both contaminants for SR1, SR2, and SR3 exceed the loads

for SK3. In Figure 3-19a, SR3 is located below the sink stream in the cascade table as it is the Pinch-causing source.

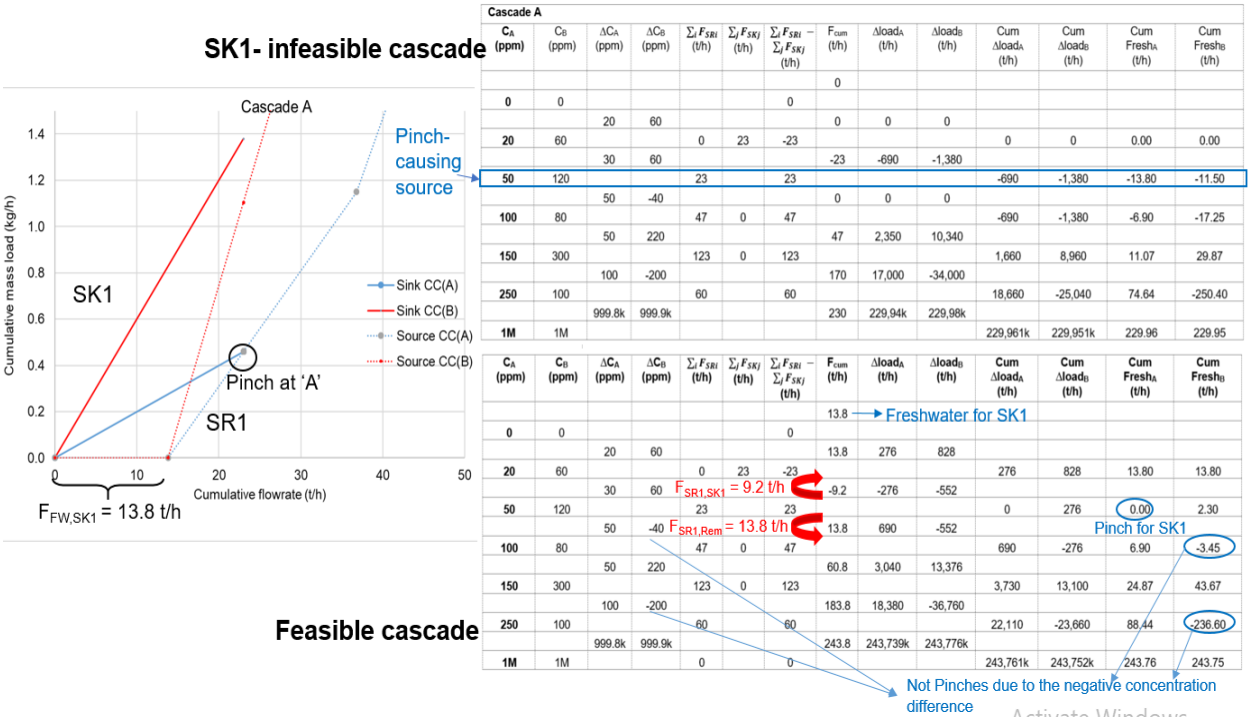

Figure 3-18; Sequential source allocation with Pinch Approach for SK1 from example 2 (a) CC Graphical representation (b) Water Cascade Table

Notice the Pinch Point occurs at contaminant 'B', but this is not the main limiting contaminant for SK3. There is still room for reduction of the freshwater requirement. The flowrate of SR3 can be reduced by mixing some of the SR4 to further reduce the freshwater target for SK3. This is because SR3 has the lowest quality in terms of contaminant 'B', and it causes the Pinch to occur at the sink's non-limiting contaminant. Based on Figure 3-9 using the manual method, SR3 can be reduced until the cumulative freshwater requirement for both contaminants is identical. Otherwise, using the numerical method, the first pair with two sources from the arranged source, i.e. SR3 and SR4. As SR1 and SR2 are clearly not enough for SK3, they are fully used for SK3. Use Eqs(4-5) to determine the flowrates of SR3 and SR4 to be allocated to SK3. As this is only two contaminants, setting the freshwater requirement- Eq(4) for A to be equal to B is enough. In step (iv), the flowrates of SR3 and SR4 that can be allocated to SK3 needs to be checked. The determined flowrates are found as: SR3 = 42.792 t/h and SR4 = 1.965 t/h. As both flowrates are not negative and are less than the available flowrates, as well as the total source flowrates (13.8+47+42.792+1.965 = 105.56 t/h) is less than sink flowrate (123 t/h), the step for SK3 is completed. Notice that in Figure 3-19b, the SR3 is no longer the Pinch-causing source since it is

reduced. SR4 becomes the new Pinch-causing source. In the cascade table, SR3 is moved to the 'high quality' source grouping, and it is located above the sink stream.

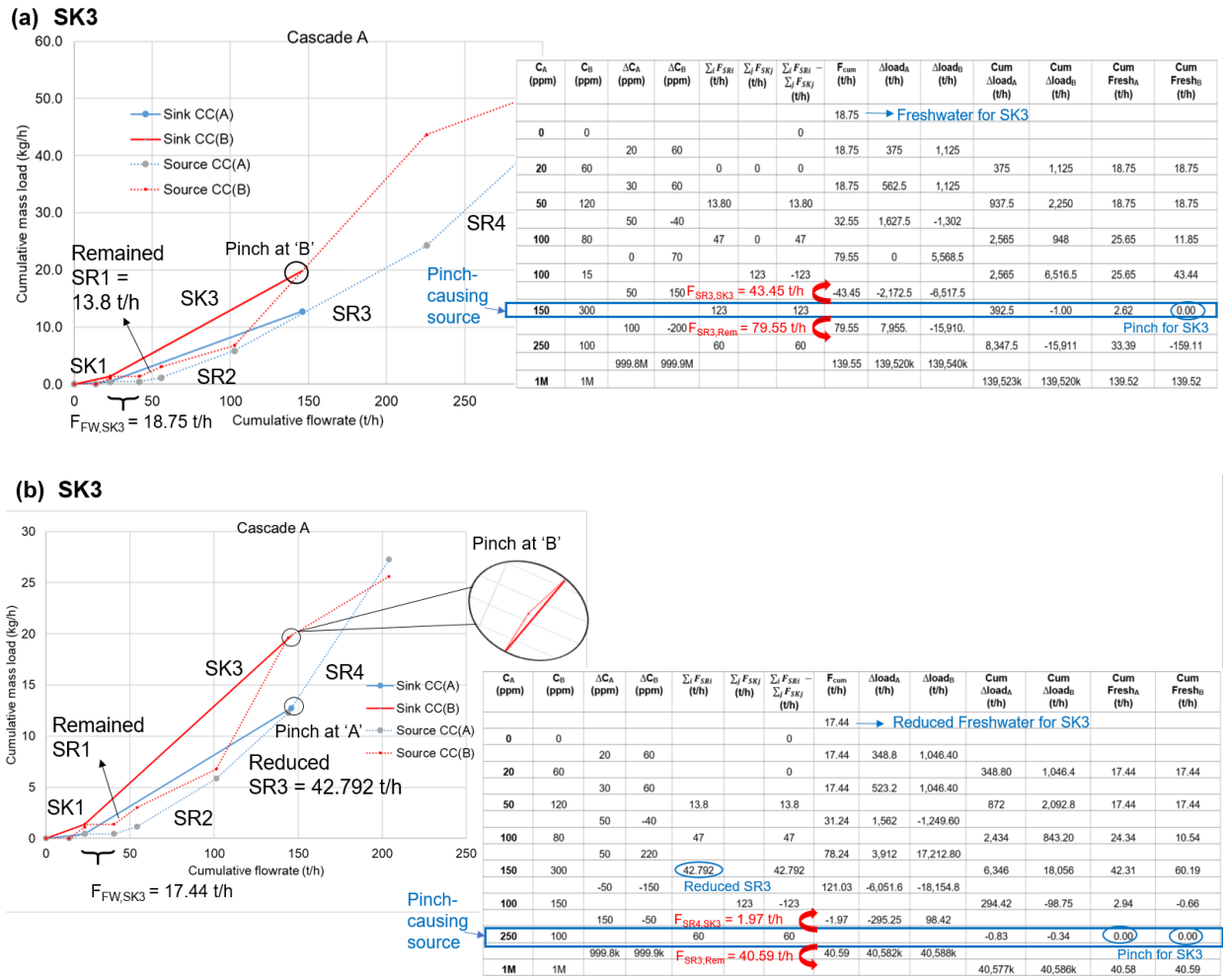

Figure 3-19; Sequential source allocation with Pinch Approach using CC graphical representation and Cascade Analysis from example 2: (a) SK3 (b) SK3 with reduced freshwater target

As for the sinks in contaminant cascade 'B', a similar methodology is applied. The source order is SR2-> SR4-> SR1-> SR3. SK2 is the first to be fulfilled. As SR2 and SR1 are already allocated to SK1 and SK3, the sources that are remained are SR4 and SR3. For SK2, the Pinch-causing source is SR4. By performing PA, the Pinch Points of both contaminants are reached for SK2, by using solely SR4 (see Figure 3-20a). This is the optimal allocation for SK2. As the SR4 is used, the remaining SR4 is not enough for SK4, and SR3 becomes the Pinch-causing source for SK4. For the next sink SK4, the Pinch Point also occurs at contaminant 'B- see Figure 3-20b, which is its main limiting contaminant. There is no room for further freshwater reduction in this case.

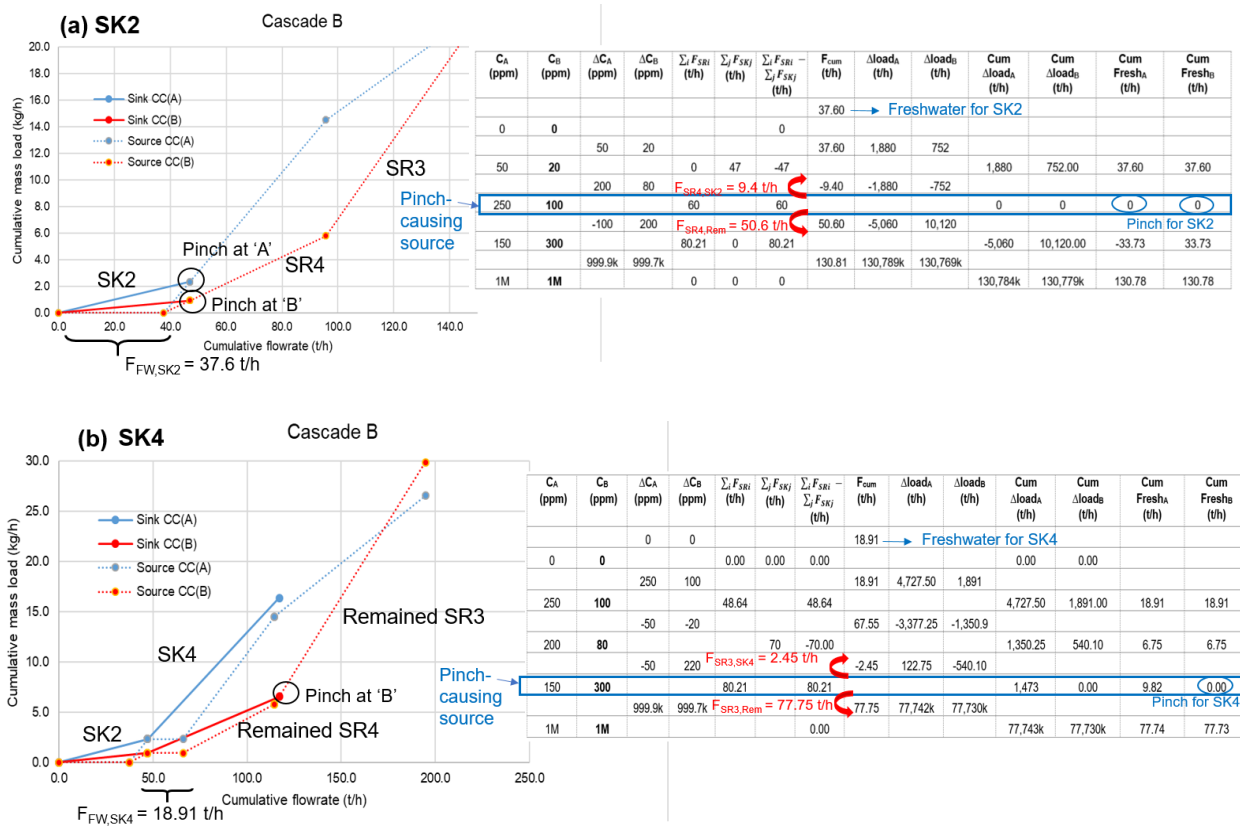

Figure 3-20; Sequential source allocation with Pinch Approach using CC graphical representation and Cascade Analysis from example 2: (a) SK2 (b) SK4

3.4.3 Non-mass transferred (fixed flowrate) vs mass transferred (fixed load) operations

Water-using operations in the chemical processes can be divided or modelled as fixed contaminant load (FL), such as absorption and reactor, or fixed flowrate (FF), such as boiler (Prakash and Shenoy, 2015). The main feature of FL operations is that they are assumed as mass transfer processes with a fixed amount of contaminant mass loads to be removed. The inlet and outlet stream flowrates are equal, and there are no water losses or gains. The FF operations do not involve mass transfer, and the principal characteristic is that water loss or gain may take place in the operation. This kind of problem also can be characterised as a water source or sink that generates or consumes a fixed quantity of water. The inlet and outlet flow rates are specified and different, while its outlet concentration must reach their maximum value and are independent of the inlet concentrations.

For mass transfer based operation, the transferred contaminant load is usually assumed as constant, see Eq(3-15). For an operation M, it has the requirement of maximum water inlet concentration

($C_{inlet,M}^{Max}$) and outlet concentration ($C_{outlet,M}^{Max}$). For the fixed load operation, the available data is usually the maximum water flowrate (f_M), which is the sink and source flowrate, and the maximum inlet and outlet concentrations.

$$\Delta load_M = f_M(C_{outlet,M}^{Max} - C_{inlet,M}^{Max}) \tag{3-15}$$

In operation involving multiple contaminants, the mass transfer occurs simultaneously, and there is a certain relationship between the contaminants. According to Wang and Smith (1995), the ratio of the mass transferred load for all contaminants is a constant, see Eq(3-16). In other words, if the inlet concentration of one contaminant, 'k1' for a fixed load operation 'M', is reduced, then the outlet concentration of contaminant 'k1' is reduced as well. This is the major assumption made by the previous literature references.

$$K_{M,k} = \frac{\Delta load_{k1,M}}{\Delta load_{k2,M}} = constant \tag{3-16}$$

In this work, the maximum concentrations of the sources and sinks (or the so-called limiting water profile) for the fixed load operation can be used to perform the Pinch Analysis, using the Load vs Flowrate diagram or the proposed Water Cascade Table analysis. In fact, the optimum freshwater requirement identified using the limiting data is the highest freshwater amount. Based on the example in Figure 3-21a, the maximum limit for contaminant 'A' has been reached for sink 1, but the limit for contaminant 'B' is not reached. This means that the sink or the inlet concentration of operation 1 does not reach the maximum for contaminant B; the source or the outlet concentration of operation 1 should not reach the maximum as well. In this case, the concentration of source 1 is not at the maximum value but rather at a reduced value, see Figure 3-21b. In this example, source 1 is recycled back for sink 1. However, if source 1 is used for other operations, the reduced concentration of source 1 could further reduce the freshwater target for other sinks as well.

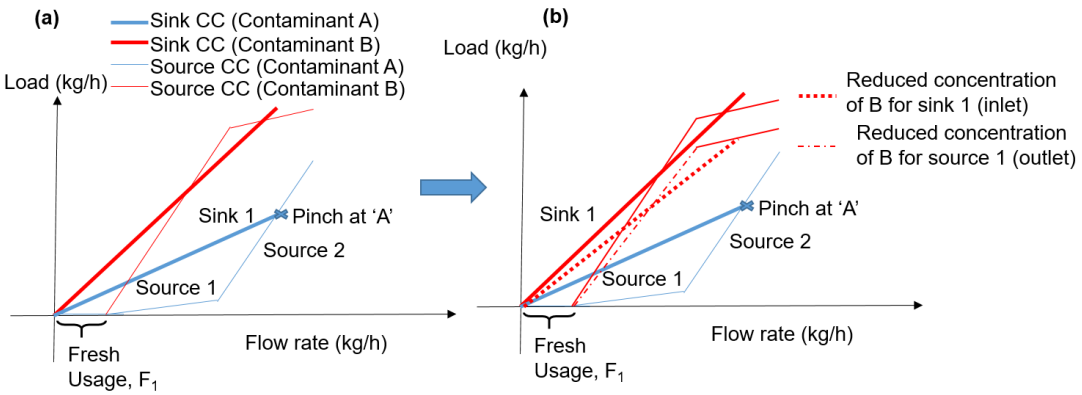

Figure 3-21: Adjusting concentrations of sinks and sources due to the fixed load operation (a) Before adjusting the concentration of sink and source (b) After adjusting the concentration of sink and source

For fixed flowrate operations, the sink and source flowrates are fixed, and the concentrations of both sinks and sources are fixed as well. However, for fixed load operations, the concentrations and the flowrates are now the degrees of freedom. In this work, the flowrate is set to be the maximum flowrates for the operation. This is because to attain the optimum freshwater target, the load in Eq(3-15) is to be reduced for an operation, and this can be done by reducing the inlet and outlet concentrations only. The freshwater target results are still identical. In fact, this is equivalent to the fixed flowrate problem, but the concentrations of contaminants are not fixed. Setting the flowrate of the operation equal to the maximum flowrates required is beneficial for a retrofit project as the capacity of a unit can be fixed. However, if the equipment capacity can be reduced to save capital cost, the flowrates can be set as the degree of freedom as well.

3.4.4 Case Study and results discussion

A case study is used to elucidate the applicability of the proposed methodology. The first case study is a three contaminant problem, with four sources and four sinks available based on Wang and Smith (1994) – see Table 3-9. These sinks and sources from this problem are from the mass-transferred operations assuming fixed transferred loads.

Table 3-9: Source and sink data for case study 1

SR	**F_{sr} (t/h)**	**$C_{A,SR}$ (ppm)**	**$C_{B,SR}$ (ppm)**	**$C_{C,SR}$ (ppm)**	**SK**	**F_{sk} (t/h)**	**$Z_{A,Sk}$ (ppm)**	**$Z_{B,SK}$ (ppm)**	**$Z_{C,SK}$ (ppm)**
1	34	160	450	30	**1**	34	0	0	0
2	75	300	270	740	**2**	75	200	100	500
3	20	1,240	1,400	1,580	**3**	20	600	850	390
4	80	800	930	900	**4**	80	300	460	400
Fw	-	0	0						

Prior to performing the Pinch Analysis, the first step is to determine the limiting contaminant for each sink and assign the sinks into proper contaminant cascade. SK1 requires pure water, so no other sources can be allocated to it. Based on Table 3-10, each sink is dedicated to different cascades. The Pinch should perform based on the descending order of flowrates of the sinks in the cascade, which is SK4->SK2->SK3.

Table 3-10: Identification of source prioritisation sequence/contaminant cascade of each sinks for case study 1

	$Z_{A,SK}/C_{A,SRmax}$ $C_{A,SRmax}$ **= 1,240 ppm**	$Z_{B,SK}/C_{B,SRmax}$ $C_{B,SRmax}$ **= 1,400 ppm**	$Z_{C,SK}/C_{C,SRmax}$ $C_{C,SRmax}$ **= 1,580 ppm**	**Minimum ratio**	**Cascade**
SK1	0	0	0	0	-
SK2	0.1613	0.0714	0.3165	0.0714	B
SK3	0.4839	0.6071	0.2468	0.2468	C
SK4	0.2419	0.3286	0.2532	0.2419	A

The Pinch-causing source and the sources that are below the Pinch have to be identified to utilise the Cascade Table for SK4. Using the heuristic proposed in Section 2.4, the source arrangement based on contaminant A is SR1->SR2->SR4->SR3. SR1 is not the Pinch-causing source as its flowrate (34 t/h) or loads for all contaminants are less than SK4. Adding SR2 to the list, SR2 becomes the Pinch-causing source as the total flowrates of SR1, and SR2 (34+75 t/h) exceeds the flowrate of SK4 (80 t/h), and SR1 should be the source located Below the Pinch. In the Cascade Table representation in Table 3-11, SR1 is placed above the SK4, and SR2 placed is below the SK4 in the table form. It shows that the freshwater requirement for SK4 is about 4.14 t/h, and the Pinch is at contaminant 'C'. However, it is worth noticing that in this case, the sources are non-conflicting in terms of contaminants 'A' and 'C', i.e. the source arrangement of both contaminants 'A' and 'C' are SR1->SR2->SR4->SR3. In this case, since the sources are already in order, there is no room for further freshwater reduction for this sink. About 41.87 t/h of SR2 and all SR1 are recycled to SK4.

Moving on to SK2, a similar procedure is repeated. The source arrangement based on contaminant 'B' is SR2->SR1->SR4->SR3. The remaining SR2 (33.14 t/h) is to be used recycled back to SK2. SR2 is the Pinch-causing source for SK2 due to its load for contaminant B (33.14 x 270 = 8,948 t/h) exceeds the load for SK2 (75 x 100 = 7,500 t/h). Table 3-12 shows the Cascade Table representation for SK2. Only about 27.78 t/h of SK2 is recycled to SR2, and additional freshwater of 47.22 t/h is required for SK2. The Pinch is at the contaminant 'B' as well, so there is no further freshwater reduction for SK2.

However, since this operation is assumed as the fixed-load mass transferred operations, as the maximum loads for contaminants 'A' and 'C' for SK2 (the inlet) are not reached, the concentrations of SR2 (the outlet) can be reduced. The concentrations of contaminants 'A' and

'C' for SK2 are reduced to (A: 27.78x300/75 = 111.12 ppm, C: 27.78x740/75=274.1 ppm). Using Eqs(3-15 to 16), the concentrations of contaminants 'A' and 'C' for SR2 are reduced to 211.11 ppm and 514.07 ppm, as shown by the calculations below.

$$K_{2,A} = \frac{\Delta load_{B,2}}{\Delta load_{A,2}} = \frac{75(270-100)}{75(300-200)} = \frac{75(270-100)}{75(C_{A,SR2}^{new}-111.12)}$$

$$C_{A,SR2}^{new} = 211.11\ ppm$$

$$K_{2,C} = \frac{\Delta load_{B,2}}{\Delta load_{C,2}} = \frac{75(270-100)}{75(740-500)} = \frac{75(270-100)}{75(C_{C,SR2}^{new}-274.1)}$$

$$C_{C,SR2}^{new} = 514.07\ ppm$$

As the concentrations of A and C for SR2 have been reduced, the freshwater requirement for SK4 actually can be reduced as well. This is because part of the SR2 is recycled to SK4. Table 3-13 shows the Cascade Table representation for SK4 after the concentrations of SR2 are reduced. It can be shown that no freshwater is required anymore for SK4. The recycled flowrate of SR2 to SK4 becomes 46 t/h. The remaining 29 t/h of SK2 is transferred to the next cascade for SK2. Table 3-14 shows the updated Cascade Table representation for SK2. Notice that since contaminant B for SK2 and SR2 are unchanged, and the Pinch for SK2 was at the contaminant B. The freshwater required for SK2 is unchanged, and the recycled flowrate of SR2 is unchanged as well (27.78 t/h). In this case, the concentrations of contaminants 'A' and 'C' for SR2 cannot be reduced anymore.

However, it is worth to be noted that SK4 now is not 'Pinched'. This is because a very high-quality SR1 in terms of contaminants A and C is fully used for SK4. SR1 should be conserved for the remaining sink: SK3. SR1 actually can be further reduced for SK4 until Pinch(s) occurs for SK4. Table 3-15 shows the final Cascade Table representation for SK4, with a reduced flowrate of SR1. It can be observed that the Pinch occurs at the Pinch-causing source: SR2 at contaminant 'C'. The SR1 is reduced to about 18.85 t/h, and the remaining SR1 can be used for SK3.

Table 3-16 shows the Cascade Table representation for the remaining SK3. The source arrangement based on contaminant 'C' is SR1->SR2->SR4->SR3. The remaining SR1 and SR2 available are about 15.15 t/h and 1.22 t/h. For SK3, the Pinch-causing source becomes SR4. The remaining SR1 and SR2 should be Below the Pinch Region for SK3, and they are located above the sink stream in Table 3-16. It shows that no freshwater is required for this sink, and there are no Pinches for this sink. Notice that the negative water surpluses shown in the last three columns are not really water deficits, but the negativity is caused by a negative concentration difference. If all SR1 was fully used for SK4, there might be additional freshwater demand for this sink. Conserving the sources are thus important when performing the Pinch Analysis for each sink sequentially.

The full design procedure is completed at this stage. Only SK1 and SK2 require freshwater. SK1 requires 34 t/h of freshwater, and SK2 requires about 47.22 t/h. The total freshwater target is determined as 81.22 t/h (34+47.22) of freshwater. The solutions obtained are similar to the results from previous works, i.e. Wang and Smith (1994) and later, Francisco et al. (2018). Although the overall framework can be fully computed automatically, the source allocation across the contaminant cascades is difficult to be identified as well. For example, the allocated SR1 to SK4 has to be conserved so that the source can be used for SK3. The algorithm can be designed as when there are still demands of resources, the sources allocations to the sinks should be conserved so that the Pinches for the sinks should be reached. However, source allocation is just a strategy for allocating the sources. When there are infeasible matches between streams, the Cascade Table or the graphical representations allow flexible tuning of the streams so that it matches the requirement of a practical plant.

3.4.5 Conclusions

This work has formulated an enhanced version of Cascade Table Analysis dedicated to multi-contaminant material recycle-reuse networks, on the example of water networks. Instead of arranging the sources solely based on the ascending order of contaminants concentrations or descending order qualities of streams, this work proposes the sources Below the Pinch should be grouped and located above the sink stream. The Pinch-causing source should be placed right under the sink in the Cascade Table representation. This alternative stream arrangement prevents the false freshwater deficit from being identified, caused by the negative concentration differences between concentration levels for multiple contaminants. If the Pinch Point occurs at the non-limiting contaminant of the sink, a source reduction can be performed to further reduce the freshwater target for that sink. Heuristics for the algorithm have been proposed.

The Cascade Table Analysis or the graphical representations provide a step-by-step procedure for multiple contaminants material network design and provides a user-friendly interface to the solutions. This is beneficial for engineers as the method shows the exact allocation of each source for each sink. Although the overall framework can be fully computed automatically, the source allocation across the contaminant cascades is difficult to identify as well. The algorithm can be designed as when there are still demands of resources, the sources allocations to the sinks should be conserved so that the Pinches for the sinks should be reached. However, the proposed source allocation procedure in Figure 3-9 is just a strategy for allocating the sources. When there are infeasible matches between streams, the Cascade Table or the graphical representations allow flexible manual tuning of the streams matches so that it fulfils the requirement of a practical plant. Future research can be focused on multiple fresh resources or water regeneration potential, as well as property-based integration.

Table 3-11: Water Cascade Table for SK4 in case study 1

C_A (ppm)	C_B (ppm)	C_C (ppm)	ΔC_A (ppm)	ΔC_B (ppm)	ΔC_C (ppm)	$\sum_i F_{SRi}$ (t/h)	$\sum_j F_{SKj}$ (t/h)	$\sum_i F_{SRi} - \sum_j F_{SKj}$ (t/h)	F_{cum} (t/h)	$\Delta load_A$ (t/h)	$\Delta load_B$ (t/h)	$\Delta load_C$ (t/h)	Cum $\Delta load_A$ (t/h)	Cum $\Delta load_B$ (t/h)	Cum $\Delta load_C$ (t/h)	Cum $Fresh_A$ (t/h)	Cum $Fresh_B$ (t/h)	Cum $Fresh_C$ (t/h)
									4.14									
0	0	0						0										
			160	450	30				4.14	661.60	1,860.75	124.05						
160	450	30				34		34					661.60	1,860.75	124.05	4.14	4.14	4.14
			140	10	370				38.14	5,338.90	381.35	14,109.95						
300	460	400					80	-80					6,000.50	2,242.10	14,234.00	20.00	4.87	35.59
			0	-190	340				-41.87	0.00	7,954.35	-14,234.10						
300	270	740				75		75					6,000.50	10,196.45	-0.10	20.00	37.76	0.00
			500	660	160				33.14	16,567.5	21,869.1	5,301.60						
800	930	900				80		80					22,568.00	32,065.55	5,301.50	28.21	34.48	5.89
			440	470	680				113.14	49,779.4	53,173.5	76,931.80						
1,240	1,400	1,580				20		20					72,347.40	85,239.00	82,233.30	58.34	60.89	52.05
			999k	999k	998k				133.14	133M	133T	133×10^{15}						
1M	1M	1M								0	0	0	133M	133T	133×10^{15}			

Table 3-12: Water Cascade Table for SK2 in case study 1

C_A (ppm)	C_B (ppm)	C_C (ppm)	ΔC_A (ppm)	ΔC_B (ppm)	ΔC_C (ppm)	$\sum_i F_{SRi}$ (t/h)	$\sum_j F_{SKj}$ (t/h)	$\sum_i F_{SRi} - \sum_j F_{SKj}$ (t/h)	F_{cum} (t/h)	$\Delta load_A$ (t/h)	$\Delta load_B$ (t/h)	$\Delta load_C$ (t/h)	Cum $\Delta load_A$ (t/h)	Cum $\Delta load_B$ (t/h)	Cum $\Delta load_C$ (t/h)	Cum $Fresh_A$ (t/h)	Cum $Fresh_B$ (t/h)	Cum $Fresh_C$ (t/h)
									47.22									
0	0	0					0	0										
			200	100	500				47.22	9,444.00	4,722.00	23,610.00						
200	100	500					75	-75					9,444.00	4,722.00	23,610.00	47.22	47.22	47.22
			100	170	-460				-27.78	-2,778.00	-4,722.6	12,778.80						
300	270	40				33	0	33					6,666.00	-0.60	36,388.80	22.22	0.00	909.72
			-140	180	-10				5.36	-749.72	963.92	-53.55						
160	450	30				0	0	0					5,916.28	963.32	36,335.25	36.98	2.14	1,211.17
			640	480	870				5.36	3,427.29	2,570.46	4,658.97						
800	930	900				80	0	80					9,343.57	3,533.79	40,994.22	11.68	3.80	45.55
			440	470	680				85.36	37,556.3	40,116.9	58,041.49						
1,240	1,400	1,580				20		20					46,899.83	43,650.70	99,035.71	37.82	31.18	62.68
			999k	999k	998k				105.36									
1M	1M	1M																

Table 3-13: Water Cascade Table for SK4 in case study 1, after reducing the concentration of SR2

C_A (ppm)	C_B (ppm)	C_C (ppm)	ΔC_A (ppm)	ΔC_B (ppm)	ΔC_C (ppm)	$\sum_i F_{SRi}$ (t/h)	$\sum_j F_{SKj}$ (t/h)	$\sum_i F_{SRi} - \sum_j F_{SKj}$ (t/h)	F_{cum} (t/h)	$\Delta load_A$ (t/h)	$\Delta load_B$ (t/h)	$\Delta load_C$ (t/h)	Cum $\Delta load_A$ (t/h)	Cum $\Delta load_B$ (t/h)	Cum $\Delta load_C$ (t/h)	Cum $Fresh_A$ (t/h)	Cum $Fresh_B$ (t/h)	Cum $Fresh_C$ (t/h)
									0									
0	0	0						0										
			160	450	30				0	0.00	0.00	0.00						
160	450	30				34		34					0.00	0.00	0.00	0.00	0.00	0.00
			140	10	370				34	4,760.00	340	12,580.00						
300	460	400					80	-80					4,760.00	340.00	12,580.00	15.87	0.74	31.45
			-89	-190	114				-46	4,088.89	8,740	-5,247.41						
211.11	270.00	514.07				75		75					8,848.89	9,080.00	7,332.59	41.92	33.63	14.26
			589	660	386				29	17,077.8	19,140	11,191.85						
800	930	900				80		80					25,926.67	28,220.00	18,524.44	32.41	30.34	20.58
			440	470	680				109	47,960.0	51,230	74,120.00						
1,240	1,400	1,580				20		20					73,886.67	79,450.00	92,644.44	59.59	56.75	58.64
			999k	999k	998k				129									
1M	1M	1M																

Table 3-14: Water Cascade Table for SK2 in case study 1, after reducing the concentration of SR2

C_A (ppm)	C_B (ppm)	C_C (ppm)	ΔC_A (ppm)	ΔC_B (ppm)	ΔC_C (ppm)	$\sum_i F_{SRi}$ (t/h)	$\sum_j F_{SKj}$ (t/h)	$\sum_i F_{SRi} - \sum_j F_{SKj}$ (t/h)	F_{cum} (t/h)	$\Delta load_A$ (t/h)	$\Delta load_B$ (t/h)	$\Delta load_C$ (t/h)	Cum $\Delta load_A$ (t/h)	Cum $\Delta load_B$ (t/h)	Cum $\Delta load_C$ (t/h)	Cum $Fresh_A$ (t/h)	Cum $Fresh_B$ (t/h)	Cum $Fresh_C$ (t/h)
									47.22									
0	0	0						0										
			200	100	500				47.22	9,444.00	4,722.00	23,610.00						
200	100	500					75	-75					9,444.00	4,722.00	23,610.00	47.22	47.22	47.22
			11	170	14				-27.78	-308.67	-4,722.60	-390.98						
211.11	270.00	514.07				29	0	29					9,135.33	-0.60	23,219.02	43.27	0.00	45.17
			-51	180	-484				1.22	-62.36	219.60	-590.57						
160	450	30				0	0	0					9,072.98	219.00	22,628.45	56.71	0.49	754.28
			640	480	870				1.22	780.80	585.60	1,061.40						
800	930	900				80	0	80					9,853.78	804.60	23,689.85	12.32	0.87	26.32
			440	470	680				81.22	35,736.8	38,173.4	55,229.60						
1,240	1,400	1,580				20		20					45,590.58	38,978.00	78,919.45	36.77	27.84	49.95
			999k	999k	998k				101.22									
1M	1M	1M				0		0										

Table 3-15: Water Cascade Table for SK4 in case study 1, after reducing the concentration of SR2 and flowrate of SR1

C_A (ppm)	C_B (ppm)	C_C (ppm)	ΔC_A (ppm)	ΔC_B (ppm)	ΔC_C (ppm)	$\sum_i F_{SRi}$ (t/h)	$\sum_j F_{SKj}$ (t/h)	$\sum_i F_{SRi} - \sum_j F_{SKj}$ (t/h)	F_{cum} (t/h)	$\Delta load_A$ (t/h)	$\Delta load_B$ (t/h)	$\Delta load_C$ (t/h)	Cum $\Delta load_A$ (t/h)	Cum $\Delta load_B$ (t/h)	Cum $\Delta load_C$ (t/h)	Cum $Fresh_A$ (t/h)	Cum $Fresh_B$ (t/h)	Cum $Fresh_C$ (t/h)
									0.00									
0	0	0						0.00										
			160	450	30				0.00	0.00	0.00	0.00						
160	450	30				18.85	0.00	18.85					0.00	0.00	0.00	0.00	0.00	0.00
			140	10	370				18.85	2,639.36	188.53	6,975.46						
300	460	400				0.00	80.00	-80.00					2,639.36	188.53	6,975.46	8.80	0.41	17.44
			-89	-190	114				-61.15	5,435.32	11,618.0	-6,975.33						
211.11	270.00	514.07				75.00	0.00	75.00					8,074.69	11,806.53	0.13	38.25	43.73	0.00
			588.9	660	385.9				13.85	8,157.64	9,142.72	5,346.08						
800	930	900				80.00	0.00	80.00					16,232.33	20,949.25	5,346.21	20.29	22.53	5.94
			440	470	680				93.85	41,295.1	44,110.7	63,819.77						
1,240	1,400	1,580				20.00		20.00					57,527.47	65,059.97	69,165.97	46.39	46.47	43.78
			999k	999k	998k				113.85									
1M	1M	1M				0.00		0.00										

Table 3-16: Water Cascade Table for SK3 in case study 1

C_A (ppm)	C_B (ppm)	C_C (ppm)	ΔC_A (ppm)	ΔC_B (ppm)	ΔC_C (ppm)	$\sum_i F_{SRi}$ (t/h)	$\sum_j F_{SKj}$ (t/h)	$\sum_i F_{SRi} - \sum_j F_{SKj}$ (t/h)	F_{cum} (t/h)	$\Delta load_A$ (t/h)	$\Delta load_B$ (t/h)	$\Delta load_C$ (t/h)	Cum $\Delta load_A$ (t/h)	Cum $\Delta load_B$ (t/h)	Cum $\Delta load_C$ (t/h)	Cum $Fresh_A$ (t/h)	Cum $Fresh_B$ (t/h)	Cum $Fresh_C$ (t/h)
0	0	0						0.00										
			160	450	30				0.00	0.00	0.00							
160	450	30				15.15	0.00	15.15					0.00	0.00	0.00	0.00	0.00	0.00
			51	-180	484				15.15	774.20	-2,726.53	7,332.46						
211.11	270.00	514.07				1.22		1.22					774.20	-2,726.53	7,332.46	3.67	-10.10	14.26
			389	580	-124				16.37	6,365.96	9,494.38	-2,031.05						
600	850	390					20.00	-20.00					7,140.16	6,767.85	5,301.42	11.90	7.96	14.73
			200	80	510				-3.63	-726.08	-290.43	-1,851.49						
800	930	900				80.00	0.00	80.00					6,414.09	6,477.42	3,449.93	8.02	6.96	3.83
			440	470	680				76.37	33,602.6	35,893.7	51,931.34						
1,240	1,400	1,580				20.00		20.00					40,016.72	42,371.14	55,381.27	32.27	30.27	35.05
			999k	999k	998k				96.37									
1M	1M	1M				0.00		0.00										

CHAPTER 4 TOTAL SITE MATERIALS HEADERS/MAINS TARGETING FRAMEWORK USING PINCH FRAMEWORK AND OPTIMISATION

This chapter presents a framework for identifying material mains/headers for internal process (Chin et al., 2021e) or at the site-level using Pinch-based concept. Section 4.1 presents the explanation of the utilisation of Pinch-based Composite Curves in identifying the headers/mains based on the sources mixing for single quality. The Total Site headers targeting ensure the cross-plant sources transfer flowrate are minimal while ensuring the overall fresh resource required are minimal as well (Chin et al., 2021b). Section 4.2 extends the analysis to multiple qualities for a problem with the same type of resources. Section 4.3 presents the mathematical optimisation framework, and a result comparison between the two approaches are presented.

4.1 Headers/Mains targeting framework for single contaminant/quality

For material-based integration in the Total Site, Karuppiah and Grossmann (2006) developed the non-linear optimisation model for Total Site Water Integration considering various contaminants types. Chew et al. (2010a) introduced the unassisted integration scheme for a cross-plant transfer involving multiple processes. The concept is to utilise the unused or purged sources of one plant to another plant to minimise the fresh resource required and the total cross-plant transfer. The framework is applied for varieties of material types involving hydrogen, water or property-based integration. Chew et al. (2010b) extended the previous approach by another assisted integration scheme, which involves using high-quality sources from one plant to replace low-quality sources for another plant. Alnouri et al. (2018) proposed central and distributed options in site-level water integration to achieve zero liquid discharge. Aguilar-Oropeza et al. (2019) studied the acceptability of the network system in an industrial water park by proposing a strategy to generate a set of solutions with trading-off objectives and minimise the compromised solutions or dissatisfaction of each plant. Jiang et al. (2019) proposed a system with a water utility generation station in an industrial park. Different types of water utilities are produced, including desalted water in the utility generation station and can be shared among the plants. Boysen et al. (2020) evaluated the economic and environmental impacts of an industrial park in Germany and suggested that water reuse is an environmentally beneficial option.

Centralised material headers/mains allow maximisation of waste resources recycling and minimisation of piping connections between industrial plants in a Total Site. Feng and Seider (2001) introduced the plant-level centralised headers/main concept for the water recycle or reuse network design with concentration identified certain heuristic. Wang et al. (2013) extended it for multiple contaminants, and Cao et al. (2004) extended the concept accounting for the regenerated water main. Using a mathematical approach, Chen et al. (2010) developed a comprehensive mixed-integer non-linear programming (MINLP) method for Total Site Integration with centralised and decentralised water mains. They studied different design objectives involving minimum fresh resource consumption and minimum total annualised cost.

Their water mains concept assumes the mains are vessels connecting various plants. Fadzil et al. (2018a) proposed a step-by-step numerical targeting framework for headers with a pre-set number of headers and contaminant concentration range for water network, and Fadzil et al. (2018b) later proposed a U-shaped two ways centralised header concept as a pipeline connecting the multiple sites.

Based on the analysis, it is proven that the material headers/mains concept could aid in promoting the resource conservation practice by reducing the network complexity and enhancing the controllability of the integrated network. Material headers/mains are essentially mixers of material sources. Their parameters, including the total number of material headers, amount and quality of the header sources, are critical for processes. The existing studies on material reuse and network design mainly pre-define the parameters based on certain heuristics and excluding alternative source mixing options for the headers. The mathematical approach could solve the issues comprehensively, but it involves non-linear formulation with the flowrates and quality of the headers sources unknown. The computation burden of the model can be rather heavy, for which the users are not able to explore different design options swiftly. In this case, Pinch Analysis provides an insightful framework aided with visualisation to the optimal resources conservation strategies, providing lower or upper bounds on certain variables to complement the mathematical approach.

The analysis also shows that the determination of the number of headers/mains, flowrates and the qualities of material header sources at both processes and Total Site levels has not been systematically investigated previously. Other than determining headers' parameters, the total amount of cross-plant transfer in the Total Site should be minimised as well to reduce the capital cost for piping and operational cost for pumps/compressors' duty.

4.1.1 Internal process headers targeting

4.1.1.1 Water mains/header targeting for single Pinch Point

The water header/main is effectively a mixer of the available water sources followed by a splitter to the water sink links. As mentioned earlier, excessive source mixing could decrease the quality of the water sources. It is critical to determine the flowrates and the contaminant concentrations of the water header. An illustrative example of a process with its Source and Sink CC is presented in Figure 4-1. It is used to demonstrate the concept and the graphical method for the optimal selection of water headers and their concentration levels for a single contaminant.

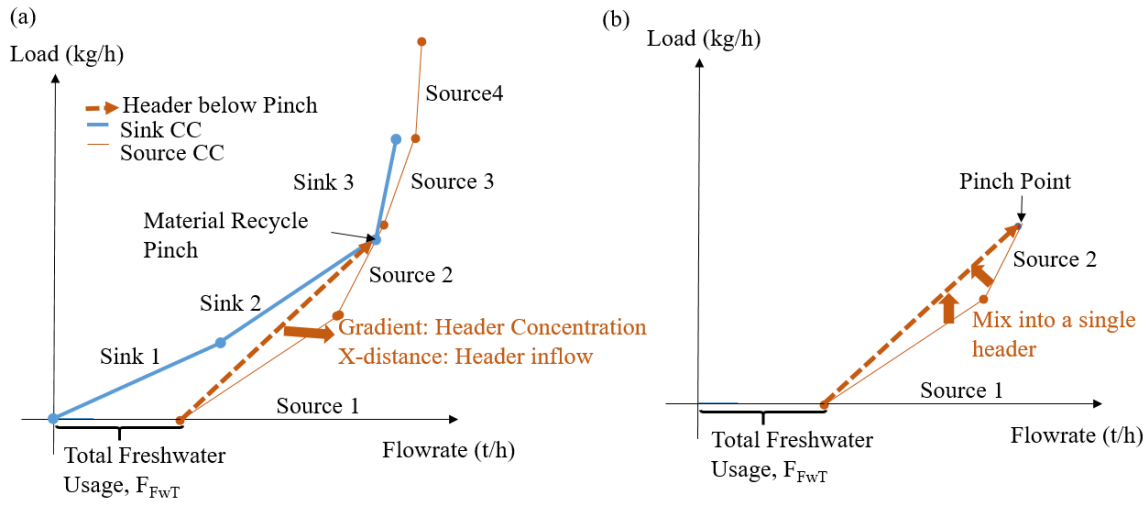

Figure 4-1: Illustrative example of constructing the header line for a single contaminant problem

Based on the configuration in Figure 4-1a, for the sinks below the Pinch Point, headers can be formed by mixing the sources in that part of the problem. The header line can be drawn from the starting point of the shifted Source CC to the Pinch Point to ensure the freshwater requirement is still minimised. The header line (the thick dashed arrow in Figure 4-1), in fact, can be regarded as another source line containing the mix of Source 1 and part of Source 2 (see Figure 4-1b). The contaminant load of the header is the summation of loads of Sources 1 and 2. The projection of the header line on the X-axis (flowrate) indicates the total sum of flowrates of the sources to be sent into the header and its gradient indicates the mixture concentration. Note that this header is responsible for supplying water to the sinks below the Pinch.

Assuming no direct recycle/reuse is allowed, another header is required for the remaining process sinks above the Pinch. A similar procedure can be followed, but the header line is drawn from the Pinch Point along the Source CC to cover the remaining sinks. The overall header targeting is shown by the demonstration in Figure 4-2. The header above the Pinch for this case is just part of Source 3. Overall, the total minimum number of headers required are four (two water-source headers with one below Pinch and one above Pinch, one freshwater header, and one wastewater header). However, in the illustrative case shown in Figure 4-2, the header above the Pinch can be just a single connection of Source 3 recycled back to Sink 3.

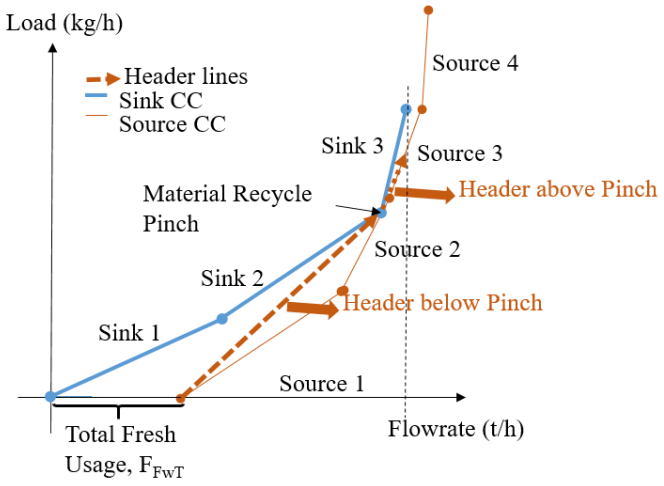

Figure 4-2: Overall water header targeting for the single contaminant illustrative process

A single header below the Pinch is usually not enough to serve all sinks without adding more freshwater. Consider a case where the header below the Pinch is drawn, but it crosses at the Sink CC (see Figure 4-3a). Note that the header line crosses the Sink CC at two points, i.e. at the Sink 1 portion and at the Pinch Point. This indicates there is too much mixing of the sources, which decreases the quality of the water in the header. This would cause an additional requirement for freshwater. The header line should be split below the Pinch to ensure that the freshwater target is still satisfied. Based on Figure 4-3b, Header 1 is formed by a part of Source 1, for which it is drawn from the starting point of Source CC and ends at the load point of Sink 1 (y-coordinate). The line for Header 2 is drawn from the ending point of Header 1 to the Pinch Point. For this scenario, there should be at least two headers formed for the sinks below the Pinch, while only one header is enough for the sink above the Pinch.

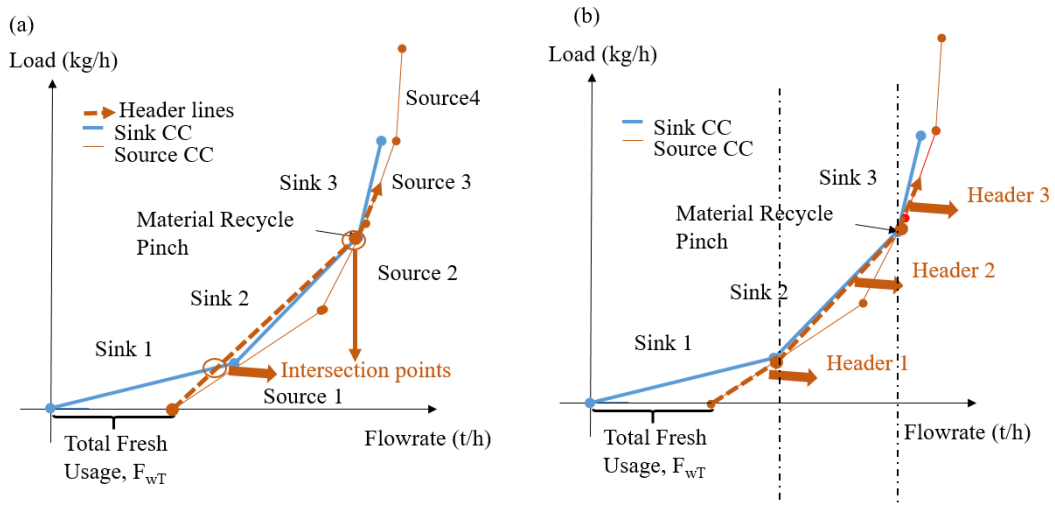

Figure 4-3: Single contaminant example (a) Single header below the Pinch is not enough (b) Another header is required by splitting the header lines

Notice that the lines representing Header 1 and Header 2 can have different lengths or different gradients. Different combinations of both header lines can be formed as long as the header lines

are below the Sink CC. This is to ensure the maximum contaminant limits for all the sinks are not violated and incurs additional freshwater requirements. It is indicated that the optimal number of water main can be identified, but the water profile (flowrate and contaminants concentrations) in the water mains are still variables. The water profile can be now targeted with the objective of minimum freshwater intake and total cost.

Similar concepts can be applied for site-level water integration. The Pinch Analysis combining the water sources and sinks from various processes can be grouped together to determine the overall water target. Headers targeting can now be performed. However, this approach assumes no internal integration at the process level. If integration at the process level is performed first, the targeting can be performed for the process before site-level integration.

4.1.1.2 Water mains/header targeting for multiple Pinch Points

There are certain occasions where there are multiple Pinch Points for the system. Figure 4-3a shows the Composite Curves representation for such a system. In this case, it is clear that a single header line is not sufficient for the sinks below the Pinch Points. Figure 4-3b shows the construction of the header lines. A single header line is drawn connecting the Source CC starting point to the first Pinch Point (header 1), and another header line is constructed connecting the First Pinch Point to the Second Pinch Point (header 2).

One can observe that the minimum number of header sources are at least equal to or larger than the number of Pinch Points for the system. For example, two Pinch Points indicate at least two headers from the sources are required. If there are no sinks above the Pinch Point, the system in Figure 4-4 require only two headers from the sources. However, the header lines might intersect at the sink CC as well. If there are any intersections at the header 1 or the header 2 lines, the header lines have to be split until no intersection occurs. The users are allowed to adjust the split ratio of the header lines at different combinations of the headers' flowrates and concentration, as long as they are below the Sink CC.

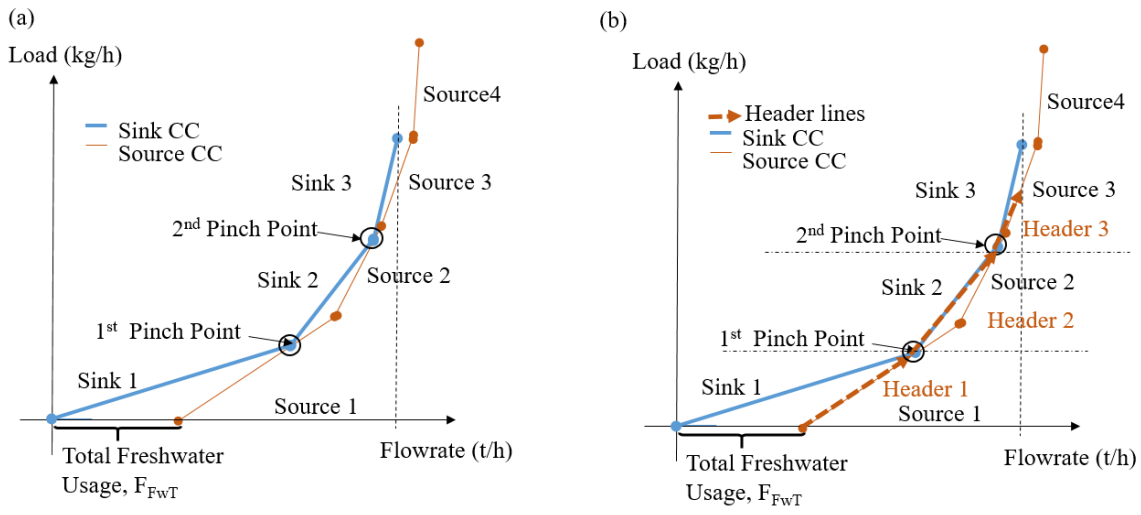

Figure 4-4: (a) Multiple Pinch Points for an illustrative system (b) Header lines construction for the Multiple Pinch Points problem

4.1.1.3 Water mains/header targeting for a threshold problem

There are also possibilities where the system is a threshold problem, i.e. no wastewater generations with or without Pinch Points. Figure 4-5a shows a scenario when there is no Pinch Point. This happens when the total flowrates of the available sources are less than the total flowrates of the sinks. In such a case, the header line is a mixture of all the sources. Another scenario when there are Pinch Point(s), but no wastewater generations are shown in Figure 4-5b. Similarly, the header line can be drawn from the Source CC starting point connecting to the Pinch Point. Note that intersection between the header lines and the Sink CC might happen as well.

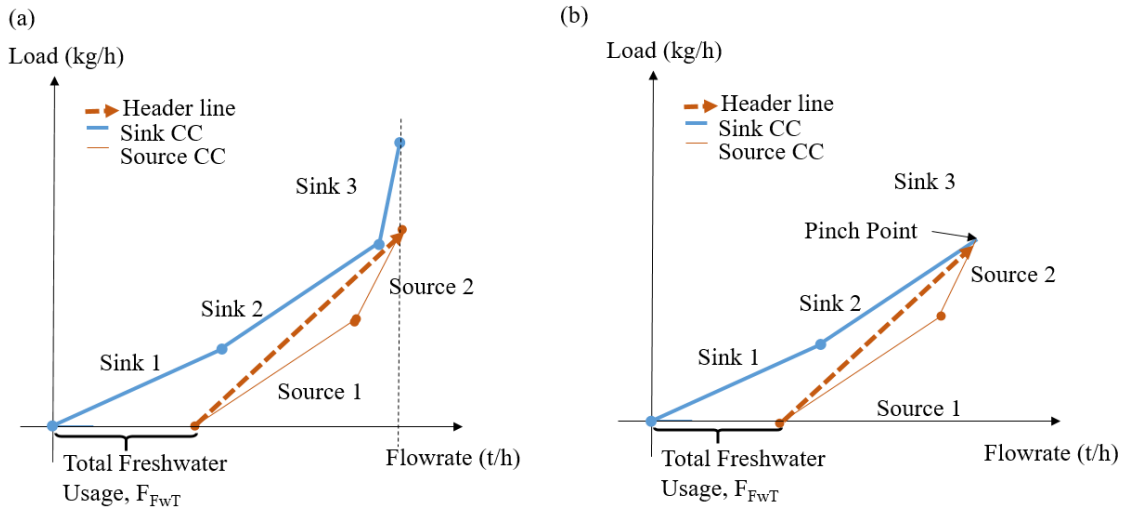

Figure 4-5: Threshold problem for an illustrative system (a) no Pinch Point (b) single Pinch Point

4.1.1.4 Overall procedure

The following procedure for headers targeting using the Composite Curves summarising the conceptual explanations from the previous sections is presented as follows:

- Construct the Composite Curves for the process/site to determine the freshwater target and Pinch Point(s).
- Draw a header line below the First Pinch Point, starting from the shifted Source CC initial point and connect to the Pinch Point(s).
- If there are multiple Pinch Points, connect the Pinch Points with the header lines
- Draw a header line above the last Pinch Point, starting from the Pinch Point along with the Source CC until the horizontal length matches where the Sink CC ends. (For single Pinch Point problem, first Pinch Point = last Pinch Point)
- Check if intersection(s) exists between the header lines and the Sink CC. If there are any, split the header lines, and draw the header lines with any combinations until the entire Header Curve is at the right side of Sink CC.

- Determine the number of headers (number of segments in the header lines), each header source's concentration (gradient) and flowrates (horizontal length).

Similar concepts can be applied for site-level Water Integration. The Pinch Analysis combining the water sources and sinks from various processes can be grouped together to determine the overall water target. Headers targeting can now be performed. However, this approach assumes no internal integration at the process level. If integration at the process level is performed first, the targeting can be performed for the process before site-level integration.

4.1.1.5 Case study and results

For internal water header design, the proposed graphical approach presented in Section 4.1.1.4 is applied to the plants specified in Table 4-1. The step-by-step framework is demonstrated in this section, and can be found in Chin et al. (2021d).

Table **4-1**: Total Site data for a single contaminant case (Fadzil et al., 2018)

	Plant 1			Plant 2			Plant 3			Plant 4			Plant 5	
	F_{SR} (t/h)	C_{TDS} (ppm)		F_{SR} (t/h)	C_{TDS} (ppm)		F_{SR} (t/h)	C_{TDS} (ppm)		F_{SR} (t/h)	C_{TDS} (ppm)		F_{SR} (t/h)	C_{TDS} (ppm)
SR1	200	50	SR1	50	50	SR1	100	130	SR1	20	50	SR1	20	130
SR2	80	100	SR2	250	100	SR2	120	290	SR2	80	100	SR2	100	130
SR3	80	100	SR3	150	130	SR3	85	300	SR3	100	125	SR3	40	250
SR4	140	150	SR4	150	250	SR4	200	350	SR4	100	150	SR4	25	400
SR5	200	200							SR5	50	800			
SR6	200	450												
	F_{SK} (t/h)	Z_{TDS} (ppm)		F_{SK} (t/h)	Z_{TDS} (ppm)		F_{SK} (t/h)	Z_{TDS} (ppm)		F_{SK} (t/h)	Z_{TDS} (ppm)		F_{SK} (t/h)	Z_{TDS} (ppm)
SK1	200	0	SK1	50	20	SK1	100	0	SK1	20	0	SK1	20	0
SK2	80	50	SK2	250	50	SK2	120	100	SK2	80	25	SK2	100	50
SK3	80	50	SK3	150	100	SK3	85	125	SK3	100	25	SK3	40	80
SK4	140	100	SK4	150	200	SK4	200	300	SK4	100	50	SK4	25	100
SK5	200	120							SK5	50	100			
SK6	200	200												

Step (i): Determine initial Composite Curves for the plant. Figure 4-6 shows the Composite Curve representation for plant 1. Figure 4-6a shows that there are two Pinch Points for the process.

Step (ii) and (iii): Construct header lines below the Pinch Point and above the Pinch Points. As the problem has two Pinch Points, a header line for the sinks below the Pinch can be drawn – Step (ii), and another header line is drawn connecting the two Pinch Points – Step (iii).

Step (iv): Check for any intersections between header lines and Sink CC. it is needed to check whether there is an intersection between the drawn header lines and the Sink CC. For plant 1, Header 1 alone is not feasible as it is above the Sink CC, and it shows there are two intersection points: the first Pinch Point and the Source CC starting point. This means another one header line is needed for below the first Pinch. Figure 4-6b shows the overall header lines with a total of three header segments. As the header curves are now entirely under Sink CC, the headers mix is feasible.

Step (v): Determine headers' properties. The headers, sources flow, and concentration can be determined. Header 1 is made up of Source 1, Header 2 is made up of the mixture of SR2, SR3 and SR4, while Header 3 is made up of SR4. The gradients of the header line segments represent the concentration of the headers. The flowrates and the concentrations of each header using the configurations in Figure 4-6b are Header 1: (200 t/h, 50 ppm), Header 2: (293.33 t/h, 122.73 ppm), Header 3: (200 t/h, 200 ppm).

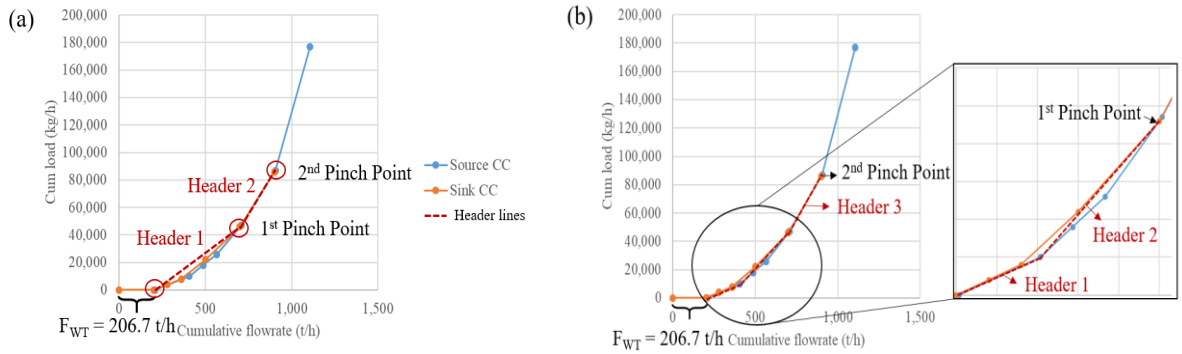

Figure 4-6: Internal water mains design for single contaminant using Composite Curves for plant 1

A similar procedure is repeated for other plants. Figure 4-7 shows the Composite Curves with all the header lines for Plants 2, 3, 4 and 5. A minimum of three headers from the mixture of sources is required for Plant 2, while Plants 3 and 4 require at least 2 headers from the sources. Only a single header is needed for Plant 5.

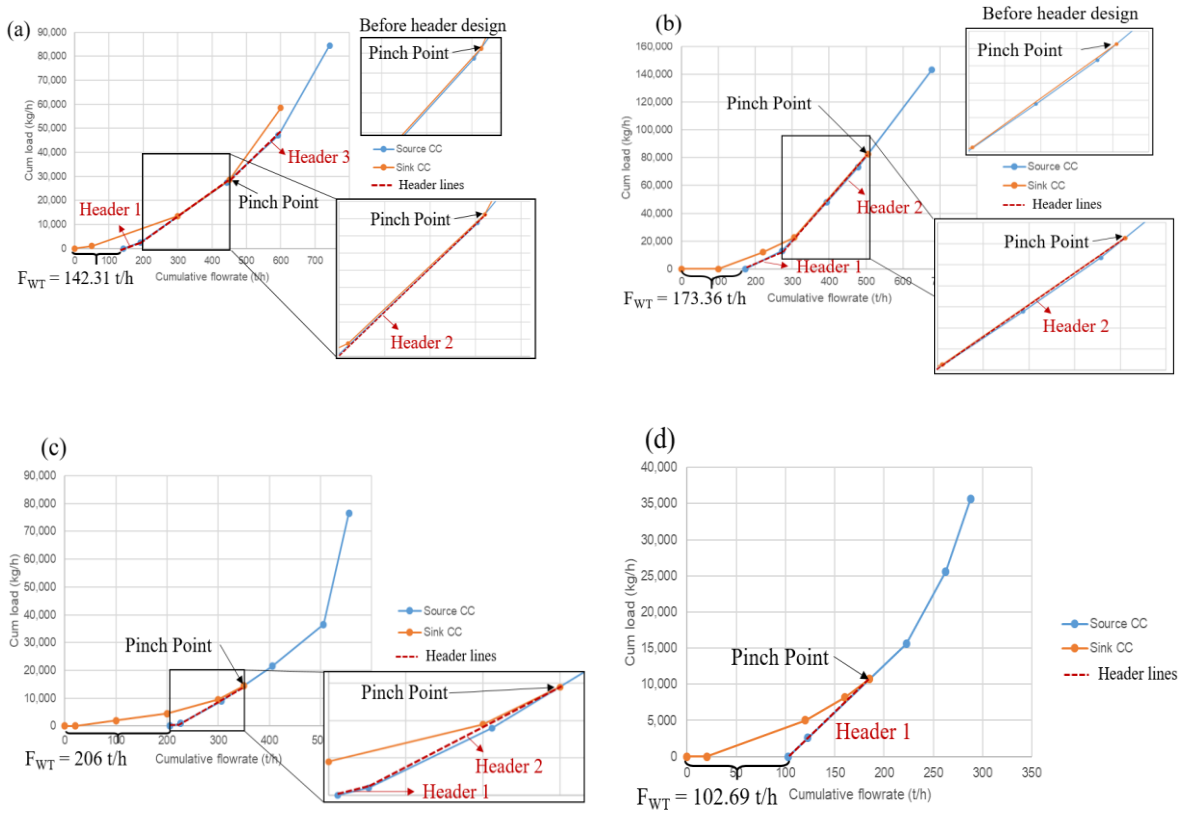

Figure 4-7: Internal water mains design for single contaminant using Composite Curves for (a) Plant 2 (b) Plant 3 (c) Plant 4 (d) Plant 5

4.1.2 Total Site headers targeting

For Total Site Material Integration, the optimal overall fresh resource consumption can be achieved by exploiting the reuse potential of the unused sources in LQR from different plants. The cross-plant transfer should also be minimised to reduce network complexity. The aim of targeting cross-plant source transfer is to minimise the total cross-plant flows while ensuring the overall fresh resource target is achieved. The fresh resource target can be identified using the Composite Curves, where all sources and sinks from each plant can be treated as they are from a single process. This approach is called the single network targeting (Chew et al., 2010a). However, this approach involves a lot of cross-plants source transfer, which require high capital cost for piping. If one is to use the typical CC to identify the network design, the sources in the HQR for different plants are actually shared among each other, which do not affect the overall fresh resource target. This is actually wasting the potential of the sources while increasing the cross-plant flow. It is first required to understand various cross-plant transfer schemes available for the Total Site to ensure effective utilisation of the sources.

4.1.2.1 Minimal cross-plant sources transfer schemes

Various feasible cross-plant transfer schemes can be identified using the Pinch-based strategy. The potentially best case for a cross-plant transfer scheme is the source transfer from the LQR of one plant to the HQR of another plant. This is because LQR does not require a fresh resource,

but HQR requires fresh resources, and source transfer from LQR to HQR could help to reduce the fresh resource intake and waste generation. It is to be noted that the mass is balanced in LQR and HQR, i.e. Inlet $flow_{HQR/LQR}$ = Outlet $flow_{HQR/LQR}$. The mass is conserved in the overall system as well. The mentioned scheme is illustrated in Figure 4-8. Using as an example a site comprising two plants, it can be noted that part of the sources from LQR in plant A (e_A) is transferred to the HQR of plant B. By material balance around LQR in plant A, the waste discharge of the plant is reduced by e_A amount. As this amount is transferred to HQR in plant B, this actually reduces the fresh resource requirement for plant B by an amount of e_A due to material balance in HQR.

The transfer is usually possible in one direction only as the LQR sources of plant A is better than the HQR of Plant B (Pinch Point of B is higher than in A). However, there can be occasions that the Pinch Point for Plant B changes as a result of the transfer from Plant A and becomes lower, and the LQR sources from Plant B have better sources. This happens as the Pinch-causing source in plant B is replaced with a source from plant A, but a new lower Pinch Point may form in plant B. For a better illustration of this scenario, the reader can refer to Section 3.2.3 Figures 11. The new LQR source from Plant B can be transferred to Plant A. Assuming part that of source (e_B) of the LQR in Plant B is transferred to the HQR in Plant A, that would reduce the fresh resource intake for Plant A as well. Overall, the total fresh resource consumption and the total waste generation are reduced by (e_A+ e_B) amounts.

This scheme is possible only when the purged source from a plant has better quality than some of the sources in another plant. For example, if the purged sources from plant A is 130 ppm, and the Pinch-causing source from plant B is 150 ppm, the transfer of purged sources from plant A to plant B could reduce the fresh resource requirements for plant B. As long as there is a transfer from an LQR of one plant to the HQR of another plant, there are guaranteed to be some reduction of fresh resource intake. This is actually the concept of an unassisted integration scheme proposed by Chew et al. (2010a).

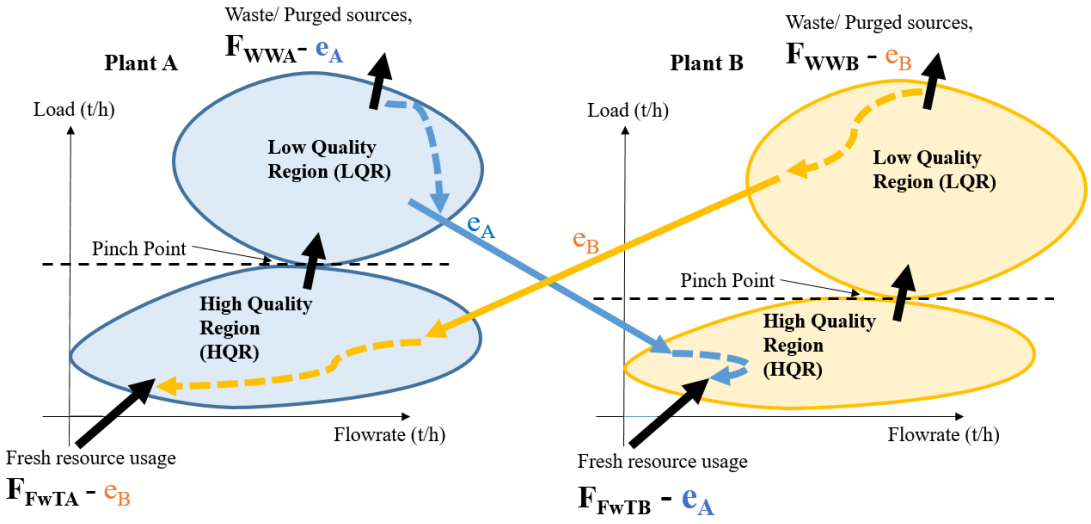

Figure **4-8**: Cross-plant transfer Scheme 1: LQR to HQR only

The transfer from the HQR of a plant to the LQR of another plant is usually not preferable as this increases the fresh resource intake for the plant that send out the sources. However, this scheme is possible if it is accompanied by another transfer from an LQR to the HQR. This is demonstrated in Figure 4-9. Plant A has sent some amount of sources (e_A) from its HQR to the LQR of plant B, and this causes the increment of fresh resources for plant A by (e_A) amount. Plant B then sends some amount of sources from its LQR to the HQR of plant A by (e_B) amount, and the changes in fresh resource intake in total is for plant A is (e_A- e_B). It is obvious that the overall fresh resource intake can be reduced only if $e_A < e_B$.

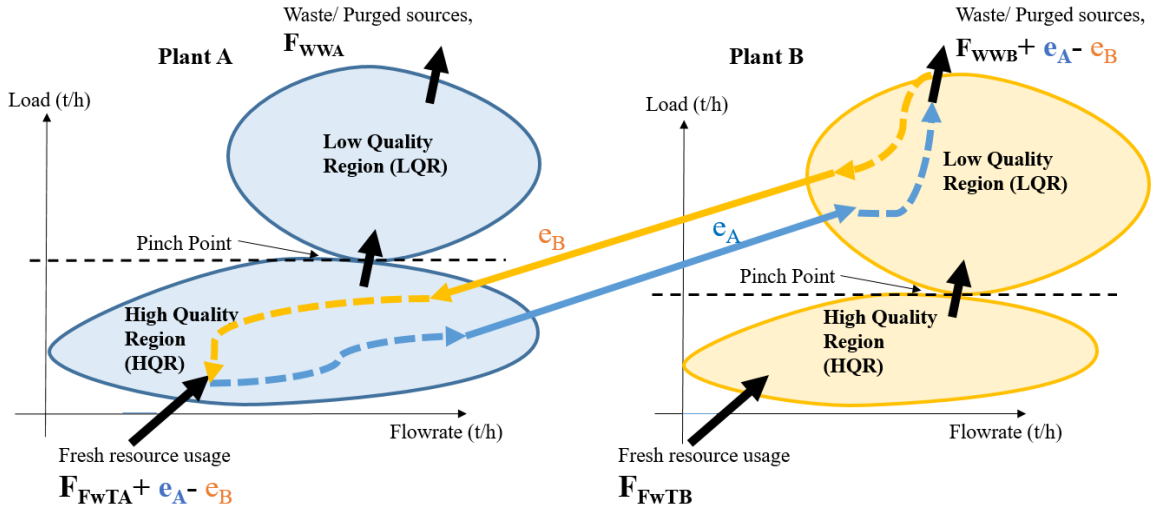

Figure **4-9**: Cross-plant transfer Scheme 2: HQR to LQR + LQR to HQR

This second scheme is applied when the Pinch-causing source of one plant is lower than the Pinch Point concentration of the Total Site. For example, let's say the Pinch concentration for the Total Site is 200 ppm (identified by the single network targeting method), and the Pinch-causing source of plant B is 150 ppm. Assuming there are sinks in the LQR, some of the Pinch-causing sources for plant B is given to the sinks in the LQR. The Pinch-causing source for plant B is actually wasted for sinks in LQR. Let's say the Pinch-causing source for plant A is 200 ppm (or ≥ 200 ppm), and this means the LQR sources in plant B has better quality than some sources in HQR in plant A. The Pinch-causing source for plant B (e_B) actually can be transferred to HQR in plant A since it is lower than the Pinch concentration of plant A, and this could reduce the fresh resource intake for plant A. The Pinch-causing source in the LQR for plant B can be replaced by using the Pinch-causing source in the HQR in plant A (e_A) To maintain the balance of the sinks in LQR for plant B. In this scenario, since the concentration of transferred sources from plant A is higher than plant B, the replacement amount from plant A (e_A) is always lower than the Pinch-causing source that is replaced in plant B (e_B) due to constant load (e_A x 200 = e_B x 150). This guarantees the reduction of fresh resource intake. This is actually the concept of assisted integration scheme proposed by Chew et al. (2010b). and the readers could refer to it for a more detailed explanation of this scheme.

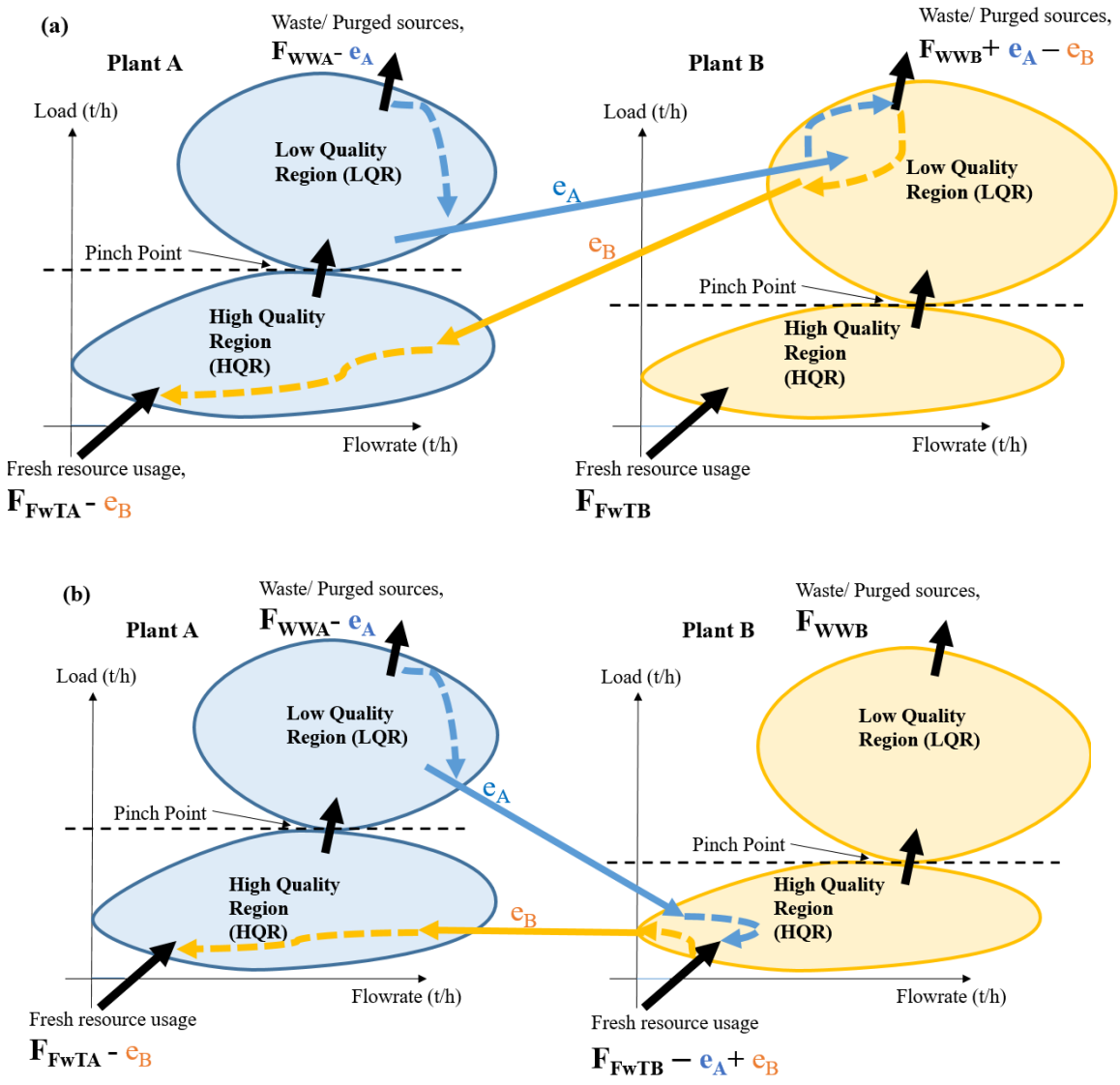

Figure 4-10: Cross-plant transfer schemes (a) Scheme 3: LQR to LQR + LQR to HQR (b) Scheme 4: HQR to HQR + LQR to HQR

Other various transfer schemes are possible. Scheme 3, according to Figure 4-10a, involves the transfer of sources from LQR to another LQR section of another plant. In the perspective of Total Site Integration, this cross-plant transfer from one LQR to another LQR is futile as the total waste generation is the same. The transfer amount (e_A) does not alter the total waste generation. If it is combined with Scheme 1 (LQR to HQR), the total fresh resource and waste generations could be reduced. Scheme 3 is only applicable when the Pinch-causing source with Site Concentration is needed. For example, let's say the Site Pinch Point is at 200 ppm. If plant B has an LQR sink that is fulfilled by a 200 ppm source, the source can be replaced by another LQR source from another plant that has ≥ 200 ppm. This is to preserve the 200 ppm source as it can be used for another plant. This is applicable when no other better quality sources are available. However, this condition is applied only when the LQR sink has a higher concentration than the replacing LQR source. If the LQR sink is 300 ppm and the replacing

source is 250 ppm, this is a feasible scheme. In such a case, replacing the source, which is 250 ppm, which requires (e_A) amount, would be lower than the replaced LQR source amount (e_B), which is 200 ppm, due to constant load (e_A x 250 = e_B x 200). Since $e_A < e_B$, both total fresh resource and waste generation can be reduced.

Similar reasons apply to Scheme 4 (Figure 4-10b) but for reducing individual fresh resource consumptions if no other transfer is possible, only if ($e_A > e_B$). This Scheme is applicable when the replacing source (e_A) has better quality than the replaced source (e_B). This is because no individual plant would sacrifice its HQR sources for other plants without benefiting from them. In this work, the focus is to reduce the total fresh resource consumption, so mainly, Scheme 1, 2 and 3 are considered in the algorithm as explained in the later section.

4.1.2.2 Data Extraction for Total Site Methodology

Prior to performing targeting for Total Site integration, it is important to extract the correct data from the process. Similar to Chew et al. (2010a), the extracted data should contain all the sources and sinks in the HQR, with the remaining unused or purged sources. The aim of the Total Site targeting is to identify the overall fresh resource target based on available sources. The sources and sinks in the HQR are selected for the Total Site because the sinks can be fulfilled by any unused/purged sources from other plants, which further reduce the individual fresh resource target. The sinks in the LQR and the sources allocated for them can be removed from Total Site targeting. This is because they are already fulfilled with no fresh resource necessary and fulfilled by the sources from the internal process.

Note that the Pinch-causing sources in the LQR should be reduced, and the quality limit for the LQR sinks should be satisfied by performing waste targeting. The procedure of data extraction follows the steps described in (Chew et al., 2010a) and is shown in Figure 4-11. Figure 4-11a represents the CC for an individual plant. The sink in the LQR and sources associated with the sink is removed, with the remaining as the extracted data for the Total Site- Figure 4-11b. The next sub-section explains the procedure to apply various cross-plant transfer schemes to achieve the overall minimum fresh resource target.

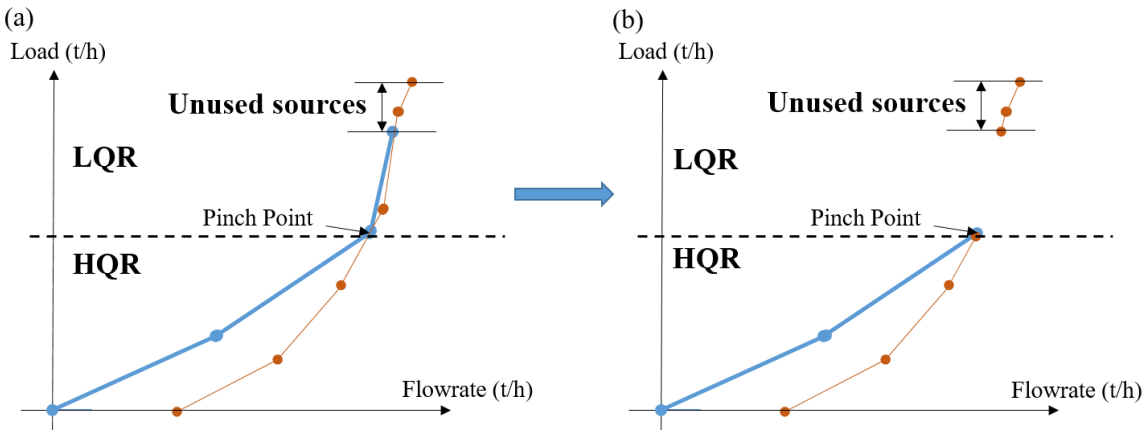

Figure 4-11: (a) Composite Curves for an individual process (b) Extracted data for Total Site targeting

4.1.2.3 Source Transfer Diagram

Based on the cross-plant transfer scheme 1 (LQR to HQR only), the unused or purged sources from LQR in one plant can be transferred to the HQR of another plant. This applies only when the purged sources have better quality than the sources in the HQR of the other plant. In this work, a diagram called Source Transfer Diagram is proposed to identify transfer the unused or purged sources for the sources in the HQR. The diagram is composed of quality (e.g. concentration for water case) in the y-axis, while the x-axis contains the load of the source streams. The reason the load is used as the x-axis instead of flowrate is that the flowrates of the unused source to be transferred are not the same as the flowrates of the HQR source to be replaced. This is due to their qualities (concentrations) are different. However, the load of the transferred source should be identical to the load of the replaced source.

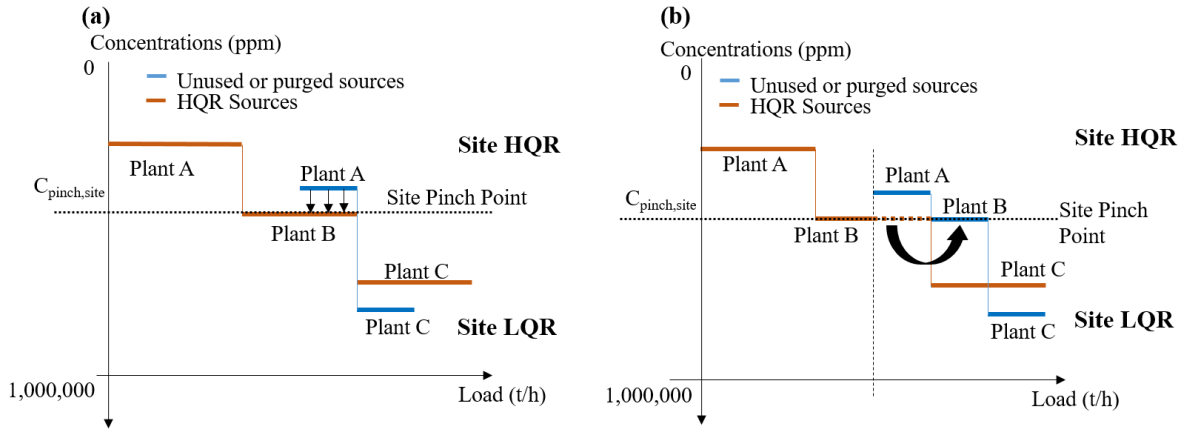

Figure 4-12: Source Transfer Diagram for (a) prior to cross-plant transfer (b) new purged sources are available with the replaced HQR sources

Two-step curves are plotted in this diagram, i.e. step curve containing HQR sources from each plant and another with the unused or purged sources. This is demonstrated in Figure 4-12. The HQR sources curve is constructing the sources in descending order of the quality (ascending order of concentrations), where each line segments represent an HQR source from a plant. The next source segment is then plotted after the previous source segment. The purged source curve is constructed in a similar manner but using the purged sources in LQR. Figure 4-12a shows the illustration of the Source Transfer Diagram prior to cross-plant transfer. The unused/purge source curve is moved until the right side of its first segment is matched with the right side of the segment of the HQR source curve right below it.

Based on Figure 4-12a, all unused sources from plant A could be transferred to plant B since the unused sources are cleaner than the HQR source in plant B. The Site Pinch Point line is also plotted in the diagram. It should be noted that the Site Pinch Point always occur at one of the HQR sources. Assuming the purged source from plant A has a lower concentration than the Site Pinch concentration, this source should be in the HQR for the Total Site, which means it should be fully reused. Replacing the HQR source in plant B helps to reduce the fresh resource intake while ensuring the purged source is utilised properly. The CC representations are shown

in Figure 4-13a and b, where the Pinch-causing source in the HQR for plant B is replaced by the unused sources from other plants. The fresh resource target can then be reduced by shifting the new Source CC in the HQR to the left until it touches the Sink CC- see Figure 4-13c. The replaced Pinch-causing source becomes the new, unused source stream and can be potentially transferred to another plant. The Source Transfer Diagram is then updated to account for the new, unused sources in Figure 4-13b. Based on the figure in this example, the new, unused sources can be further transferred to the HQR of plant C.

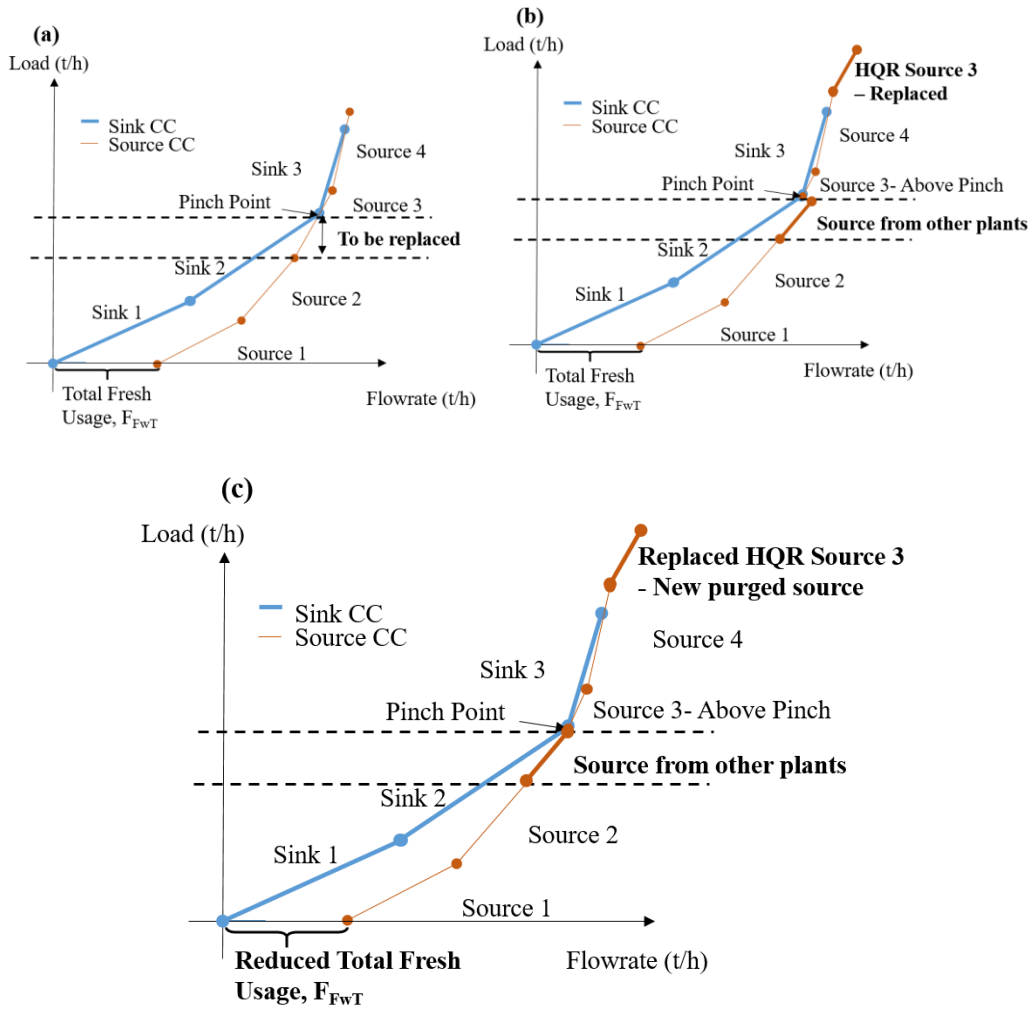

Figure 4-13: (a) The source to be replaced by the purged sources from other plants (b) Source from other plants replace the original source (c) freshwater target for the individual plant is reduced and the replaced source becomes the new purged source.

However, replacing the HQR sources with cleaner purged sources not always results in the same Pinch Point as the original identified Pinch Point. This scenario is demonstrated in Figures 4-14a and b. In Figure 4-14b, Source 1 becomes the new Pinch-causing source for the process, and the subsequent sources become the LQR sources. In this case, the Source Transfer Diagram has to be updated with the new purged sources.

The Source Transfer Diagram is mainly to match the unused sources from the LQR of one plant with the sources in the HQR for another plant. This follows the cross-plant transfer scheme 1 with LQR to HQR transfer only. Scheme 2 (HQR to LQR + LQR to HQR) requires manual identification of the Pinch-causing source that has a lower concentration than the Total Site Pinch Point. The cross-plant source transfer has to be identified after the data extraction step. The full cross-plants source targeting and network design framework are described in Section 4.1.2.5

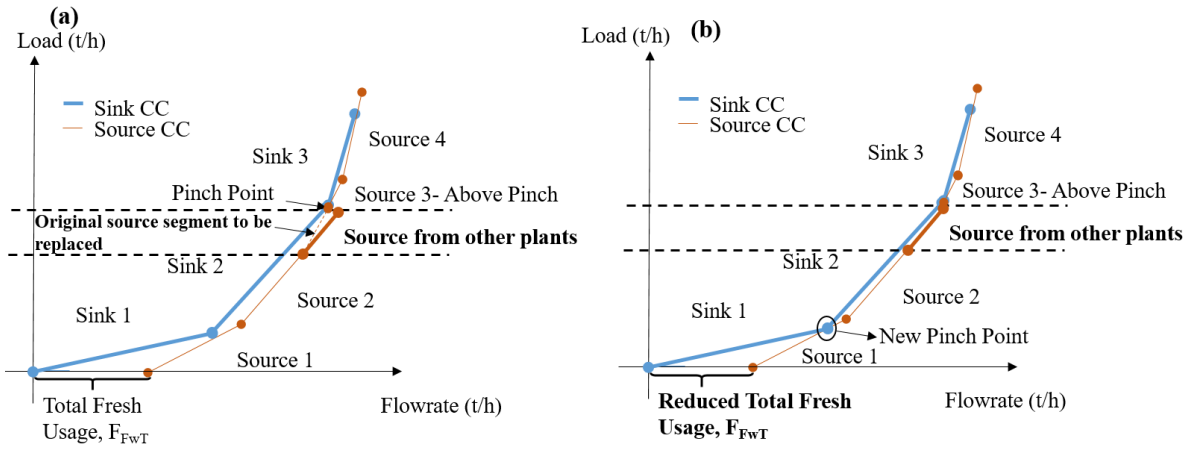

Figure 4-14: (a) Replacement of sources in the HQR by sources from other plants (b) New Pinch Point is formed at a higher quality (lower concentration)

Figure 4-15a shows a case where one of the purged sources from a plant and the HQR source from another plant have lower concentrations than the Site Pinch Point. In this case, the cleanest purged source can be reused to replace the HQR source in plant B, as shown. However, this transfer is actually less effective and require more cross-plant transfer (total 4 transfers). The cleanest purged source from plant A is supposed to be in the HQR for the Total Site. Using it to replace the HQR source in plant B, which is also in the HQR for the Total Site, actually does not alter the total fresh resource target when both of them are in the HQR. The cleanest purged source from plant A can instead be used to replace the HQR sources from other plants that have lower qualities than the Site Pinch Point (in LQR for Total Site) – see Figure 4-15b. The plant A purged source can be used to replace plant C sources, and the replaced source as well as the plant B purged source can be used to plant D. This transfer scheme requires fewer cross-plant transfers (total 3 transfers) and would yield the similar fresh resource target as compared to Figure 4-15a. This is actually similar to swapping the arrangement of the source in the Site Source CC arrangement. Even though replacing the plant B source shown in Figure 4-15a could yield better quality purged sources, a more cross-plant transfer is needed and can be unnecessary for Total Site fresh resource targeting.

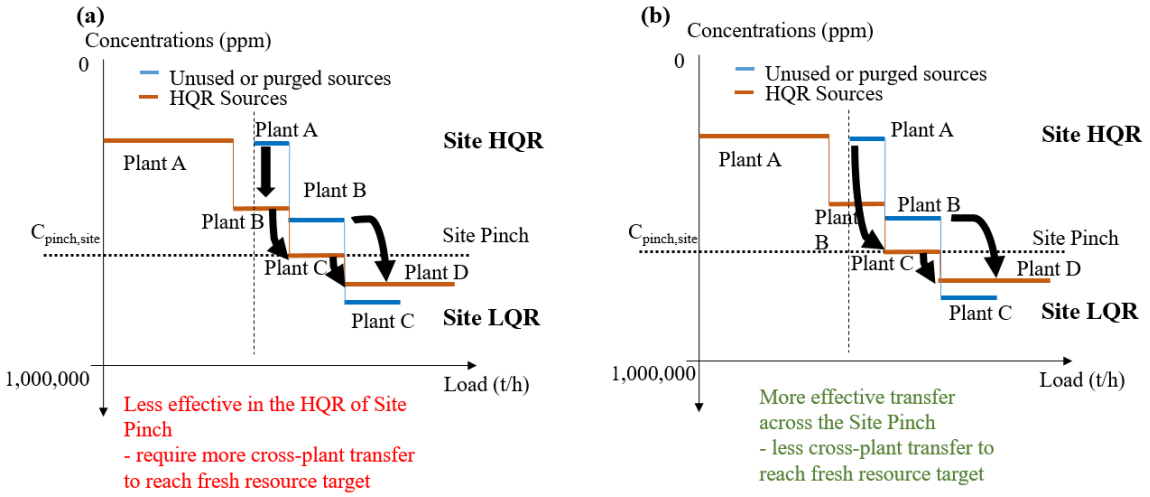

Figure 4-15: (a) Less effective Source Transfer in the HQR of Total Site (b) Better Source Transfer with the purged source to the HQR sources across the Site Pinch Point

Similar reasoning applies to the transfer of the source in the LQR of Total Site. The purged sources transfer to the HQR sources, which are in the Site LQR, is less effective in reducing the fresh resource - see Figure 4-16a. Even though some reduction in the fresh resource can be obtained, in Site CC, these sources do not alter the fresh resource target. The cleaner source is not fully utilised. The transfer is more effective when the purged source has at least higher quality (lower concentration) than the Site Pinch- see Figure 4-16b.

Based on this observation, it is thus proposed that the purged source should always transfer across or at the Site Pinch. The purged source should replace the HQR sources, which are at least lower quality (higher concentration) than the Site Pinch Point, or the purged source should always at least higher quality (lower concentration) than the Site Pinch Point. It should be noted that the Site Pinch Point always exists at one of the HQR sources.

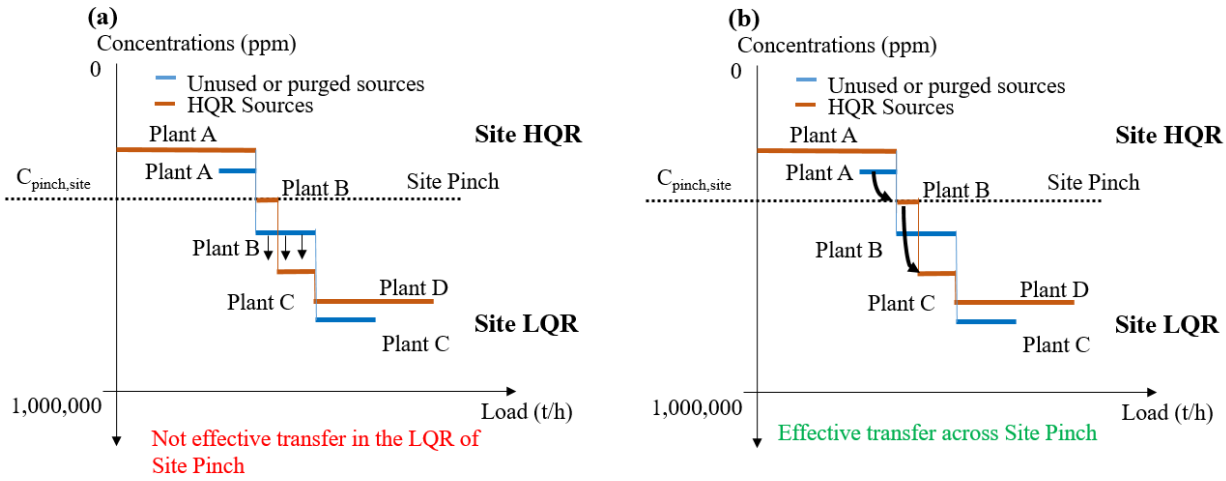

Figure 4-16: (a) Less effective Source Transfer in the LQR of Total Site (b) Better Source Transfer with the purged source to the HQR sources across the Site Pinch Point

4.1.2.4 Headers Targeting for Total Site

Identification of the headers using the Total Site Composite Curves requires first the determination of which sources are the cross-plant transfer source streams in the Site Source CC. The targeting of minimal cross-plant source transfer and the network design should be performed prior to header targeting and design. The Site Composite Curves containing the extracted sources and sinks from individual plants can then be constructed, and the cross-plant source streams can be identified. Figure 4-17a shows an example of the Site Composite Curves, with labelled cross-plant streams. The cross-plant source streams can then be mixed to determine the flowrate and the quality of the Total Site header. In the example of Figure 4-17b, it shows a single header below the Site Pinch Point is enough for the sinks. It is worth noting that in this example, the identification of the header is similar to swapping the position of cross-plant Source 2 and Source 1 (see Figure 4-17b). As identified earlier in Section 3.1, swapping the position of the source streams below the Pinch Point or the HQR do not alter the overall fresh resource requirement.

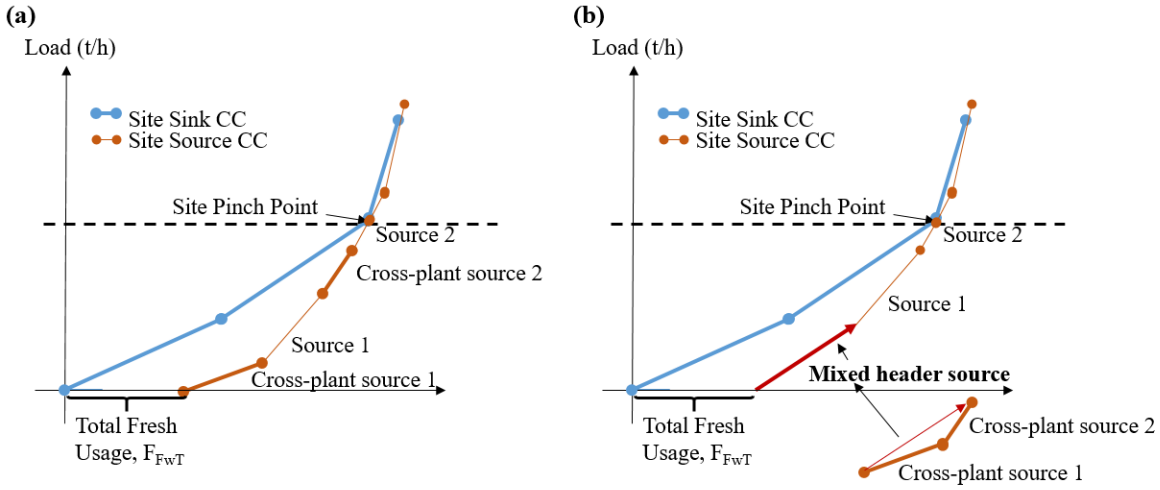

Figure 4-17: (a) Site Composite Curves with labelled cross-plant source streams (b) Mixed header source from the cross-plant sources streams.

In Figure 4-17b, the header source formed by the mixture has a higher quality than Source 1, and so its segment should be located before Source 1. Since the source segments are in ascending order, the new Source CC with the header segment should be located at the right of Sink CC without an interception point. If the header source mix causes the intersection between Source CC and Sink CC – see Figure 4-18a, this indicates not all cross-plant source streams can be mixed. In the example in Figure 4-18, at least two headers are required for the Total Site network. One of the options for this example is to not mix both cross-plant sources at all, and each of them can represent a single header- Figure 4-18b. However, this is not the only solution. The cross-plant Source 1 can be mixed with part of the cross-plant Source 2 to form a header. As explained before, as long as the Site Source CC with the headers does not cross the Site Sink CC, the headers mix is feasible with the identified fresh resource target. Note that this

applies when the Site Source CC segments are arranged in ascending order of the sources' gradient (impurity) only.

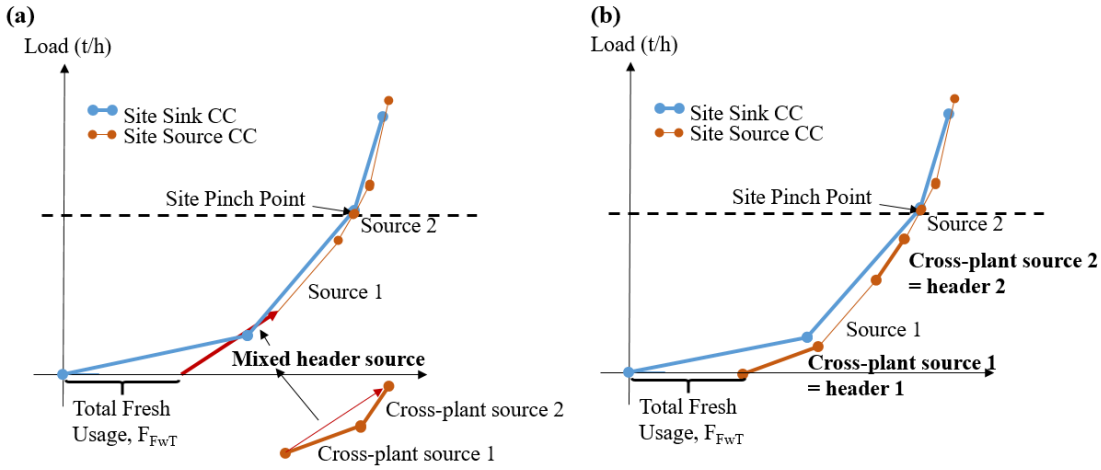

Figure 4-18: (a) Site Source CC with header segment crosses at the Site Sink CC (b) Two headers below the Site Pinch Point with both cross-plant source streams are not mixed

As a summary, the Total Site headers/mains targeting step can be summarised as follows:

a. Construct the Site Composite Curves to determine the fresh resource target for direct recycling or reuse with the cross-plant source streams marked.

b. For below the Pinch region (HQR), to group the cross-plant source segments below the Pinch together in the Site Source CC. Draw a header line by mixing all the cross-plant sources.

c. Arrange the Site Source CC with a header segment with ascending order of the gradient.

d. Check if intersection(s) exists between the new Site Source CC and the Site Sink CC. If there are any, split the header line, and draw the header lines with any combinations (along with the cross-plant source streams segments) until the entire Site Source CC is at the right side of Sink CC. (No. of intersections = minimum no. of headers below Pinch).

e. Repeat steps (ii) to (iv) above the Pinch region (LQR).

f. Determine the number of headers (number of segments in the header lines), each header source's concentration (gradient) and flowrates (horizontal length).

4.1.2.5 Overall framework

The overall proposed Total Site Material Headers/Main targeting and design framework summarising the conceptual explanation in Section 4.1.2 is presented in Figure 4-19. The general framework can be divided into four main hierarchical steps:

(i) Data extraction from each individual process
(ii) Identification of Site Pinch Point and minimum total fresh resource intake with CC
(iii) Optimise the cross-plant source transfer and fresh resource intake
(iv) Headers targeting and network design for Total Site.

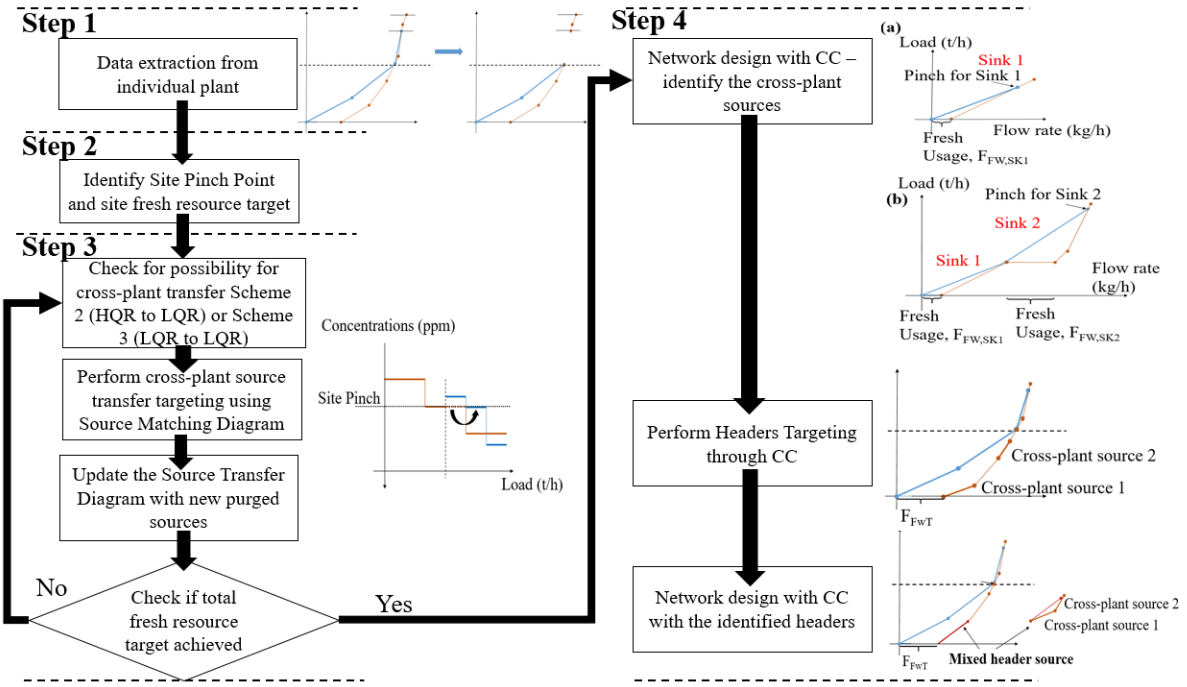

Figure 4-19: Flowchart of the proposed Total Site Material Integration with a headers design framework

The first step involves the data extraction stage, where the CCs are first constructed for each individual plant. Sources and sinks in the HQR and the unused sources in the LQR are extracted – see Section 4.1.2.2. The second step involves the identification of the Pinch Point and the minimum fresh resource for the Total Site. The fresh resource target identified serves as the ultimate goal of this framework. The third step is to determine the optimal cross-plant source transfer by reusing the unused or purged sources from each plant. It is first required to check whether there is a possibility to transfer sources from HQR to LQR with Scheme 2 (where the Pinch-causing source of one plant has a lower concentration than the Site Pinch Point), or LQR to LQR with Scheme 3 (where an LQR source of a plant higher than Site Pinch Point can be used to replace the LQR Pinch-causing source of another plant, provided the impurity of the LQR sink fulfilled by the Pinch-causing source is higher than the Site Pinch Point). If a Pinch-causing source has a lower concentration than the Site Pinch Point, all of it should be in the HQR of the Total Site, and it should not be wasted to use for sinks in the LQR. The sinks in the site LQR should be fulfilled by the site LQR sources as well. The readers are referred to as Chew et al. (2010b) for the detailed method for Scheme 2. The Source Transfer Diagram is proposed as the graphical tool to determine the optimal utilisation of the purged sources (cross-plant transfer Scheme 1: LQR to HQR only). The new source allocation has to be checked with CCs for each plant. This step is carried out iteratively until the total fresh resource requirement is identical to the resource target for the Total Site identified in the second step. The final step is to identify the cross-plant source streams, and they are used to determine the minimum number of headers, optimal flowrates and concentrations of the headers/mains. The full methodology is demonstrated with a case study in the following section.

4.1.2.6 Case study and results

The selected case study is the water allocation problem with a single contaminant. The data required for this study are presented in Table 4-1. Details can be found in Chin et al. (2021b)

Step 1: Data extraction from each plant. The Total Site sources and sinks are first extracted from the individual plant. The sources and sinks in the HQR and the unused sources in the LQR are extracted to the Total Site. The LQR unused sources should also contain the Pinch-causing source as the waste targeting should be performed on the sinks in the LQR. The Composite Curves for each plant are now shown. Table 4-2 shows the extracted data for each plant. The freshwater targets and the Pinch-causing sources are targeted. Note that in Plant 1, the Pinch-causing source is supposed to be SR5. However, as SK6 has identical flowrates and quality with SR5, the entire SR5 is used for SK6. The SR4, which is better quality than SR5, is preserved, and it becomes another Pinch-causing source. This plant contains two Pinch-causing sources, but SR4 is the primary Pinch-causing source (150 ppm). The summation of the freshwater requirement for all plants is 831.03 t/h.

Step 2: Identification of Site Pinch Point and minimum total fresh resource intake. The next step then involves the identification of the Site Pinch Point and the minimum fresh resource intake using the extracted data. Using the Composite Curve representation, the Site Pinch Point is determined as 130 ppm, and the overall fresh resource target is identified as 765.96 t/h, as shown in Figure 4-20. This clearly shows that there is room for improvement.

Step 3: Optimise the cross-plant source transfer and fresh resource intake.

Step 3a: First iteration. According to the flowchart presented in Figure 4-19, it needs to be checked whether any Pinch-causing source has a lower concentration than the Site Pinch Point (for Scheme 2). If it has a lower concentration than the Site Pinch Point, all of it should be in the site HQR, and it should not be wasted to use for sinks in the LQR of the process. From the extracted data in Table 4-2, it can be seen that the Pinch-causing source for Plant 4 has a concentration of 125 ppm (SR3), which is lower than Site Pinch Point (130 ppm). The SR3 allocated for the sinks in LQR can be replaced by a lower quality source ($\geq$ 130 ppm) in HQR of other plants. However, all of the sinks for Plant 4 are actually in the HQR, and they are not removed. In this case, there is no need for cross-plant transfer Scheme 2 (HQR to LQR + LQR to HQR), and the cross-plant transfer Scheme 1 (LQR to HQR only) should be enough to reach the overall fresh resource target.

The Source Transfer Diagram is plotted using the extracted unused/purged sources and the HQR sources in Figure 4-21. The purged source curve should be moved until its first segment is on top of the HQR source of the first segment. It can be seen that the Pinch-causing source for Plant 4 (SR3) in the LQR (125 ppm) could be used to replace the HQR sources with various concentrations: 130 ppm, 150 ppm and 290 ppm. As mentioned earlier, the most effective cross-plant sources transfer is to transfer the purged sources across the Site Pinch. The cross-plant flows can be reduced while ensuring the fresh resource target is still achieved. The

transfer of sources is shown later, where using the 125 ppm source to replace 290 ppm sources is better than replacing 130 ppm sources.

Table **4-2**: Extracted Total Site data. '*' denotes the Pinch-causing sources for each plant, and red texts denote removed sources or sinks

	Plant 1			Plant 2			Plant 3			Plant 4			Plant 5	
	F_{SR}/ t/h	C/ ppm		F_{SR}/ t/h	C/ ppm		F_{SR}/ t/h	C/ ppm		F_{SR}/ t/h	C/ ppm		F_{SR}/ t/h	C/ ppm
	HQR			**HQR**			**HQR**			**HQR**			**HQR**	
Fw	**206.7**	**0**		**142.3**	**0**		**173.4**	**0**		**206**	**0**		**102.7**	**0**
SR1	40	50	SR1	50	50	SR1	100	130	SR1	20	50	SR1	20	130
SR2	80	100	SR2	250	100	SR2	120	290	SR2	80	100	SR2*	62.3	130
SR3	80	100	SR3*	7.69	130	SR3	85	300	SR3*	44	125			
SR4*	133.3	150				SR4*	26.6	350						
	LQR Unused			**LQR Unused**			**LQR Unused**			**LQR Unused**			**LQR Unused**	
SR4*	6.667	150	SR3*	79.8	130	SR4*	173.4	350	SR3*	56	125	SR2*	37.7	130
SR5*	0	200	SR4	62.5	250				SR4	100	150	SR3	40	250
SR6	200	450							SR5	50	800	SR4	25	400
	F_{SK}/ t/h	Z/ ppm		F_{SK}/ t/h	Z/ ppm		F_{SK}/ t/h	Z/ ppm		F_{SK}/ t/h	Z/ ppm		F_{SK}/ t/h	Z/ ppm
SK1	200	0	SK1	50	20	SK1	100	0	SK1	20	0	SK1	20	0
SK2	80	50	SK2	250	50	SK2	120	100	SK2	80	25	SK2	100	50
SK3	80	50	SK3	150	100	SK3	85	125	SK3	100	25	SK3	40	80
SK4	140	100	SK4	0	200	SK4	200	300	SK4	100	50	SK4	25	100
SK5	200	120							SK5	50	100			
SK6	0	200												

The method is demonstrated by replacing 130 ppm sources with the SR3 from Plant 4 first, then the replacing of the 290 ppm source is shown later. In this case study, both Plant 2 and Plant 5 have HQR sources with 130 ppm. The 125 ppm purged source can be transferred to Plants 2 or 5. Figure 4-21b shows the replacement of part of the 130 ppm HQR sources with the 125 ppm purged source, and the replaced source is purged and can be used to replace the others. As the replaced source becomes part of the unused source, the total load of the 130 ppm unused source can then be used to replace the HQR source with 150 ppm (Plant 1). Notice that

all these source transfers happen around the Site Pinch Point, which is effective. The 150 ppm source from Plant 1 is now replaced, and theoretically, it can be used to replace the HQR sources in Plant 2 (290 ppm, 300 ppm, 350 ppm); however, as these sources have a higher concentration than the Site Pinch Point (130 ppm), which should be in the LQR of the Total Site. Using LQR source to replace other LQR sources is futile for the overall integration. This scenario indicates the purged sources lower than 130 ppm is needed.

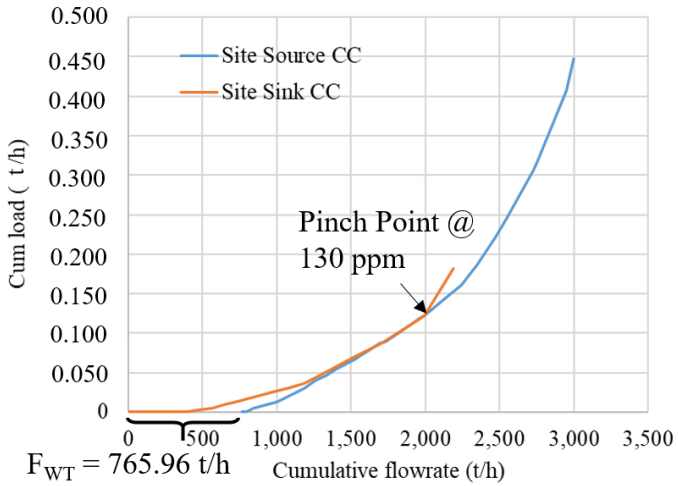

Figure 4-20: Identification of Pinch Point and fresh resource target for the Total Site

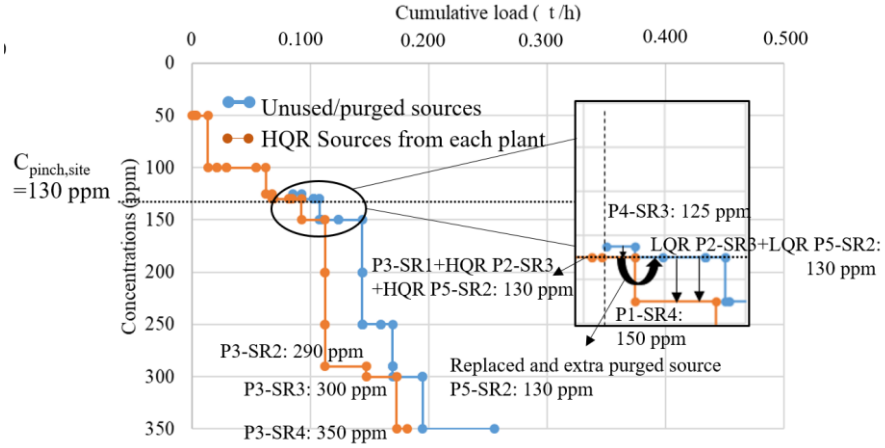

Figure 4-21: Source Transfer Diagram for the case study- 1st round iteration

Transferring 56 t/h of SR3 from Plant 4 to Plant 5 and 153.84 t/h of sources from Plant 5 and Plant 2 to Plant 1 (133.33 x 150/130), the targets for the individual plant need to be updated. The Total Site data is updated after the first iteration of cross-plant transfer and shown in Table 4-3. Based on the results, they are transferring 56 t/h of Plant 4 SR3 to Plant 5 yields about an additional 53.85 t/h of SR2 with 130 ppm. Notice that the freshwater target for Plant 5 is reduced from 102.7 to 100.5 t/h. The total amount of unused SR2 from Plant 5 becomes 91.55 t/h (53.85 + 37.7) of SR2 that can be transferred to Plant 1. The remaining 130 ppm source to be supplied for Plant 1 can be obtained from Plant 2 SR2, which is about 62.29 t/h (153.84-91.55). After supplying these sources to Plant 1, based on Table 4-3, a new Pinch Point is

formed at 50 ppm (SR1), and the freshwater target is reduced from 206.7 to 200 t/h for Plant 1. Notice that since a new Pinch Point is formed, the Pinch-causing source for Plant 1 is now the SR1(50 ppm), and part of it (about 22.5 t/h) can be purged for reusing in other plants. SK2-6 become the LQR sinks, and SR2-5 are all allocated to the LQR sinks, so they are removed since they can be fulfilled without a fresh resource supply. As of now, the 150 ppm source (SR4) from Plant 1 is categorised as an LQR source; the replacing SR2 amount from Plant 5 and SR3 from Plant 1 should be updated as well. It is not necessary to replace all of SR4 Plant 1, and

Table **4-3**: Updated Total Site data with the 1st iteration of the cross-plant transfer. '*' denotes the Pinch-causing sources for each plant. Red font denotes removed sources or sinks.

	Plant 1			Plant 2			Plant 3			Plant 4			Plant 5	
	F_{SR}/ t/h	C/ ppm		F_{SR}/ t/h	C/ ppm		F_{SR}/ t/h	C/ ppm		F_{SR}/ t/h	C/ ppm		F_{SR}/ t/h	C/ ppm
	HQR			**HQR**			**HQR**			**HQR**			**HQR**	
Fw	**200**	**0**		**142.3**	**0**		**173.4**	**0**		**206**	**0**		**100.5**	**0**
SR1*	160	50	SR1	50	50	SR1	100	130	SR1	20	50	SR1	20	130
	LQR Unused		SR2	250	100	SR2	120	290	SR2	80	100	SR2*	8.462	130
SR1*	22.5	50	SR3*	7.69	130	SR3	85	300	SR3*	44	125			
SR2	0	100				SR4*	26.6	350						
SR3	0	100		**LQR Unused**			**LQR Unused**			**LQR Unused**			**LQR Unused**	
SR4	140	150	SR3*	17.5	130	SR4*	173.4	350	SR4	100	150	SR3	40	250
SR5	0	200	SR4	62.5	250				SR5	50	800	SR4	25	400
SR6	198.3	450												
				Transferred						**Transferred**			**Transferred**	
			SR3 - to P1	62.30	130				SR3 - to P5	56	125	SR2 - to P1	91.55	130
	F_{SK}/ t/h	Z/ ppm		F_{SK}/ t/h	Z/ ppm		F_{SK}/ t/h	Z/ ppm		F_{SK}/ t/h	Z/ ppm		F_{SK}/ t/h	Z/ ppm
SK1	200	0	SK1	50	20	SK1	100	0	SK1	20	0	SK1	20	0
SK2	0	50	SK2	250	50	SK2	120	100	SK2	80	25	SK2	100	50
SK3	0	50	SK3	150	100	SK3	85	125	SK3	100	25	SK3	40	80
SK4	0	100	SK4	0	200	SK4	200	300	SK4	100	50	SK4	25	100
SK5	0	120							SK5	50	100			
SK6	0	200												

the transferred 130 ppm source should be minimised for Plant 1. Multiple source targeting can be performed – see Foo (2007) in this case. The identified transferred amount is 162.50 t/h (70.95+91.55). The total freshwater target identified are reduced to 822.20 t/h (200 + 142.31 + 173.35 + 206 +100.54) at current iteration, which is still higher than 765.96 t/h.

Step 3b: Second iteration. As the freshwater target is still not matched with the site target, the step is repeated. It is then required to check for a possibility for applying Scheme 2 or 3. For Plant 3, the Pinch-causing source is at 350 ppm, and SR2 and SR3 are both HQR sources with lower quality than the Site Pinch Point. This indicates that it is still not fully exploiting the source potential from other plants. The currently available sources are SR1 from Plant 1 (22.5 t/h with 50 ppm) and SR3 from Plant 2 (17.5 t/h with 130 ppm). These sources are not enough to the sources from Plant 3. However, it should be noted that in Plant 2, the sink in LQR (SK4) has 200 ppm and the Pinch-causing source is 130 ppm. In fact, since SR4 from Plant 1 is unused now, this source actually can replace the Pinch-causing source in the LQR for Plant 2, preserving it for Plant 3. This is actually the cross-plant transfer Scheme 3, where the source from LQR of Plant 1 is used to transfer to the LQR of Plant 2, which then the replaced source is transferred to HQR of plant 3 – see Section 3.2.1 The amount is determined and tabulated in Table 4-4, where 67.8 t/h of SR1 from Plant 1 is transferred to Plant 2. An additional amount of SR3 is unused in Plant 2, which is now about 80 t/h. Since new purged and HQR sources are found, the Source Transfer Diagram can be updated to show the reusing potential of the remaining SR1 from Plant 1, shown in Figure 4-22.

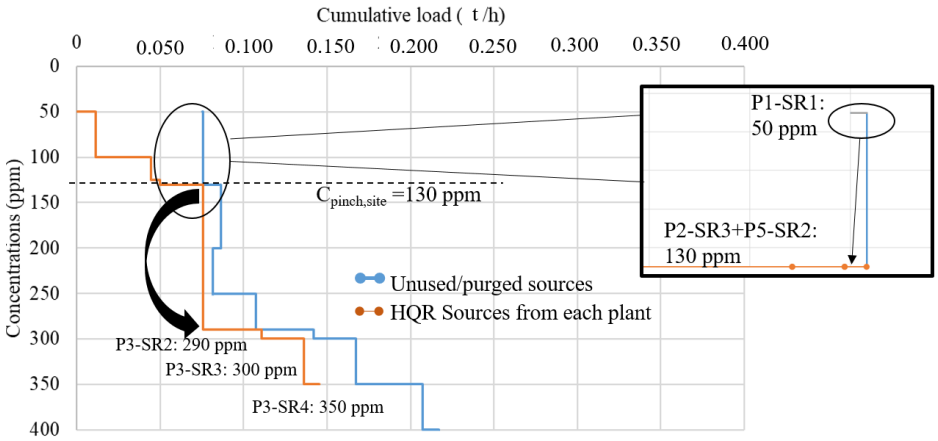

Figure 4-22: Source Transfer Diagram for the case study – 2nd round iteration

The new purged source SR1 from Plant 1 can be used to replace HQR sources in any other plant since its concentration is the lowest (50 ppm). However, it is more effective to transfer the source at or across the Site Pinch. In this case, Plant 1 SR1 can be used to replace the HQR sources, which have the Site Pinch concentration: 130 ppm. Since Plants 2, 3 and 5 all have HQR sources with 130 ppm, the unused SR1 can be used for any of them.

Table **4-4**: Updated Total Site data with 1st iteration of cross-plant transfer, applying cross-plant Scheme 3 in Plant 1. '*' denotes the Pinch-causing sources for each plant, red texts denote removed sources or sinks

	Plant 1			Plant 2			Plant 3			Plant 4			Plant 5	
	F_{SR}/ t/h	C/ ppm		F_{SR}/ t/h	C/ ppm		F_{SR}/ t/h	C/ ppm		F_{SR}/ t/h	C/ ppm		F_{SR}/ t/h	C/ ppm
	HQR			**HQR**			**HQR**			**HQR**			**HQR**	
Fw	**200**	**0**		**142.3**	**0**		**173.4**	**0**		**206**	**0**		**100.5**	**0**
SR1*	160	50	SR1	50	50	SR1	100	130	SR1	20	50	SR1	20	130
	LQR Unused		SR2	250	100	SR2	120	290	SR2	80	100	SR2*	8.462	130
SR1*	22.5	50	SR3*	7.69	130	SR3	85	300	SR3*	44	125			
SR2	0	100				SR4*	26.6	350						
SR3	0	100		**LQR Unused**			**LQR Unused**			**LQR Unused**			**LQR Unused**	
SR4	72.2	150	SR3*	71.36	130	SR4*	173.4	350	SR4	100	150	SR3	40	250
SR5	0	200	SR4	75	250				SR5	50	800	SR4	25	400
SR6	198.3	450												
	Transferred			**Transferred**						**Transferred**			**Transferred**	
SR4– to P2	67.8	150	SR3 - to P1	70.95	130				SR3 - to P5	56	125	SR2 - to P1	91.55	130
	F_{SK}/ t/h	Z/ ppm		F_{SK}/ t/h	Z/ ppm		F_{SK}/ t/h	Z/ ppm		F_{SK}/ t/h	Z/ ppm		F_{SK}/ t/h	Z/ ppm
SK1	200	0	SK1	50	20	SK1	100	0	SK1	20	0	SK1	20	0
SK2	0	50	SK2	250	50	SK2	120	100	SK2	80	25	SK2	100	50
SK3	0	50	SK3	150	100	SK3	85	125	SK3	100	25	SK3	40	80
SK4	0	100	SK4	0	200	SK4	200	300	SK4	100	50	SK4	25	100
SK5	0	120							SK5	50	100			
SK6	0	200												

Note that if all purged SR1 from Plant 1 is transferred to Plant 2, the Pinch-causing source for Plant 2 is changed to SR2 (not shown). This means an additional source with 100 ppm is available for Plant 3. However, this causes additional cross-plant transfer, as explained in Section 4.1.2.3 earlier. The better way is to transfer the SR1 from Plant 1 to either Plant 3 or Plant 5. Transferring the source to Plants 3 or 5 does not change the Pinch-causing sources. The updated Total Site results are presented in Table 4-5.The total freshwater target now becomes 765.96 t/h (200 + 142.31 + 117.11 + 206 +100.54). This coincides with the target in Step 2. The total cross-plant sources transfer amount is identified as 374.14 t/h. The full network design is presented in Figure 4-23.

Step 3c: Further optimisation- Revised first iteration. However, the total cross-plant transfer can be reduced further. In the first round of iteration, the SR3 from Plant 4 (56 t/h) is transferred to Plant 5 to replace sources with 130 ppm. It is actually better to replace the 290 ppm sources in Plant 3, where the SR3 from Plant 4 is transferred across the Site Pinch (130 ppm). This could yield lower cross-plant transfers and achieving the total fresh resource target as well. The full network design using this strategy is shown in Figure 4-24, with the total cross-plant transfers amount as 320.3 t/h. This clearly shows that the source transfer across the Site Pinch is beneficial in reducing the cross-plant flow.

Table **4-5**: Updated Total Site data with the 2nd iteration of the cross-plant transfer. '*' denotes the Pinch-causing sources for each plant, and red texts denote removed sources or sinks

	Plant 1			Plant 2			Plant 3			Plant 4			Plant 5	
	F_{SR}/ t/h	C/ ppm		F_{SR}/ t/h	C/ ppm		F_{SR}/ t/h	C/ ppm		F_{SR}/ t/h	C/ ppm		F_{SR}/ t/h	C/ ppm
	HQR			**HQR**			**HQR**			**HQR**			**HQR**	
Fw	**200**	**0**		**142.3**	**0**		**117.1**	**0**		**206**	**0**		**100.5**	**0**
SR1*	160	50	SR1	50	50	SR1*	85.4	130	SR1	20	50	SR1	20	130
	LQR Unused		SR2	250	100				SR2	80	100	SR2*	8.462	130
SR1*	22.5	50	SR3*	7.69	130				SR3*	44	125			
SR2	0	100												
SR3	0	100		**LQR Unused**			**LQR Unused**			**LQR Unused**			**LQR Unused**	
SR4	72.2	150	SR3*	0	130	SR3	19.6	300	SR4	100	150	SR3	40	250
SR5	0	200	SR4	75	250	SR4	200	350	SR5	50	800	SR4	25	400
SR6	198.3	450												
	Transferred			**Transferred**						**Transferred**			**Transferred**	
SR4– to P2	67.8	150	SR3 - to P1	70.95	130				SR3 - to P5	56	125	SR2 - to P1	91.55	130
SR1- to P3	22.5	50	SR3 – to P3	65.34	130									
	F_{SK}/ t/h	Z/ ppm		F_{SK}/ t/h	Z/ ppm		F_{SK}/ t/h	Z/ ppm		F_{SK}/ t/h	Z/ ppm		F_{SK}/ t/h	Z/ ppm
SK1	200	0	SK1	50	20	SK1	100	0	SK1	20	0	SK1	20	0
SK2	0	50	SK2	250	50	SK2	120	100	SK2	80	25	SK2	100	50
SK3	0	50	SK3	150	100	SK3	85	125	SK3	100	25	SK3	40	80
SK4	0	100	SK4	0	200	SK4	0	300	SK4	100	50	SK4	25	100
SK5	0	120							SK5	50	100			
SK6	0	200												

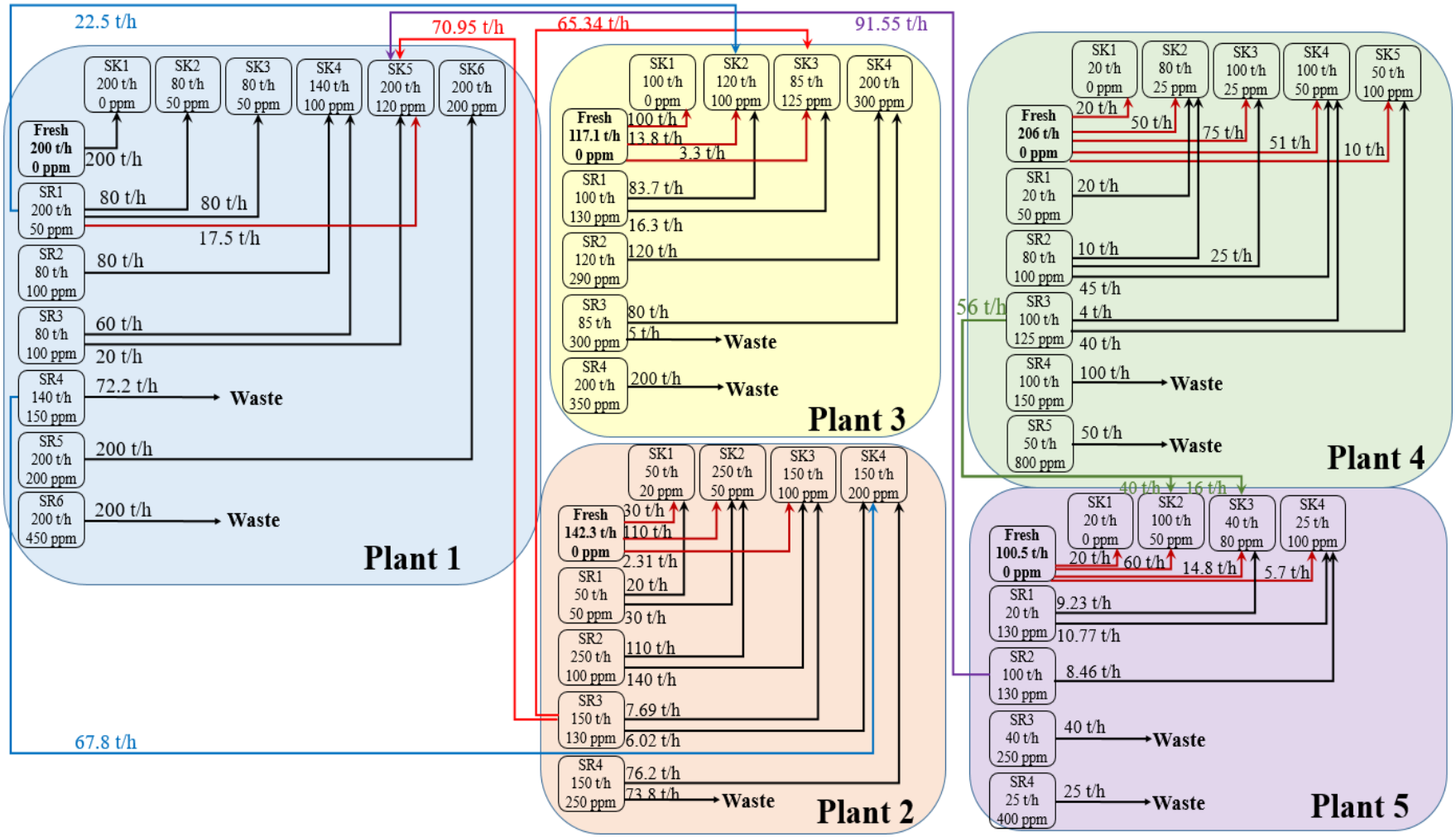

Figure 4-23: Network design for Total Site- Plant 4 SR3 is transferred to Plant 5 in 1st iteration. The total cross-plant transfer amount is 374.14 t/h.

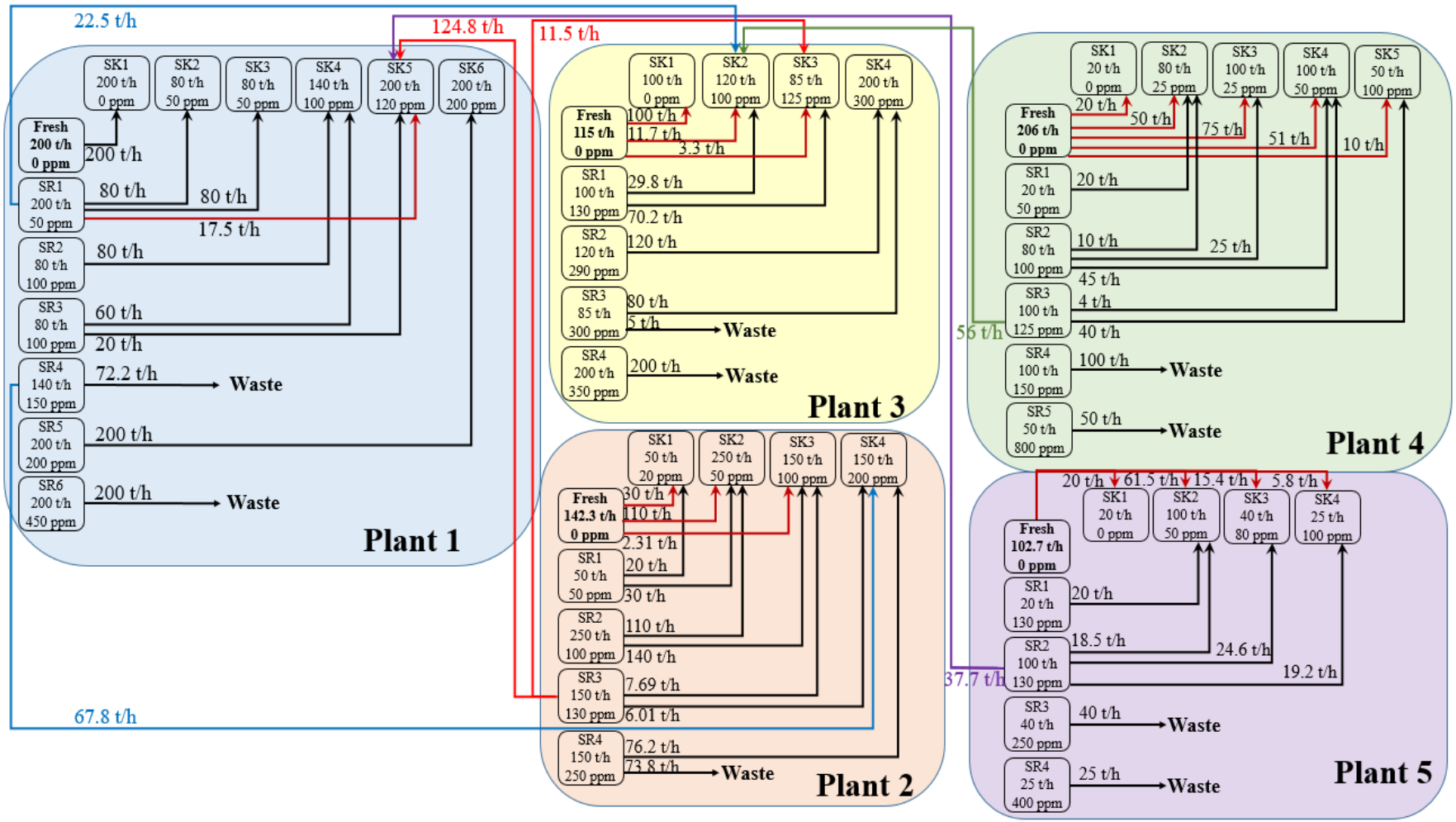

Figure 4-24: Network design for Total Site – Plant 4 SR3 is transferred to Plant 3 instead of Plant 5 in 1st iteration. The total cross-plant transfer amount is 320.3 t/h.

Step 4: Headers targeting and network design. The cross-plant sources have to be identified first to design the headers. The minimum numbers of headers, flowrates and the concentration of the headers are identified using the Site CC using the cross-plant sources in Figure 4-24 with a minimal cross-plant transfer and are presented in Figure 4-25. It is shown that if only two headers from the sources are formed, where one header below the Site Pinch (252.5 t/h with 121.8 ppm) and another above the Site Pinch (67.8 t/h with 150 ppm), the Site Source CC actually crosses the Site Sink CC. This means the additional fresh resource is required with only two headers. By checking the CC for individual plants, Plant 3 actually requires more freshwater with the headers. The CC for Plant 3 with the headers is presented in Figure 4-26a, as the header crosses the Sink CC for Plant 3. A higher-quality header is needed if cross-plant source transfer is minimal. As shown in Figure 4-26b, a separate header formed by any combinations of cross-plant sources for Plant 3 is required.

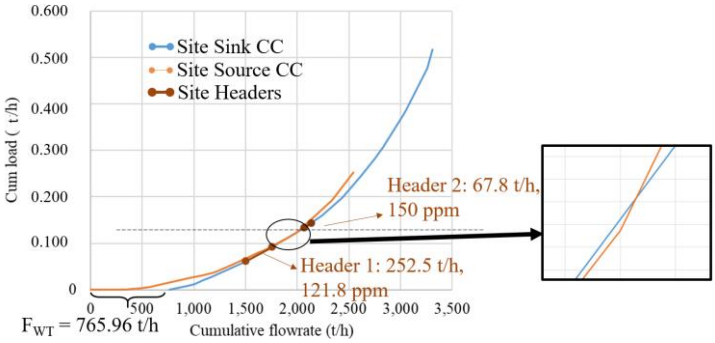

Figure 1: Site CC with the mixed header sources

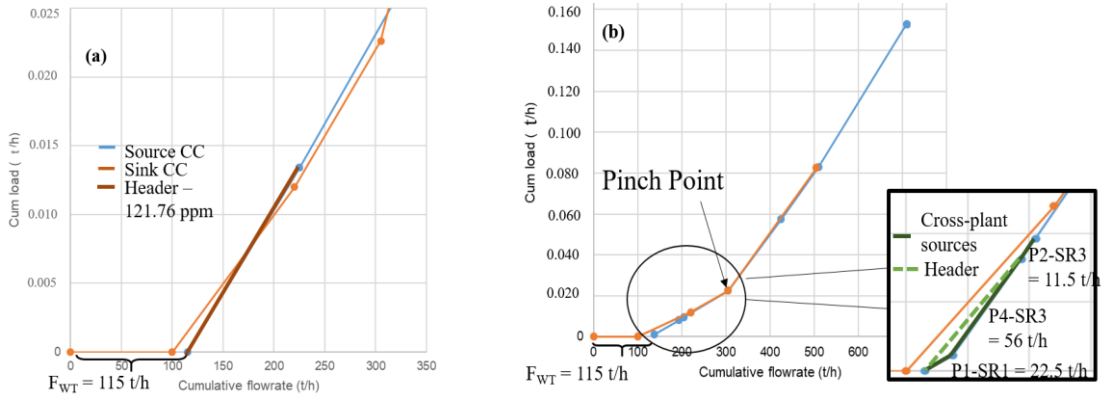

Figure 4-26: CC for plant 3 (a) The header causes the target to increase (b) New header mix for plant 3

By forming another header with cross-plant sources for Plant 3, the full network design is updated and shown in Figure 4-27. It can be seen that the minimal cross-plant transfer (or the total flow inside the headers from the cross-plant sources) is 320.3 t/h with 765.96 t/h freshwater, which coincides with the minimal results identified earlier. The internal headers for each process can be determined as well using individual CCs (see Supplementary Material). The full network design with the site headers and internal headers is shown in Figure 4-28.

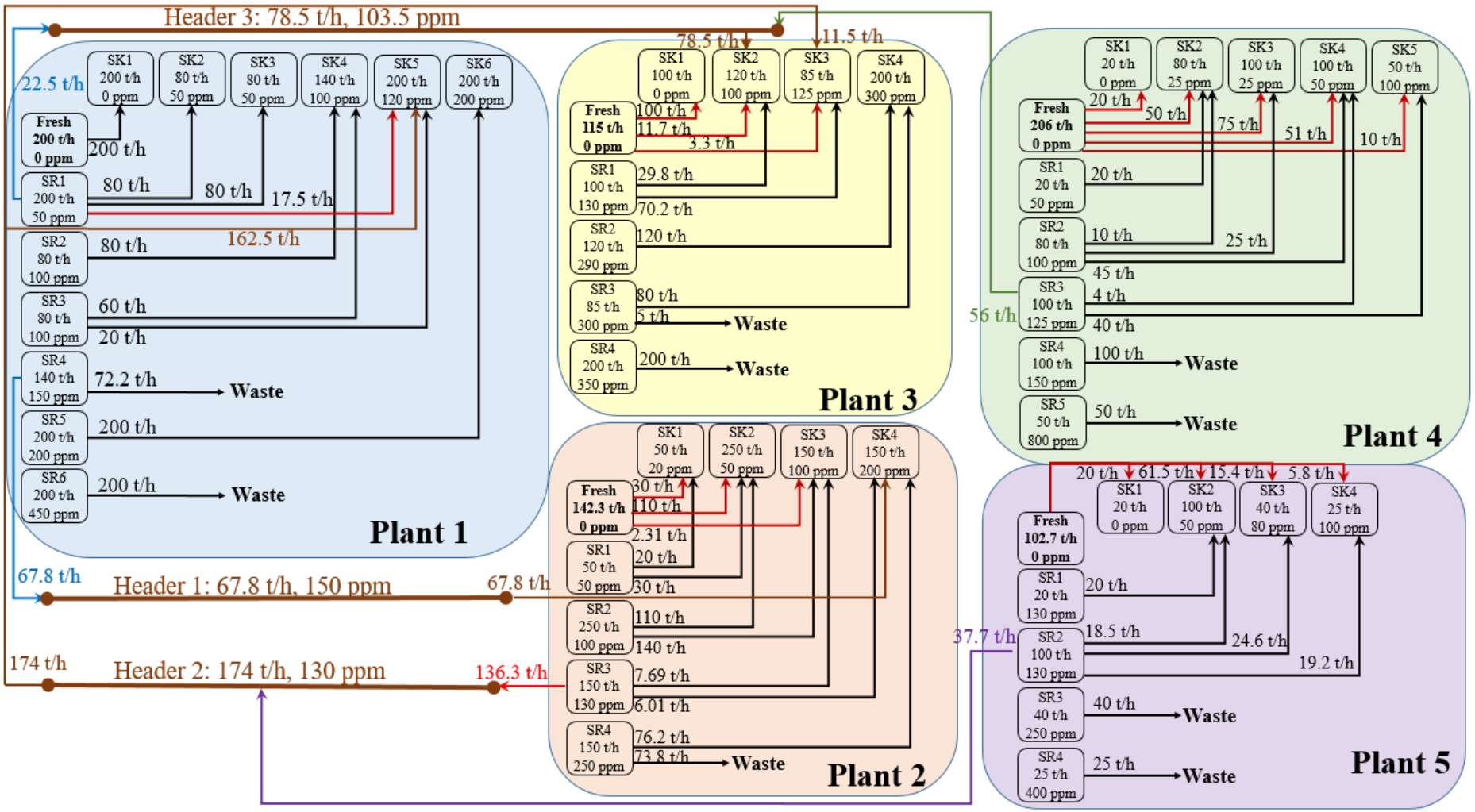

Figure 4-27: Network design for Total Site with three site headers from cross-plant sources. The overall freshwater target is 765.96 t/h with minimal total cross-plant transfer (total flowrates of headers sources) is 320.31 t/h

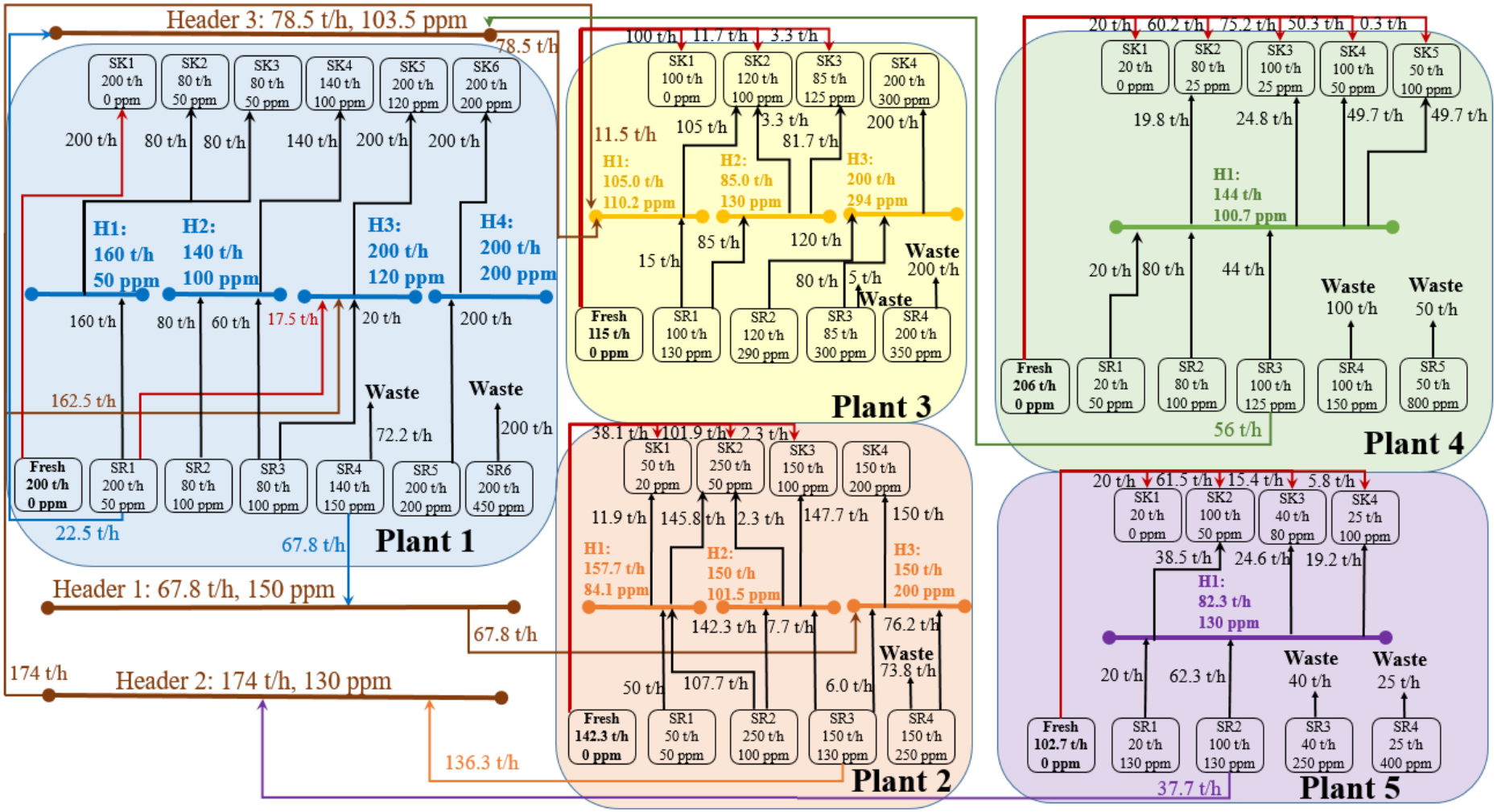

Figure 4-28: Network design for Total Site with site headers and internal process headers. The overall freshwater target is 765.96 t/h with minimal total cross-plant transfer (total flowrates of headers sources) is 320.31 t/h

4.2 Headers/Mains targeting framework for multiple contaminant/quality

4.2.1 Internal process headers targeting

The freshwater targeting procedure, using the Composite Curves for multiple contaminants, is more complicated than the case of a single contaminant. Based on Chin et al. (2021c), first requires determining the limiting contaminants for each sink. The individual source-to-sink allocation is then performed with CCs with the arrangement of sources based on the limiting contaminant of each sink and needs to check which contaminants limits are not fulfilled. Those that are not satisfied require some shifting (Figure 4-29), as discussed next. Note that Figure 4-29a considers Sink 1 only, and Figure 4-29b is a continuation dedicated containing Sinks 1 and 2, then Figure 4-29c displays further the steps for Sinks 1, 2 and 3. Figure 4-29a is a partial construction in Figure 4-29b, and Figure 4-29b is a partial construction for Figure 4-29c.

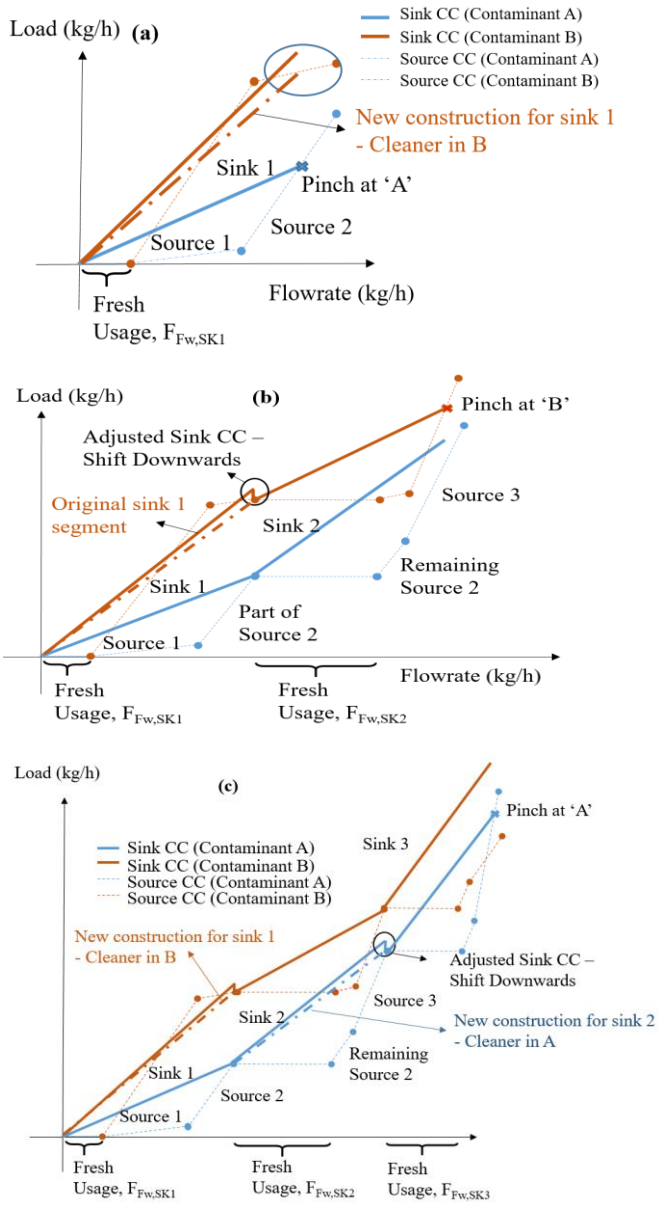

Figure 4-29: Sequential source allocation with a developed methodology for multiple contaminants, adapted from Chin et al. (2021d)

Notice that in Figure 4-29a, by performing the typical Pinch Analysis on Sink 1 only, the Pinch Point is at contaminant A for Sink 1, while for contaminant B, the maximum contaminant limit is not reached- the Source CC is below the endpoint of the sink (see the circled part). In fact, the only constraint, in this case, is that the Source CC should be below the endpoints of Sink CC. For contaminant B, although the Source CC crosses at Sink CC, the Source CC is still below the endpoint of Sink CC, which indicates the total contaminant flowrates/loads are still below the sink's loads. This is actually a feasible source-sink matching that follows the Polygon Rule of CC- see Chin et al. (2021c), which term originated from Yang et al. (2014)

Based on Figure 4-29a, the contaminant B limit for Sink 1 is not reached, but the contaminant A limit is achieved. The total allocated sources to Sink 1 are actually cleaner in terms of contaminant B, but the load of contaminant A is identical to that of the sink. As a load of Sink 1 for contaminant B is now lower than the original load, the real load of contaminant B (instead of the original load) should be the one cascaded to the next sink. This means the real concentration of contaminant B for Sink 1 actually becomes lower, and this should be used when constructing the segment of Sink 1 in the Sink CC. In Figure 4-29b, the starting point of the sink 2 segment has to be matched with the real contaminant loads for Sink 1. The starting point of Sink CC of contaminant B for Sink 2 has to move downwards to match with the new constructed Sink 1 segment. Similarly, for Sink 2 in Figure 4-29c, the contaminant A limit is not reached but the contaminant B limit is satisfied for Sink 2, so the Sink 3 segment has to move downwards (contaminant A) to match with the new constructed Sink 2 segment. The Composite Curves for the overall system are shown in Figure 4-30. Note that the vertical shifting of the Sink CC does not alter the specification of the streams but only accounted for the cleaner water supply not reaching the contaminants limits of the sinks.

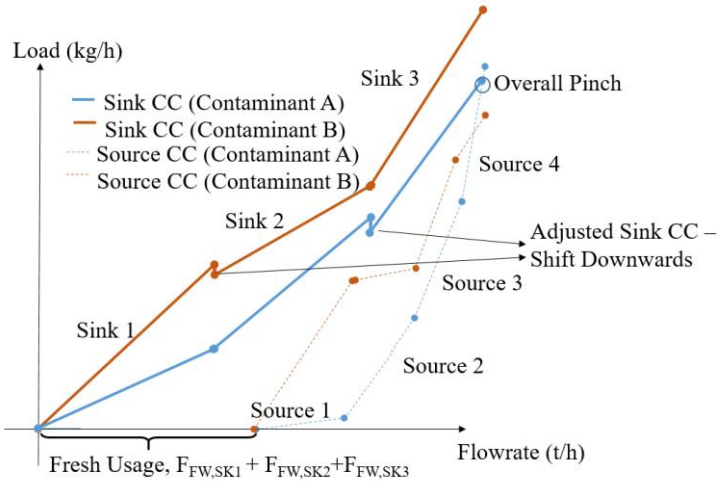

Figure 4-30: Overall Source and Sink CC for the multiple contaminants illustrative example

However, the optimal source allocation does not rely solely on the prioritisation of the sources due to the multiple constraints of the contaminants – see Chapter 3 Section 3.3.

4.2.1.1 Header targeting and design with Composite Curves

The water header targeting procedure is similar to the single contaminant case. Consider a two contaminants example, and the sinks are assigned to the contaminant cascade A, which means their main limiting contaminant is A. Assuming that in this case, both contaminants A and B are fulfilled, the sink CCs for contaminants A and B are expected with no vertical shifting as the limits are fulfilled. Figure 4-31 shows the examples after the freshwater target for each sink is identified. In the example of Figure 4-31, only a single header is sufficient to cover the sinks, and the freshwater requirement is similar, provided that the header source for the non-limiting contaminant (contaminant B) still satisfies all the sinks' limits. If the header causes any other contaminant limits (A/B) to be unfulfilled, this causes additional freshwater requirements to the overall system; an additional header is required – see Figure 4-32.

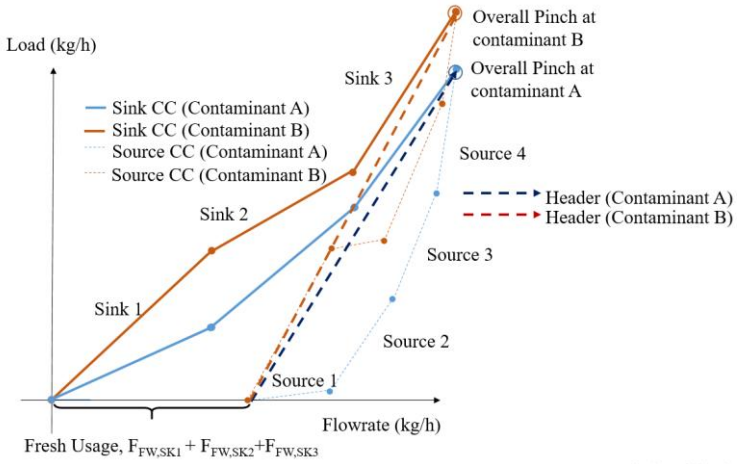

Figure 4-31: Illustrative example of constructing header lines for multiple contaminants – all contaminant limits are reached

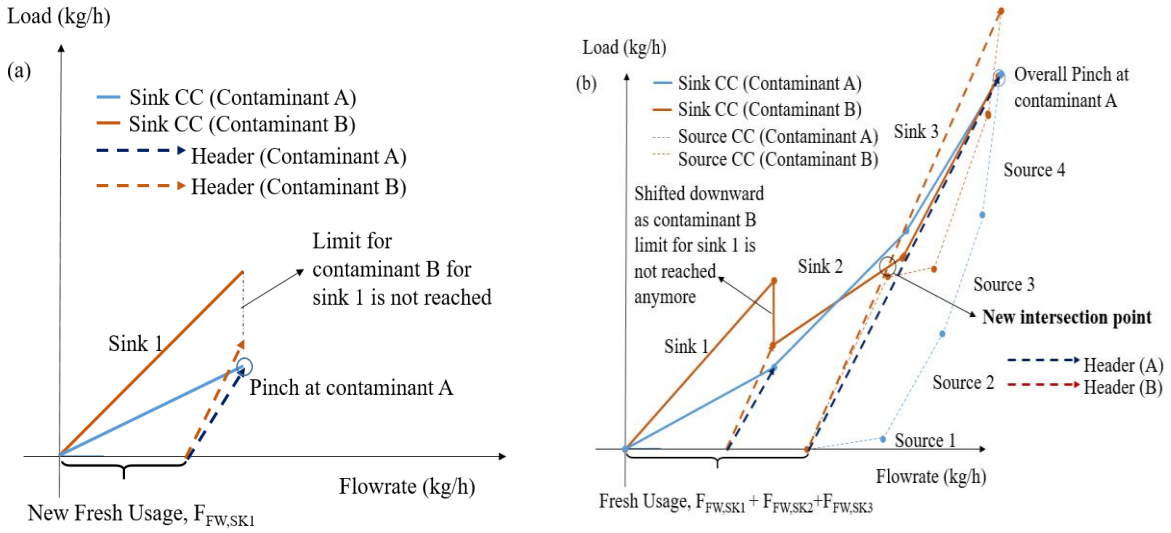

Figure 4-32: Illustrative example of constructing a single header line for multiple contaminants is not enough (a) the contaminant B limit for sink 1 is supposed to be fulfilled, but not fulfilled due to the header (b) the header mix becomes infeasible for the overall system

In Figure 4-32a, the contaminant B limit for sink 1 is supposed to be fulfilled in Figure 4-31 but not fulfilled due to the header mix. The single header mix becomes infeasible for the overall system without adding more freshwater, see Figure 4-32b, where a new intersection point between the header lines and the sink CC occurs. This suggests that the number of fulfilled contaminant limits for all sinks is smaller than the number of headers to allow for degrees of freedom in source mixing to achieve this.

Another case is considered next, where only the limit for the main limiting contaminants is reached for the sinks. In the demonstration example, only the limit of Contaminant A (the limiting contaminant) is reached. It can be seen that in this case, the Sink CC for contaminant B requires some vertical shifting at Sink 1 and Sink 2 as their contaminant limits are not reached. According to Figure 4-33, the initial observation is that only a single header is enough to satisfy all the sinks without causing additional freshwater requirements.

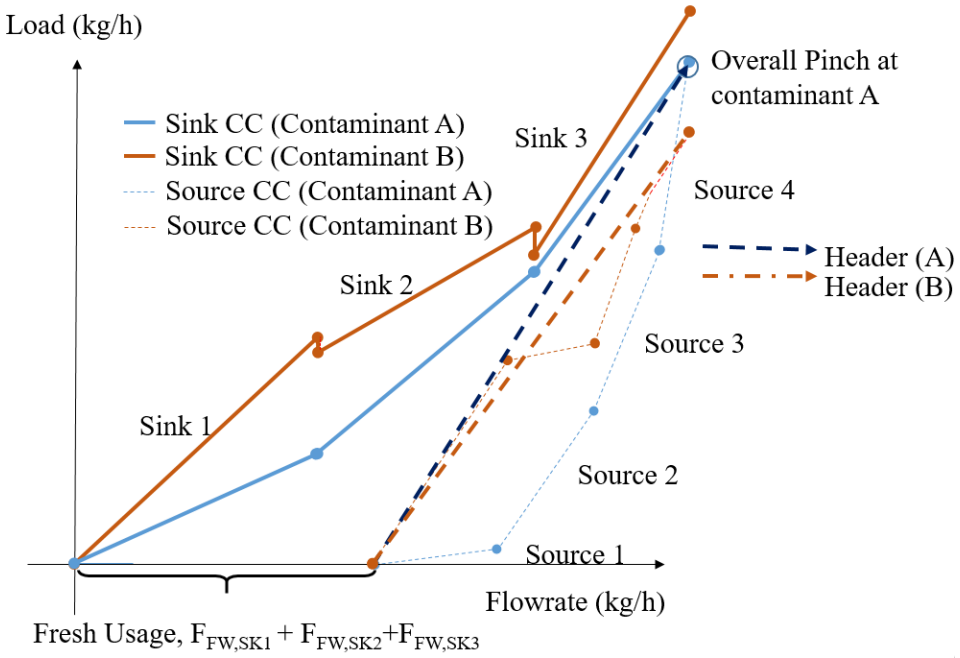

Figure 4-33: Illustrative example of constructing header lines for multiple contaminants – one of the contaminants limits are reached only

However, this might not be the case because the sources are mixed into the headers, which would alter the quality levels of the sources for both contaminants. As the sources are mixed, some of the sink's limiting contaminant (e.g. A) might become the non-limiting, while the non-limiting one (e.g. B) becomes the limiting contaminant. This can cause additional freshwater requirement for the sink and for the overall target. That case is illustrated on a modification of the previous example that shows the individual header-to-sink CC in Figure 4-34a. It can be seen that for Sink 1, the contaminant A limit is still satisfied without violating contaminant B. However, for the case of Sink 2, the header for contaminant B becomes limiting, and additional freshwater is required for Sink 2, which causes the increment of the overall freshwater target identified by multi-contaminant Pinch Analysis. This suggests that a single header using the

mix of the source below the overall Pinch Point is not enough to cover the sink without adding more fresh resources. An additional header is required to ensure contaminant A is the limiting one for sink 2. The additional header line can be drawn starting from the Source CC starting point, and the endpoint can be many points along with the Source CC as the locus path – see Figure 4-35. Notice that the order of sources in the Source CC can be altered, depending on the individual source-to-sink allocation.

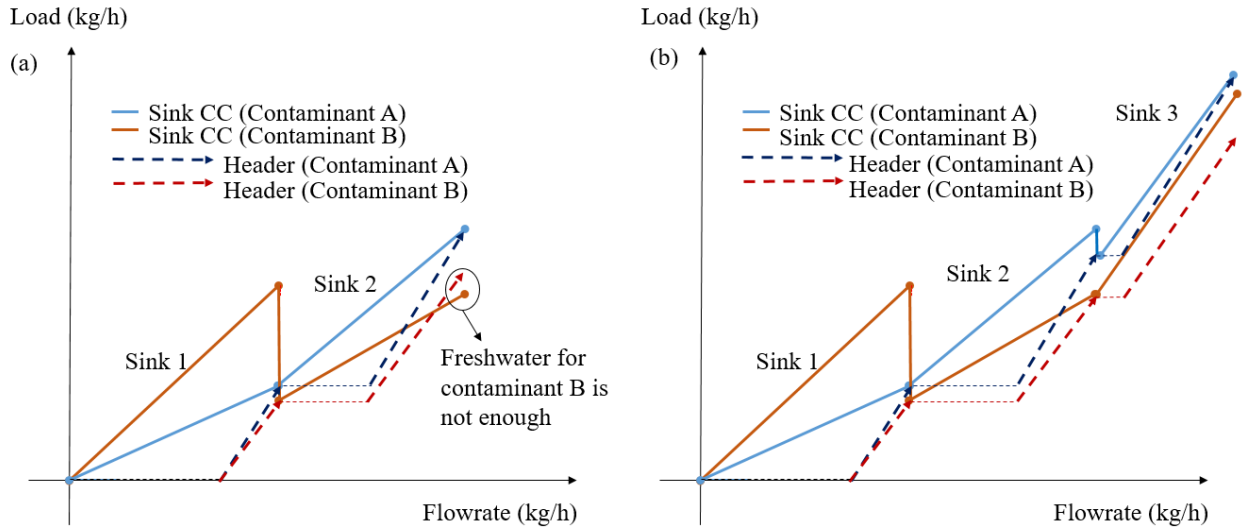

Figure 4-34: (a) The header line for sink 2 for contaminant B (which is supposed to be the unsatisfied contaminant) becomes the limiting (b) Sink CC for contaminant A at Sink 3 is shifted downwards.

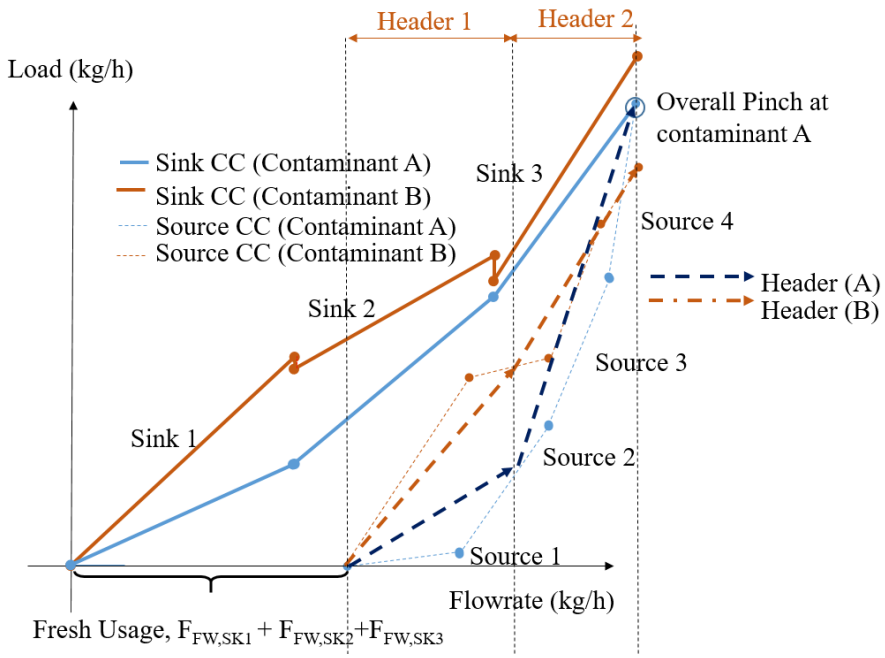

Figure 4-35: Example of construction of multiple header lines for multiple contaminants

Based on the explanations above, the water header/main targeting steps for multiple contaminants can be summarised as follows:

- Construct an initial multi-contaminant Pinch Analysis for the process/site to determine the overall freshwater target for direct recycle or reuse. Perform vertical shifting of the sink CC if necessary.
- Draw a header line below the Pinch Point(s), starting from the shifted Source CC initial point and connect to the Pinch Point(s).
- Check if intersection(s) exists between the header lines and the Sink CC. If there are any, split the header lines, and draw the header lines with any combinations until the entire header curve is at the right side of Sink CC. (No. of intersections = minimum no. of headers below Pinch).
- Check for individual source-sink allocation, whether the supposing fulfilled contaminant limit is fulfilled using the header sources. If no, go to step (v), else go to step (vi).
- Split the header line and draw an additional header line(s) using Source CC as the locus path. Go back to step (iv). (No. of fulfilled contaminant limits for all sinks = no. of headers)
- Repeat the steps for sinks that are above the Pinch Point(s).
- Determine the no. of a header, each header source's concentration (gradient) and flowrates (horizontal length).

4.2.2 Total Site headers targeting

4.2.2.1 Minimal cross-plant sources transfer schemes

The multiple qualities problem can have a similar representation using Composite Curves as well. Each quality has an individual High-Quality Region and Low-Quality Region, as shown in Figure 4-36. The Pinch Points of individual plants and the Site Pinch Point(s) can be identified with Composite Curves. A feasible and effective cross-transfer scheme can be identified in a similar manner.

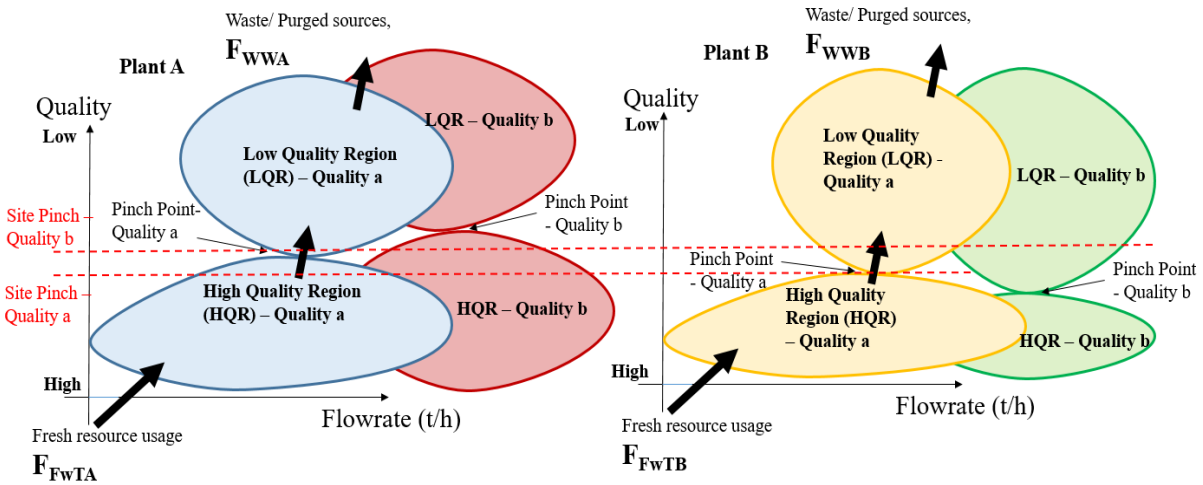

Figure 4-36: Division into High-Quality Region and Low-Quality Region with two qualities (both qualities have Pinch Points)

It has been shown in the previous section that the supplier plants with Pinch Points lower than the Site Pinch Points can transfer their sources to receiver plants with Pinch Points higher than the Site Pinch Points. Figure 4-37 shows an example of a feasible transfer scheme (Scheme 1) for the two qualities problem. The supplier plant (Plant B) has Pinch Points lower or equal to the Site Pinch Points for both qualities, and the receiver plant (Plant A) has higher Pinch Points than the Site Pinch Points for both qualities. Note that the Pinch Points are the real Pinch Points, not the 'pseudo' Pinch Points.

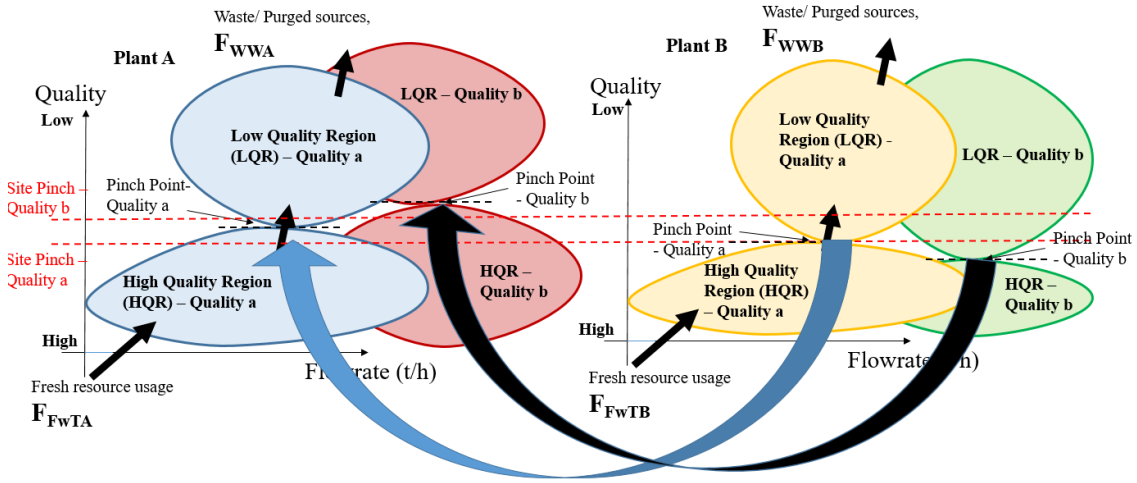

Figure 4-37: Plant B send its unused sources (LQR) to Plant A (HQR higher than Site Pinch Points)

In the demonstration shown in Figure 4-38, it is shown that the receiver and supplier both have lower Pinch Point for Quality B. In terms of Quality A, Plant B can supply its source from its LQR to Plant A's HQR since Plant A has a higher Pinch Point than the Site Pinch Point. Since both plants have lower Pinch Points for Quality B, the transfer can be ineffective for Quality B but effective for Quality A. Since also Plant B has a lower Pinch Point in Quality B than Plant A, the transfer from Plant B LQR to Plant A HQR is still effective and feasible.

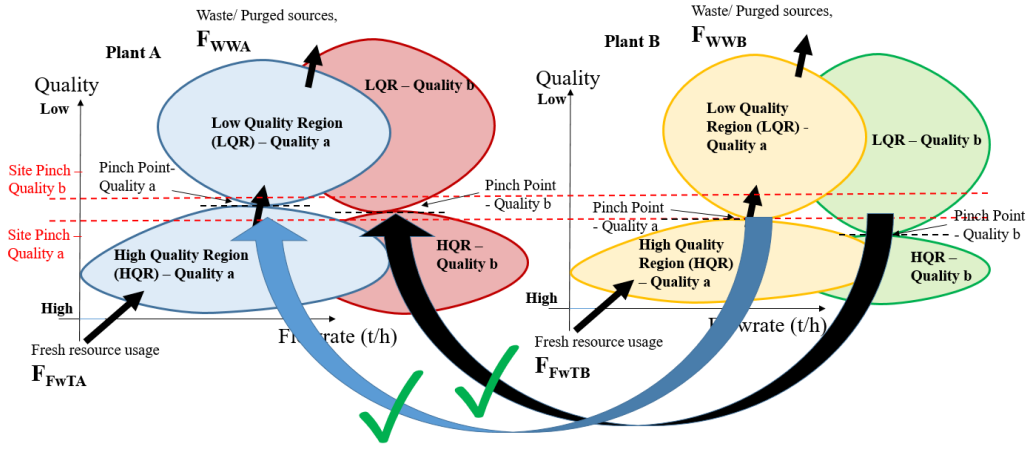

Figure 4-38: Plant B send its unused sources (LQR) to Plant A (HQR). Plant A has a higher Pinch Point than Site Pinch for Quality A but a lower Pinch Point than Site Pinch for B.

However, in the case where Plant B has a higher Pinch Point in Quality B than the Site Pinch Point - see Figure 14, the cross-plant transfer of LQR (Plant B) to HQR (Plant A) is actually ineffective, although it is effective in terms of Quality A. The alternative schemes presented in the previous section should be sought out instead. The cross-plant transfer strategies from the single quality representation are applicable to multiple qualities as well, but the transfer should be checked for all qualities. The Pinch Points for multiple qualities are also strongly dependent on the source-to-sink allocation strategy, so it is required that the network design should be known prior to analysing the Composite Curves.

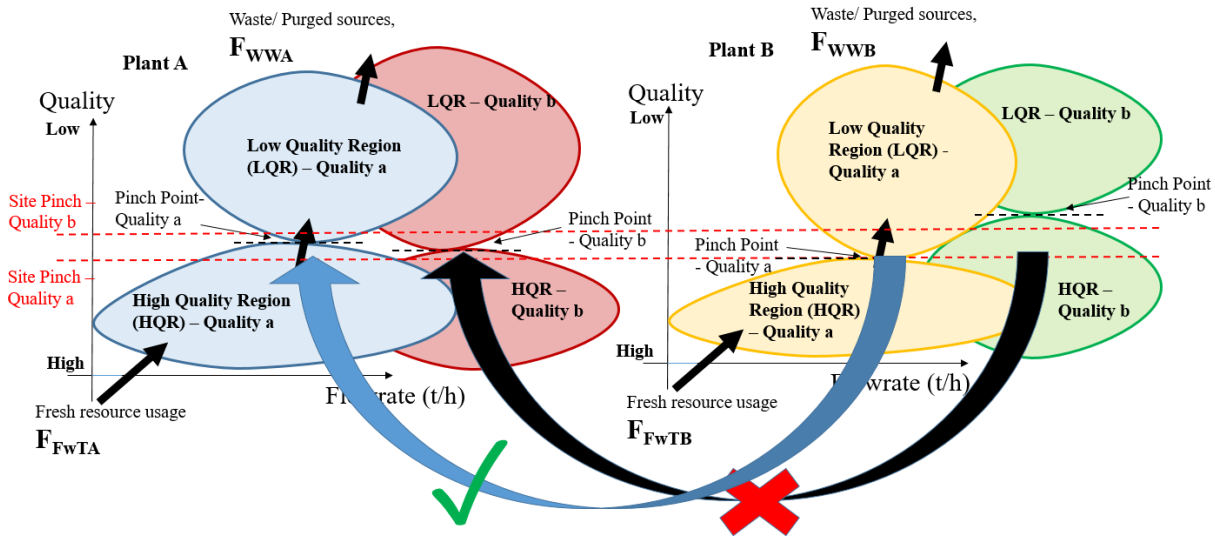

Figure 4-39: Plant B cannot send its unused sources (LQR for Quality A, but HQR for Quality B) to Plant A (HQR) due to Pinch Point for Quality B for Plant B is higher than the Site Pinch

4.2.2.2 Overall headers targeting framework

The headers targeting for single quality/contaminant problem is straightforward, just using the Composite Curves as shown in Figure 4-40, with all the sources and sinks from all the plants stacked in the Site Source and Sink CC. The header lines can be easily drawn from the Site Source Composite Curves, with a mix of cross-plant sources. However, in the case of multiple qualities, the individual allocation of the headers should be checked when there are Pinch Points in various qualities. In this case, an iterative procedure is proposed to determine the headers' properties as well as the individual allocation as well- Figure 4-41.

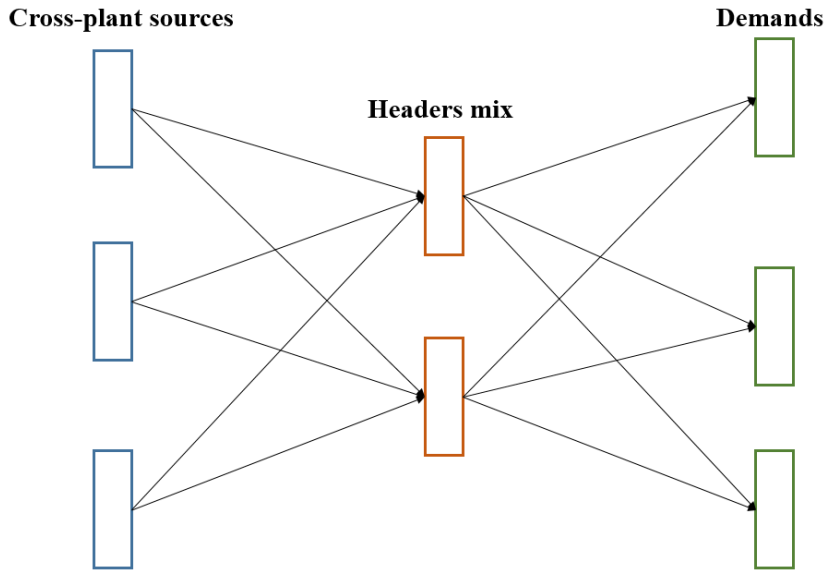

Figure **4-40**: Site-level headers mixed with cross-plant sources and sent to the demands/sinks

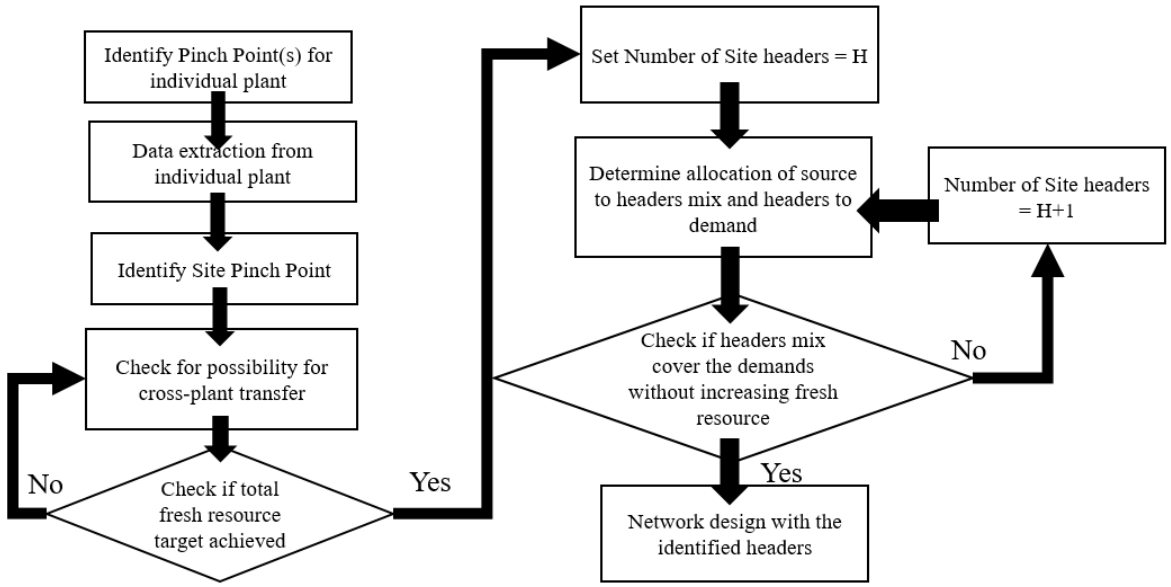

Figure **4-41**: Site-level headers targeting and design for multiple qualities problems

For site-level framework, the first step involves identifying the cross-plant sources first by analysing the Pinch Points of all plants through the Composite Curves. With the cross-plant sources, an iterative allocation procedure with the pre-set number of headers is determined first, with the freshwater requirement determined from an individual approach with a mathematical approach. In the first iteration, the number of the header can be set to one (H=1). It is then checked that the number of the header is sufficient to fulfil the demands without incurring an increment on the fresh resource. If not, the number of headers is increased by one, and the procedure is repeated.

4.2.2.3 Case studies and results – Internal and Site Headers

Internal Headers Targeting For a problem with multiple contaminants, the headers targeting framework can be used for data in Table 4-6. The step-by-step framework is demonstrated in this section.

Table **4-6**: Total Site data for multiple contaminants case (Chin et al., 2021d)

	Plant 1					Plant 2					Plant 3			
	F_{SR} (t/h)	C_A (ppm)	C_B (ppm)	C_C (ppm)		F_{SR} (t/h)	C_A (ppm)	C_B (ppm)	C_C (ppm)		F_{SR} (t/h)	C_A (ppm)	C_B (ppm)	C_C (ppm)
SR1	45	15	400	35	SR1	45	15	400	35	SR1	15	140	105	15
SR2	34	117.7	12,500	168.2	SR2	34	150	250	169	SR2	15	205	55	40
SR3	8.01	103.8	45	125,000	SR3	59	110	45	125	SR3	10	410	205	55
SR4	19	22	120	30	SR4	19	22	120	30	SR4	11	5	10	5
SR5	44.8	225	229	307.5	SR5	43	225	229	305	SR5	25	600	230	35
SR6	170	4.7	1.2	2,000	SR6	170	20	30	200	SR6	30	70	300	45
SR7	29	173.7	3,500	205	SR7	29	150	350	205	SR7	20	250	1,100	150
										SR8	25	150	660	90
	F_{SK} (t/h)	Z_A (ppm)	Z_B (ppm)	Z_C (ppm)		F_{SK} (t/h)	Z_A (ppm)	Z_B (ppm)	Z_C (ppm)		F_{SK} (t/h)	Z_A (ppm)	Z_B (ppm)	Z_C (ppm)
SK1	45	0	0	0	SK1	45	0	0	0	SK1	15	5	7	5
SK2	34	17.6	294.3	33.1	SK2	34	8	94	33	SK2	15	5	7	5
SK3	8.01	3.7	20	5	SK3	59	3.7	20	5	SK3	10	25	100	15
SK4	19	0	0	0	SK4	19	0	0	0	SK4	11	30	130	20
SK5	815	7.5	200	17.5	SK5	890	7.5	160	17.5	SK5	25	200	210	50
SK6	170	0	0	0	SK6	170	0	0	0	SK6	30	150	100	20
SK7	29	3.7	20	5						SK7	20	475	300	100
										SK8	25	200	120	40

Step (i): Construct initial multi-contaminant Composite Curves. To identify the freshwater target using Composite Curves, the first step is to classify the sinks into the contaminant cascades by determining their main limiting contaminant – see the detailed procedure in Chin et al.[21]. Using Plant 2 as the example, Table 4-7 shows the classification of sinks to the proper cascade by determining the concentration ratio- Eq(2). It shows that SK3 and SK2 are classified to cascade C, while SK5 and SK7 are classified to cascade A. Cascade A should be targeted first due to its total sink flowrate allocated to it is higher than the one in cascade C. Using the source allocation step for each sink in Figure 3-9, the overall Composite Curves representation for both cascades are shown in Figure 4-42. It shows the Pinch Points are at all of the contaminants.

Table 4-7: Classification of sinks to the contaminant cascade for plant 2.

	$Z_{A,SK}/C_{A,SRmax}$ $C_{A,SRmax}$= 225 ppm	**$Z_{B,SK}/C_{B,SRmax}$ $C_{B,SRmax}$= 12,500 ppm**	**$Z_{C,SK}/C_{C,SRmax}$ $C_{C,SRmax}$= 125,000 ppm**	**Minimum ratio**	**Cascade**
SK4	0	0	0	0	A/B/C
SK1	0	0	0	0	A/B/C
SK6	0	0	0	0	A/B/C
SK3	0.0247	0.0500	0.0244	0.0244	C
SK7	0.0247	0.0500	0.0244	0.0244	A
SK5	0.0500	0.5000	0.0854	0.0500	A
SK2	0.1173	0.7358	0.1615	0.1173	C

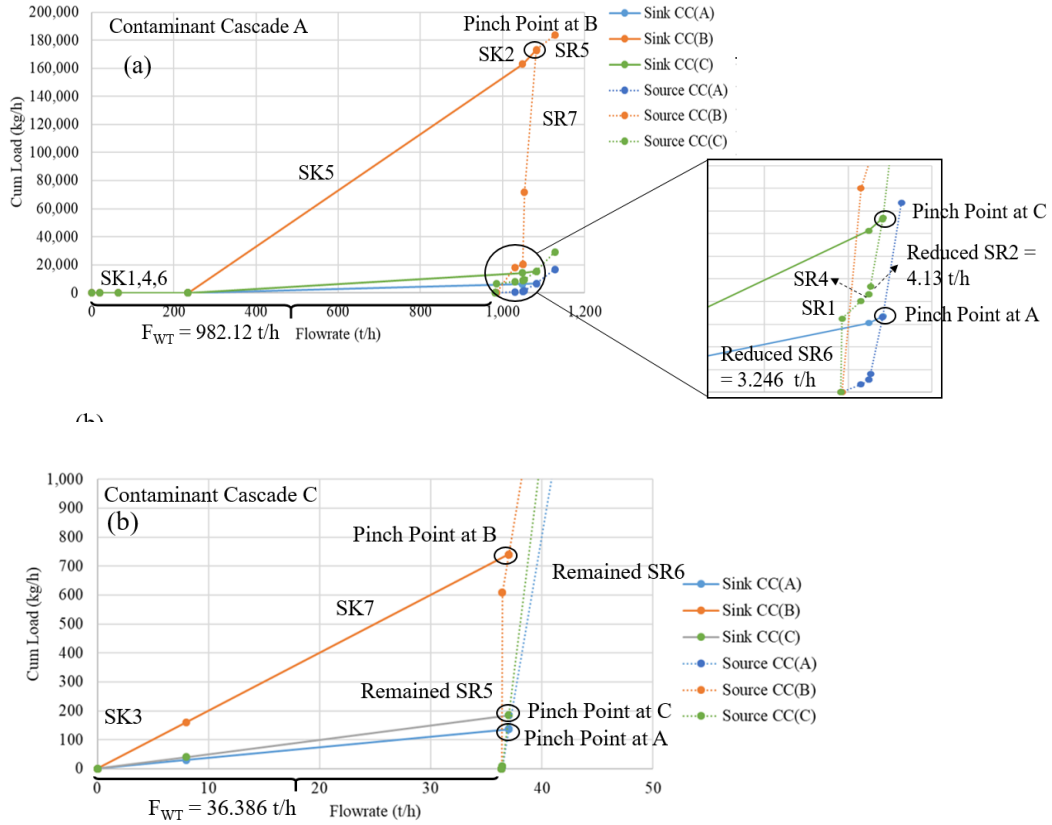

Figure 4-42: Source and Sink Composite Curves for Plant 2

Step (ii): Construct initial Multi-Contaminant Composite Curves. The combined representation of the Source and Sink CCs are combined in a single diagram shown in Figure 4-43. In this representation, the contaminant cascade A is drawn before the contaminant cascade C. According to Figure 4-43, a single header line below the Pinch Point can be drawn (only intersects at Pinch Points). The initial observation shows that a single header from the source is sufficient for the process. However, it must be checked with the source-to-sink allocation.

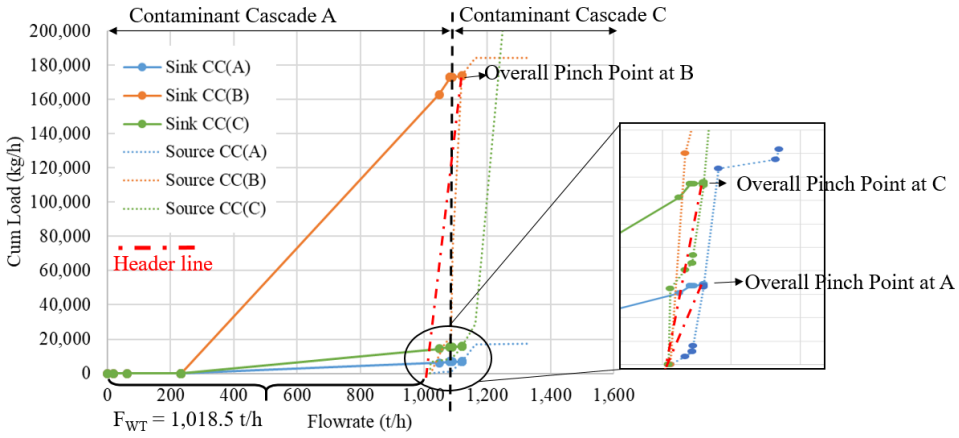

Figure 4-43: Combining Composite Curves for cascade A and C, with an internal header line for plant 2

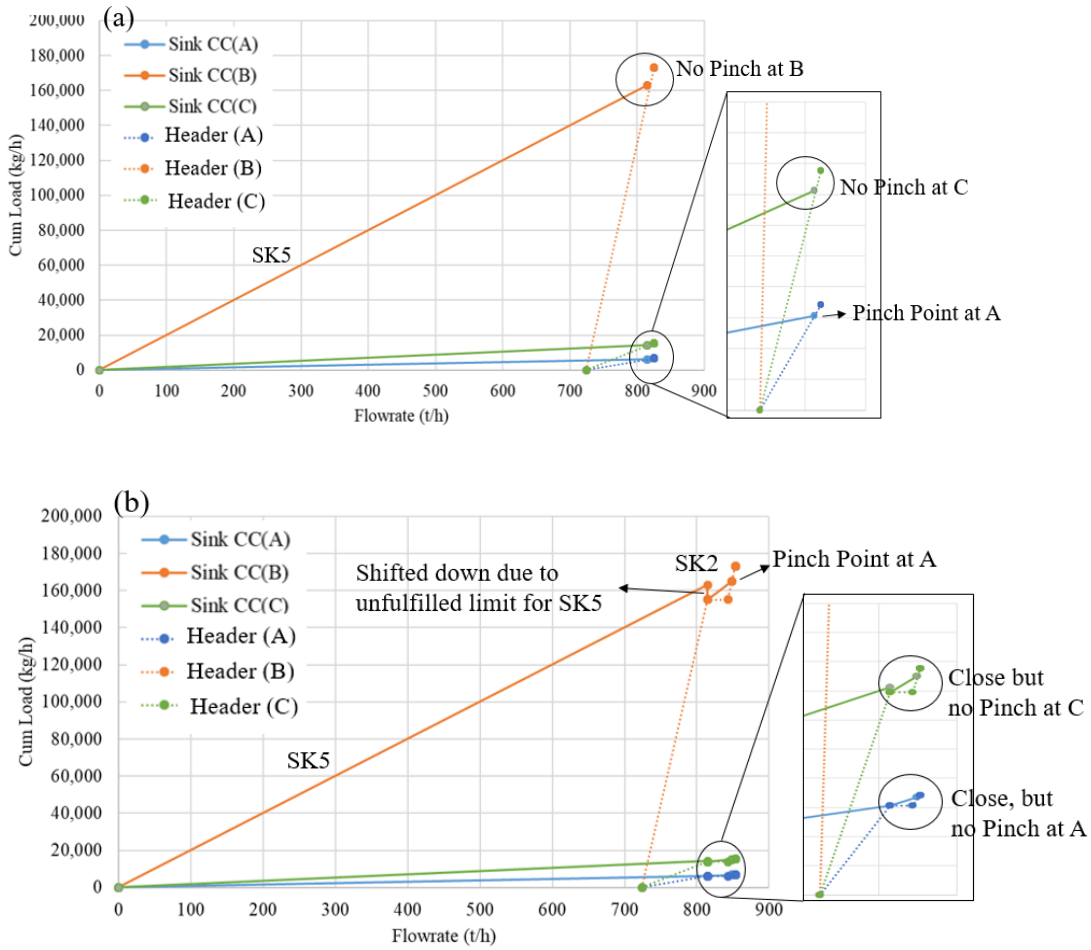

Figure 4-44: Checking individual source-to-sink allocation using the single header mixed sources (a) SK5 (b) SK5 and SK2 for plant 2

Figure 4-44 shows the allocation of the header for SK5. For SK5, the only Pinch Point formed is at contaminant A, but not at contaminant B and C- see Figure 4-44a. However, it is shown that this header mix is for the scenario where all Pinch Points for three contaminants for all sinks, see Figure 4-42, where no vertical shifting in the Sink CCs for all contaminants. The fact that no vertical shifting indicates that all contaminant limits for all sinks are fulfilled. Using the single header mix, vertical shifting of the Sink CCs at Sink 5 are required as the limit for contaminants B and C are not fulfilled for sink 5- see Figure 4-44b. It is also worth noting that for SK2, the only Pinch is at Contaminant A. The vertical shifting of the Sink CCs results in that the header mix identified earlier is not feasible (without adding more freshwater). This requires multiple header lines to be identified. Since the source allocation identified with the Pinch Analysis shows all contaminants limits for all the sinks are fulfilled, this means at least 3 headers from the sources (as there are 3 contaminants) are required to allow for degrees of freedom to achieve all contaminant limits for all sinks.

Another simpler case from Plant 1 is used to demonstrate the procedure. Table 4-8 shows the classification of sinks to the proper cascade by determining the concentration ratio. It shows that all of the sinks should be classified to cascade A. Figure 4-45 shows the Source and Sink

Composite Curves with the internal water header line for the process with 2 overall Pinch Points at contaminants A and C. Single header line is drawn with only intersection point at the Pinch Points. Note also no vertical shifting of the sink CCs for contaminant A and C, which mean those contaminant limits for all sinks are fulfilled.

Table 4-8: Classification of sinks to the contaminant cascade for plant 1.

	$Z_{A,SK}/C_{A,SRmax}$ $C_{A,SRmax}$= 150 ppm	$Z_{B,SK}/C_{B,SRmax}$ $C_{B,SRmax}$= 400 ppm	$Z_{C,SK}/C_{C,SRmax}$ $C_{C,SRmax}$= 205 ppm	Minimum ratio	Cascade
SK1	0	0	0	0	-
SK4	0	0	0	0	-
SK6	0	0	0	0	-
SK3	0.0247	0.0500	0.0244	0.0244	A
SK5	0.0500	0.4000	0.0854	0.0500	A
SK2	0.0533	0.2350	0.1610	0.0533	A

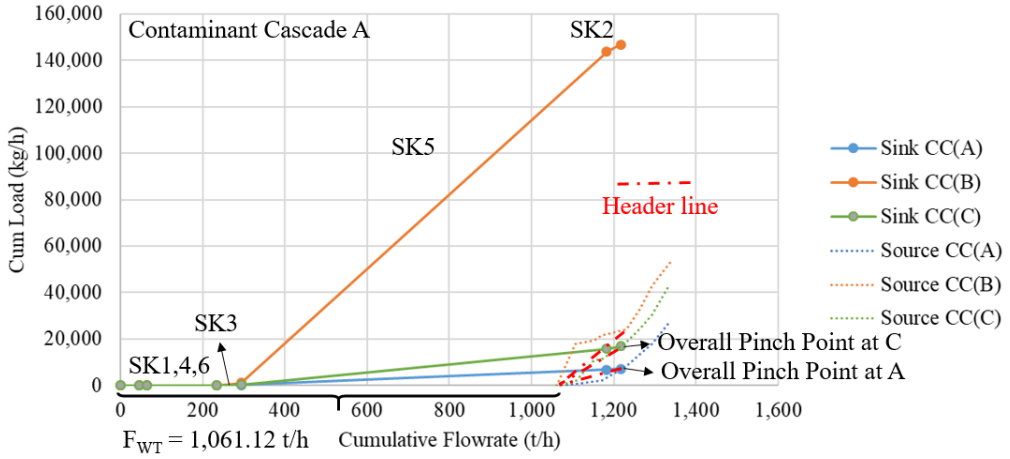

Figure 4-45: Source and Sink Composite Curves, with internal header lines for plant 1

Figure 4-46a shows the allocation of the header mix for SK3. The only Pinch Point formed is at contaminant C, but not at contaminant A. Using the single header mix, vertical shifting of the Sink CCs at Sink 3 are required as the limit for contaminant C is not fulfilled for sink 3- see Figure 4-46b. The contaminant limit for B is still not fulfilled for SK3, and this does not affect the overall target as in Figure 4-45 the contaminant B is not fulfilled overall. It is worth to also note that for SK5, the only Pinch is at the contaminant C. Since the source allocation identified with the Pinch Analysis shows both contaminants A and C limits for all the sinks are fulfilled, this means at least 2 headers from the sources (as there are 2 contaminants limits reached) are required to allow for degrees of freedom to achieve the required contaminant limits for sinks.

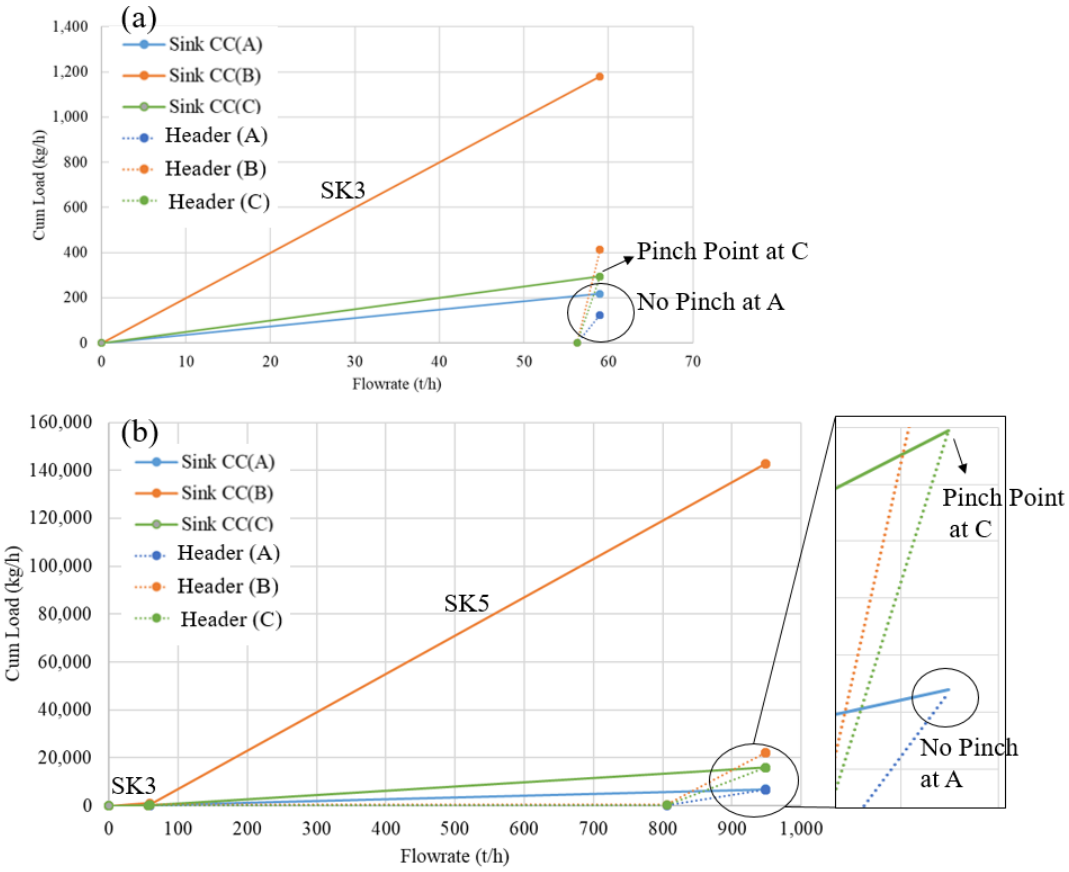

Figure 4-46: Checking individual source-to-sink allocation using the single header mixed sources (a) SK3 (b) SK3 and SK5 for plant 1

Total Site Headers Targeting. For site-level headers synthesis, it is first required to determine the Pinch Points for all the three plants for the case study. By performing Multi-Contaminant Pinch Analysis, it can be shown that the Pinch Points for each plant are: Plant 1: {225 ppm, 12,500 ppm, 2,000 ppm}, Plant 2: {110 ppm, ∞, 200 ppm} and Plant 3: {600 ppm, 300 ppm, ∞}. The total fresh resources required are about 2,190 t/h. The minimum fresh resources and the Pinch Points for the Total Site can be identified using various methods such as Mathematical Programming, Pinch-based Composite Curves, Water Source Diagram and concentration potential. In this case, a mathematical approach is used. It is identified that the fresh resources required are 2,074.06 t/h, and the Pinch Points are {600 ppm, ∞, 2,000 ppm}. The study is divided into just two plants studies (Plant 1 and 2) and three plant studies (Plant 1, 2 and 3).

4.2.2.3.1 Two plants

If the industrial site only contains two plants, the total minimal fresh resource is 2,074.67 t/h, with Pinch Points {225 ppm, 12,500 ppm, 2,000 ppm}, which follows the Pinch Points of Plant 1 for contaminants A, B and C. This means that Plant 1 is the limiting one, and its fresh resources can be further reduced. The current total fresh resource without site integration is 2,079.6 t/h, which is higher than the fresh resource with site integration. It can be seen that the LQR of SR2 contains sources that have better qualities than the Site Pinches. Since the

Pinch Points for Plant 2 are all lower than the Site Pinch Points, Plant 2 could send its LQR sources to Plant 1. The Pinch-causing sources for Plant 2 are SR3 for contaminant A and SR6 for contaminants C. It is obvious that SR6 is a better source compared to SR3 since its contaminants concentrations for A and B are better than SR3, and the target is to reduce the limits of contaminants A and B for Plant 1.

A new source, SR6 from Plant 2, is available for Plant 1. The flowrate of the required cross-plant transfer is mainly to replace the SR2 in Plant 1. By using the optimisation method, it is determined that the flowrate of SR6 is 5.99 t/h. A single transfer from Plant 2 is enough to achieve the fresh resource for the Total Site (2,074.67 t/h). Since only a single cross-plant source, a single header is enough for both plants. Figure 4-47 shows the header construction for two plants, where the SR6 from Plant 2 is the header source, and it is sent to SK2 and SK5 from Plant 1 (where the results are from mathematical optimisation).

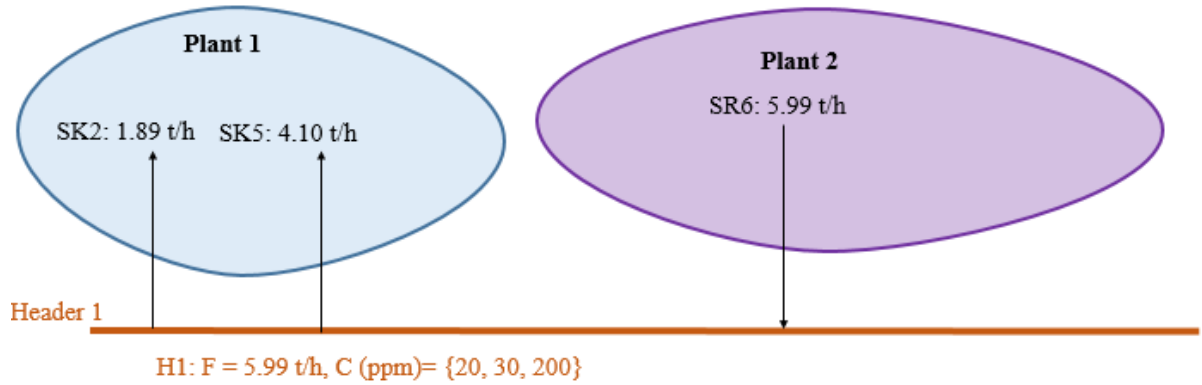

Figure 4-47: Total Site headers allocation for multiple qualities: Two plants study

4.2.2.3.2 Three plants

For the three plants study, the Pinch Points for each plant are: Plant 1: {225 ppm, 12,500 ppm, 2,000 ppm}, Plant 2: {110 ppm, ∞, 200 ppm} and Plant 3: {600 ppm, 300 ppm, ∞}. The total fresh resources required are about 2,190 t/h. The fresh resources for the Total Site required are 2,074.06 t/h, and the Pinch Points are {600 ppm, ∞, 2,000 ppm}. The Pinch Points for individual plants should be lower or equal to the Site Pinch Points. By analysing the Pinch Points, several insights can be identified:

(i) Plant 1 can send its LQR sources as its Pinch Points for contaminants A & B are lower than the Site Pinch Points, and its Pinch Point for contaminant C is identical to Site Pinch.

(ii) Plant 2 can send its LQR sources as its Pinch Point for contaminants A, B & C are lower than the Site Pinch

(iii) Plant 3 has Pinch Point for contaminant C higher than the Site Pinch, it can obtain sources transfer from other plants. It can send its LQR sources to other plants as well.

For further fresh resource reduction, the Pinch Points for each plant can be examined. The fresh resource for Plant 1 is limited by contaminant B as its Pinch Point is at 12,500 ppm, and it can be replaced by other sources. The candidate sources would be the LQR sources that have lower concentrations than the Pinch Points from Plant 2 and Plant 3. The ideal one would be SR3 and SR6 from Plant 2 since it has lower contaminants B, as discussed in the previous section. Plant 2 SR2 have lower qualities than SR3 in all contaminants, so SR3 should be used before SR2. The same reasoning applies to SR6 and SR5.

Plant 3 have potential LQR sources that are lower than the Site Pinch Points: SR7 and SR8. However, since SR8 has lower contaminants than SR7, SR8 should be prioritised. The Pinch-causing sources from Plant 3 in the LQR region can be used as well (SR5 and SR6). Since Plant 3 has Pinch Point for contaminant C higher than the Site Pinch, it can obtain sources from other plants as well. The candidate source would be the Plant 1 SR6, which is the Pinch-causing source for contaminant C for Plant 1. The minimal total cross-plant transfers with detailed allocations are solved using mathematical optimisation. The minimal cross-transfer sources are determined as 108.9 t/h with minimal fresh resources. The procedure in Figure 4-41 is then used to determine the number of headers required. By solving the number of headers iteratively with the cross-plant sources, it is determined that three headers are sufficient to cover the demands. Figure 4-48 shows the header sources mix from each plant and its allocation to each sink.

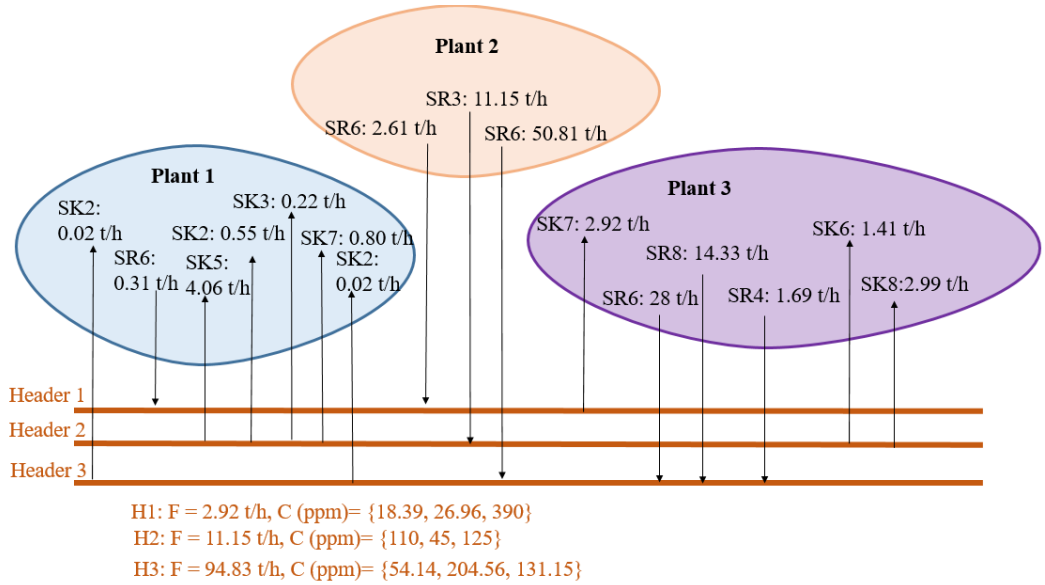

Figure 4-48: Total Site headers allocation for multiple qualities: Three plants study

4.3 Mathematical Optimisation approach (Results comparison)

This section presents the comparison of the results between the proposed Pinch-based approach with the mathematical optimisation approach. The full model is presented in Appendix B, and the results comparison is presented in Appendix C.

Several assumptions or parameters required for the optimisation model are listed as follows:

(a) The unit price for fresh resource cost, wastewater treatment cost and electricity are $ 1/t, $ 0.5/t and $ 0.1/kWh

(b) The annual operating hours (Op) for the plants are 8,000 h/y

(c) The interest rate (IR) is 10 %, and the operating life (n_{life}) for all the plants are 20 y.

(d) Stainless steel (F_M = 2) pump with type factor (F_t = 1.50) and 1,800 shaft rpm is used to pump water in all piping connections[27]. The friction of the pipe is neglected.

(e) The distance between units in each process is 0.1 km, while the distance between plant 'p' and plant 'p+1' is 1 km. This means, for example, the distance between Plant 1 and Plant 2 is 1 km, and the distance between Plant 1 and Plant 3 is 2 km. The distance between the process and the Total Site headers to be built is 0.4 km. The piping length is assumed similar to the elevation length.

(f) The water header/main is assumed as a vessel containing a mixture of water sources.

4.4 Conclusion

This work has proposed a header targeting and design approach for Water Integration problems using the Material Recovery Pinch Diagram. The freshwater target is identified first using the Pinch Analysis, and the header curves are constructed by mixing some of the source segments in the Source Composite Curve. The study is also applied for both single- and multiple-contaminant cases. The approach can target the header source flowrates, the concentration of the header's mix, and the minimum number of headers required to achieve the identified freshwater target. A mathematical model is also formulated by accounting for the piping cost, pumping cost and the water header capital cost. The results show the Total Site minimum TAC for the single contaminant study is 12.9 M$/y, while for multiple contaminants case is 20.0 M$/y, which are compromised by higher freshwater intake due to more expensive capital expenditure.

This approach is beneficial as it provides a graphical interface to the users. The users could manipulate the headers' flow and concentrations by adjusting the length and gradients of the header lines based on their preferences. The header lines can be adjusted by using the Source Composite Curve as the locus path, and the header lines should be located below the Sink Composite Curve to guarantee a minimum fresh resource target.

Several findings are obtained from this work:

- Swapping the order of sources within HQR (or LQR) does not alter the fresh resource requirement (or waste generation) for a process.
- The combination of cross-plant transfer Scheme 2 (HQR to LQR) and Scheme 3 (LQR to LQR) with Scheme 1 (LQR to HQR) yields the optimal total fresh resource target with the minimal cross-plant transfer.

- Transferring purged sources from one plant to replace the HQR sources from another plant is more effective when the transfer happens across the Site Pinch Point than within just the site HQR or site LQR. The overall cross-plant transfer can be minimised while the total fresh resource target that can be obtained is still identical.
- A minimum number of headers in the Total Site can be identified with Site CC that guarantees fresh resource intake is minimal, but the total cross-plant sources transfer is not minimal, which may require more capital and operational cost.

However, the header design using the Composite Curves depends on the source-to-sink allocation strategy. For the single contaminant case, the Pinch-based strategy of allocating source is to satisfy the maximum limit of the sinks (below the Pinch). For the multiple contaminants case, the individual source-to-sink allocation defines the Pinch Points and specify the vertical shifting of the Sink/Source CC (where sinks' contaminant limits are not reached below the Pinch). It is an iterative procedure to check whether the header mix is feasible with the source-to-sink allocation for multiple contaminants cases. In this work, the source-to-sink allocation strategy is to fulfil all the contaminant limits for every sink as much as possible. Different approaches such as concentration potential, Water Source Diagram or Mathematical Programming approach can be used to determine the individual source-to-sink allocation first, and then the Composite Curves can be drawn to determine the number of headers, the flowrates and the concentrations. The solutions obtained may differ for each approach.

CHAPTER 5 GAME THEORY APPROACHES IN DERIVING A BALANCED ECONOMIC POLICY OF WASTES RECYCLING IN TOTAL SITE/ECO-INDUSTRIAL PARK

This chapter aims to identify the distribution of stable and fair profits to the plants from the government to each stakeholder with the Cooperative Game approach. Designing water symbiosis networks in an industrial site is aimed to solve the water quality and security problem by minimising freshwater consumption or pollutant discharge. However, implementing the symbiosis requires an expensive capital cost on the site and may need cost compensation by the authority to facilitate the operation. This study considers the grand coalition of finite players (industrial plants/stakeholders) with authority to facilitate water recycling in an eco-industrial park. The first stage includes the determination of the park authority's objectives (i.e., to minimise cost, resource usage, or pollutants discharge) if the stakeholders cooperate. In the next stage, the park authority can then compensate the cost by providing fair incentives or subsidies for the stakeholders that participate in the symbiosis (Section 5.2). The incentives can be a rewarding scheme for the recycling efforts, while the subsidies are the money required to build the facilities. The stakeholders are then allowed to decide the recycling amount that maximises their economic interests. A wastewater tax can be imposed by the authority to the stakeholders to stimulate them to take part in the symbiosis while generating the money source for subsidisation. Proper game analysis is provided to analyse the Nash Equilibrium solutions of the tax rate (Section 5.3). Section 5.4 presents the overall framework, and Section 5.5 presents the case study and results

5.1 Introduction

A possible approach to finding a fair distribution of cost and resources is to apply the Cooperative Game Theory (CGT). This is expected to ensure stable and efficient operation in an eco-industrial park. One example is from Lozano et al. (2013) for transportation and logistic cost-sharing. Most of the current research has focused on the waste recycling of products generated by social services and consumption, such as waste recycling and distribution (He et al., 2019) and recycling path selection and optimisation (Herczeg et al., 2018). In the field of Process Integration, Hiede et al. (2012) studied energy integration between companies by using Pinch Analysis and Cooperative Game approach to explore the allocation of utility savings. Chang et al. (2014) proposed a game-theoretic method in optimising the configuration of site-level plant Heat Integration schemes. Chang et al. (2018) later provided a stepwise development of the indirect Heat Integration schemes using the game theory approach. Jin et al. (2018) proposed innovative risk-based Shapley values for exploring the cost savings for site-level Heat Integration problems. Wang et al. (2020) introduced a method ensuring fair and stable cost allocation for site-level Heat Integration problems using an ideal expert model. Carmen (2019) utilised different utility allocation schemes for water distribution networks for agriculture industries, including social welfare, Nash Bargaining Solution and Russian Welfare strategies. These strategies ensure the fair

design of the water distribution scheme. Ramos et al. (2018) formulated a multi-leader-followers and single-leader-follower framework for synthesising an eco-industrial park. They consider the possibility that the authority or the stakeholders can be the leaders as well as the followers. Chhipi-Shrestha et al. (2019) applied game theory in selecting sustainable municipal water reuse applications, and Jato-Espino and Ruiz-Puente (2021) strengthen the waste exchange scheme in industrial parks using Game Theory as well. Cruz-Aviles et al. (2021) incorporated fairness in their approach in designing water networks in eco-industrial parks. Jin et al. (2020) proposed a hybrid of government value compensation model and game theory approach for waste recycling in an industrial park.

Jacobsen (2006) have conducted an economic and environmental analysis on the water and steam exchanges in Kalundborg industrial park, where it shows that the long-term resource saving benefits can be minor, but the crucial part is the economic benefits for each participating plant to facilitate industrial symbiosis. As mentioned above, most of the works related to water industrial park design did not account for fair cost or resources allocation among different plants. Another issue is the lack of studies that consider scientific subsidising strategies by the authority to the stakeholders, which hinders the application of the industrial park. The cost of waste recycling or treatment can be very high for the stakeholder to bear, which further affects the enthusiasm and initiatives of the company (Chen et al., 2019). A very little research has been conducted on how the government should compensate firms for waste recycling in industrial parks.

This study aims to apply the game theory and value compensation approaches to determine the optimal incentives and subsidising strategy from the government for each plant. The ideal case where all the plants cooperate to achieve pollution reduction goals can be designed with Cooperative Game Theory (CGT) approaches. The stable and fair cost allocation among the stakeholders can be evaluated using the CGT strategies. A game analysis on the taxation system by the authority as a stimulation for the stakeholders is also provided. The following section explains the proposed methodology used in this work.

5.2 Government subsidies/incentives allocations with Cooperative Game Theory

Each plant in the industrial site might be reluctant to participate in the symbiosis programme even though the minimal total TAC is identified through optimisation. This is because the additional cost they need to pay to build the overall system may exceed the resources cost-saving, which they might not obtain any profit. This hinders the practical implementation of the proposed scheme. In this case, the authority plays a central role in providing subsidies to the plants to convince them to take part in the industrial symbiosis for greater environmental benefits. Jin et al. (2020) have developed a framework for the government subsidisation strategy in a competitive environment, where each plant and the government only concern about their own benefits. However, this approach may raise dissatisfaction from the stakeholders on the subsidised amount provided by the government, as some might receive a larger or smaller amount. In fact, they should cooperate in formulating a fair (minimising

dissatisfaction) and stable subsidisation allocation contract among the stakeholders while minimising the budget required by the government. It is also necessary to ensure the subsidies allocated for the grand cooperation are greater than the subsidies the stakeholders can obtain if they do not participate in the symbiosis. This is to ensure they are more willing to join the symbiosis to achieve Total Integration.

Identification of the incentives and subsidisation allocation to each plant is not an obvious task. It is required to know the contribution of each plant to the total TAC, the total resource-saving or the waste discharge. However, a smaller plant may contribute less to the resources saving as they require a lesser amount of fresh resources. The scale of the plant is also an important factor in allocating the cost as well. An analytical approach is required to determine the fair cost distribution among the plants so that the satisfaction of all the plants can be maximised. The Cooperative Game Theory is the most suitable concept in establishing fair resources sharing contract between stakeholders. Figure 5-1 shows the conceptual framework for this study, where the first stage involves the determination of the solutions for all possible coalitions. The subsequent stages are the subsidies or incentives allocations by the park authority.

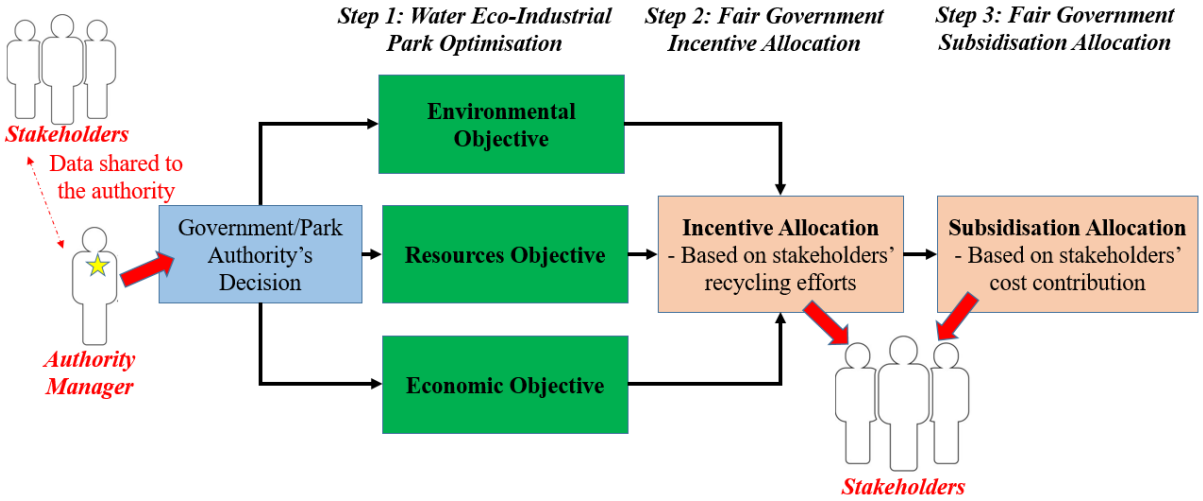

Figure **5-1**: A general proposed framework of government incentive and subsidisation allocation on water eco-industrial park

5.2.1 Fair allocation with Point solution concepts

In the solution concept of a cooperative game, the aim of the approach is to identify a fair and equitable cost or profit distribution to different players (plants). A cost savings allocation problem can be modelled as a cooperative game with transferable utility, i.e., a pair (N, CS) where N = {1, 2, …, P} denotes the whole set of companies, also known as the grand coalition. The characteristic function CS assigns to any non-empty coalition S, and the Cost Savings CS(S) is obtained if the companies in S cooperate. The cost savings for the industrial symbiosis can be in different contexts, i.e. the utility cost savings or the total annualised cost savings. The two conditions of a Cooperative Game are super-additivity and monotonicity- Eq(5-1).

Super-additivity: $CS(S \cup T) \geq CS(S) + CS(T) \qquad \forall S,T \subseteq N, S \cap T = \varnothing$

Monotonicity: $CS(S) \leq CS(T) \quad \forall S \subseteq T \subseteq N$ (5-1).

Super-additivity implies that the cost savings resulting from merging any two coalitions are larger than the sum of the separate cost savings of those coalitions. This provides an incentive to form the grand coalition. Analogously, monotonicity implies that a larger coalition is more beneficial than a smaller coalition.

In the perspective of industrial symbiosis, these properties hold true as well. The super-additivity property means that the stakeholders are only convinced to join in the grand symbiosis (with all other stakeholders) only if the overall benefits are bigger than the benefits without resource exchange with other stakeholders. Otherwise, it is preferable to perform Process Integration alone rather than combining efforts with others. The monotonicity property suggests a similar concept, for which the stakeholders obtain greater benefits by cooperating with more stakeholders instead of forming a smaller coalition.

There is an additional property, convexity, that implies the incentives for a new plant joining a symbiosis network increase as the network grows (Shapley, 1971) - Eq(5-2). However, this property does not always hold true for industrial symbiosis. This is because the cost required to integrate with the newcomer may be higher due to the geographical location of the new plant from other plants, or it has a low-quality waste discharge and high fresh resource requirements. However, considering the resource and environmental objectives, this property might hold true as the more collaboration between plants, the resources savings and pollutants discharged reduction can be maximised.

$$CS(S \cup \{i\}) - CS(S) \leq CS(T \cup \{i\}) - CS(T) \quad \forall S \subseteq T \text{ and } i \notin T \tag{5-2}$$

The main purpose of forming a water eco-industrial park is to minimise the reliance on fresh resources and to minimise wastewater discharge. In this case, the authority could provide an incentive scheme for the stakeholders depending on how much they can save on resource consumption and waste discharge. This is provided that the authority has additional income and decides to reward the participating stakeholders. The incentives could stimulate the stakeholders to maximise their water recycling rates. This work proposes an incentive allocation strategy for the government or park authority using the Cooperative Game approach. In this specific case, the annual cost savings (CS^{inc}) represents the operating cost saving for all coalition 'S', which is represented in Eq(5-3).

$$CS^{inc}(S) = UP_{FW}\left(F_{FW,O}(S) - F_{FW,T}(S)\right) + UP_{WW}\left(F_{WW,O}(S) - F_{WW,T}(S)\right) \quad \forall S \in N \tag{5-3}$$

There are varieties of Cooperative Game Theory approaches for allocation of incentives, namely the Shapley Value (Shapley, 1953), nucleolus (Schmeidler, 1969), the Least Core method (Drechsel and Kimms, 2010), the min-max core (Drechsel and Kimms, 2010) and the τ-value (Tijs and Driessen, 1986). The Shapley Value is the most common approach in the literature, where the marginal contribution of the stakeholder in the grand coalition is considered. The cost or profit is then allocated to them based on their marginal contribution. The calculated Shapley Value represents the amount of incentive allocated to each plant. The nucleolus approach aims to minimise the largest dissatisfaction of the stakeholders, while the τ-value concept is to find the allocation solutions between the marginal contribution of the stakeholder and the minimal rights of the stakeholder. The formulations of these approaches are shown in Appendix C.

5.2.2 The Core methods

The incentives allocation by the authority can be optional depending on the authority's choice. However, subsidies from the park authority are needed to support the cost of building the industrial park if the savings on recycling sources are outweighed by the capital cost. The annual cost saving with government incentives for each plant 'p' can be calculated using Eq(5-4). It is easy to determine the minimum amount of subsidies such that all the stakeholders at least do not suffer economic loss. The minimum subsidisation for each stakeholder can be determined by solving the industrial symbiosis model with capital cost by setting the profit constraint to be at least zero- Eq(5-5) with the symbiosis model and determine the minimum subsidies amount.

$$CS^{sub}(p) = TAC_o(p) - TAC(p) + Incentives(p)\ \forall p \in P \tag{5-4}$$

$$Profit(p) = CS^{sub}(p) + Subsidy(p)\ \forall p \in P \tag{5-5}$$

However, in order to further stimulate the stakeholders to participate in the symbiosis, more subsidies can be allocated to the stakeholders according to their contribution to the total cost saving. In this work, it is proposed that the subsidy allocation to the stakeholders, similar to incentive allocation, has to be fair to all the stakeholders so that the dissatisfaction of the stakeholders can be minimised. A similar game-theoretical approach can be applied for subsidisation allocation by accounting for the annualised capital cost in the annual cost saving.

In this study, it is proposed that the government subsidisation must fulfil the super-additivity and monotonicity properties of cost savings, i.e. the subsidised profit for a larger coalition is greater than merging smaller coalitions, as well as the subsidised cost saving is more beneficial for the larger coalition- see Eq(5-1). The grand coalition of all the stakeholders does not necessarily yield lower annualised cost compared to other smaller coalitions. This is because of the expensive capital of building the facilities, such as piping connection and pumps. If these properties do not hold, the grand coalition scheme is not interesting for any rational stakeholders anymore, and they might not be interested in joining the symbiosis.

The modified ε-core method for subsidies allocation to account for super-additivity and monotonicity is presented in Eqs(5-6 to 11). In this approach, the $x(p)$ is a profit variable, which represents the additional profit that each plant 'p' can obtain from the authority, apart from the subsidies. However, the main purpose of the method is to identify the minimum subsidies amount. The preferred solution for $x(p)$ contains all zeros. In Eq(5-6), the value of ε^{sub} is minimised as well. If $\varepsilon^{sub}< 0$, this means that the core is not empty, i.e. the profits of each plant in the grand coalition is larger than any other coalition. The stakeholders have no reasons to not join the grand symbiosis if this is the case. However, if $\varepsilon^{sub}> 0$, this means there are other smaller coalitions better than the grand coalitions. The stakeholders could obtain more profits in a smaller coalition. In fact, the value of ε^{sub} can be interpreted as the following:

(i) The authority has to pay a specific stakeholder amount of ε^{sub} so that the stakeholders are willing to join the grand integration scheme, assuming the stakeholders are rational.

(ii) The participated stakeholder must pay a penalty ε^{sub} if they want to quit the grand integration scheme. This helps the authority to formulate a cost binding contract with the stakeholders.

Eq(5-9) indicates the total subsidies must be lower than the budget of the park authority, Eq(5-10) ensures the subsidies allocated are at least larger than the minimum requirement of the cost for each plant 'p', to ensure at least each plant does not suffer economic loss while Eq(5-11) ensures the super-additivity properties hold for the subsidies allocation. In this work, only semi-super-additivity is assumed, where the cost savings for individuals are lower than the cost savings in the grand coalition. The formulation of the subsidy allocation model using another variant of the game theory tool (modified min-max core) is presented in Appendix D.

$$Modified\ LeastCore:\ Min\ \sum_{p} Subsidise\ (p) + \varepsilon^{sub} \tag{5-6}$$

$$\sum_{p\in S} x\ (p) - \sum_{p\in S} Subsidise\ (p) \geq CS^{sub}(S) - \varepsilon^{sub} \quad \forall S \in N \tag{5-7}$$

$$\sum_{p\in N} x\ (p) - \sum_{p\in N} Subsidise\ (p) = CS^{sub}(S) \quad S = N \tag{5-8}$$

$$\sum_{p} Subsidise\ (p) \leq Budget \tag{5-9}$$

$$Subsidise\ (p) \geq |CS^{sub}(p)|\ \ if\ CS^{sub}(p) < 0, \forall p \in P \tag{5-10}$$

$$\text{Semi-superadditivity: } CS^{sub}(\{i\}) - \sum_{p\epsilon ps} Subsidise\ (p) \leq CS^{sub}(S), \quad S = N, where\ i \in S \tag{5-11}$$

5.3 Taxation policy on waste discharge

The park authority or manager could impose a wastewater tax on the park to further stimulate the stakeholders to implement as much recycling as possible. The tax received could be used as a source of income to subsidise the stakeholders (Figure 5-2), which means that the tax money received from one stakeholder could be used as subsidies for other stakeholders. A wastewater tax can be calculated as the tax imposed on the wastewater pollutant discharge for each plant 'p'- see Eq(5-12).

$$Tax(p) = t\left(\sum_{i\epsilon I} F_{p,SRi,WW} C_{p,SRi}\right), \text{ where t = tax rate/kg of pollutant} \quad (5\text{-}12)$$

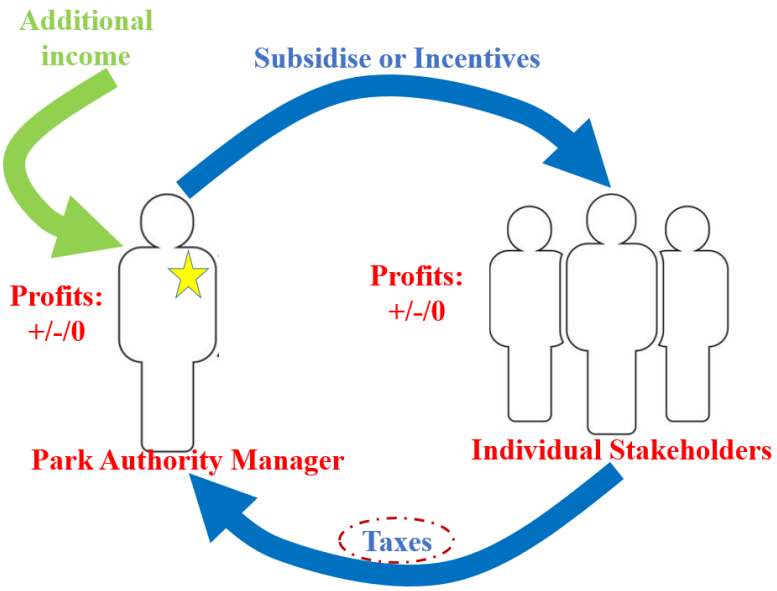

Figure **5-2**: A wastewater tax can be used as a source of income to subsidise the eco-industrial park

However, the tax rate 't' should be properly set to encourage the stakeholders to perform recycling, as they are more pressured to recycle more water to reduce the pollutants discharge load. The behaviours of the stakeholders and the tax rate are related indirectly as well. The tax rate should also be set so that the park authority can reduce its regulatory frequency while more money to cover subsidies the cost. In this case, a game analysis between the park authority and all stakeholders is required to investigate the effect of the tax rates on their behaviours. The possible scenario tree analysis is presented in Figure 5-3. The following assumptions for the game analysis are stated as follow:

(i) The park authority could enforce the tax regulation on the industrial plants. The probability of regulation (willingness of regulation) is $\emptyset$ where they have to pay certain regulatory cost $Cost_{\emptyset}$.

(ii) The owners of the plants have the choices to implement recycling or not, with the probability of recycling (willingness to recycle) denoted as θ for all stakeholders. They need to pay certain cost $Cost_{\theta}$ when implementing the recycling, and cost $Cost_{\theta_o}$ when

they do not implement recycling- the fresh resource and waste treatment cost. As the cost of implementing the recycling scheme is expected to be more expensive compared to without recycling, it is assumed that $Cost_{\theta} > Cost_{\theta_o}$.

(iii) The subsidies by the park authority $sub(p)$ are provided only if the stakeholders implemented the recycling scheme. They are not entitled to receive any subsidies otherwise.

(iv) The park authority does not know the stakeholders are willing to participate in the water symbiosis, while the stakeholders do not know whether the park authority will impose the tax regulation or not.

(v) Each stakeholder and the park authority are rational, where they will play the strategies that maximise their own benefits.

5.3.1 Nash Equilibrium analysis

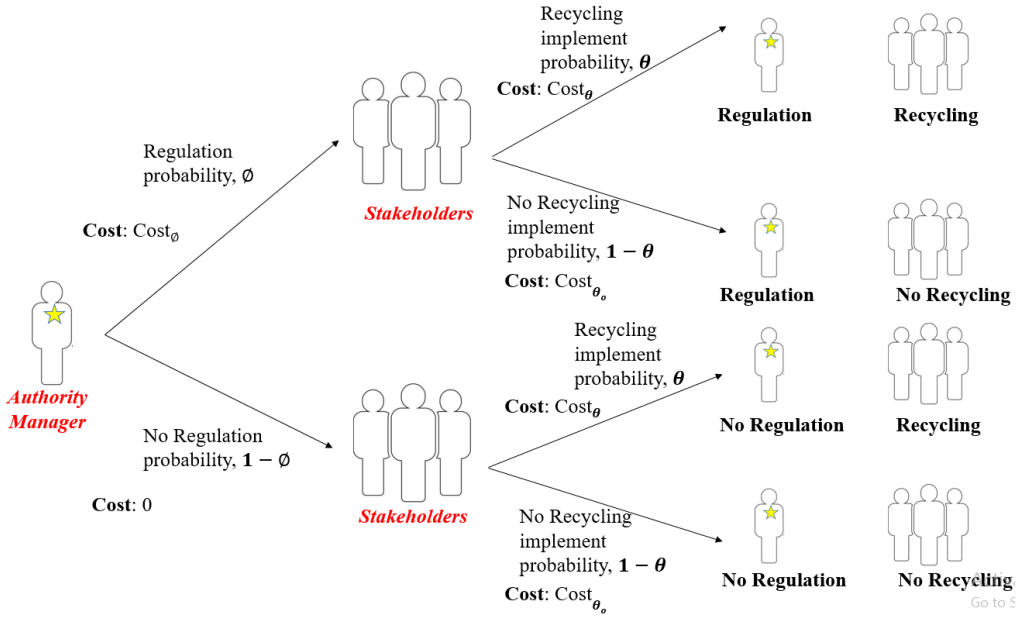

Figure **5-3**: Possible scenarios between park authority and stakeholders

Assuming the park authority and stakeholders do not know the strategies of each other, a Nash Equilibrium analysis is required to understand their own optimal strategies and behaviours. The Nash Equilibrium points of a game (Nash, 1950) is the optimal strategy of a player, given that the other players' strategies are known. For example, with two players (Player 1 and 2), the strategy (A, B) is a Nash Equilibrium point, where the optimal strategy for Player 1 is 'A' given Player 2 has played 'B'. The same reasons apply to Player 2 as well, where his/her optimal strategy is 'B' given Player 1 has played 'A'. This can be applied to the industrial park analysis that involves park authority and stakeholders as two separate players. It is crucial to analyse their behaviours under the effects of taxation policies and subsidies, and the tax rate can be set properly. A pure strategy for a game is not available if there are no Nash Equilibrium points for all players. In this case, a mixed strategy can be played. Table 5-1 presents the payoff table

of each party. $Tax_o(p)$ is the waste discharge tax imposed on plant 'p' if they do not implement the recycling strategy. The tax can be calculated using Eq(5-12). Note that in this work, the considered game is played between all stakeholders and the park authority manager.

Table 5-1: Payoff table for park authority (G) and all stakeholders/plants

		Stakeholders/Plants (P)	
		Recycle (θ)	No Recycle ($1-\theta$)
Park Authority (G)	Regulation ($\emptyset$)	**G**:$-Cost_{\emptyset} - \sum_p sub(p) + \sum_p Tax(p)$ **P**: $-Cost_{\theta} + \sum_p sub(p) - \sum_p Tax(p)$.	**G**:$-Cost_{\emptyset} + \sum_p Tax_o(p)$ **P**: $-Cost_{\theta_o} - \sum_p Tax_o(p)$
	No Regulation ($1-\emptyset$)	**G**: 0 **P**: $-Cost_{\theta}$	**G**: 0 **P**: $-Cost_{\theta_o}$

$$\theta = \frac{-Cost_{\emptyset} + \sum_p Tax_o(p)}{\sum_p Tax_o(p) + \sum_p sub(p) - \sum_p Tax\,(p)} \tag{5-13}$$

$$\emptyset = \frac{Cost_{\theta} - Cost_{\theta_o} - \sum_p sub(p) + \sum_p Tax\,(p)}{\sum_p Tax_o(p)} \tag{5-14}$$

The Nash Equilibrium solutions for the strategies ($\emptyset$ and θ) of both parties are presented in Eqs(5-13 to 14), where their derivations can be found in Supplementary Material - Appendix E. Several intuitions can be obtained from the payoff table (Table 5-1) and equilibrium solutions:

(a) If the tax rates and subsidies are low, the 'no recycling' strategy might be the dominant strategy of the stakeholders regardless of authority strategies, as $Cost_{\theta} > Cost_{\theta_o}$.

(b) If the regulatory cost of authority ($Cost_{\emptyset}$) is high, the stakeholders recycling probability (θ) decreases. This is because the rational stakeholders think that the authority is more reluctant to pay the regulatory cost, which indirectly reduces the willingness of recycling.

(c) The increases in the subsidies obviously increase the recycling probability (θ), motivating the stakeholders to invest in the recycling scheme. This also decreases the probability of the authority regulation ($\emptyset$) as well.

(d) The increases of the wastewater tax rate 't' reduces the authority regulation probability ($\emptyset$), and increases the recycling probability of the stakeholders (θ)

(e) Assuming the regulatory cost of authority ($Cost_{\emptyset}$) is a negligible cost, the 'regulation' strategy from the authority is the dominant strategy regardless of stakeholders' strategies, provided if $\sum_p sub(p) \leq \sum_p Tax(p)$, i.e. the total taxes received are at least equal to the total subsidies. In this case, the recycling probability (θ) will be close to one as well.

(f) If authority has chosen 'regulation', it is obvious that recycling is the optimal strategy provided if the payoff for recycling is larger than without recycling, i.e., $-Cost_{\theta} + \sum_p sub(p) - \sum_p Tax(p) \geq -Cost_{\theta_o} - \sum_p Tax_o(p)$. However, this condition might yield lower tax rates, which reduces the profits for the authority. In fact, it is actually sufficient to specify that the payoff for recycling is larger than the cost without recycling activity, i.e., $Cost_{\theta} + \sum_p sub(p) - \sum_p Tax(p) \geq -Cost_{\theta_o}$

Based on the mentioned intuitions, the determination of the wastewater tax has to fulfil either one of the two conditions – Eqs(5-15 to 16).

Condition 1: $\sum_p sub(p) \leq \sum_p Tax(p)$ (5-15)

Condition 2: $\sum_p Tax(p) \leq Cost_{\theta_o} - Cost_{\theta} + \sum_p sub(p)$ (5-16)

Condition 1 represents the minimum tax amount is larger than the total subsidies so that the park authority do not suffer economic loss. This is based on the assumption that the regulatory cost ($Cost_{\emptyset}$) is negligible or can be sponsored by additional sources of income or the extra environmental benefits. This condition is actually benefitting the authority the most. Condition 2 represents the maximum tax amount, such that the payoff for recycling should be larger than the payoff without recycling if to strongly attract the stakeholders. This condition is to maximise the benefit of the stakeholders while encouraging the stakeholders to recycle.

These conditions are based on the fact that both players get the most benefits. However, these two conditions are based on the major assumptions that no additional income to subsidise, as well as the stakeholders, are willing to or capable to pay the tax. The overall flow of the money is balanced as presented in Figure 5-2, which might not be the case realistically as there are additional incomes/cost for both parties. Even though the conditions are obvious, this analysis provides a threshold estimation of the tax rates as well as the subsidies.

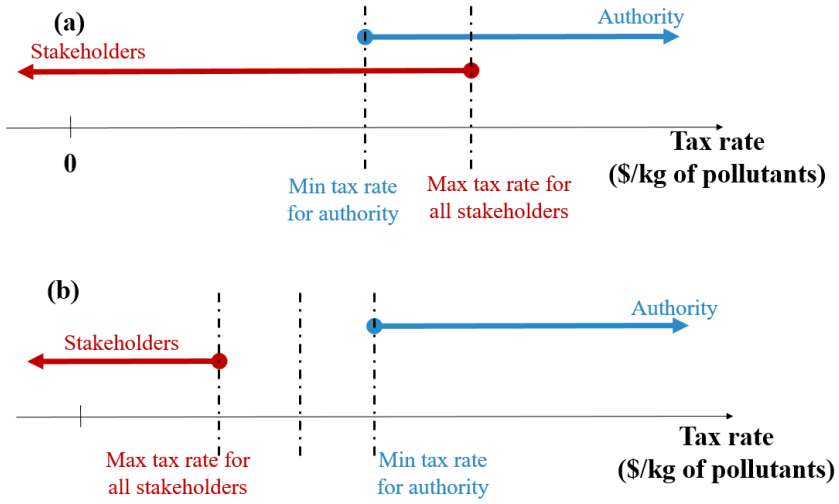

Figure **5-4**: Possible tax rates for stakeholders and authority (a) Feasible tax rates (b) Infeasible tax rates

There are different scenarios when considering the tax rates specification for stakeholders and authority. Figure 5-4a shows the feasible tax rates for both parties, based on Condition 1 and Condition 2 as defined. The minimum tax rate for authority (Condition 1) is lower than the maximum tax rate for stakeholders (Condition 2), for which the overlapped region represents the feasible tax rates for both parties. However, it is possible that the maximum tax rates of stakeholders are smaller than the tax rates for the authority (Figure 5-4b). This is due to the fact that the stakeholders are not able to pay the high amount of tax. Specifying higher tax rates may incur dissatisfaction, and the stakeholders are more reluctant to conduct any recycling activities. In this case, additional income is needed for the authority to provide more incentives for the stakeholders.

Figure 5-5 shows the minimum additional income is required by the authority. With the additional income, the minimum tax rate for authority can be reduced as they do not need to just rely on the taxes as a source of income for subsidy. Providing incentives to the stakeholders also could increase the maximum tax rates allowable for stakeholders that they are willing to participate in the grand symbiosis. It is crucial to leverage the tax rates between the authority and the stakeholders. The extension of both tax rates where the threshold tax rates coincide, as shown in Figure 5-5 represents the optimal tax rates for both stakeholders and authorities.

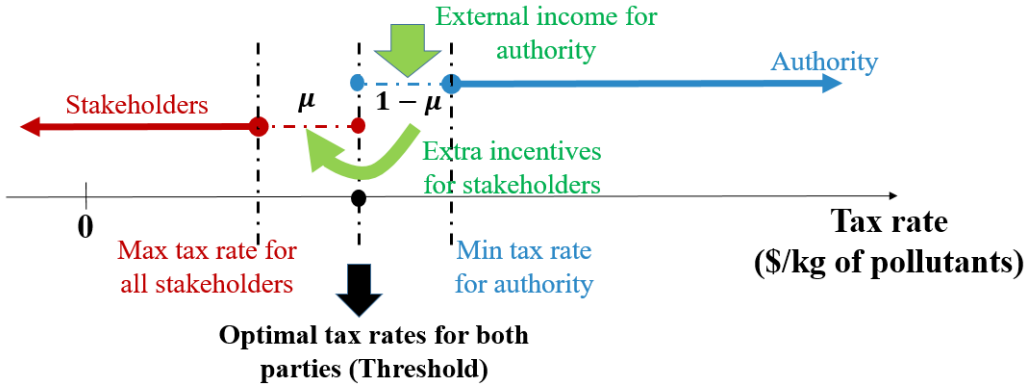

Figure **5-5**: Additional income is needed for the authority to provide incentives for stakeholders to set the tax rates

5.4 Multi-stage Game Theory approaches

The proposed framework for identifying the optimal incentives and subsidies allocation from the park authority for a water eco-industrial park is summarised in Figure 5-6.

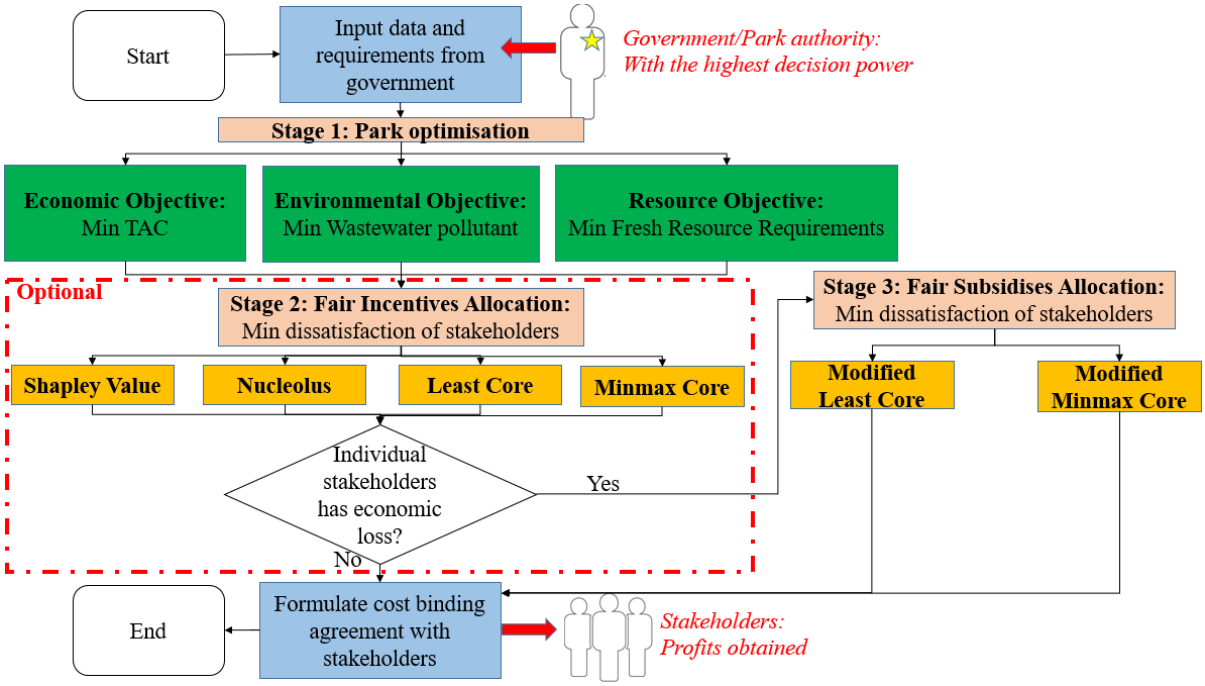

Figure **5-6**: Proposed framework of determining authority compensation for a water eco-industrial park

The compensation framework can be distinguished into three main stages. The first stage involves the identification of objectives by the government, either minimising cost, minimising the environmental burdens or minimising TAC for all possible coalitions of stakeholders. The government has the highest decision power. The cross-plant flow transfer scheme is then identified for the grand coalition. The second stage then determines the fair incentives allocation to each stakeholder using a game-theoretical approach resulted in the saving of total operating cost. This stage is optional, depending on the budget of the park manager. The detailed method is explained in Section 5.2. It is then needed to check whether the incentives are high enough to cover the capital cost required. In the third stage, determine the minimum budget required from the government in ensuring all the stakeholders do not suffer economic loss. The subsidies allocation can be further increased and readjusted using the game-theoretical approach presented in Section 5.2.2. A binding agreement can be formulated between the stakeholders and the park authority using the solutions from the modified core methods.

The authority decides on the fresh resources allocation as well as the subsidies or incentives amount. As each stakeholder is only concerned with their own economic benefits, the stakeholders could determine the recycled water flowrates with the profits obtained from the authority. This can be solved using Eqs(B1-B8) with the objective of minimising TAC for each plant with fixed freshwater flows. The overall multi-stage framework is presented in Figure 5-7. This framework structure is analogous to a Stackelberg-Nash game model, where the leader (authority) has the highest decision power and should decide first. The followers (stakeholders) only decide based on the decision from the leader.

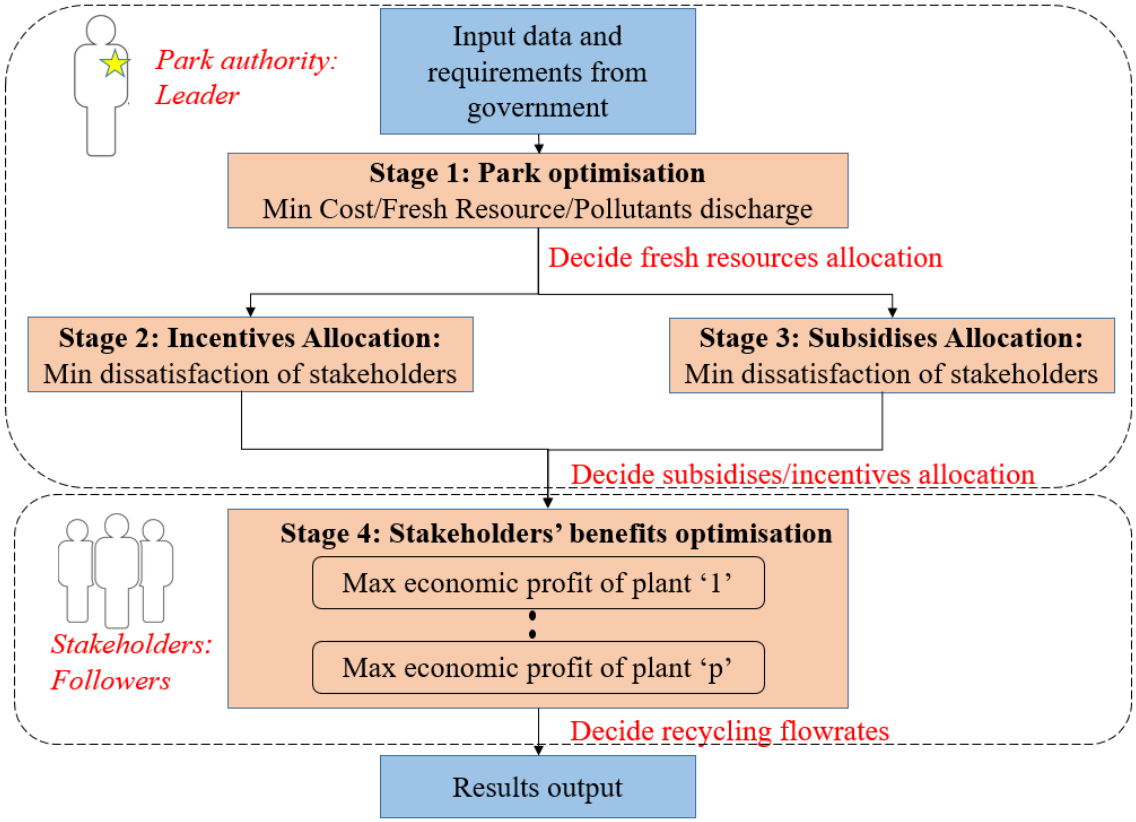

Figure **5-7**: Overall framework of determining a compensated water eco-industrial park

5.5 Case studies and results

The framework is applied to an illustrative industrial site case study with the data for this study features a single contaminant water recycling problem with five plants from Fadzil et al. (2018), for which the contaminants are the Total Dissolved Solid (TDS). The water streams data are presented in Chapter 4, Table 4-1. The original practice of the site is assumed as all the sources are discharged as wastewater (2,540 t/h), and the freshwater requirement is equal to all the flowrates of the sinks (2,540 t/h). The total freshwater required is equal to the wastewater flow. Several assumptions or parameters are assumed similar to parameters from Chapter 4 Section 4.3.

Stage 1: Park optimisation. Based on the overall framework presented in Figure 5-7, the optimisation of the eco-industrial park is performed first from the perspective of park authority. The model with Eqs(1-8) is solved repeatedly for all possible coalitions consisting of all the plants, considering either resources objectives, environmental objective or cost objective. The total number of the possible coalition, S, is 31 ($2^5 - 1$). Table 5-2 shows the optimisation results considering the resources objective, while Table 5-3 is for the environmental objective. The results for the cost objective are not shown.

From the perspective of resources objectives, it can be seen that the freshwater requirement for a larger coalition is lower than merging any smaller coalitions. For example, the

freshwater requirement for coalition {ABCDE} is 795.96 t/h, which is lower than the freshwater requirement merging single plant integration results (206.67 + 142.21 + 173.36 + 206 + 102.69 = 921.03 t/h), and any other coalitions. If resource-saving is the main objective, this suggests that the cooperation of stakeholders could achieve freshwater saving and wastewater savings, complying with the environmental objectives. However, in the perspective of the environmental objective, the fresh resource required for the grand coalition {ABCDE} is 967.01 t/h, which is larger than the resource objective. Also, it is to note that the resource requirement for smaller coalitions are lower, e.g. the fresh resource for {ACD} +{B}+ {E} (631.29 + 219.62 + 102.69 = 953.60 t/h), which is lower than the grand coalition. The same applies to wastewater flowrate as well. Plant B and Plant E might not be willing to join the grand coalition. Similar reasons apply to pollutants discharge as well.

Table 5-2: Optimisation results for resources objective.

Coalition, S	TAC ($/y)	Freshwater, F_{WT} (t/h)	Wastewater, Fww (t/h)	Pollutant discharge (kg/h)	Cost savings, TAC_o-TAC ($/y)
A	6,538,902	206.67	206.67	91.00	4,517,922
AB	19,837,791	330.00	330.00	119.57	-1,135,501
ABC	47,208,209	474.50	474.50	178.73	-22,004,674
ABCD	91,157,248	667.50	667.50	244.68	-61,415,889
ABCDE	312,504,369	765.96	765.96	264.58	-280,109,138
ABCE	252,363,561	568.66	568.66	205.46	-224,506,155
ABD	47,351,620	532.31	532.31	179.00	-24,111,505
ABDE	77,201,265	635.00	635.00	203.90	-51,307,278
ABE	48,143,441	431.15	431.15	143.42	-26,787,278
AC	22,316,560	376.21	376.21	151.68	-4,758,492
ACD	51,400,574	544.17	544.17	214.70	-29,304,681
ACDE	262,700,137	641.83	641.83	238.58	-237,950,373
ACE	48,337,027	455.10	455.10	176.58	-28,125,087
AD	31,067,274	403.33	403.33	153.00	-15,472,626
ADE	50,004,537	501.00	501.00	186.59	-31,756,017
AE	24,561,662	304.33	304.33	117.87	-10,850,966
B	5,792,901	142.31	142.31	35.58	1,852,566
BC	19,706,621	273.27	273.27	87.88	-5,559,911
BCD	42,898,873	477.12	477.12	158.57	-24,214,338
BCDE	71,180,289	579.81	579.81	183.08	-49,841,882
BCE	44,950,202	375.96	375.96	118.34	-28,149,619
BD	21,917,726	348.00	348.00	96.27	-6,323,078
BDE	39,523,973	448.85	448.85	122.01	-21,275,453
BE	21,770,904	245.00	245.00	53.77	-8,060,208
C	6,107,333	173.36	173.36	60.68	393,911
CD	19,860,428	337.50	337.50	135.27	-8,821,359
CDE	38,106,603	437.88	437.88	147.58	-24,413,662
CE	20,841,919	251.10	251.10	86.78	-11,686,802
D	6,326,586	206.00	206.00	62.00	-1,788,762
DE	19,125,314	306.54	306.54	86.90	-11,933,618
E	4,997,023	102.69	102.69	24.90	-2,343,151

Table 5-3: Optimisation results for environmental objective

Coalition, S	TAC ($/y)	Freshwater, F_{WT} (t/h)	Wastewater, Fww (t/h)	Pollutant discharge (kg/h)	Cost savings, TAC_o-TAC ($/y)
A	6,266,739.85	207.26	207.26	91.00	4,790,084
AB	24,436,212.03	740.40	740.40	117.00	-5,733,922
ABC	37,957,942.07	582.63	582.63	177.68	-12,754,407
ABCD	65,726,117.48	929.10	929.10	239.68	-35,984,759
ABCDE	123,351,944.96	967.01	967.01	265.07	-90,956,714
ABCE	93,962,931.21	822.50	822.50	202.58	-66,105,524
ABD	50,083,890.82	911.37	911.37	179.00	-26,843,776
ABDE	83,427,175.40	875.79	875.79	203.90	-57,533,189
ABE	52,053,732.49	795.42	795.42	141.90	-30,697,570
AC	19,446,690.08	382.75	382.75	151.68	-1,888,622
ACD	39,243,867.18	631.29	631.29	213.68	-17,147,975
ACDE	92,218,436.28	795.13	795.13	238.58	-67,468,672
ACE	38,047,542.87	491.12	491.12	176.58	-17,835,602
AD	20,081,228.78	427.86	427.86	153.00	-4,486,581
ADE	39,115,528.95	561.07	561.07	177.90	-20,867,009
AE	21,636,459.19	541.71	541.71	115.90	-7,925,763
B	6,489,186.50	219.62	219.62	26.00	1,156,280
BC	17,880,308.46	347.36	347.36	86.68	-3,733,598
BCD	44,548,612.71	653.44	653.44	148.68	-25,864,078
BCDE	80,354,566.82	700.79	700.79	173.58	-59,016,160
BCE	37,017,103.34	449.05	449.05	111.58	-20,216,520
BD	19,215,826.50	423.14	423.14	88.00	-3,621,178
BDE	47,581,307.15	633.43	633.43	112.90	-29,332,787
BE	18,051,373.29	287.68	287.68	50.90	-4,340,677
C	5,887,328.29	173.75	173.75	60.67	613,916
CD	18,452,943.50	361.99	361.99	122.68	-7,413,875
CDE	36,720,418.91	473.80	473.80	147.58	-23,027,478
CE	21,293,060.93	338.13	338.13	85.58	-12,137,944
D	6,156,576.53	206.57	206.57	62.00	-1,618,752
DE	17,769,104.65	325.97	325.97	86.90	-10,577,408
E	4,996,142.01	102.69	102.69	24.90	-2,342,270

It is a different case when the cost is considered. Based on Table 5-2, it is obvious that the TAC for coalition {ABCDE} (312 M$/y) is much larger than the TAC{A}+TAC{B}+TAC{C}+TAC{D}+TAC{E} (about 23 M$/y). This is due to the expensive capital of building the capital of cross-plant water recycling to cope with the minimum fresh resources. In such a case, any rational stakeholder might not be willing to participate in the grand coalition. In order to facilitate the practical realisation of the industrial symbiosis, government subsidisation is crucial. It is proposed in this work that the government subsidisation amount must ensure the partial super-additivity and monotonicity properties of cost savings, i.e. the subsidised cost saving for the grand coalition is greater than merging smaller coalitions, as well as the subsidised cost saving is more beneficial for the grand coalition. It is also to be noted that the cost savings of the coalition are negative, which means the capital is much higher than the utility cost-saving.

Stage 2: Fair incentives allocation (Optional). The park authority could decide on the incentives rewards to the stakeholders based on the utility savings they achieved, provided if there is spare money. For this case study, the incentive rate, σ is fixed at 70 %. Using

game theory approaches demonstrated in Section 5.2.2, the fair distribution of incentives shares can be identified. For resources objectives, the resource requirement and wastewater flowrates for the grand coalition {ABCDE} are lower compared to other coalitions, which suggests that the utility saving is the greatest. Using other variants of Cooperative Game Theory tools, the fair and stable incentives allocations are solved using R programming software with the 'CoopGame' packages. The results are presented in Figure 5-8. The Shapley Value approach determines the marginal contribution of each plant and determines the incentives share. It is interesting to note that the nucleolus approach determines slightly higher incentives share for Plant C to minimise their dissatisfaction by taking away some shares from other plants. The solutions for nucleolus and τ-value are close to each other. Using the core methods (The Core, Least Core and Minmax Core), the solutions are close as well, but The Core method estimates higher incentives share for Plant A and C.

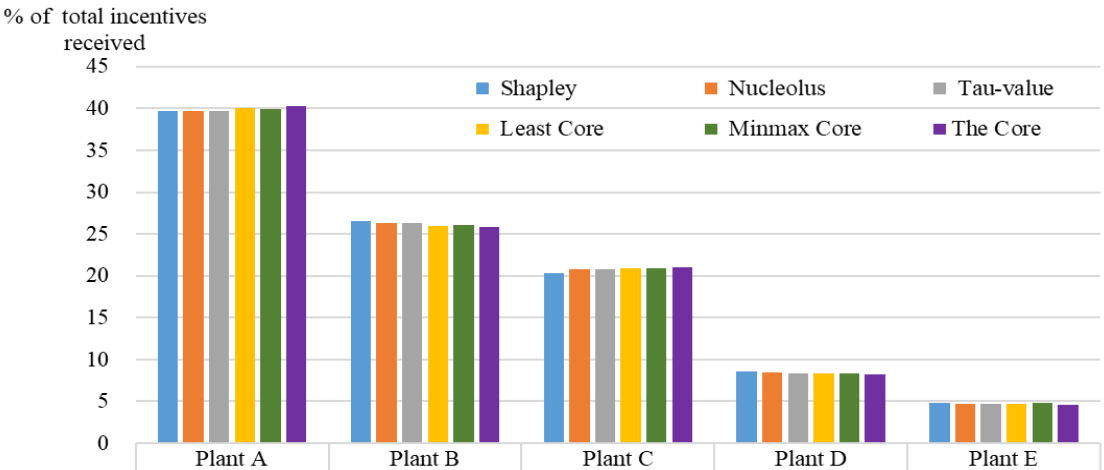

	Plant A	Plant B	Plant C	Plant D	Plant E
Shapley	39.69	26.51	20.31	8.61	4.88
Nucleolus	39.68	26.31	20.81	8.44	4.76
Tau-value	39.72	26.32	20.83	8.36	4.76
Least Core	40.02	25.97	20.95	8.33	4.73
Minmax Core	39.95	26.06	20.86	8.33	4.80
The Core	40.24	25.80	21.08	8.24	4.64

Figure 5-8: Results of fair incentives allocation for resources objective. Total incentive = 21,288,462 $/y

However, for the environmental objective, the point solution method (Shapley Value, Nucleolus and τ-value) are not suitable since the grand coalition does not yield the greatest utility saving. The Least Core and Minmax Core methods should be used to determine the incentives shares, also the additional fee to be paid by the authority to convince the stakeholders to join the symbiosis. Table 5-4 shows the incentives obtained by each plant for all three objectives. The incentives that can be obtained for resource objectives are the highest among the three due to its resource-saving is the largest. It can be noted that for the resource objective, the value of ε for Least Core method is less than zero (and the value of $n \geq 1$ for the min-max core), which indicates the core is not empty. If the stakeholders leave

the grand coalition, they risk losing a profit of 9,231 $/y. For cost and environmental objectives, the values of ε for Least Core method are positive (and the value of $n < 1$ for min-max core), which indicates the authority may have to pay extra ε to convince the stakeholders to join in the coalition. This is due to smaller coalitions are better than grand coalitions.

Table 5-4: Annual incentives of each plant for different objectives

	Incentives share (%)					
	Cost objective		Resource objective		Environmental Objective	
Methods	Least Core	Minmax	Least Core	Minmax	Least Core	Minmax
Plant A	40.46	40.15	40.02	39.95	41.63	41.16
Plant B	26.50	26.07	25.97	26.06	25.24	24.66
Plant C	20.79	20.95	20.95	20.86	21.85	20.77
Plant D	7.76	8.15	8.33	8.33	7.77	8.52
Plant E	4.48	4.68	4.73	4.80	3.52	4.89
Total ($/y)	20,512,960	20,512,960	21,288,462	21,288,462	18,875,929	18,875,929
Penalty, ε ($/y)	286,918	-	-9,231	-	540,561	-
n	-	0.97	-	1.00	-	0.93

Stages 3 & 4: Fair subsidies allocation and profit maximisation for each plant. Using a similar approach, the subsidies share can be distributed among the players using the modified core methods, as presented in Section 5.2.2. Table 5-5 shows the subsidies share among the plants without considering the incentives identified from Stage 2. The subsidies also do not consider the semi-superadditivity constraint-Eq(5-12) and the minimum cost required for each plant- Eq(5-11). The distribution of the subsidies is quite equitable among the plants, and the solutions for both approaches are similar.

Table 5-5: Annual subsidies of each plant for different objectives (without incentives), without considering minimum cost required and without semi-superadditivity.

	Subsidies share (%)					
	Cost objective		Resource objective		Environmental Objective	
Methods	Least Core	Minmax	Least Core	Minmax	Least Core	Minmax
Plant A	16.88	16.88	24.23	24.23	15.41	15.41
Plant B	14.93	14.93	11.46	11.46	20.06	20.06
Plant C	18.97	18.97	23.70	23.70	17.78	17.78
Plant D	22.89	22.89	20.51	20.51	23.15	23.15
Plant E	26.33	26.33	20.09	20.09	23.61	23.61
Total ($/y)	57,286,735	57,286,735	280,109,138	280,109,140	90,956,715	90,956,714
Penalty, ε ($/y)	20,837,806	-	162,409,320	-	35,674,121	-
n	-	0.00	-	0.00	-	0.00

The values of ε for the Least Core method are all positive, and values of $n < 1$ for min-max core, indicating the cost savings for grand integration are lower compared to the smaller group integration. The park authority needs to pay an extra amount to accommodate the profit loss of the stakeholders to attract them to join in the coalition, e.g. the required budget

for the park authority is actually about 77 M$/y (57,286,735 + 20,837,806). The subsidies results are compared between without semi-superadditivity constraint vs with semi-super additivity, considering the minimum cost requirements, as presented in Table 5-6, Table 5-7 and Table 5-8.

Table 5-6: Annual subsidies of each plant for different objectives (without incentives), considering minimum cost requirement (Cost objective)

	Subsidies amount ($/y)				Profits, x ($/y)	
	With semi-superadditivity		Without semi-superadditivity		With semi-superadditivity	
Methods	Least Core	Minmax	Least Core	Minmax	Least Core	Minmax
Plant A	9,671,835	12,478,439	7,738,224	8,858,563		997,482
Plant B	11,966,612	9,850,158	9,850,158	9,850,158	3,414,436	686,220
Plant C	10,866,923	10,866,923	11,959,441	10,839,102		657,869
Plant D	13,405,394	13,405,394	13,405,394	13,405,394	293,069	675,392
Plant E	15,083,477	14,393,328	14,333,518	14,333,518		690,543
Total ($/y)	60,994,241	60,994,242	57,286,735	57,286,735		
Penalty, ε ($/y)	20,837,806		21,678,898		-	-
n		0.0573		0	-	-

Table 5-7: Annual subsidies of each plant for different objectives (without incentives), considering minimum cost requirement (Resource objective)

	Subsidies amount ($/y)				Profits, x ($/y)	
	With semi-superadditivity		Without semi-superadditivity		With semi-superadditivity	
Methods	Least Core	Minmax	Least Core	Minmax	Least Core	Minmax
Plant A	67,857,936	67,857,936	67,857,936	20,911,322	0	936,759
Plant B	53,871,023	53,871,023	50,163,517	62,542,801	3,707,506	721,229
Plant C	66,392,540	66,392,540	66,392,540	63,531,493	0	864,416
Plant D	39,411,214	39,411,214	39,411,214	66,097,628	0	486,947
Plant E	56,283,930	56,283,930	56,283,930	67,025,894	0	698,154
Total ($/y)	283,816,643	283,816,643	280,109,137	280,109,138	-	-
Penalty, ε ($/y)	162,409,320	-	162,409,320		-	-
n	-	0.0129	-	0.00	-	-

Table 5-8: Annual subsidies of each plant for different objectives (without incentives), considering minimum cost requirement (Environmental objective)

	Subsidies amount ($/y)				Profits, x ($/y)	
	With semi-superadditivity		Without semi-superadditivity		With semi-superadditivity	
Methods	Least Core	Minmax	Least Core	Minmax	Least Core	Minmax
Plant A	17,720,450	17,720,450	14,012,944	7,738,224	3,707,506	858,060
Plant B	18,242,171	18,242,171	18,242,171	44,640,476	0	739,433
Plant C	16,173,414	16,173,414	16,173,414	10,839,102	0	639,902
Plant D	21,053,129	21,053,129	21,053,129	13,405,394	0	740,803
Plant E	21,475,057	21,475,057	21,475,057	14,333,518	0	729,307
Total ($/y)	94,664,221	94,664,221	90,956,715	90,956,714	-	-
Penalty, ε ($/y)	35,674,121	-	35,674,121	-	-	-
n	-	0.0381	-	0	-	-

In Table 5-6, Table 5-7 and Table 5-8, it can be observed that the total subsidies for all objectives required are higher as compared to without semi-superadditivity constraint – Eq(5-12). The additional amount is to ensure a fair and equitable distribution while ensuring the profits for the grand coalition is higher than any other smaller coalitions. It is also interesting to note that the profit allocated for each plant for the Least Core method contains extreme solutions, i.e. only one plant receives the profit. This shows that the extreme solutions where either one of the five plants received profits are feasible. For Minmax core, the profits are more equitably distributed among the plants, as the aim of the method is to minimise the dissatisfaction among the plants.

After the subsidies have been determined, each plant can further maximise its profit by deciding the recycling flowrates. This is equivalent to setting the cost objective for the overall design of the park using the allocated resources. The full network design is not shown for brevity.

Final stage: Tax rates. The sources of subsidies money can be generated from the imposed tax on the stakeholders. Table 5-9 shows the maximum tax rates that can be imposed by the authority to the stakeholders, which can be determined by Eqs(5-14 to 15). Note that in this case, since the total subsidies are equal to the cost difference between recycling and non-recycling, the right-hand side of Condition 2- Eq(5-15) is zero for all objectives. An additional source of income is needed, and more incentives should be given to the stakeholders to ensure both benefits of authority and stakeholders. The incentives can be based on the operating cost saving as identified by Stage 2, but the authority should get the extra income for incentives from external sources. The additional income can be imposed by the higher rank authority, for example, the environmental benefits given to the park authority in terms of cost. The extra amount needed can be estimated as μ x tax amount, where μ ranges from 0 to 1. In this case, the value of μ is 0.5 so that both tax rates coincide. This means that at least μ*Tax amount of additional income is required for the authority in order to realise the industrial symbiosis.

Table 5-9: Tax rates for different objectives

	Tax rate ($/kg of TDS)		
Plants	Cost objective	Resource objective	Environmental Objective
Condition 1: Minimum tax for authority	28.34	132.33	42.97
Condition 2: Maximum tax for stakeholders	0	0	0
Optimal tax rates for both parties (μ = 0.5)	Authority: 28.34 (1-μ) Stakeholders: 28.34 (μ)	Authority: 132.33 (1-μ) Stakeholders: 132.33 (μ)	Authority: 42.97 (1-μ) Stakeholders: 42.97 (μ)

It can be observed that the imposed tax rates are very high for resources objectives. The stakeholders might raise dissatisfaction, especially smaller stakeholders, as they might not afford the very high price. It is also to be observed that tax rates are directly affected by the subsidies amount. As the subsidies are higher, this means more recycling to be performed and the tax rate to be imposed is higher to stimulate the recycling desires among the stakeholders. At this rate, the stakeholders might be more interested in building in-house waste resource treatment to satisfy their own demands rather than supplying to other plants. The centralised waste treatment hub or in-house treatment can be considered in future work to balance the tax rates, subsidies and environmental emissions.

5.6 Conclusions

This work has considered the fair and equitable subsidies or incentives allocations to facilitate the realisation of water symbiosis in an eco-industrial park. The park authority should distribute the money so that the stakeholders are more willing to join in the grand symbiosis scheme while ensuring their dissatisfactions are minimised. It is also proposed in this work that the cost allocation should be convincing enough for the stakeholders to participate in the grand coalition rather than forming smaller collaborations. This is because more coalitions could save more resources and waste discharges but required higher cost. A multi-stage cooperative game theory approach is proposed to evaluate the distribution scheme. The park authority has the highest decision power to decide on the subsidies or incentives to be allocated and the resources allocated. The stakeholders can then decide on the recycling flows based on the authority's decision. The framework is followed by a game analysis on tax rates that can be imposed by the authority to encourage recycling activities while also generating a source of income for the subsidies.

An illustrative study is used to demonstrate the proposed framework. The following results are obtained using the approach:

a) Incentives can be provided by the authority as a reward for the efforts of operating cost savings. The nucleolus/τ-value approaches could identify the incentives allocations that minimise the largest dissatisfaction of the players, as compared to Shapley Value, which only considers the marginal contribution of each plant. The Core methods could determine the set of solutions for the incentives or subsidies while ensuring fair distribution.

b) The cost and environmental objectives incur a higher operating cost in the grand coalition compared to some smaller coalitions. The stakeholders could obtain more incentives when forming smaller coalitions, but the environmental impacts are not minimised. The Core methods could identify the additional amount for the authority to convince the stakeholders. In this study, the additional amount is 287 k$/y considering the cost objective and 541 k$/y for the environmental objective.

c) The stakeholders could hold the bargaining power to request more subsidies in the grand coalition. The Least Core and min-max core methods identify the additional money that

should be provided by the authority to convince the stakeholders to participate in the grand symbiosis. In this study, the additional amount identified is about 21 M$/y for cost objective, 162 M$/y for resource objective and 36 M$/y for environment objective. The solutions from Minmax core are more equitable and fairer than the Least Core method.

d) Additional subsidies are required to ensure the grand coalition has better profit than any other smaller coalition for any of the objectives (semi-superadditivity).

e) Game analysis on the taxation policy also suggests that higher tax rates could stimulate the recycling activities from the stakeholders. For this specific case, assuming the taxes are to be used for subsidies, the minimum tax rate per kg of TDS discharged can range from 28.34 $/kg to 132.33 $/kg, which depends on the objectives of the park manager.

f) Additional income for authority is needed to leverage the imposed wastewater tax rate so that the benefits of both sides are guaranteed. Additional incentives should be given to the stakeholders as well. The environmental benefits in terms of cost for the authority obviously stimulate the authority to implement the regulation as well, which allows lowering the tax rates. The leverage rate of the tax rate is identified as $\mu = 0.5$.

This study is primarily focused on fair subsidies or incentives allocation methods and analysis of the tax rates. Notice that the approach assumes rationalities between stakeholders, i.e., each stakeholder wants to get the subsidies/incentives at least larger in the collaboration than what they can get without collaboration (super-additivity/monotonicity). In reality, this may not be the solution as the certain firm could have more negotiation powers over the others and, in turn, affects the allocation solutions. A stakeholder may decide to enter/quit the coalition at any time over the planning horizons when they could get better benefits. A proper evolutionary game analysis on the collaborative firms should be conducted to determine behaviours of the firms that reflect the realistic scenario.

It is also worth noting that probably the super-additivity requirements are not always satisfied in a large collaborative group without additional compensation from the government. This is especially when the cost or environmental emissions are the main objectives of the industrial park formation. This implies that a smaller collaboration cluster (integration in smaller clusters) could be more beneficial than a full large collaboration (integration between all firms). More realistic issues such as variations of supply and demand can yield very different results. The tax rates on pollutants discharge are also based on a single contaminant only, which are supposed to be weighted by the priority of the pollutants. The prices for the freshwater source are also fixed.

CHAPTER 6 APPLICATION OF THE PINCH FRAMEWORK IN OPPORTUNISTIC MAINTENANCE MANAGEMENT AND TASKS ALLOCATION

This study presents an extension of the Process Integration tool in opportunistic maintenance and maintenance tasks allocations problem. These problems are presented as a resource conservation problem, where the cost is the resources for opportunistic maintenance and human labours working hour is the resource for the task allocation problems. Section 6.2 presents the Pinch Analysis in opportunistic maintenance framework based on the publication in Chin et al. (2019), and Section 6.3 in maintenance tasks allocation according to Chin et al. (2020a).

6.1 Introduction

Maintenance plays an essential role in a production process to ensure the equipment or assets are repaired, replaced or modified according to the production requirements. The efficacy of the maintenance policy for complex and expensive chemical processes is critical for reliable operations. Basri et al. (2017) highlighted that the opportunistic grouping of maintenance planning could be practical and effective in the process industries. For such maintenance policy, it relies on various opportunities such as production stoppages, economic considerations and environmental conditions. For example, a failure event in the separation system in oil refineries is likely to shut down the oil export system. The maintenance team may take the equipment failure opportunity to perform preventive maintenance for other components (Truong Ba et al., 2017). Another example would be the sugarcane processing system. The supply of sugarcane is stopped during rainy seasons, which the production has to be stopped and creates an opportunity for maintenance (Jiao et al., 2005). Substantial cost and time can be saved using this policy when compared to awaiting the regular maintenance schedule. The problem of maintenance management, especially opportunistic maintenance, can be regarded as a resource conservation problem, where the cost is the primary resource to be minimised, and the main constraint (quality) is the time of the failure or maintenance. Similar reasoning applies to maintenance task scheduling with human labour working hours as well.

6.2 Pinch Analysis in opportunistic maintenance management

Failure occurs randomly in any chemical process. If any failure occurs, the maintenance crew has to react proactively to the unit repair. This creates an opportunity to perform the scheduled maintenance together with the unit repair. This opportunistic maintenance strategy could reduce the production stoppage cost or downtime, which also fully utilise the available resources. This strategy is in line with the concept of Circular Economy.

After determining the maintenance intervals and frequencies, the expected cost due to failure of components i can be calculated using Eq(6-1).

$$C_{F,ik} = (C_o^c + C_i^c) \int_{T_{i,k}^*}^{(k+1)T} f_i(t)dt \quad \forall i,k \tag{6-1}$$

Where $C_{F,ik}$ represents the expected failure cost of component i at time interval [$T^*_{i,k}$, (k+1)T], C_o^C is the common set-up cost due to the failure, C_i^C is the corrective replacement cost for component i, and $T^*_{i,k}$ is the last periodic maintenance for component i- Eq(6-2). The common set-up cost, C_o^C is the summation of the cost for mobilising repair crews, safety provision, disassembling, transportation and production loss. Each failure incurs an emergency stoppage to the process, which requires a common set-up cost. In this study, a constant value is assigned to the set-up cost of $30,000 (Laggoune et al., 2009). Notice that the calculation in Eq(6-1) only consider a single failure per component, which is also the assumption of this study. The system is also assumed to be a series process in which the failure of one component induces the system failure. The term $T^*_{i,k}$ is required as each maintenance action improves the reliability of the component. This study assumes the maintenance is perfect, which means the maintenance action restores the reliability of the component back to its original state. $T^*_{i,k}$ can be computed using Eq(6-2) as follows:

$$T_{i,k}^* = \begin{cases} kT & , k \bmod F_i = 0 \\ T_{i,k-1}^* & , else \end{cases} \quad \forall i,k \tag{6-2}$$

The condition statement from Eq(6-2) signifies that $T^*_{i,k}$ equals to kT, only if the k modulo the maintenance frequency of component i, F_i is zero (k divides F_i does not have remainders). Take an example from Figure 6-1, at time 2T, as the last maintenance of component 2 is at time T, the failure probability should be evaluated from T ($T^*_{i,1}$). As for component 1 at time 2T, since it is not maintained at time T (k mod $F_1 \neq 0$ as $F_1=2$ and k=1), the failure probability is evaluated from time 0 ($T^*_{i,0}$) to 2T.

The opportunistic cost saving for each component and each time period can be computed using Eq(6-3).

$$C_{OS,ik} = (C_o^p + C_i^p)\left(1 - \int_{T_{i,k}^*}^{(k+1)T} f_i(t)dt\right) - C_i^p\left(1 - \prod_{j\neq i} \int_{T_{i,k}^*}^{(k+1)T} f_j(t)dt\right) \quad \forall i,k \tag{6-3}$$

Where $C_{OS,ik}$ represents the expected cost saving due to opportunistic rescheduling of component i at time interval [$T^*_{i,k}$, (k+1)T], C_o^P is the common set-up cost due to preventive maintenance (assumed $ 20,000 <C_o^C), C_i^P is the preventive maintenance cost for components i and j which are the failed components (j≠i). The first term in Eq(6-3) represents the expected preventive maintenance cost between [$T^*_{i,k}$, (k+1)T]. In this study, the expected preventive maintenance cost for each component are still considered for each time period. This is because the maintenance schedule is still expected to be changed from the determined schedule. The second term represents the cost incurred for opportunity maintenance. It considers the probabilities of other component j have been failed, thus creating an opportunity to maintain non-failed component i. Notice that C_o^P is not considered in this term due to the corrective set-

up cost has been incurred (C_o^C) as failure happens. Figure 6-1 is presented to allow the illustration of the concepts explained.

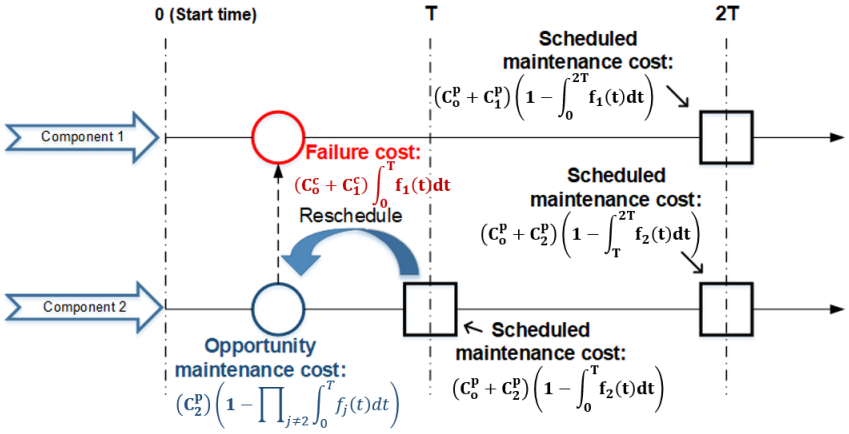

Figure 6-1: Demonstration of a maintenance cycle for a system of two components

The step-by-step framework for constructing the Composite Curves is presented as follow:

(i) Identify the maintenance cycles for each component. In this study, the time length is fixed when all the components have at least undergone maintenance once.

(ii) Determine the expected failure cost ('Sinks') using Eq(6-1) and expected opportunistic cost-saving ('Sources') using Eq(6-3) for each time interval.

(iii) Plot the Failure Cost Composite Curve ('Sinks'), with cumulative cost as x-axis and time intervals as y-axis. Please refer to Figure 6-2a.

(iv) Plot the Opportunistic Cost-Saving Composite Curve ('Sources') in the same figure.

(v) Shift the Source Composite Curve horizontally until it is on the right side of the Sink Composite Curve. The reason is that the expected cost-saving has to be larger than the failure expected cost at a given time. This is to ensure sufficient cost to mitigate the expected failure at the given time. The point where both of the curves meet is called the 'time pinch'. It is the time where the cost saved from opportunistic maintenance is just enough to cover the failure cost. The cost saved before this period (below the pinch region) cannot be transferred to cover the expected failure cost beyond this period (above the pinch region) – Figure 6-3a.

The proposed methodology is applied to a hydrogen gas centrifugal compressor of the catalytic reforming unit in Skikida refinery. It was determined as the leading cause of the catalytic reformer breakdowns (Laggoune et al., 2009). For a reformer, the role of a compressor to maintain the pressure of hydrogen gas helps in reducing coke formation and production losses. As such, the maintenance of compressor plays an important part in ensuring the process reliability to drive larger profit. The detailed process description can be found in Laggoune et al. (2009). The data required for this study are presented in Table 6-1.

Table 6-1: Cost data and the Weibull parameters of system components (Laggoune et al., 2009)

Component i	C_i^C ($)	C_i^P ($)	B_i	n_i	$MTBF_i^a$ (d)
Sheathing (C1)	14,868	3,639	1.73	486	433
Sheathing (C2)	39,204	5,438	1.88	507	450
Tightness (C3)	44,880	7,398	2.43	286	254
Stub bearing (C4)	57,876	8,277	2.53	898	797
Tightness ring (C5)	73,860	13,554	2.14	905	801
Carrying bearing (C6)	46,752	14,130	3.55	736	663
Stub bearing (C7)	48,568	21,356	2.68	1,094	973
Labyrinth support (C8)	74,232	24,348	2.09	1,388	1,229

Figure 6-2a shows the plot of the Composite Curves, as mentioned in section 2.3 steps (i)-(iv). Note that the time interval is fixed as 244 d, for which the maintenance is carried out slightly before the minimum MTBF (254 d) (Table 6-1). The values are set for demonstration purposes only and can be modified according to preferences. As can be seen that after time 488 d, the expected failure cost is higher than the expected opportunistic cost savings. Extra cost has to be invested in mitigating the expected failures after that time. Figure 6-2b shows the Grand Composite Curve, which is the cost difference between Source Composite Curve and Sink Composite Curve.

Based on step (v), the Source Composite Curve is shifted to the right horizontally until it is at the right side of the Sink Composite Curve. The shifted amount is the extra cost needed to mitigate the expected failure of the system. According to Figures 6-3a and b, an extra $ 422,183 has to be paid to cover the failures that are expected to happen at an earlier time. A total amount of $ 789,270 (about 65 % or total failure cost) can be saved from the opportunistic maintenance policy (overlapped regions).

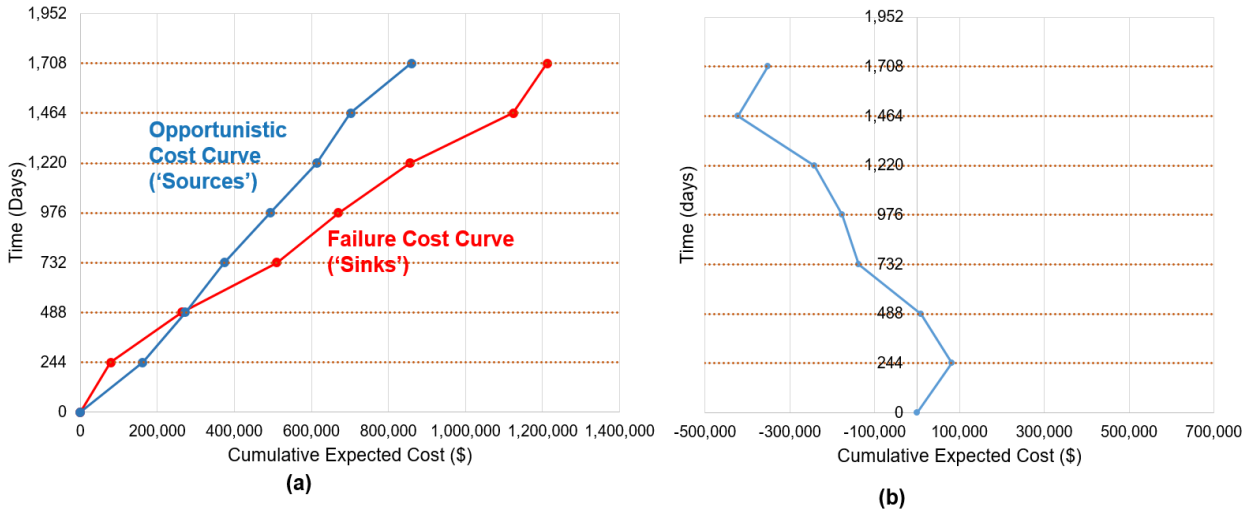

Figure 6-2: Graphical representation of the Pinch Analysis framework before shifting (a) Composite Curves (b) Grand Composite Curve

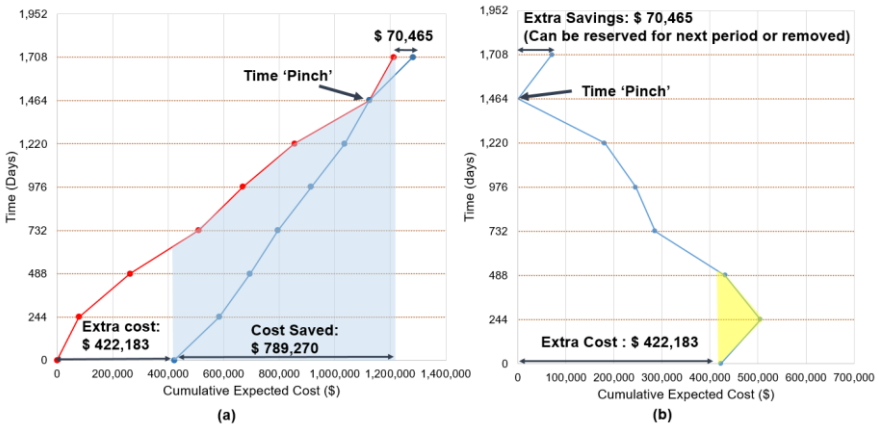

Figure 6-3: Graphical representation of the Pinch Analysis framework after shifting (a) Composite Curves (b) Grand Composite Curve

The interception of the two Composite Curves at 1,464 d, called Time Pinch, signifies that the cost saved from opportunistic maintenance is just enough to cover the expected cost due to failures. The cost saved before this period (Below Pinch Region) is not able to cover the expected failure after this period (Above Pinch Region). Extra $70,465 saved at the end of the period can be reserved for the next period or to handle emergencies. This amount can also be further reduced by removing unnecessary maintenance grouping. The discussions above are just demonstrations of the proposed methodology and strategy for maintenance management. Further development and solution benchmarking with the real case studies are required to confirm the legitimacy of the proposed framework.

6.3 Pinch Analysis in tasks allocations and scheduling

The objective is to allocate the means of maintenance with minimum use of human and material resources in line with the objectives of the circular economy. This could result in better resource utilisation and equipment longevity, allowing a greater number of inner material circulations.

After the individual maintenance time ($t_{i,j}$) are found, the maintenance grouping model is then solved to determine the optimal maintenance tasks clusters. The model is presented in Eqs (6-4 to 9).

$$h_{i,j} = Cc_i * \left(\frac{x_i + dt_{i,j}}{\theta_i}\right)^{b_i} - \left(\frac{x_i}{\theta_i}\right)^{b_i} - dt_{i,j}E\left(\frac{C}{x}\right) \tag{6-4}$$

$$dt_{i,j} > -x_i \tag{6-5}$$

$$t^*_{i,j} = t_{i,j} + dt_{i,j} = \sum_{k \epsilon K} z_{i,j,k} T_k \tag{6-6}$$

$$\sum_{i \in I, j \in J} z_{i,j,k} \leq 1 \tag{6-7}$$

$$Setr_k = \left(\sum_{i \in I, j \in J} (z_{i,j,k} - 1) S \right) \left(\sum_{i \in I, j \in J} z_{i,j,k} \right) \quad (6\text{-}8)$$

$$Max\ EP = - \sum_{i \in I, j \in J} h_{i,j} + \sum_{k \epsilon K} Setr_k \quad (6\text{-}9)$$

where $h_{i,j}$ is the penalty cost for shifting maintenance activities for equipment items i and j-th maintenance, $dt_{i,j}$ is the amount of time shift, T_k is the maintenance execution time for group k, $z_{i,j,k}$ is the binary variables to specify that whether the j-th maintenance task for equipment i is in group k, $Setr_k$ is the set-up cost reduction for group k and EP is the economic profit for grouping maintenance tasks.

The main objective in this model is to identify the shifting time ($dt_{i,j}$) that maximises the economic profit gain (EP) from grouping maintenance activities together. More information on such models can be found in Do et al. (2015). The step-by-step framework for applying Pinch Analysis in maintenance scheduling is presented as follow:

(a) Identify the optimal maintenance cycles and clusters for each equipment

(b) In each cluster k, arrange the daily maintenance tasks based on the priority level and determine the latest finish date of the tasks. The work is limited to at least 8 h works per day. Plot the curve with cumulative duration (h) on the x-axis and time (days) on the y-axis. This is the Tasks Composite Curve ('Demand/Sinks').

(c) Determine the available manhour and their daily work schedule in the plant. Plot a similar curve in the same figure, with the duration represented by the daily shift hours. This is the Manhour Composite Curve ('Supply/Sources').

(d) Shift the Manhour Composite Curve horizontally until it is on the right side of the Tasks Composite Curve. The reason is that on a specific day, cumulative available man-hours should be larger or equals to the duration of the cumulative task. This is also to ensure the tasks are finished before the deadlines. Please refer to Figure 6-4.

The proposed methodology is applied to a small scale chemical process, which is the Tennessee Eastman Problem. Table 6-2 shows the list of equipment with their corresponding failure and maintenance data. In this study, the set-up cost is assigned to a value of $ 1,000. The starting time, t_{begin} and operational time before t_{begin}, d_i are assumed to be zero. The time length is fixed as all the equipment are maintained at least once, i.e. $t_{end} = \max(t_{i,j})$.

Table 6-2: Equipment failure and maintenance data (Nguyen and Bagajewicz, 2010)

Equipment	Quantity	MTBF, (d)	$\theta_i b_i$	CM duration (h)	PM duration (h)	Priority	Production Loss ($/d)
Valves	11	1,000	1.55	3.5	3	3	1,000
Compressors	1	381	1.7	15	6	1	60,000
Pumps	2	381	1.75	8	5	4	10
Heat Exchanger	2	1,193	1.8	13	7	2	60,000
Flash Drum	1	2,208	2	42	12	1	60,000
Stripper	1	2,582	2	72	12	1	60,000
Reactor	1	1,660	2	42	12	1	60,000

Table 6-3 below shows the optimisation results using models. It shows that the optimal maintenance grouping strategy is divided into four groups that yield the highest economic profit.

The schedule at k=3 and at 134th week is chosen due to the longer task duration at that week to demonstrate the approach of Pinch Analysis. Figures 6-4a to d shows the plot of infeasible and feasible Composite Curves for a single worker. The shift hour for the worker is 8 h/d for 5 d/week. Notice that an extra 22 h of working hours are needed at the beginning of the time, and an extra 8 h at the end is wasted. The worker is expected to take a weekend break, as shown in a longer vertical line at 6th and 7th d. The 'pinch' point is expected at the 8th d due to the cumulative working hours are just enough to complete the cumulated tasks before this day. It suggests that the worker can take a leave at 11th d as all the tasks are expected to finish.

For this case, the workers' daily shift schedules are changed to 12 h/d for 4 d/week. Figure 6-5 (a) and (b) shows the Composite Curves and the Grand Composite Curves. The extra working hour is reduced to 13 h, and the Pinch point is at 7th d. The 22 h at the end are not needed, and this suggests that the worker can take the leave as the tasks are expected to finish at 9th d.

Table 6-3: Long-term maintenance planning results

Equipment	Quantity	Optimal maintenance time, $t^*(i,j)$ (weeks)			
		k=1	k=2	k=3	k=4
Valves	11	63	134	134	124
Compressors	1	63	38	38	38
Pumps	2	63	134	134	124
Heat Exchanger	2	63	38	74	74
Flash Drum	1	63	134	134	146
Stripper	1	63	134	134	146
Reactor	1	63	134	134	124
$EP/(T_{end}-T_{begin})$ ($/weeks)	**-**	**-134.79**	**13.63**	**17.92**	**18.22**

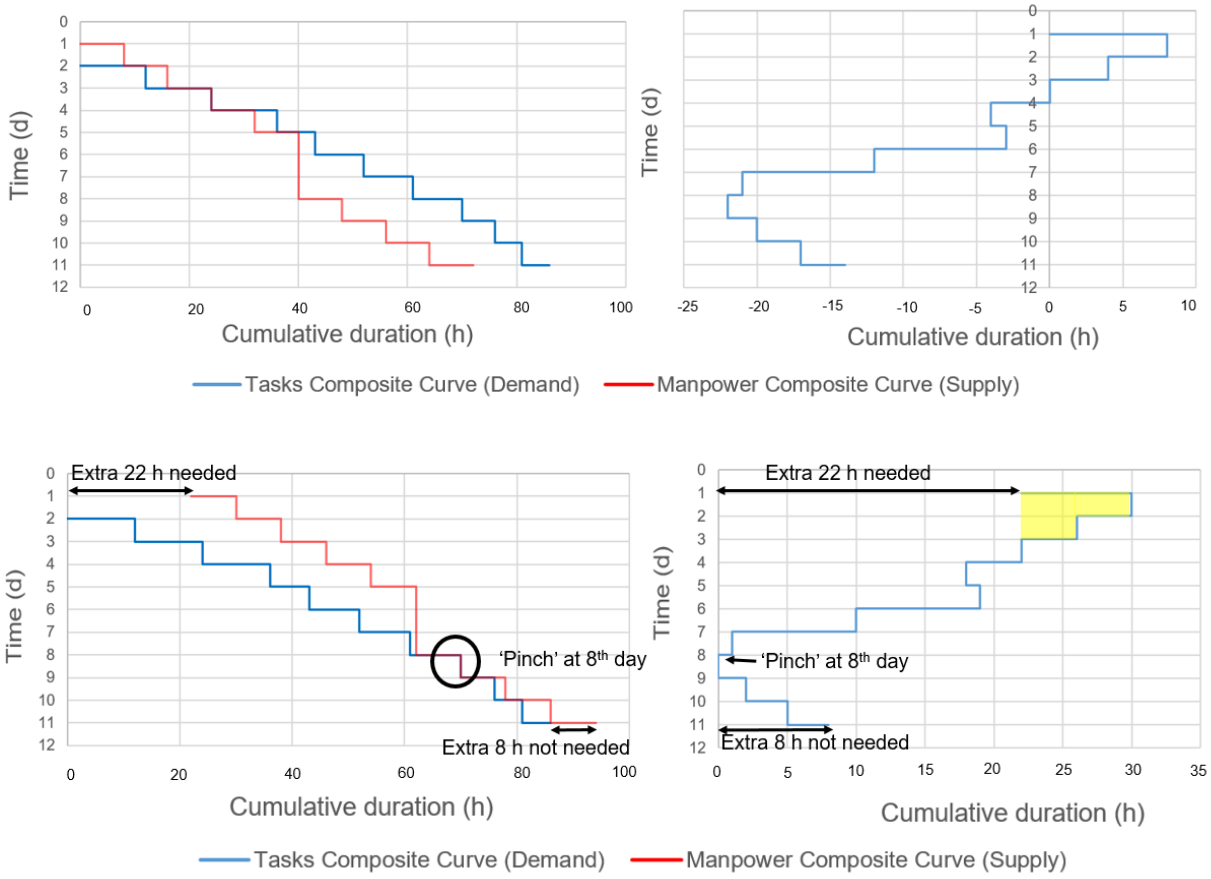

Figure 6-4: Pinch Analysis framework (8 h/d shift for 5 d shift) with (a) Infeasible Composite Curves matching (b) Infeasible Grand Composite Curve (GCC) (c) Feasible Composite Curves matching after shifting (d) Feasible GCC after shifting

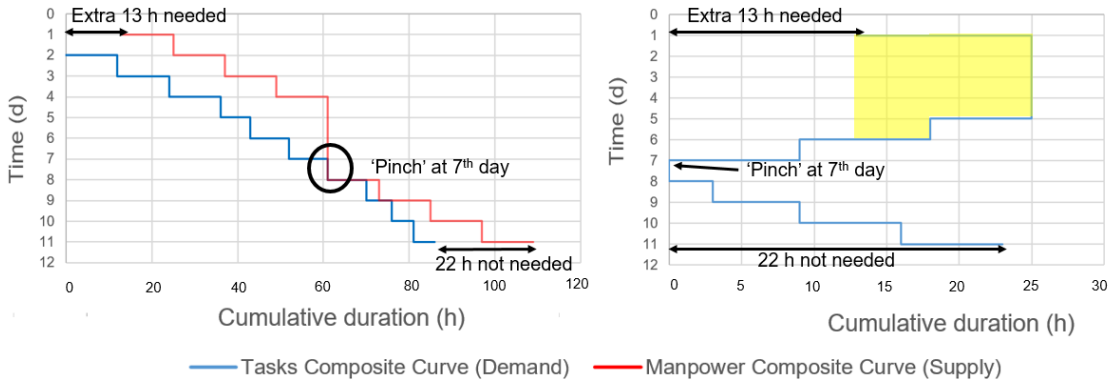

Figure 6-5: Pinch Analysis framework (12 h/d for 4 d shift) with (a) Composite Curves (b) GCC

6.4 Conclusion

The graphical strategy to facilitate opportunistic maintenance management can identify the cost saved from the maintenance policy used to cover the expected failure cost. A case study of component replacement of a hydrogen gas compressor is used to demonstrate the methodology. The result shows that about 35% of the failure cost from the start time has to be paid at extra cost. The remaining 65 % can be covered by applying a maintenance policy. The extra cost savings at the end of the period also suggest that the maintenance grouping can be further reduced. This concept is highly dependent on maintenance schedules. The solution might change as the schedule has been modified. The updates on the reliability function after maintenance rescheduling are also ignored in this study. The potential future research would be the full maintenance scheduling using a similar approach considering the availability of the resources (manpower, time and spare parts). Criticality analysis and the concept of the circular economy can also be incorporated to assess the maintenance policy. Solution benchmarking is also necessary to determine its accuracy and legitimation

For the maintenance task scheduling approach, this work proposed a combination of mathematical optimisation and graphical strategy to facilitate long-term and short-term maintenance planning. A case study of a small scale plant is used to demonstrate the methodology. For a single maintenance crew, an extra 22 h is needed to complete the tasks with an 8 h/d for 5 d working hours, while an extra 13 h is needed with a 12 h/d for 4 d shifts. Depending on the minimum finished date difference for the tasks, extra working hours are needed to account for uncertainties. Pinch Analysis provides an excellent visualisation interface for the scheduler to plan for daily maintenance tasks. The limitation of this concept is that the problem is solved sequentially, which global optimality is not guaranteed. For future study, a scenario can be created where the maintenance tasks require specific skillsets from a worker, i.e. workers are either dealing with rotating equipment, heat exchangers or large equipment. The uncertainties of equipment failure can also be incorporated so that the engineers can tackle emergencies with sufficient resources.

CHAPTER 7 ASSET INVESTMENT AND MAINTENANCE DECISION-MAKING FRAMEWORK FOR A PROCESS SYSTEM

This chapter brings an innovative algorithm combining process and asset optimisation for a chemical process system. The model integrates assets' lifetime and reliability functions to visualise the benefits of the hybrid process and asset optimisation. A Mixed Integer Linear Programming (MILP) model is formulated for investment and maintenance planning. The operating life of the network is discretised into multiple periods, and a decision is made within each period: whether to upgrade the equipment, purchase new equipment – for replacement or adding to the network, maintain the unit or perform nothing.

7.1 Optimisation approach in asset lifetime modelling

The investment planning model consists of a set of logical actions to commission or decommission the heat exchangers. The model is adapted and modified according to (Butun et al., 2019). The sets of the exchangers are categorised into two, which are set *'kn'* ($kn \in \boldsymbol{KN} \subseteq \boldsymbol{K}$) which represents the new heat exchanger units and set *'ko'* ($ko \in \boldsymbol{KO} \subseteq \boldsymbol{K}$) which represents the existing exchanger units in the HEN. Both set '*KN*' and *'KO'* are subsets of the heat exchangers set *K*, and the union of both sets are the set *K* itself, i.e. $KN \cup KO = K$.

At each period *'p'*, a decision to commission or decommission each heat exchanger *'k'* is made. The commission decision is represented with buying action, which is modelled as a binary variable $xb_{k,p}$. The decommission actions are divided into two types, which are either selling the unit ($xs_{k,p}$) or scrapping the unit ($xd_{k,p}$) when the exchanger has reached the end of its lifetime. To keep track of the exchangers' existence, another binary variable is introduced, $xe_{k,p}$. If the exchanger exists ($xe_{k,p}=1$), it has to be decommissioned first before it is repurchased. The existence constraints are defined from Eq(7-1) below:

$$xe_{k,p} = \sum_{(i,j)} B^{C}_{i,j,k,p} + \sum_{p' \in \{1 \dots p\}} xb_{k,p'} - xs_{k,p'} - xd_{k,p'} \quad \forall k \in KO, \forall p \in P \quad (7\text{-}1)$$

The following equation illustrates the formulation of constraints that compute the exchangers' sizes from the commission and decommission actions.

$$Ae_{k,p} = \begin{cases} A^{init}_{k} + Ab_{k,p} - As_{k,p} - Ad_{k,p} & \forall k \in K,\ p = 1 \\ Ae_{k,p-1} + Ab_{k,p} - As_{k,p} - Ad_{k,p} & \forall k \in K,\ \forall p < |P| \\ 2Ae_{k,p-1} - As_{k,p} - Ad_{k,p} & \forall k \in K,\ p = |P| \end{cases} \quad (7\text{-}2)$$

Where $Ae_{k,p}$ is the existing area of exchanger *'k'* at time period *'p'*, A^{init}_{k} is the initial area of exchanger *'k'*, $Ab_{k,p}$ is the purchased area of exchanger *'k'* at period *'p'*, $As_{k,p}$ is the sold area of exchanger *'k'* at time *'p'* and $Ad_{k,p}$ is the dead area of exchanger *'k'* at period *'p'*. Eq(7-2), along with Eq(7-10), ensure that the purchasing action is only allowed to be performed before the period ends ($p<|P|$). Also, as Eq(7-7) ensures that the decommissioning action must be performed at the end of the period, and only one of selling or scrapping the unit is allowed. Eq(7-9) ensures that either $As_{k,p}$ or $Ad_{k,p}$ to be equal to $Ae_{k,p-1}$ (see Eq(7-8) and (7-9)). At $p=|P|$,

the area of the exchangers is enforced to be similar to the area at the previous period. The existing area fulfils the HEN retrofit model (P1), which is reformulated into Eq(7-3).

$$Ae_{k,p}Ue_{k,p} = (UA)_{k,p} \tag{7-3}$$

7.1.1 Decommissioning

The following set of constraints provides the logical actions about the decommissioning of the exchangers in the HEN.

$$xd_{k,p} + xs_{k,p} \leq xe_{k,p-1}\ \forall k \in K,\ \forall p \in P\ \&\ p \neq 1 \tag{7-4}$$

$$xd_{k,p} + xs_{k,p} = 0\ \ \forall k \in KN,\ \forall p \in P\ \&\ p = 1 \tag{7-5}$$

$$xd_{k,p} + xs_{k,p} \leq 1\ \ \forall k \in KO,\ \forall p \in P\ \&\ p = 1 \tag{7-6}$$

$$xd_{k,p} + xs_{k,p} = xe_{k,p-1}\ \forall k \in K,\ \forall p \in P\ \&\ p = |P| \tag{7-7}$$

Eq(7-4) defines that for any heat exchanger *k*, it can be decommissioned if it exists in the previous period only. The decommission action could only be either selling or scraping the unit. For new heat exchanger, it is not allowed to be decommissioned since it is not existed at the start of the project (Eq(7-5)), whereas the existing exchangers can be decommissioned at the start of the project, and new exchangers could be purchased to replace them – Eq(7-6). Eq(7-7) enforces that at the end of the period, all exchangers that exist must be decommissioned. The following equations then define the formulation of the decommissioned exchangers' sizes, where $As_{k,p}$ is the size of the sold unit and $Ad_{k,p}$ is the dead size (scrapping) of the unit. It is apparent that Eq(7-8)and (7-9) are non-linear. The linear reformulation of both equations is presented in Appendix F.

$$As_{k,p} = \begin{cases} A_{k,p}^{init}\ xs_{k,p} & \forall k \in K,\ \forall p \in P\ and\ p = 1 \\ Ae_{k,p-1}\ xs_{k,p}\,, & \forall k \in K,\ \forall p \in P\ and\ p \neq 1 \end{cases} \tag{7-8}$$

$$Ad_{k,p} = \begin{cases} A_{k,p}^{init}\ xd_{k,p} & \forall k \in K,\ \forall p \in P\ and\ p = 1 \\ Ae_{k,p-1}\ xd_{k,p}\,, & \forall k \in K,\ \forall p \in P\ and\ p \neq 1 \end{cases} \tag{7-9}$$

7.1.2 Commissioning

The constraints related to the commissioning action, i.e. the purchasing action, are presented in this section. The purchase size of a unit $Ab_{k,p}$ should be within a logical range ($Amin_{k,p} \leq Ab_{k,p} \leq Amax_{k,p}$) that are available in the market. Eq(7-10) below shows the connection between the binary variable $xb_{k,p}$ and the continuous variable $Ab_{k,p}$. In this work, the minimum purchased area is set to be the initial area of the exchangers, i.e. $Amin_{k,p}=A^{init}_{k}$. For the set of new unit *'KN'*, the initial area is zero. Likewise, the maximum area is set to be the 'big M' variable defined in section 2.1, i.e. $Amax_{k,p}=M$. While Eq 55 defines the range of the sizes for the bought units, it also ensures that if a unit needs to be bought, the binary variable $xb_{k,p}$ is activated.

$$A_{k}^{init}\ xb_{k,p} \leq Ab_{k,p} \leq M\ xb_{k,p}\ \forall k \in K,\ \forall p \in P \tag{7-10}$$

To ensure that the purchasing action is not performed at the end of the investment project, Eq(7-11) below is formulated.

$$\sum_k Ab_{k,p} = 0 \;\; \forall p \in P \;\&\; p = |P| \tag{7-11}$$

7.1.3 Service life of exchangers

The heat exchanger is still functional as long as its end-of-life has not been reached. An integer, $L_{k,p}$ is used to indicate the remaining service life of the exchangers. Constraints 57 to 65 are formulated to relate the remaining service life to the investment planning actions, which are adapted and modified from Butun et al. (2019). The descriptions of the constraints are as follow:

(i) Eq(7-12): An exchanger can only exist if its remaining service life is non-zero only

(ii) Eq (7-13): If an exchanger has a remaining service life, then it exists in the HEN

(iii) Eq (7-14): At the first period, the remaining service life is equal to the life span of the unit ($L^{span}{}_k$), if a new unit is commissioned. If it is decommissioned, its service life is equal to the difference between the life span and its initial service life ($L^{init}{}_k$). Before it is commissioned, it has to be decommissioned first. At the other periods, the remaining service life decreases by one period compared to the previous period, if it still exists. The buying action restores the service life of the exchanger, and the selling action decreases the service life, which $Ls_{k,p}$ represents the life of the sold exchanger.

(iv) Eq (7-15): If the remaining service life of exchanger at previous period minus its current sold life is greater than 1, buying action is not activated. This means that a unit cannot be re-purchased before it is decommissioned or sold.

(v) Eq (7-16): If the remaining service life of the exchanger at the previous period is greater than 1, the exchanger is not dead and cannot be scrapped. The unit is scrapped only if its previous age is 1 year or less.

(vi) Eq (7-17): An exchanger can only be sold if the remaining service life of the exchanger at the previous period is greater than or equal to 2.

(vii) Eqs (7-18) to (7-19): If sold life of the exchanger is non-zero, then the selling action is activated, and the sold life is equal to the previous service life minus one.

$$xe_{k,p} \leq L_{k,p} \;\; \forall k \in K, \forall p \in P \tag{7-12}$$

$$L_{k,p} \leq xe_{k,p} L_k^{span} \;\; \forall k \in K, \forall p \in P \tag{7-13}$$

$$L_{k,p} = \begin{cases} xb_{k,p} L_k^{span} + \left(L_k^{span} - L_k^{init}\right)\left(1 - xs_{k,p} - xd_{k,p}\right) & \forall k \in K, \forall p \in P, p = 1 \\ L_{k,p-1} - xe_{k,p} + L_k^{span} xb_{k,p} - Ls_{k,p} & \forall k \in K, \forall p \in P, p \neq 1 \end{cases} \tag{7-14}$$

$$L_{k,p-1} - Ls_{k,p} - 1 \leq \left(1 - xb_{k,p}\right) L_k^{span} \;\; \forall k \in K, \forall p \in P \;\&\; p \neq 1 \tag{7-15}$$

$$L_{k,p-1} - 1 \leq \left(1 - xd_{k,p}\right) L_k^{span} \;\; \forall k \in K, \forall p \in P \;\&\; p \neq 1 \tag{7-16}$$

$$L_{k,p-1} - 2 \leq \left(2 - xe_{k,p-1} - xs_{k,p-1}\right) L_k^{span} \;\; \forall k \in K, \forall p \in P \;\&\; p \neq 1 \tag{7-17}$$

$$Ls_{k,p} \geq L_{k,p-1} - xe_{k,p-1} - \left(1 - xs_{k,p-1}\right) L_k^{span} \;\; \forall k \in K, \forall p \in P \;\&\; p \neq 1 \tag{7-18}$$

$$Ls_{k,p} \leq L_{k,p-1} - xe_{k,p-1} \quad \forall k \in K, \forall p \in P \,\&\, p \neq 1 \tag{7-19}$$

$$Ls_{k,p} \leq xs_{k,p} L_k^{span} \quad \forall k \in K, \forall p \in P \tag{7-20}$$

7.1.4 Cost model

The cost model constraints are formulated to calculate the cash flows, relating the decommissioning and commissioning actions to the NPV evaluation. The investment in HTE and purchasing units are considered as negative cash flows. The yearly reduced operating cost due to utility reductions compared to the base case is considered as the positive cash flow. The bought exchangers are susceptible to depreciation. The remaining value of the sold exchangers, as well as the salvage value of the exchangers, are the positive cash flows during each period. Eqs(7-21) to (7-29) are formulated to compute the cost for the exchangers due to the decommissioning and commissioning, adapted and modified from Butun et al. (2019).

(i) Eq (7-21): The buying cost ($Cb_{k,p}$) is the investment cost for the exchanger represented in Eq (7-1) .

(ii) Eq (7-22): The heat exchanger starts to lose its economic value once it is purchased. At the start of the project, only the base unit is susceptible to depreciation, while new units have no remaining value ($Crv_{k,p}$). A double-declining depreciation is used, where i^{dep}_k is the depreciation rate. At other periods, the remaining value is the summation of the previous remaining value and purchasing cost, minus the sold value ($Csv_{k,p}$), dead value ($Cdv_{k,p}$) and depreciated value ($Cdep_{k,p}$) from the previous period.

(iii) Eq (7-23): The formula to calculate the depreciated value of the exchanger k, based on the straight-line depreciation method

(iv) Eqs (7-24) to (7-25): The sold value of heat exchanger k. If the selling action is not activated, the sold value is zero. Notice that Eq 7-25 is a bilinear function. The linearisation procedure is presented in Appendix F.

(v) Eqs (7-26) to (7-27): The dead value of heat exchanger k. If the scrapping action is not activated, the dead value is zero. Notice that Eq 7-27 is a bilinear function; the linearisation procedure is presented in Appendix F.

(vi) Eq (7-28): The scrap price of the exchanger k ($Csc_{k,p}$) is equal to the salvage value if the scrapping action is activated. It is equal to zero otherwise.

(vii) Eq (7-29): The selling price of the exchanger k ($Cs_{k,p}$) is equal to the maximum of sold value and the scrapping value if the selling action is activated. It is equal to zero otherwise. The linearisation procedure of the maximum function is given in Appendix F.

$$Cb_{k,p} = Inv_{k,p} \quad \forall k \in K, \forall p \in P \tag{7-21}$$

$$Crv_{k,p} =$$

$$\begin{cases} Cb_{k,p}(1-2i_{dep})^{L_k^{init}} & \forall k \in KO, \forall p \in P \text{ and } p = 1 \\ 0 & \forall k \in KN, \forall p \in P \text{ and } p = 1 \\ Cb_{k,p-1} + Crv_{k,p-1} - Csv_{(k,p-1)} - Cdv_{k,p-1} - Cdep_{k,p-1} & \forall k \in K, \forall p \in P \text{ and } p \neq 1 \end{cases} \quad (7\text{-}22)$$

$$Cdep_{k,p} = (Cb_{k,p} - Csv_{k,p} - Cdv_{k,p} + Crv_{k,p})i_{dep} \ \forall k \in K, \forall p \in P \quad (7\text{-}23)$$

$$Crv_{k,p} - (1 - xs_{k,p})M \leq Csv_{k,p} \leq Crv_{k,p} \ \forall k \in K, \forall p \in P \quad (7\text{-}24)$$

$$Csv_{k,p} = xs_{k,p}Crv_{k,p} \ \forall k \in K, \forall p \in P \quad (7\text{-}25)$$

$$Crv_{k,p} - (1 - xd_{k,p})M \leq Cdv_{k,p} \leq Crv_{k,p} \ \forall k \in K, \forall p \in P \quad (7\text{-}26)$$

$$Cdv_{k,p} = xd_{k,p}Crv_{k,p} \ \forall k \in K, \forall p \in P \quad (7\text{-}27)$$

$$Csc_{k,p} = xd_{k,p}Csal_k \ \forall k \in K, \forall p \in P \quad (7\text{-}28)$$

$$Cs_{k,p} = \max(Csv_{k,p}, xs_{k,p}Csal_k) \ \forall k \in K, \forall p \in P \quad (7\text{-}29)$$

7.2 Mean-residual life of the equipment

The failure analysis based on past failure data is usually performed during the design stage to determine the equipment's survival or reliability function. The time-to-failure for the equipment is fitted with appropriate failure probability using statistical functions, such as Weibull, Exponential or Normal distributions. The most popular distribution model for the reliability function is the Weibull model. It is widely used to study the lifetime of components with different hazard rate functions due to its flexibility in parameter tuning. In this study, the individual failure probabilities of the exchangers are modelled using the Weibull model, as shown in Eq(7-30).

$$f_k(t) = \frac{B_k}{n_k}\left(\frac{t}{n_k}\right)^{B_k-1} e^{-\left(\frac{t}{n_k}\right)^{B_k}} \quad \forall k \in K \quad (7\text{-}30)$$

Where $f_k(t)$ is the failure probability of unit *k*, B_k and n_k are the shape parameter, and the scale parameter for exchanger *k* and *t* is the time of the operation. The reliability function, i.e. the probability of the exchanger still function at time *t* is represented as follow:

$$R_k(t) = \int_t^{\infty} fk(t)dt = e^{-\left(\frac{t}{n_k}\right)^{B_k}} \quad (7\text{-}31)$$

In this work, the mean residual life (MRL) or the remaining useful life (RUL) is used as the reliability indicator for heat exchangers. MRL is the remaining time of the unit before the failure occurs, given that the unit has operated longer than a certain period *'t'*. It is more useful than the reliability function as it evaluates the performance of the exchanger over a long time horizon, while the reliability function or hazard rate just measures the probability of failure

instantaneously. The MRL measures the remaining life of the exchanger, given it is operated after a certain amount of time. This gives valuable information about the assets' performance over time and provides guidelines to engineers to plan maintenance or replacement actions. This is especially useful for heat exchangers as the tube materials undergo corrosion and fatigue over time. Engineers often apply this indicator in the plant's assets to decide whether to perform maintenance or delay it, as stopping the production incurs an expensive cost. The equation governing the MRL is shown in Eq(7-32):

$$MRL_k(t) = E_t(T - t|T > t) = \frac{\int_t^{\infty} R_k(u)du}{R_k(t)} = \frac{\int_0^{\infty} R_k(g+t)dg}{R_k(t)} \quad (7\text{-}32)$$

Note that in this work, the MRL is assumed to indicate various failure events caused by, such as tube corrosion. The maintenance action is assumed to be the combination of cleaning action or bundles replacement, regardless of the number of cleaning cycles. The detailed cleaning schedule is ignored here as this would be the problem for short-term planning. For simplicity sake, it is also assumed that a spare is readily available when maintenance is performed, so the utility penalty is ignored in this work. The integration of an exponential function is infeasible to solve, especially the upper bound is infinity. An accurate approximation using Gauss-Lauguerre quadrature is applied in this work. Linearisation is then performed on the approximated MRL model. Please refer to Appendix F for the approximation and linearisation approach.

7.3 Results and discussion

The HEN retrofit, investment and maintenance planning model is solved using commercial MILP solver: CPLEX, with a model formulated in the General Algebraic Modelling System (GAMS) software version 29.1. the solver with a relative gap set as at least 0.1-0.2. The laptop used is a HP EliteBook 820 G3 with Intel Core i5-63000 M (2.50 GHz) processor, and 16 GB RAM is used to solve the model. The average Central Processing Unit (CPU) time for the generation of solutions for the HEN retrofit model is 30 s, but for the multi-period model could take up to 1,000-5,000- s with each iteration.

The optimal investment and maintenance planning for the HEN is determined for a horizon of 20 years. The retrofit option is first limited to enhancing the heat exchangers with HTE and replacing old exchangers without topological modifications. For case study 1- see Chin et al. (2020b), the optimal NPV obtained is about 3.1 M$, with utility saving of a maximum 24 %. The total investment in purchasing new exchangers have estimated to be about 0.97 M$, while the investment in the HTE technologies is estimated to be about $ 10,506. Table 7-1 shows the optimal investment solutions for individual exchangers. It is assumed that once any exchanger k is replenished, purchasing action is activated, and the exchanger is replaced. It can be shown that the decision to purchase new exchangers are mainly activated in the first period for E1 to E4, but not E5. This is because the cost for utilities is much higher than the capital cost itself, so more utility saving is encouraged to yield a higher NPV. When the units have reached the

end of service life, it is inevitable to invest in new heat exchangers. Bigger sizes of heat exchangers (E1, E2, E3 and E4) are purchased at the start of the project to enhance the utility saving further, while the similar size of E5 is used until it reaches the end of its life (15 years). After it is scrapped, a new and slightly larger E5 is bought. Earlier investments are more beneficial due to the time value of money. Figure 7-1 shows the HEN layout.

Only some of the exchangers are equipped with enhancement technologies. The new exchanger E3 is implemented with external fins (EF) on its shell-side to enhance the heat transfer. The tube-side heat transfer of E5 is enhanced through internal fins (InF) as well before it is scrapped in the 15th year. The newly bought E5 is not equipped with any enhancement technologies. The reasons for not implementing the technologies are probably due to the utility saving is given more priority due to the high utility cost, so purchasing new and larger exchangers are preferred to yield higher NPV.

As for the maintenance periods, Figure 7-2 clearly shows the mean residual life (MRL) behaviours for different exchangers. The blue dotted line represents the original MRL distribution of the heat exchangers, derived from Eq 77. Due to the assumptions of the increasing failure rate of all the exchangers, the MRL decreases gradually as time progresses. The jump between points or constant behaviours of the orange line represents the maintenance performed on the exchanger. Based on the results, E1, E2 and E3 are not maintained too often, probably due to relatively lower fouling resistances. As for E4, it is encouraged to maintain the exchangers annually after year 2 to ensure the energy efficiency of the exchanger. This is mostly due to the higher fouling resistance of E4, which could incur expensive operating cost if it is not maintained. The maintenance cost is relatively cheaper, so it is recommended to maintain the exchanger more often to reduce the fouling resistance. The reason for the jump of MRL distribution (blue dotted line) for E5 is because of the buying action. As a new exchanger is bought, the age and its MRL is restored.

Table 7-1: Optimal investment in heat exchangers for case study 1 (consider intensification only), with values in bracket represent the period.

Exchangers	E1	E2	E3	E4	E5
Tube Intensification technologies	None	None	None	None	InF (P1-P15) None (P15-P20)
Shell Intensification technologies	None	None	EF	None	None
Purchasing size of exchangers (m^2)	1,554.9 **(P1)**	4,718.8 **(P1)**	275.4 **(P1)**	244.35 **(P1)**	37.4 **(P16)**
Selling size of exchangers (m^2)	1,554.9 **(P20)**	4,718.8 **(P20)**	275.4 **(P20)**	244.35 **(P20)**	37.4 **(P20)**
Dead size (Scrapped) of exchangers (m^2)	590.7 **(P1)**	2,508.2 **(P1)**	269.2 **(P1)**	220.2 **(P1)**	31.0 **(P16)**
Investment on heat exchangers ($)	326,888	992,053	95,677	51,370	7,870
Investment in HTE ($)	-	-	9,422 (P1)	-	1,084.2 (P1)
Selling price of exchangers ($)	44,158	134,012	12,924	6,939	5,163
Scrap price of exchangers ($)	5,000	5,000	5,000	5,000	5,000

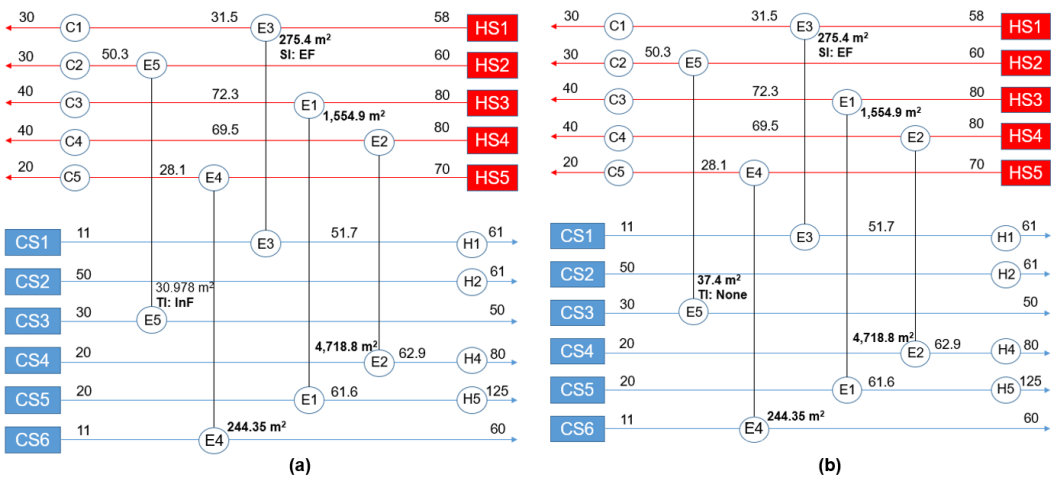

Figure 7-1: HEN layout for case study 1 after the retrofit, consider HI only: (a) Period 1-15 (b) Period 16-20, with temperatures are represented by the values on the streams

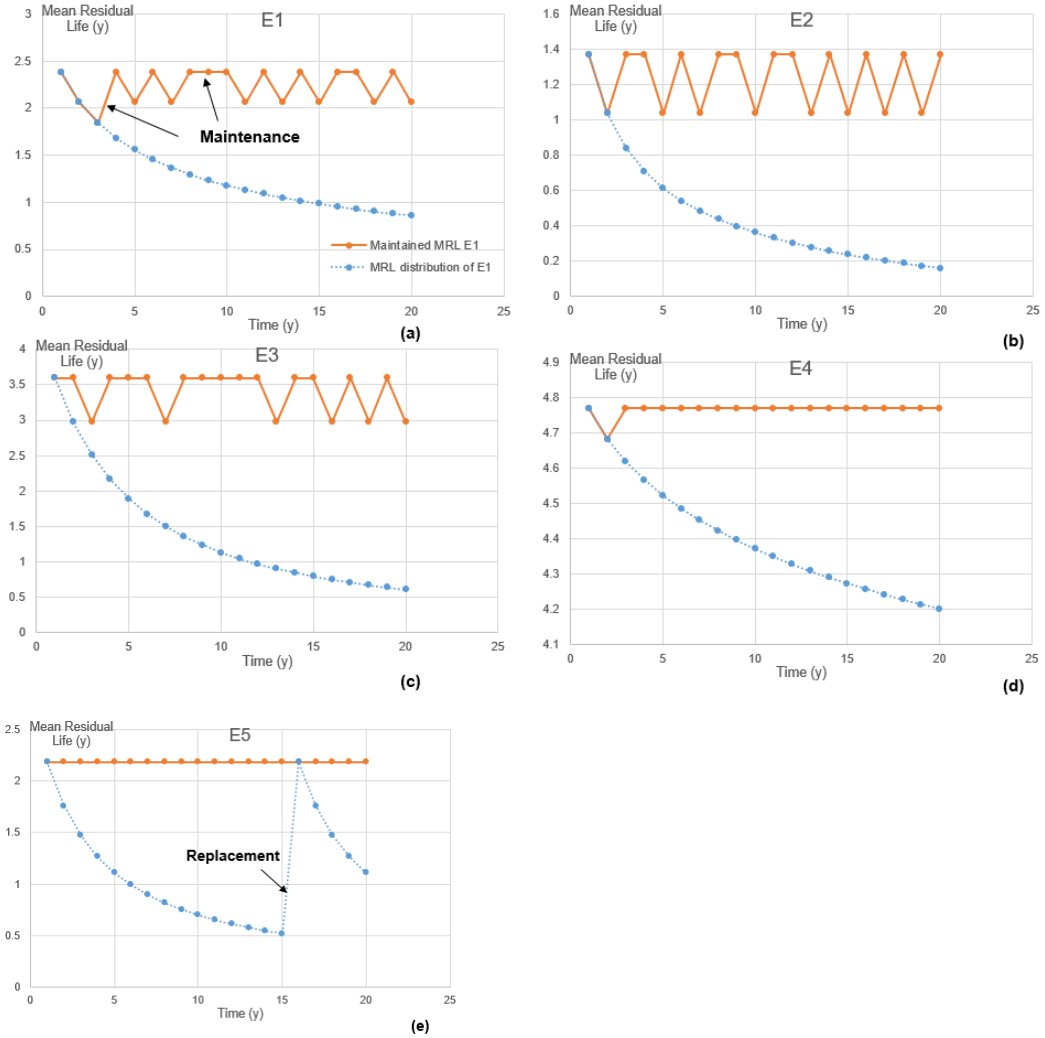

Figure 7-2: Mean residual life of the exchangers equipped with HTE technologies (a) E1 (b) E2 (c) E3 (d) E4 (e) E5

For case study 2 – see Chin et al. (2020b), the optimal NPV obtained is about 147 k$, with utility saving of an average of 32 %. The total investment in purchasing new exchangers have estimated to be about $ 52,931, while the investment in the HTE technologies is estimated to be about $ 6,600. Table 7-2 shows the optimal investment solutions for individual exchangers. The investment is suggested to be at the start of the project. The single exchanger E1 is recommended to change to a bigger size and is equipped with coiled wire plus internal fins (CWIF) on its tube side. This is because the cost for utilities is much higher than the capital cost itself, so more utility saving is encouraged to yield a higher NPV. The investment is started in the first period to yield higher utility savings. Figure 7-3 shows the HEN layout. Based on Figure 7-4, the exchanger is also recommended to maintain once every two years to ensure consistent performance.

Table 7-2: Optimal investment in heat exchangers for case study 2 (consider intensification only), with values in bracket represent the period.

Exchangers	E1
Tube Intensification technologies	CWIF
Shell Intensification technologies	None
Purchasing size of exchangers (m^2)	120.0 **(P1)**
Selling size of exchangers (m^2)	120.0 **(P20)**
Dead size (Scrapped) of exchangers (m^2)	8.31 **(P1)**
Investment in new exchangers ($)	52,931
Investment in HTE ($)	6,600
The selling price of exchangers ($)	7,150
Scrap price of exchangers ($)	5,000

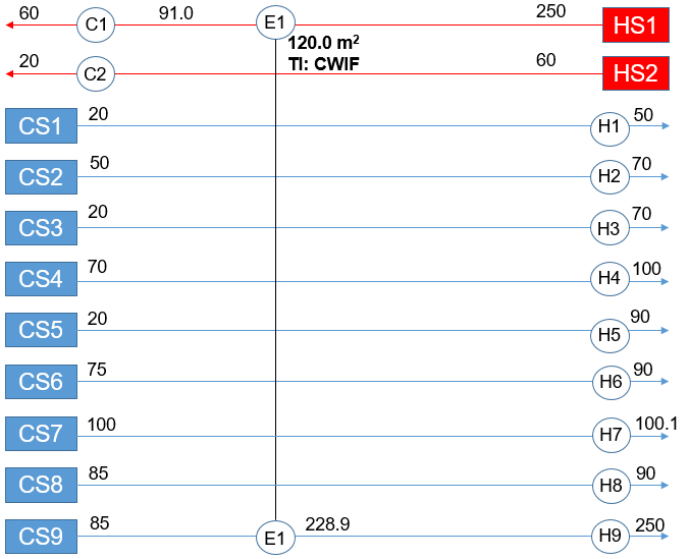

Figure 7-3: HEN layout for case study 2 after the retrofit, consider HI only

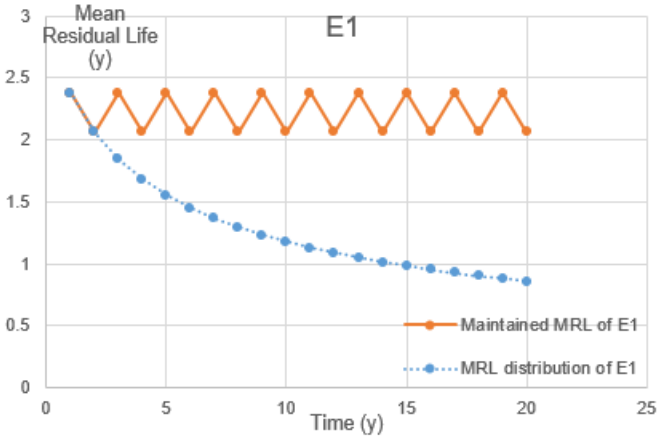

Figure 7-4: Mean residual life of the exchangers equipped with HTE technologies for case study 2: E1

Adding extra exchangers. The optimal investment and maintenance planning for the HEN is now considering the option for topological modifications (i.e. adding new exchangers). For case study 1, the number of additional units is determined to be 2. The optimal NPV obtained is about 3.8 M$, with a utility saving of still about 51 %. The total investment in purchasing new exchangers are lower than just considering the heat intensification only, estimated to be about 0.77 M$, while the investment in the HTE technologies is estimated to be about $ 180,560. In this scenario, all exchangers except E2 are replaced with new and larger exchangers. The new exchanger E6 is recommended to install twisted tape and internal fins (TTIF) on its tube-side, while the exchanger E7 should equip with an external fin (EF) on its shell-side.

It is surprising to show that the enabling options to add new exchangers yield higher NPV while paying less on the investment. This is due to the capital cost is an exponent function, which cost increases exponentially when the area is increased. The option to add new exchangers is comparatively cheaper than using a very large heat exchanger. As shown in Table 7-2, about two-time expansion is needed for E2 and E1 to yield better profit. Table 7-3 shows the optimal investment solutions for individual exchangers. Figure 7-5 shows the HEN layout for different periods.

As for the maintenance periods, all the exchangers are expected to be maintained annually, except that E2 is to be maintained annually after the 2nd year to ensure the operating efficiency of the exchangers. Only exchanger E2 is shown in Figure 7-6, which illustrate its mean residual life (MRL) behaviours. Due to the buying action of E2 in the 11th year, the MRL distribution is restored to its original value. Note that in this work, the exchanger is assumed to be restored back to the original MRL of the specific exchanger but not improved MRL.

Table7-3: Optimal investment in heat exchangers for case study 1 (consider intensification + adding new exchangers), with values in bracket represent the period.

Exchangers	E1	E2	E3	E4	E5	E6	E7
Tube Intensification technologies	None	None	None	None	None	TTIF	None
Shell Intensification technologies	None	None	None	None	None	None	EF
Purchase size of exchangers (m^2)	847.6 **(P1)**	2,508.5 **(P11)**	348.6 **(P1)**	244.4 **(P1)**	37.4 **(P1)**	2,205 **(P1)**	2,009 **(P1)**
Selling size of exchangers (m^2)	-	2,508.5 **(P20)**	-	-	-	2,205 **(P20)**	2,009 **(P20)**
Dead size (Scrapped) of exchangers (m^2)	590.7 **(P1)** 847.6 **(P20)**	2508.2 **(P11)**	269.2 **(P1)** 348.6 **(P20)**	220.2 **(P1)** 244.4 **(P20)**	31.0 **(P16)** 37.4 **(P20)**	-	-
Investment on heat exchangers ($)	126,488	278,392	117,876	87,636	21,170	268,905	262,779
Investment in HTE ($)	-	-		-		110,248	70,312
The selling price of exchangers ($)	-	30,371	-	-	-	9,308	8,480
Scrap price of exchangers ($)	10,000	5,000	10,000	10,000	10,000	-	-

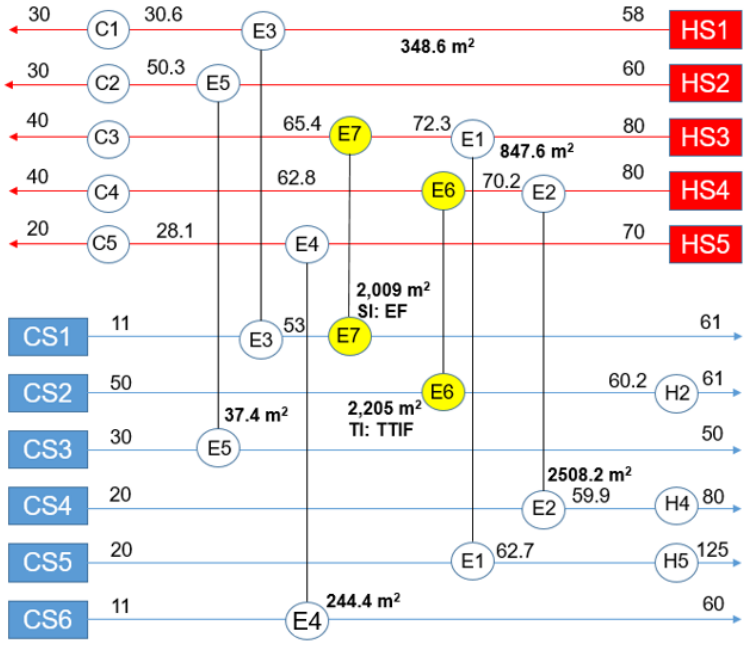

Figure 7-5: HEN layout for case study 1 after the retrofit, consider HI and new exchangers:

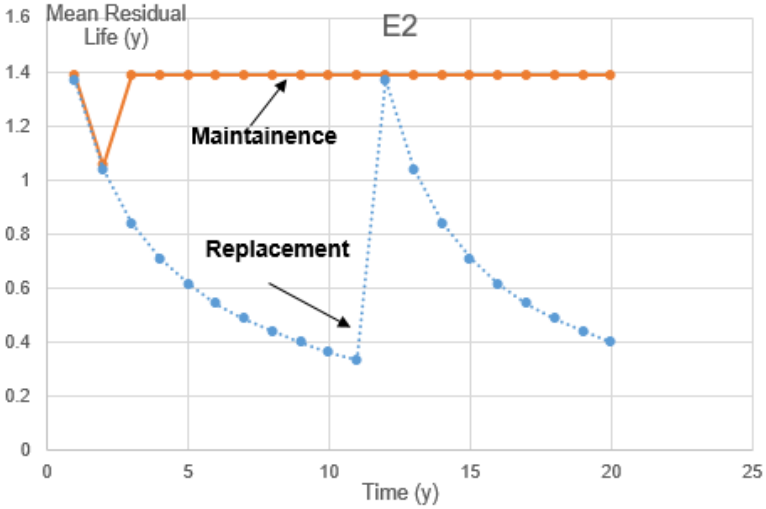

Figure 7-6: Mean residual life for case study 1: E2 (consider HTE and adding new exchangers)

Similarly, for Case Study 2, the optimal investment and maintenance planning are conducted for a horizon of 20 y, considering the topological modification options. Three additional units are recommended to be installed. In this case, the optimal NPV is about 320 k$. The investment in new exchangers is all conducted at the beginning of the period. Notice that the investment is higher than considering the intensification only (see Table 7-4). This is logical as more area is required if the operating cost needs to be reduced. Even though the investments are higher, the income generated from scrapping the exchangers and the utility saving justify the cost,

which yields a higher NPV. Maintenance is needed to conduct annually to ensure the consistent performance of the network. Figure 7-7 shows the HEN layout.

Table 7-4: Optimal investment in heat exchangers for Case Study 2 (consider intensification + adding new exchangers) with values in bracket represent the period.

Exchangers	E1	E2	E3
Tube Intensification technologies	CWIF	None	None
Shell Intensification technologies	None	None	None
Purchasing size of exchangers (m^2)	92.1 **(P1)**	10.4 **(P1)**	25.8 **(P1)**
Selling size of exchangers (m^2)	-	-	-
Dead size (Scrapped) of exchangers (m^2)	92.1 **(P20)**	10.4 **(P20)**	25.8 **(P20)**
Investment in new exchangers ($)	57,425	33,918	39,188
Investment in HTE ($)	5,065.5	-	-
The selling price of exchangers ($)	-	-	-
Scrap price of exchangers ($)	5,000	5,000	5,000

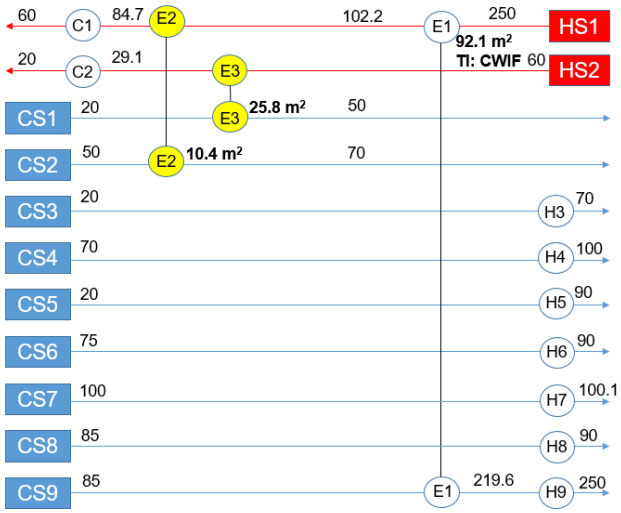

Figure 7-7: HEN layout for case study 2 after the retrofit, consider HI and new exchangers for 20 y period

7.4 Conclusion

This work considers the long-term investment and maintenance planning within the context of HEN retrofit. The HEN retrofit model is formulated based on the concept of SRTGD, which clearly shows the matches between cold and hot streams. Most of the works on HEN retrofit considers investment and uses NPV as the objective function, but they do not include the opportunity to invest in exchangers at different time period throughout the lifetime of the HEN. This work considers the simultaneous optimisation of HEN retrofit, investment and maintenance planning. A sequential solution strategy is proposed as well to solve the integrated model. The HEN retrofit model is first solved to obtain the streams' temperature and exchangers' areas. Subsequently, the first stage solution is used as the initial points to the second stage, which is the linearised model of integrated HEN retrofit, investment and maintenance planning.

For the Kraft Pulp mill case study, The obtained solution shows that the combination of heat transfer enhancement and installation of extra exchangers provide more significant economic benefit than just heat intensification only. Investment in larger exchangers are preferred in the first period or after the exchanges' service life has ended. A total NPV of 3.8 M$ was obtained by implementing the intensification technologies and adding new exchangers, with utility savings of about 51 % (under the 20 y time horizon). An NPV of 3.1 M$ is obtained for HEN retrofit without topological modification. It is worth noting that the investment in exchangers considering the topological changes is higher than the retrofit option without topological changes, but the NPV is higher. This is due to the utility cost is much higher than the capital cost, so the optimisation solver sought to maximise the utility saving by adding a new heat transfer area. Similar results are obtained for another case study in the sunflower oil production plant, in which the implementation of both HTE and adding extra exchangers are cost-effective. Even though the investment in exchangers is about 40-60 % higher than without adding new exchangers, the utility saving and the income generated from selling or scrapping the exchangers balance the cost, which yields a higher NPV. The obtained NPV is also higher compared to previous works, with 17 % higher for case study 1 and 14 % higher for case study 2. This proves the advantages of a retrofit with replacing old exchangers, with intensification as well as adding new exchangers.

The exchanger with the highest fouling resistance is maintained more often, preferably annually, compared to other exchanges. This is to ensure the operating cost is minimised. From the MRL plot of individual exchangers, the engineers could monitor the exchangers' failure behaviour and track their maintenance status. However, the set of new exchangers invested are assumed to have similar performance characteristics to the base exchangers (i.e. fouling resistance and failure behaviour), which might not be the optimal option in the perspective of investment. Another significant issue is that the data availability of exchangers' performance (i.e. corrosion or reliability) is low. In this work, only the mean failure time taken from the literature source is used to infer the failure behaviour, which can be inaccurate practically.

CHAPTER 8 CONCLUSIONS AND PROPOSED FUTURE DEVELOPMENT

8.1 Conclusions of the PhD study

The PhD study has been carried out to extend the Pinch-based analysis on the material resources conservation network to multiple qualities, Total Site synthesis considering materials headers, and maintenance planning

8.1.1 Pinch Analysis in material resources conservation

The study is initiated with an analysis on Mass-Based Pinch Analysis considering multiple qualities. The analysis shows that each sink is limited by at least one qualities indicator. Following the limiting qualities indicator, the sinks should be targeted using the sources with the ascending order sequence of the limiting qualities. It is also required to check the detailed allocation of sources to sinks when constructing the Composite Curves as there might have an unfulfilled qualities limit, which may result in the more fresh resource.

A headers targeting framework is also proposed using the Pinch-based Composite Curves. The header lines can be drawn by merging the segments of the Source Composite Curve. It is also shown that the number of headers are at least the number of Pinch Point of a specific problem. For site-level headers targeting and synthesis, the Pinch Point(s) are first identified for the overall network using the Material Recovery Pinch Diagram for all the qualities. The guideline for the cross-plant material sources transfer is then built upon the concept of the Pinch Point(s) for all the qualities indicators. The objective is to ensure the cross-plant sources flowrate or the number of cross-plant connections is minimal. The number of headers required for the individual processes can be identified by analysing the Composite Curves with the cross-plant sources while ensuring the fresh resources required is minimal. An iterative headers targeting framework is then proposed to determine the flowrates and the qualities of the headers. Two case studies, which have single and multiple qualities Total Site water recycling network, are used to demonstrate the proposed framework, comparing results obtained using direct integration and centralised headers. This framework provides a proper analysis of the problem, which allows users to explore various source mixing options for the identified minimum number of headers. The proposed method also solves the site level network synthesis with the centralised headers problem, which is a non-linear problem.

8.1.2 Game Theory in water symbiosis

This work also has considered the fair and equitable subsidies or incentives allocations to facilitate the realisation of water symbiosis in an eco-industrial park. The park authority should distribute the money so that the stakeholders are more willing to join in the grand symbiosis scheme while ensuring their dissatisfactions are minimised. It is also proposed in this work that the cost allocation should be convincing enough for the stakeholders to participate in the grand coalition rather than forming smaller collaborations. This is because more coalitions could save more resources and waste discharges but required higher cost. A

multi-stage cooperative game theory approach is proposed to evaluate the distribution scheme. The park authority has the highest decision power to decide on the subsidies or incentives to be allocated and the resources allocated. The stakeholders can then decide on the recycling flows based on the authority's decision. The framework is followed by a game analysis on tax rates that can be imposed by the authority to encourage recycling activities while also generating a source of income for the subsidies. Notice that the approach assumes rationalities between stakeholders, i.e., each stakeholder wants to get the subsidies/incentives at least larger in the collaboration than what they can get without collaboration (super-additivity/monotonicity). In reality, this may not be the solution as the certain firm could have more negotiation powers over the others and, in turn, affects the allocation solutions. A stakeholder may decide to enter/quit the coalition at any time over the planning horizons when they could get better benefits. A proper evolutionary game analysis on the collaborative firms should be conducted to determine behaviours of the firms that reflect the realistic scenario.

8.1.3 Asset maintenance and management

The asset maintenance planning resembles the resource conservation problem as it involves resource planning as well – labour/time/spare/cost. This thesis has extended the Process Integration tools in asset management planning, including opportunistic maintenance management and tasks allocation. Cost is treated as the main resource for opportunistic maintenance management, while labour working hour is the resource for task allocation. A more sophisticated Pinch-based strategy can be applied to opportunistic maintenance as well to identify an optimal maintenance grouping strategy. This tool can be integrated with the proposed short-term maintenance task scheduling strategy. The failure of the equipment failure or operating data could be collected to predict the failure behaviour To facilitate accurate asset management and maintenance planning. This serves as the base for asset performance and can be readily integrated into the proposed asset optimisation framework, allowing a robust and smart retrofit framework to be developed.

8.2 Novel contributions

The novel contributions lie in the following aspects:

(i) The first contribution is to extend the Pinch-based framework to material conservation networks multiple qualities as well as headers targeting and synthesis for both process and site level. (Chapters 3-4). It provides the fundamental understanding of material recycling or reuse network problems with multiple qualities. The contributions also allow exploring sources mixing options for intermediate resource storage, either internal or in an industrial site with minimal fresh resource.

(ii) The second contribution involves the investigation of the resources allocation and operational management in the Game Theory perspective, which provides solutions in rational or collaborative perspectives (Chapter 5). The approach provides a

guideline to formulate a balanced economic policy between stakeholders and the government or authorities, through fair subsidies and tax implementation to facilitate the Circular Economy system

(iii) The third contribution is the integration of assets performance studies into resources conservation network studies in industrial sites (Chapter 6 – 7). The contribution not only focuses on resources conservation, but also considers an integrated framework on asset and process optimisation in the chemical industry. It incorporates the reliability issues, the service life of equipment and depreciation of the units. Utilising Pinch approach in planning maintenance inspection and tasks scheduling enables the resources (time, cost, work force) to be saved in a simpler way.

8.3 Future Development

As a scientific research work aiming to seek solutions and inspire new studies, this thesis also identifies the following aspects worth further investigation. The first point is the lack of a materials database with quality parameters. It is difficult to identify a more accurate global resources conservation without a proper database to target for the Circular Economy. The second aspect, which has been common in existing assessment/optimisation tools, is to improve the feasibility in the practical implementation of the site-level resources conservation planning. Although Game Theory could provide rational perspectives for the government and each individual plant, it does not provide an optimal solution for the environment. A management contract should be established to ensure the accuracy of resource sharing information. The last point worth further investigation is that in a combination of resources management combining material and energy resources. The energy sources, including renewable resources (e.g. hydropower, solar power, coal-fired power), should be incorporated so that an ideal Circular Economy system with maximum recyclability of the sources can be achieved as much as possible in a realistic scenario.

In terms of asset maintenance modelling, the following potential advancement on maintenance optimisation is identified in the review:

(i) Opportunistic maintenance of equipment exploiting production stoppage. The current works mostly dealt with the maintenance of multiple components in a single piece of equipment, while multi-unit systems are considered with at most two dependent components

(ii) Data-driven joint optimisation of spare parts ordering policy with maintenance planning should be considered. Currently, there are a lack of practical studies on maintenance optimisation with resource limitations

(iii) Evolving Non-stationary data on assets' condition and hazardous risk should be utilised. Not many works have considered both quantitative and qualitative data. Both types of data should be combined with well-informed maintenance planning.

(iv) Fault propagation effect from one unit to another should be incorporated into maintenance optimisation, especially in Total Site/Industrial Site planning. Not only structural interdependencies but the unit failure could affect the operating parameters, causing major damage.

More attention should be paid to the sustainability impacts caused by equipment maintenance and breakdown. Greener and more efficient technologies can be installed into the assets (retrofit), other than the maintenance of the equipment. Life-cycle sustainability assessment of the asset management methods can be performed to evaluate the sustainability index of the assets. Advanced development of assets maintenance planning and scheduling models concerning the environmental burden is needed so that the process can advance toward a Circular Economy.

REFERENCES

Aguirre, A.M., Papageorgiou, L.G., 2017. Resource-constrained formulation for production scheduling and maintenance, in: Espuña, A., Graells, M., Puigjaner, L. (Eds.), Computer Aided Chemical Engineering, 27 European Symposium on Computer Aided Process Engineering. Elsevier, pp. 1375–1380.

Ahmed Q., Moghaddam K.S., Raza,S.A., Khan F.I., 2015. A multi-constrained maintenance scheduling optimisation model for a hydrocarbon processing facility. Proceedings of the IMechE 229, 151–168.

Allwood J.M., 2014. Squaring the Circular Economy: The Role of Recycling within a Hierarchy of Material Management Strategies, in: Worrell, E., Reuter, M.A. (Eds.), Handbook of Recycling. Elsevier, Boston, pp. 445–477.

Alnouri SY, Linke P, El-Halwagi MM, 2014. Optimal interplant water networks for industrial zones: addressing interconnectivity options through pipeline merging. AIChE Journal, 60(8), 2853-2874

Alnouri SY, Linke P, El-Halwagi MM, 2018. Accounting for central and distributed zero liquid discharge options in interplant water network design**.** Journal of Cleaner Production, 171, 644-661

Alrabghi A., Tiwari A., 2015. State of the art in simulation-based optimisation for maintenance systems. Computers & Industrial Engineering, 82, 167–182.

Alva-Argáez A., Kokossis A.C., Smith R., 2007. The design of water-using systems in petroleum refining using a water-pinch decomposition. Chemical Engineering Journal, 128, 33–46.

Alva-Argáez A., Vallianatos A., Kokossis A., 1999. A multi-contaminant transhipment model for mass exchange networks and wastewater minimisation problems. Computers & Chemical Engineering, 23, 1439–1453.

Aviso KB, Tan RR, Culaba AB, Cruz JB, 2010. Bi-level fuzzy optimization approach for water exchange in eco-industrial parks. Process Safety and Environmental Protection, 88, 31-40.

Baaqeel H., El-Halwagi M.M., 2018. Optimal Multi-scale Capacity Planning in Seawater Desalination Systems. Processes, 6, 68.

Bakirtzis G.A., Biskas P.N., Chatziathanasiou V., 2012. Generation Expansion Planning by MILP considering mid-term scheduling decisions. Electric Power Systems Research, 86, 98–112.

Bandyopadhyay S, 2006. Source Composite Curve for Waste Reduction. Chemical Engineering Journal, 125, 99–110.

Banjevic D., 2009. Remaining useful life in theory and practice. Metrika, 69, 337–49.

Boix M, Montastruc L, Pibouleau L, Azzaro-Pantel C, Domenech S, 2012. Industrial water management by multiobjective optimization: from individual to collective solution through eco-industrial parks. Journal of Cleaner Production, 22 (1), 85-97

Boysen B, Cristobal J, Hilbig J, Guldemund A, Schebek L, Rudolph K-U, 2020. Economic and environmental assessment of water reuse in industrial parks: case study based on a Model Industrial Park, Journal of Water Reuse and Desalination, 10(4), 475-489.

Bressanelli G., Perona M., Saccani N., 2019. Challenges in supply chain redesign for the Circular Economy: a literature review and a multiple case study. International Journal of Production Research 57, 7395–7422.

Bütün H, Kantor I, Maréchal F., 2019. An Optimisation Approach for Long-Term Industrial Investment Planning. Energies,12,1–33.
Calixto E.E.S., Francisco F.S., Pessoa F.L.P., Queiroz EM, 2015. A Novel Approach to Predict Violations and to Define the Reference Contaminant and Operation in Water Using Networks, in: Gernaey, K.V., Huusom, J.K., Gani, R. (Eds.), Computer Aided Chemical Engineering, 12 International Symposium on Process Systems Engineering and 25 European Symposium on Computer Aided Process Engineering. Elsevier, pp. 1901–1906.
Carlo F.D., Arleo M.A., 2017. Imperfect Maintenance Models, from Theory to Practice, in: Volosencu, C. (Ed.), System Reliability. InTech, London, UK.
Castaño J.A., Higuita J.C., 2016. Using turbidity for designing water networks. Journal of Environmental Management, 172, 129–135.
Chen CL, Hung SW, Lee JY, 2010. Design of Inter-Plant Water Network with Central and Decentralized Water Mains. Computers & Chemical Engineering, 34(9), 1522–1531.
Chen JY, Dimitrov S, Pun H, 2019. The impact of government subsidy on supply Chains' sustainability innovation. Omega, 86, 42-58,
Chew IML, Foo DCY, Ng BKS, 2010a. Flowrate Targeting Algorithm for Interplant Resource Conservation Network. Part 1: Unassisted Integration Scheme. Industrial Engineering & Chemistry Research, 49, 6439-6455.
Chew IML, Foo DCY, Ng BKS, 2010b. Flowrate Targeting Algorithm for Interplant Resource Conservation Network. Part 2: Assisted Integration Scheme. Industrial Engineering & Chemistry Research, 49, 6456-6468.
Chew IRM, Tan RR, Foo DCR, Chiu ASF, 2009. Game theory approach to the analysis of inter-plant water integration in an eco-industrial park, Journal of Cleaner Production, 17(18), 1611-1619.
Chhipi-Shrestha G, Rodriguez M, Sadiq R, 2019. Selection of sustainable municipal water reuse applications by multi-stakeholders using game theory. Science of the Total Environment, 650, 2512-2526.
Chin HH, Varbanov PS, Klemeš JJ, 2020a. Short Term Maintenance Tasks Scheduling with Pinch Methodology. Chemical Engineering Transactions, 78, 499-504.
Chin HH, Varbanov PS, Klemeš JJ, Lam HL, 2019. Application of Pinch aAnalysis to Opportunistic Maintenance Management. Chemical Engineering Transactions, 76, 535-540
Chin HH, Varbanov PS, Klemeš JJ, Liew PY, 2021a. Enhanced Cascade Table Analysis to target and design multi-constraint resource conservation networks. Computers & Chemical Engineering, 148, 107262.
Chin HH, Varbanov PS, Klemeš JJ, Wan-Alwi SR, 2021b. Total Site Material Recycling Network Design and Headers Targeting Framework with Minimal Cross-Plant Source Transfer. Computers & Chemical Engineering, 151, 107364.
Chin HH, Varbanov PS, Liew PY, Klemeš JJ, 2021c. Pinch-Based Targeting Methodology for Multi-Contaminant Material Recycle/Reuse. Chemical Engineering Science, 230, 116129.
Chin HH, Jia X, Varbanov PS, Klemeš JJ, Liu Z-Y, 2021d. Internal and Total Site Water Networks Design with Water Mains Using Pinch-Based and Optimisation Approaches. ACS Sustainable Chemistry & Engineering, 9(19), 6639-6658.

Chin HH, Jia X, Varbanov PS, Klemeš JJ, Wan-Alwi SR, 2021e. Targeting Flowrates and Concentrations in Internal or Total Site Water Mains for Single Contaminant. Chemical Engineering Transaction, 86, 895-900

Chin HH, Wang B, Varbanov PS, Klemeš JJ, Zeng M, Wang QW, 2020b. Long-term Investment and Maintenance Planning for Heat Exchanger Network Retrofit. Applied Energy, 279, 115713.

Dakwala M., Mohanty B., Bhargava R., 2009. A process integration approach to industrial water conservation: a case study for an Indian starch industry. Journal of Cleaner Production, 17, 1654–1662.

Dal-Mas M., Giarola S., Zamboni A., Bezzo F., 2011. Strategic design and investment capacity planning of the ethanol supply chain under price uncertainty. Biomass and Bioenergy, 35, 2059–71.

de Jonge B., Scarf PA, 2019. A review on maintenance optimisation. European Journal of Operational Research., 285(3), 805-824.

Dedopoulos I.T., Shah N., 1995. Preventive maintenance policy optimisation for multipurpose plant equipment. Computers & Chemical Engineering, European Symposium on Computer Aided Process Engineering,3-5, 19, 693–698.

den Hollander M.C., Bakker C.A., Hultink E.J., 2017. Product Design in a Circular Economy: Development of a Typology of Key Concepts and Terms. J of Industrial Ecology, 21, 517–525.

Do P., Vu H.C., Barros A., Bérenguer C., 2015. Maintenance grouping for multi-component systems with availability constraints and limited maintenance teams. Reliability Engineering & System Safety, 142, 56–67

Dong H, Zhang L, Geng Y, Li P, Yu C, 2021. New insights from grey water footprint assessment: An industrial park level, Journal of Cleaner Production, 285, 124915.

Drechsel J, Kimms A, 2010. Computing core allocations in cooperative games with an application to cooperative procurement. International Journal of Production Economics, 128, 310-321

Drechsel J, Kimms A, 2011. Cooperative lot sizing with transshipments and scarce capacities: solutions and fair cost allocations. International Journal of Production Research, 9(1), 2643-2668

El-Halwagi M.M., Gabriel F., Harell D., 2003. Rigorous Graphical Targeting for Resource Conservation via Material Recycle/Reuse Networks. Industrial Engineering Chemistry Research, 42, 4319–4328.

El-Halwagi MM, Gabriel F, Harell D, 2003. Rigorous Graphical Targeting for Resource Conservation via Material Recycle/Reuse Networks. Industrial & Engineering Chemistry Research, 42(19), 4319–4328.

El-Halwagi, MM (Ed.), 2006. Synthesis of mass exchange networks: A graphical approach, in: Process Systems Engineering, Process Integration. Academic Press, 87–136.

Ellen MacArthur Foundation, 2013. Towards the circular economy, Economic and business rationale for an accelerated transition. <https://www.ellenmacarthurfoundation.org/assets/downloads/publications/Ellen-MacArthur-FoundationTowards-the-Circular-Economy-vol.1.pdf> accessed 07.08.2020

Eurostat, 2018. Circular material use rate: calculation method. <ec.europa.eu/eurostat/documents/3859598/9407565/KS-FT-18-009-EN-N.pdf/b8efd42b-b1b8-41ea-aaa()-45e127ad2e3f> accessed 07.08.2020

Faccio M, Persona A, Sgarbossa F, Zanin G., 2014. Industrial maintenance policy development: A quantitative framework. International Journal of Production Economics, 147, 85–93.

Fadzil AFA, Wan-Alwi SR, Manan Z, Klemeš JJ, 2018. Industrial Site Water Minimisation via One-Way Centralised Water Reuse Header. Journal of Cleaner Production, 200, 174–187.

Fan X.Y., Klemeš J.J., Jia X., Liu Z.Y., 2019. An iterative method for design of total water networks with multiple contaminants. Journal of Cleaner Production, 240, 118098.

Foo D.C.Y., 2009. State-of-the-Art Review of Pinch Analysis Techniques for Water Network Synthesis. Industrial Engineering Chemistry Research, 48, 5125–5159.

Geissdoerfer M., Savaget P., Bocken N.M.P., Hultink E.J., 2017. The Circular Economy - A new sustainability paradigm?. Journal of cleaner production, 143. 757-768.

Geng Y., Fu J., Sarkis J., Xue B., 2012. Towards a national circular economy indicator system in China: an evaluation and critical analysis. Journal of Cleaner Production, 23(1), 216-224.

Gomes J.F.S., Queiroz E.M., Pessoa F.L.P., 2007. Design procedure for water/wastewater minimisation: single contaminant. Journal of Cleaner Production. 15, 474–485.

González JD, Rodríguez ES, 2007. A natural selection from the core of a TU game: the core-center. International Journal of Game Theory, 36, 27-46

Govindarajan V., 2018. Water pinch analysis : a review of recent peer-reviewed publications. Vatten, 3, 147–152

Hallale N., 2002. A new graphical targeting method for water minimisation. Advances in Environmental Research, 6, 377–390.

Haupt M., Vadenbo C., Hellweg S., 2017. Do we have the right performance indicators for the circular economy?: insight into the Swiss waste management system. Journal of Industrial Ecology, 21(3), 615-627.

He P, He Y, Xu H, 2019. Channel structure and pricing in a dual-channel closed-loop supply chain with government subsidy. International Journal of Production Economy, 213, 108-123

Herczeg G, Akkerman R, Hauschild MZ, 2018. Supply chain collaboration in industrial symbiosis networks. Journal of Cleaner Production, 171, 1058-1067

Idris M.M.M., 2016. Turnaround Maintenance Planning for a Network of Plants Using Mathematical Programming Model (masters). King Fahd University of Petroleum and Minerals, Dhahran, Saudi Arabia.

ISO 55000, 2014. Asset management — Overview, principles and terminology <https://www.iso.org/standard/55088.html> accessed 07.08.2020

Jacobsen NB, 2006. Industrial Symbiosis in Kalundborg, Denmark A Quantitative Assessment of Economic and Environmental Aspects, Journal of Industrial Ecology, 10, 1-2.

Jato-Espino D, Ruiz-Puente C, 2021. Bringing Facilitated Industrial Symbiosis and Game Theory together to strengthen waste exchange in industrial parks. Science of the Total Environment, 771, 145400.

Jiang W, Zhang Z, Deng C, Tang X, Feng X, 2019. Industrial park water system optimisation with joint use of water utility sub-system, Journal of Cleaner Production, 147, 119-127.
Jin Y, Tang Z, Zhou Q, Zeng H, Mo S, 2020. A government value compensation model of waste recycling in an industrial park: A game theory approach. Journal of Cleaner Production, 275, 122976.
Jóźwiak I.J., 1997. An introduction to the studies of reliability of systems using the Weibull proportional hazards model. Microelectronics Reliability, 37, 915–8.
Kalmykova Y., Sadagopan M., Rosad, L., 2018. Circular economy – From review of theories and practices to development of implementation tools. Resources, Conservation and Recycling, 135, 190–201.
Kirchherr J., Reike D., Hekkert M., 2017. Conceptualising the circular economy: An analysis of 114 definitions. Resources, Conservation and Recycling, 127, 221-232.
Klemeš J.J., Varbanov P.S., Walmsley T.G., Jia X., 2018. New directions in the implementation of Pinch Methodology (PM). Renewable and Sustainable Energy Reviews, 98, 439–468.
Komonen K., 2008. A Strategic Asset Management Model: A framework of a plant level model for strategic choices and actions. Proceedings of Euromaintenance 2008 Conference on asset management & production reliability, Brussel, 8 - 10 April 2008, pp. 1-10.
Laggoune R., Chateauneuf A., Aissani D., 2009. Opportunistic policy for optimal preventive maintenance of a multi-component system in continuous operating units. Computers & Chemical Engineering, 33, 1499–1510.
Lal N.S., Walmsley T.G., Walmsley M.R.W., Atkins M.J., Neale J.R., 2018. A novel Heat Exchanger Network Bridge Retrofit method using the Modified Energy Transfer Diagram. Energy, 155, 190–204.
Lambert R.S.C, Maier S., Shah N., Polak J.W.,2016. Optimal phasing of district heating network investments using multistage stochastic programming. International Journal of Sustainable Energy Planning and Management, 9, 57–74.
Li AH, Fan X.Y., Klemeš, J.J., Liu Z.Y., 2017. Concentration potential concepts: Powerful tools for design of water-using networks with multiple contaminants. Journal of Cleaner Production 165, 254–261.
Liao ZW, Wu JT, Jiang BB, Wang JD, Yang YR, 2007. Design methodology for flexible multiple plant water networks. Industrial Engineering & Chemistry Research, 46(14), 4954-4963
Lim S-R, Park JM, 2010. Interfactory and intrafactory water network system to remodel a conventional industrial park to a green eco-industrial park. Industrial Engineering & Chemistry Research, 49(3), 1351-1358.
Linnhoff B., Townsend D.W., Boland D., Thomas B.E.A., Guy A.R., Marsland R.H., 1982, A user guide on process integration for the efficient use of energy (2nd ed). IChemE, Rugby, UK.
Liu H., Ren L., Zhuo H., Fu S., 2019. Water Footprint and Water Pinch Analysis in Ethanol Industrial Production for Water Management. Water, 11, 518.
Liu L, Wang J, Song H, Du J, Yang F, 2017. Multi-period water network management for industrial parks considering predictable variations. Computers & Chemical Engineering, 104, 172-184.

Liu S, Papageorgiou LG., 2013. Multi-objective optimisation of production, distribution and capacity planning of global supply chains in the process industry. Omega, 41, 369–82.
Liu Z.Y., Yang Y., Wan L.Z., Wang, X., Hou, K.H., 2009. A heuristic design procedure for water-using networks with multiple contaminants. AIChE Journal, 55, 374–382.
Lozano S, Moreno P, Adenso-Díaz B, Algaba E, 2013. Cooperative game theory approach to allocating benefits of horizontal cooperation, European Journal of Operational Research, 229(2), 444-452.
Mabitla S.S., Majozi T., 2019. A hybrid method for synthesis of integrated water and regeneration networks with variable removal ratios. Journal of Environmental Management, 231, 666–678.
Manan ZA, Tan YL, Foo DCY, 2004. Targeting the Minimum Water Flow Rate Using Water Cascade Analysis Technique. AIChE Journal, 50(12), 3169–3183.
Mann, J.G., Liu, Y.A., 1999. Industrial Water Reuse and Wastewater Minimization. McGraw Hill Professional, NY, USA.
Manne, M. G. A. S.,1967. Investments for Capacity Expansion: Size, Location and Time-phasing. Studies in the Economic Development of India, 77,614–6.
Mayer A., Haas W., Wiedenhofer D., Krausmann F., Nuss P., Blengini G. A., 2019. Measuring Progress towards a Circular Economy: A Monitoring Framework for Economy-wide Material Loop Closing in the EU28. Journal of Industrial Ecology, 23(1), 62-76
Megow N., Möhring R.H., Schulz J., 2010. Decision Support and Optimisation in Shutdown and Turnaround Scheduling. INFORMS Journal on Computing, 23, 189–204.
Milios L., 2018. Advancing to a Circular Economy: three essential ingredients for a comprehensive policy mix. Sustain Sci, 13, 861–878.
Mohammadnejad S., Bidhendi G.R.N., Mehrdad, N., 2011. Water pinch analysis in oil refinery using regeneration reuse and recycling consideration. Desalination, 265, 255–265.
Monstastruc L, Boix M, Pibouleau L, Azzaro-Pantel C, Domenech S, 2013. On the flexibility of an eco-industrial park (EIP) for managing industrial water. Journal of Cleaner Production, 43, 1-11.
Morseletto P., 2020. Targets for a circular economy. Resources Conservation and Recycling, 153, 104553.
Munguía-López ADC, Sampat AM, Rubio-Castro E, Ponce-Ortega JM, Zavala VM, 2019. Fairness-guided design of water distribution networks for agricultural lands, Computers & Chemical Engineering, 130, 106547.
Murray A., Skene K., Haynes K., 2017. The Circular Economy: An Interdisciplinary Exploration of the Concept and Application in a Global Context. Journal of Business Ethics, 140, 369–380.
Nakamura S., Kondo Y., 2018. Toward an integrated model of the circular economy: Dynamic waste input–output. Resources, Conservation and Recycling, 139, 326-332.
Nash J, 1950. Equilibrium points in n-person games. Proceedings of the National Academy of Sciences, 36(1), 48-49.
Nemati-Amirkolaii K., Romdhana H., Lameloise M.L., 2019. Pinch Methods for Efficient Use of Water in Food Industry: A Survey Review. Sustainability, 11, 4492.

Nguyen D., Bagajewicz M., 2010. Optimisation of Preventive Maintenance in Chemical Process Plants. Industrial & Engineering Chemistry Research, 49, 4329–4339.
OECD, Environmental Outlook to 2050, 2021. <https://www.oecd.org/env/indicators-modelling-outlooks> [accessed 16/4/2021]
Olesen S.G., Polley G.T., 1997. A Simple Methodology for the Design of Water Networks Handling Single Contaminants. Chemical Engineering Research and Design, 75, 420–426.
Pereira S., Ferreira P., Vaz A.I.F, 2017. Generation expansion planning with high share of renewables of variable output. Applied Energy, 190,1275–88
Potting J., Hekkert M.P., Worrell E., Hanemaaijer A., 2017. Circular Economy: Measuring Innovation in the Product Chain, 2544, PBL Environmental Assessment Agency, Netherland.
Ramin E, Bestuzheva K, Gargalo CL, Ramin D, Carina S, Ramin P, Flores-Alsina X, Andersen MM, Gernaey KV, 2021. Incremental design of water symbiosis networks with prior knowledge: The case of an industrial park in Kenya. Science of the Total Environment, 751, 141706.
Redlarski G, Krawczuk M, Kupczyk A, Piechocki J, Ambroziak D, Palkowski A., 2017. Swarm-Assisted Investment Planning of a Bioethanol Plant. Pol J Environ Stud, 26,1203–14.
Sahinidis NV, Grossmann IE, Fornari RE, Chathrathi M.,1989. Optimisation model for long range planning in the chemical industry. Computers & Chemical Engineering, 13,1049–63.
Sahinidis NV, Grossmann IE.,1991. Multiperiod investment model for processing networks with dedicated and flexible plants. Industrial Engineering Chemistry Research, 30, 1165–71.
Schmeidler D, 1969.The nucleolus of a characteristic function game. SIAM Journal of Applied Mathematics, 17, 1163-1170
Seider WD, Lewin DR, Seader JD, Widagdo S, Gani R, Ng KM, 2016. Product and Process Design Principles: Synthesis, Analysis and Evaluation, Fourth Edition, Wiley: New York, USA.
Shapley LS, 1953. A value for n-person games. Annals of Mathematics Studies, 28, 307-317
Shapley LS, 1971. Cores of convex games. International Journal of Game Theory, 1(1), 1971, 11-26.
Skouteri G., Ouki S., Foo D., Saroj D., Altini M., Melidis P., Cowley B., Ells G., Palmer S., O'Dell S., 2018. Water footprint and water pinch analysis techniques for sustainable water management in the brick-manufacturing industry. J of Cleaner Production, 172, 786–794.
Stackelberg HV, 1952. The theory of the market economy. Oxford University Press, Oxford, UK.
Tan R.R., Aziz M.K.A., Ng D.K.S., Foo D.C.Y., Lam H.L., 2016. Pinch analysis-based approach to industrial safety risk and environmental management. Clean Technologies and Environmental Policy, 18, 2107–2117.
Tan Y.L., Foo D.C.Y., Tan R.R., 2007. Approximate Graphical Targeting for Water Network with Two Contaminants, in: 10th Process Integration, Modeling and Optimisation for Energy Saving and Pollution Reduction (PRES 2007), Ischia, Italy.

Tian J.R., Zhou P.J., Lv B., 2008. A process integration approach to industrial water conservation: A case study for a Chinese steel plant. Journal of Environmental Management, 86, 682–687.

Tijs SH, Driessen TSH, 1986. Game theory and cost allocation problems. Management Science, 32, 1015-1028.

Tiu BTC, Cruz DE, 2017. An MILP model for optimizing water exchanges in eco-industrial parks considering water quality. Resources, Conservation and Recycling, 119, 89-96.

Tseng T.L. (Bill), Hvolby, H.H., Fraser, K., 2015. Maintenance management models: a study of the published literature to identify empirical evidence: A greater practical focus is needed. Int J Qual & Reliability Mgmt, 32, 635–664.

Tura N., Hanski J., Ahola T., Ståhle M., Piiparinen S., Valkokari P., 2019. Unlocking circular business: A framework of barriers and drivers. Journal of Cleaner Production, 212, 90-98.

UNEP, The United Nations World Water Development Report, 2019. United Nations Educational, Scientific and Cultural Organization, Paris, France, ISBN: 978-92-3-100309-7

Valkokari P., Hanski J., Ahonen T., 2017. Impact of maintenance on circular economy, in: Proceedings of the 2nd Annual SMACC Research Seminar 2017. Presented at the Annual SMACC Research Seminar 2017, Tampere University of Technology, pp. 20–23.

Vilarinho S., Lopes I., Oliveira J.A., 2017. Preventive Maintenance Decisions through Maintenance Optimisation Models: A Case Study. Procedia Manufacturing,11,1170–7.

Wang B, Klemeš JJ, Varbanov PS, Chin HH, Wang Q-W, Zeng M., 2020. Heat exchanger network retrofit by a shifted retrofit thermodynamic grid diagram-based model and a two-stage approach. Energy, 198,117338.

Wang K., Djurdjanovic D., 2018. Joint Optimisation of Preventive Maintenance, Spare Parts Inventory and Transportation Options for Systems of Geographically Distributed Assets. Machines, 6, 55.

Wang YP, Smith R, 1994. Wastewater Minimisation. Chemical Engineering Science, 49 (7), 981–1006.

Wickart M., Madlener R., 2007. Optimal technology choice and investment timing: A stochastic model of industrial cogeneration vs. heat-only production. Energy Economics, 29, 934–52.

Wiesner A, Schlegel M, Oldenburg J, Würth L, Hannemann R, Polt A., 2008 Model-based investment planning model for step-wise capacity expansions of chemical plants. In: Braunschweig B, Joulia X (Eds). Computer Aided Chemical Engineering, 25, 307–12.

Xu J, Hou S, Xie H, Lv C, Yao L, 2018. Equilibrium approach towards water resource management and pollution control in coal chemical industrial park. Journal of Environmental Management, 219, 56-73.

Yazdi M, Nedjati A, Abbassi R., 2019. Fuzzy dynamic risk-based maintenance investment optimisation for offshore process facilities. Journal of Loss Prevention in the Process Industries,57, 194–207.

Zhang X., Shahidehpour M., Alabdulwahab A., Abusorrah A., 2015. Optimal Expansion Planning of Energy Hub With Multiple Energy Infrastructures. IEEE Trans on Smart Grid, 6, 2302–11.

Zhao H.P., Yang Y., Liu Z.Y., 2019. Design of heat integrated water networks with multiple contaminants. Journal of Cleaner Production. 211, 530–536.

APPENDICES

A: Derivation of freshwater target equation in Chapter 3

Given a process that has several water-using operations, with a set of water sinks $j \in \boldsymbol{J}, |J| = N_{sinks}$ and water sources $i \in \boldsymbol{I}, |I| = N_{source}$ (Figure A1) are available. Each sink 'j' requires a flowrate F_{SKj} with maximum allowable concentration ($Z_{k,SKj}$) of different species $k \in \boldsymbol{K}, |k| =$ No. of contaminants, i.e. $Z_{SKj}^{\max} = (Z_{1,SKj}, Z_{2,SKj} \dots Z_{K,SKj})$. The set of process sources can be recycled or reused to fulfil the sinks. Similarly, each source has a given flowrate F_{SRi} with the composition of different contaminants ($C_{k,SRi}$), i.e. $C_{SRi} = (C_{1,SRi}, C_{2,SRi} \dots C_{K,SRi})$. An external fresh resource with flowrate F_{FW} is available to supplement the use of internal sources. The fresh resource is also composed of contaminants with concentration ($C_{k,FW}$), i.e. $C_{FW} = (C_{1,FW}, C_{2,FW} \dots C_{K,FW})$.

The typical source-sink allocation model of the water network presented in Figure 3-1 gives rise to four governing equations – Eqs (A1)-(A4). The problem maps to an optimisation formulation. Its objective function is expressed in Eq (A1), which stipulates the minimisation of the total required freshwater, which is the freshwater target.

Eqs (A2) and (A3) express the mass balances for sources and sinks, while Eq (A4) represents the contaminant constraints for individual sinks. Note that as proven by El-Halwagi et al. (2003), the composition of the sink should represent the maximum contaminant concentration to minimise the use of a fresh resource. These equations are crucial for understanding the model characteristics to derive the proper procedures for obtaining the optimal freshwater target.

$$Min\ F_{FWT} = \sum_j F_{Fw,SKj} \tag{A1}$$

$$F_{SRi} = \sum_j F_{SRi,SKj} + F_{SRi,WW} \quad \forall \text{ i} \tag{A2}$$

$$F_{SKj} = \sum_i F_{SRi,SKj} + F_{Fw,SKj} \quad \forall \text{ j} \tag{A3}$$

$$\sum_i F_{SRi,SKj} C_{k,SRi} + F_{Fw,SKj} C_{k,Fw} \leq F_{SKj} Z_{k,SKj} \quad \forall \text{ j } \forall \text{ k} \tag{A4}$$

Where F_{FWT} represents the total freshwater flowrate, $F_{Fw,SKj}$ is freshwater to sink 'j' flowrate, F_{SRi} is source 'i' flowrate, $F_{SRi,SKj}$ is source 'i' to sink 'j' flowrate, $F_{SRi,WW}$ is source 'i' to waste flowrate, F_{SKj} is the sink 'j' flowrate, $C_{k,SRi}$ is the concentration of contaminant 'k' in source 'i', $C_{k,Fw}$ is the concentration of contaminant 'k' in freshwater, and $Z_{k,SKj}$ is the concentration of contaminant 'k' in sink 'j'.

Taking one of the $F_{SRis,SKj}$ ($i=i_s$) out from Eq(A3) and inequality (A4) become:

$$F_{SKj} = \sum_{i=1}^{i_s-1} F_{SRi,SKj} + F_{SRi_s,SKj} + \sum_{i_s+1}^{I} F_{SRi,SKj} + F_{Fw,SKj} \quad \forall \text{ j} \tag{A5}$$

$$\sum_{i=1}^{i_s-1} F_{SRi,SKj} C_{k,SRi} + F_{SRi_s,SKj} C_{k,SRi_s} + \sum_{i_s+1}^{I} F_{SRi,SKj} C_{k,SRi} + F_{Fw,SKj} C_{k,Fw} \leq F_{SKj} Z_{k,SKj} \quad \forall \text{ j } \forall \text{ k} \tag{A6}$$

$F_{SRis,SKj}$ represents the reference source. Now replace the term $F_{SRis,SKj}$ in inequality (A4) by substituting Eq(A5):

$$\sum_{i=1}^{i_s-1} F_{SRi,SKj}C_{k,SRi} + \left(F_{SKj} - \sum_{i=1}^{i_s-1} F_{SRi,SKj} - \sum_{i_s+1}^{I} F_{SRi,SKj} - F_{Fw,SKj}\right)C_{k,SRi_s} + \sum_{i_s+1}^{I} F_{SRi,SKj}C_{k,SRi} + F_{Fw,SKj}C_{k,Fw} \le F_{SKj}Z_{k,SKj} \quad \forall \text{ j } \forall \text{ k} \tag{A7}$$

Move $F_{Fw,SKj}$ to the left hand side of inequality (A7)

$$F_{Fw,SKj}\left(C_{k,Fw} - C_{k,SRi_s}\right) \le \sum_{i=1}^{i_s-1} F_{SRi,SKj}\left(C_{k,SRis} - C_{k,SRi}\right) + \sum_{i_s+1}^{I} F_{SRi,SKj}\left(C_{k,SRis} - C_{k,SRi}\right) + F_{SKj}(Z_{k,SKj} - C_{k,SRi_s}) \quad \forall \text{ j } \forall \text{ k} \tag{A8}$$

As $\left(C_{k,Fw} - C_{k,SRi_s}\right)$ is less than zero, changing its order becomes:

$$-F_{Fw,SKj}\left(C_{k,SRi_s} - C_{k,Fw}\right) \le \sum_{i=1}^{i_s-1} F_{SRi,SKj}\left(C_{k,SRis} - C_{k,SRi}\right) + \sum_{i_s+1}^{I} F_{SRi,SKj}\left(C_{k,SRis} - C_{k,SRi}\right) + F_{SKj}(Z_{k,SKj} - C_{k,SRi_s}) \tag{A9}$$

Divide both side with $-\left(C_{k,Fw} - C_{k,SRi_s}\right)$:

$$F_{Fw,SKj} \ge \sum_{i=1}^{i_s-1} F_{SRi,SKj}\left[-\frac{\left(C_{k,SRi_s} - C_{k,SRi}\right)}{\left(C_{k,SRi_s} - C_{k,Fw}\right)}\right] + \sum_{i_s+1}^{I} F_{SRi,SKj}\left[-\frac{\left(C_{k,SRi_s} - C_{k,SRi}\right)}{\left(C_{k,SRi_s} - C_{k,Fw}\right)}\right] + F_{SKj}\left[-\frac{Z_{k,SKj} - C_{k,SRi_s}}{\left(C_{k,SRi_s} - C_{k,Fw}\right)}\right] \quad \forall \text{ j } \forall \text{ k} \tag{A10}$$

$$F_{Fw,SKj} \ge \sum_{i=1}^{i_s-1} F_{SRi,SKj}\left[-\frac{\left(\left(C_{k,SRi_s} - C_{k,Fw}\right) - \left(C_{k,SRi} - C_{k,Fw}\right)\right)}{\left(C_{k,SRi_s} - C_{k,Fw}\right)}\right] + \sum_{i_s+1}^{I} F_{SRi,SKj}\left[-\frac{\left(\left(C_{k,SRi_s} - C_{k,Fw}\right) - \left(C_{k,SRi} - C_{k,Fw}\right)\right)}{\left(C_{k,SRi_s} - C_{k,Fw}\right)}\right] + F_{SKj}\left[-\frac{Z_{k,SKj} - C_{k,Fw} - \left(C_{k,SRi_s} - C_{k,Fw}\right)}{\left(C_{k,SRi_s} - C_{k,Fw}\right)}\right] \quad \forall\, j \ \forall\, k \tag{A11}$$

Finally the freshwater target for SKj becomes. $F_{SRis,SKj}$ can be included in here because based on Eq(A9), $\left(C_{k,SRi_s} - C_{k,SRi}\right) = 0$ when $i=i_s$

$$F_{Fw,SKj} \geq \sum_{i=1}^{I} F_{SRi,SKj}\left[\frac{(C_{k,SRi}-C_{k,Fw})}{(C_{k,SRi_s}-C_{k,Fw})}-1\right] + F_{SKj}\left[1-\frac{(Z_{k,SKj}-C_{k,Fw})}{(C_{k,SRi_s}-C_{k,Fw})}\right] \quad \forall j \ \forall k \tag{A12}$$

The freshwater target for SKj in Eq(A12) is the largest amount required for all contaminant 'k'. Each contaminant level requires different amount of freshwater, but the largest value indicates the exact required freshwater for the SKj. Eq(A13) becomes:

$$F_{Fw,SKj} \geq \max_{k}\left[\sum_{i=1}^{I} F_{SRi,SKj}\left[\frac{(C_{k,SRi}-C_{k,Fw})}{(C_{k,SRi_s}-C_{k,Fw})}-1\right] + F_{SKj}\left[1-\frac{(Z_{k,SKj}-C_{k,Fw})}{(C_{k,SRi_s}-C_{k,Fw})}\right] \quad \forall j \right] \tag{A13}$$

Also, let's choose $C_{k,SRis}$ be the maximum source concentration for contaminant 'k', i.e. $C_{k,SRis} = C_{k,SRmax} = \max_{i}(C_{k,SRi})$. The reason the reference source concentration is chosen as the maximum amount is that it can be the normalisation constant for the coefficients of the sources flowrates in Eq(A13).

Since in Eq(A13), $F_{SRi,SKj}$ is a variable, the constant term $F_{SKj}\left[1-\frac{(Z_{k,SKj}-C_{k,Fw})}{(C_{k,SRi_s}-C_{k,Fw})}\right]$ governs the sources to be allocated to the sink. If this constant term is the largest for contaminant 'k', then SK_j is limitied by contaminant 'k'. In this case, $F_{FW,SKj}$ is likely to follow the prioritisation sequence for contamination level 'k'. Notice that for certain contaminant 'k', the cleaner sources are prioritised because the coefficients of the $F_{SRi,SKj}$ has larger negative values, which means that using the cleaner sources could reduce the minimum value of $F_{Fw,SKj}$. However, this can be traded-off by other contaminants due to different source arrangement.

The total freshwater target (F_{FWT}) then is the summation of all required freshwater for all sinks:

$$F_{FWT} = \sum_{j}^{J} F_{Fw,SKj} \tag{A14}$$

As different sinks are to follow different contaminant cascades (source arrangement), it means that the total target in Eq(A14) is the summation of all the freshwater in all contaminant cascades, i.e.:

$$F_{FWT} = \sum_{j\in jk1} F_{Fw,SKj} + \sum_{j\in jk2} F_{Fw,SKj} + \cdots + \sum_{j\in jK} F_{Fw,SKj} \tag{A15}$$

Where jk represents the set of sinks 'j' that belong to the contaminant cascade 'k', and the jk1, jk2,…,jK are all mutually exclusive sets.

B: Total Site synthesis model with headers for Section 4.3

The network synthesis model for either Internal or Site-level Water Integration is based on the can be solved with the mathematical optimisation approach. Figure B-1 shows the superstructure of the water network design with water headers for intra-process or site level. It consists of the schematic representation of the connections between water-using processes/units and water mains/header. The mathematical formulation is presented in the following sub-sections.

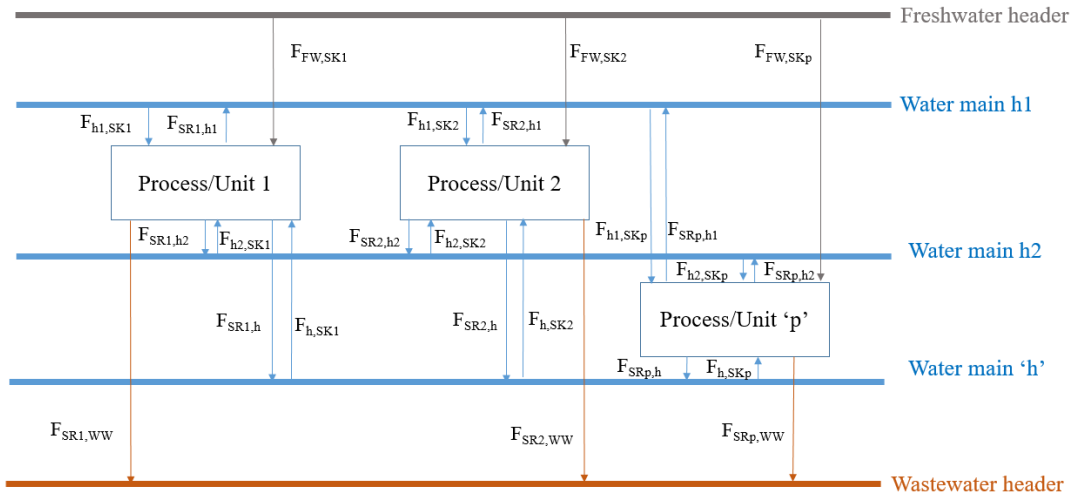

Figure **B-1**: Water headers/mains design for internal process level or site level

Mass balance constraints for internal water mains

The following equations denote the mass balance equations. Eq(B-1) specifies the mass sink balance for all sink 'j' - the summation of the water source from each header 'h' ($F_{h,SKj}$) with the freshwater ($F_{FW,SKj}$) equals to the flowrate of the sink (F_{SKj}). Eq(B-2) denotes the source mass balance for all source 'i', i.e. the summation of the water flow sent to each header 'h' by source 'i' ($F_{SRi,h}$) and the water sent to the wastewater header ($F_{SRi,WW}$) is equals to the flowrate of the source (F_{SRi}). Eq(B-3) specifies the mass balance around the headers. The total outlet water flow from header 'h' is equal to the total inlet water flow to header 'h', and the total water flow is equal to the header flowrate (F_h).

$$\sum_{h \epsilon H} F_{h,SKj} + F_{FW,SKj} = F_{SKj} \quad \forall j \tag{B-1}$$

$$\sum_{h \epsilon H} F_{SRi,h} + F_{SRi,WW} = F_{SRi} \quad \forall i \tag{B-2}$$

$$\sum_{j \epsilon J} F_{h,SKj} = \sum_{i \epsilon I} F_{SRi,h} = F_h \quad \forall h \tag{B-3}$$

The allocation of the sources must fulfil the contaminant limits as well. Eqs(B-4 and B-5) are formulated to ensure the maximum limits for contaminants are not violated.

$$\sum_{i\epsilon I} F_{SRi,h}\, C_{k,SRi} = F_h C_{k,h} \quad \forall k,h \tag{B-4}$$

$$\sum_{h\epsilon H} F_{h,SKj} C_{k,h} + F_{FW,SKj} C_{k,FW} \leq F_{SKj} Z_{k,SKj} \quad \forall k,j \tag{B-5}$$

Eq(B-4) specifies that for contaminant 'k', the load of the contaminants from all the sources sent to each header 'h' ($F_{SRi,h}C_{k,SRi}$), where $C_{k,SRi}$ is the concentration of contaminant 'k' for source 'i' is equal to the contaminant load inside header 'h' ($F_h C_{k,h}$), where $C_{k,h}$ is the concentration of contaminant 'k' in the water header 'h'. Eq(B-5) is formulated to ensure the maximum contaminant limit for the sink for each contaminant 'k' is not violated. The contaminant load from the header ($F_{h,SKj}C_{k,h}$) plus the contaminant load from the fresh resource $F_{FW,SKj}C_{k,FW}$ has to be equal or lower than the contaminant load of a sink $F_{SKj}Z_{k,SKj}$, where $C_{k,FW}$ and $Z_{k,SKj}$ are the respective concentration of contaminant 'k' in freshwater and sink 'j'.

Note that with a process that involves water gains and loss, the following water balance equation- Eq(B-6) for a unit is used to check the flowrates of the sink and source are satisfied.

$$F_{SKj} + F_{gain,j} = F_{SRi} + F_{loss,i} \quad \forall j \mid j = i \tag{B-6}$$

<u>Mass balance constraints for Total Site water mains</u>

The mass balance equations for Total Site water mains design are similar to the equations for internal water mains, but the extra source or sinks from another plant 'p' have to be considered.

$$\sum_{h\epsilon H} F_{h,p,SKj} + F_{FW,p,SKj} + \sum_{i\epsilon I} F_{p,SRi,SKj} = F_{p,SKj} \quad \forall j,p \tag{B-7}$$

$$\sum_{h\epsilon H} F_{p,SRi,h} + F_{p,SRi,WW} + \sum_{j\epsilon J} F_{p,SRi,SKj} = F_{p,SRi} \quad \forall i,p \tag{B-8}$$

$$\sum_{p\epsilon P} \sum_{j\epsilon J} F_{h,p,SKj} = \sum_{p\epsilon P} \sum_{i\epsilon I} F_{p,SRi,h} = F_h \quad \forall h \tag{B-9}$$

Eq(B-7) specifies the mass balance for all sinks 'j' for a specific process 'p'- the summation of the water from each header 'h' ($F_{h,p,SKj}$), the freshwater ($F_{FW,p,SKj}$), and the internal source 'i' from process 'p' itself ($F_{p,SRi,SKj}$) equals to the flowrate of the sink ($F_{p,SKj}$). Eq(B-8) denotes the source mass balance for all source 'i' and process 'p', i.e. the summation of the

water flow sent to each header 'h' by source 'i' from process 'p' ($F_{p,SRi,h}$), the water sent to the wastewater header ($F_{p,SRi,WW}$), and the internal recycling of source 'i' to all sinks in the process 'p' itself ($F_{p,SRi,SKj}$) is equals to the flowrate of the source ($F_{p,SRi}$). Eq(B-9) specifies the mass balance around the headers. The total outlet water flow from header 'h' is equal to the total inlet water flow to header 'h', and the total water flow is equal to the header flowrate (F_h).

Eqs(B-10 to B-11) are formulated to ensure the maximum limits for contaminants are not violated, similar to the single contaminant case.

$$\sum_{p\in P}\sum_{i\epsilon I} F_{p,SRi,h}\, C_{k,p,SRi} = F_h C_{k,h} \quad \forall k,h \tag{B-10}$$

$$\sum_{h\epsilon H} F_{h,p,SKj} C_{k,h} + \sum_{i\in I} F_{p,SRi,SKj} C_{k,p,SRi} + F_{FW,p,SKj} C_{k,FW} \leq F_{p,SKj} Z_{k,p,SKj} \quad \forall k,j,p \tag{B-11}$$

Note that the model specified Eqs(B-7 to B-11) allow the options for internal process recycling, along with the water use by the headers. If only headers are allowed, the term $F_{p,SRi,SKj}$ can be removed.

Objective functions

In this work, two objective functions are specified to investigate the sets of solutions produced. The first objective function is the minimisation of fresh resource usage, as denoted in Eq(B-12). This is coherent with the solutions from the Pinch-based approach as it targets the minimum freshwater requirements.

$$Obj = \min F_{FW,T} = \min \sum_{p\in P}\sum_{j\epsilon J} F_{FW,p,SKj} \text{ or } \min \sum_{j\epsilon J} F_{FW,SKj} \tag{B-12}$$

To identify the solutions that have the optimal cost performance, the Total Annualised Cost (TAC) is used as another criterion to be minimised- see Eq(B-13). Eq(B-14) shows the formulation of the TAC estimation equation. In this work, the covered capital cost is the cost for piping connection (Cap_{piping}), the cost for building the water header/mains (Cap_{mains}) and cost for purchasing the pumps (Cap_{pump}), for which all are multiplied with annualised factor (AF). The operating cost included the cost of purchasing fresh resources, wastewater treatment cost, and the electricity cost dedicated to pumping power requirements. The unit price for each of the operational cost is assumed constant and known, i.e. UP_{FW}, UP_{WW} and UP_{elec}. The operating cost is then converted to annual cost using the specified annual operating hours: Op.

$$Obj = \min TAC \tag{B-13}$$

$$TAC = \left(Cap_{piping} + Cap_{mains} + Cap_{pump}\right)AF + \left(UP_{FW}\left(F_{FW,T}\right) + UP_{WW}\left(F_{WW,T}\right) + UP_{elec}Elec\right)Op \quad \text{(B-14)}$$

$$AF = \frac{IR}{1-(1+IR)^{-n_{life}}} \quad \text{(B-15)}$$

Overall, the internal water main design model is formulated with either objective function Eq(B-12) or Eq(B-13), subject to the constraints of Eqs(B-1 to B-5). For the Total Site model, similar equations for the objective functions can be used but subjected to constraints Eqs(B-7 to B-11). The main variables to be identified are (a) Flowrates allocated to headers, (b) concentration of headers, (c) number of headers, (d) Flowrates recycled internally (for Total Site model). Note that the model is a Non-Linear Programming (NLP) due to the bilinear terms in the water header calculations, where both flowrates (F_h) and its concentration ($C_{k,h}$) are variables. The computation of the capital cost for piping, water heater, and pumps are shown below.

The computation of capital cost for pumps is based on Seider et al. (2016). It is assumed in this work that each piping connection connecting the source and sink requires a single pump. The equations below explain the computation of the pumping capital cost. Eq(B-16) require the calculation of the size factors for the pumps. The head range for the pump is from 50-200 ft, which in this work, the pump head is assumed as 175 ft. Eq(B-17) is the base cost for purchasing the pumps (in 2002), multiplied by the material factor (F_m) and pump type factor (F_t). The value of F_m used in this work is 2.0 for stainless steel, and F_t used is 1.50. The base cost is multiplied by the Chemical Engineering Index (CEPCI). The CEPCI in 2002 is 396 (Turton et al., 2018), and the CEPCI in 2019 is 607.5 (Chemical Engineering, 2019). Eq(B-18) is the total purchase cost for the pump for the water eco-industrial park.

$$S_{p,i,j,p'} = Q_{p,i,j,p'}H_{pump}^{0.5} \quad \text{(B-16)}$$

$$Cap_{pump_{p,i,j,p'}} = F_M F_t \left(e^{12.1656 - 1.1448\log\left(S_{p,i,j,p'}\right) + 0.0862\left(\log\left(S_{p,i,j,p'}\right)\right)^2}\right)\left(\frac{CEPCI_{2019}}{CEPCI_{2002}}\right) \quad \text{(B-17)}$$

$$Cap_{pump} = \sum_{h\in H, p\in P, j\in J, p'\in P} Cap_{pump_{p,,i,j,p'}} \quad \text{(B-18)}$$

Where $S_{p,i,j,p'}$ is the pump size factors for the piping connection correspond to the flowrates of the water sources. $Q_{p,i,j,p'}$ is the volumetric flowrates of the water sources in gal/min. H_{pump} represents the head of the pump. The unit for capital cost is in dollars ($).

(i) Capital cost for piping

The cost for the piping is dependent on the selection of the diameter of the pipes, which is dependent on the velocity of the water flows. To ensure the feasible flow of the water, it is recommended the water velocity should be between 1-2 m/s. The diameters for the pipes are estimated using Eq(B-19) – see (USDA, 2020).

$$D = \left[\frac{0.408\,Q}{V}\right]^{0.5} \tag{B-19}$$

Where D is the diameter of the pipe, Q is the volumetric flowrate of the water flow in gal/min, and V is the velocity of the water inside the pipe in ft/s. For conservative design, the velocity of the water is set as 5.5 ft/s. The unit price for the pipes is presented in Table S1.

Table B-1: Unit price of piping for different pipe diameters (Bütün et al., 2019)

D_{pipe} (mm)	20	40	80	100	200	300	400	500	600	800	1,000	1,500
Price/length, C_{pipe} (€/m)	96	166	312	387	775	1,180	1,588	2,008	2,434	3,304	4,192	6,474

As the selection of pipes is a discrete selection, the binary variables $x_{h,p,j,s}, x_{p,i,h,s}, x_{p,i,j,s}$ are introduced to denote the selection of the pipe size, $d \in D$. Eqs(B-20-B-21) indicate the constraints introduced into the optimisation model.

$$D_{p,i,j,p'} = \left[\frac{0.408\,Q_{p,i,j,p'}}{V_{p,i,j,p'}}\right]^{0.5} \tag{B-20}$$

$$D_{p,i,j,p'} - \frac{D_{pipe_S}}{1000} \leq M(1 - x_{p,i,j,p',d}) \tag{B-21}$$

$$F_{p,i,j,p'} \leq M \sum_{d\in D}\left(x_{p,i,j,p',d}\right) \tag{B-22}$$

$$\sum_{d\in D}\left(x_{p,i,j,p',d}\right) \leq 1 \tag{B-23}$$

Eq(B-21) ensures that the selection of the pipe must be larger than the calculated pipe diameter. The binary variables are forced to be zero when the selection of pipe is shorter than the calculated pipe sizes. Eq(B-22) enforces that the pipe is selected when only non-zero water flows exist. It also enforces that when there is a water flow, the pipes must be selected. Eq(B-23) ensures that only a single pipe or none (when zero flows) are selected. The total capital cost for the piping is computed with Eq(B-24).

The big 'M' in Eqs(B-21 to B-22) can be set as the maximum values of the source flowrates. However, in this study, we assume no maximum values for the flowrates, so we set M = 1,000 for all Eqs(B-21) and all case studies. As for Eqs(B-22), we set higher M=10,000 because the diameter is in mm, and the highest diameter is 1,500 mm.

$$Cap_{piping} = \sum_{p\in P, i\in I, j\in J, d\in D, p'\in P}\left(x_{p,i,j,p',d} C_{pipe_d}\right) \quad \text{(B-24)}$$

C: Optimisation results for Section 4.3

C1: Single Contaminant

Internal Process headers. Table C-1 shows the comparison of the results. If the cost is considered as the criterion, it indicates that 4 headers (excludes freshwater and wastewater headers) yield the solution with the optimum cost, 2.80 M$/y (see the column with H=4) compared to other header design options. It is due to the capital cost is more expensive than the freshwater and wastewater cost to some extent, and building more internal water mains could reduce the number of piping connections. Beyond the specification of H>4, the optimal TAC increases as the piping, pumps and water mains cost become higher. However, the optimum no. of headers for the objective of minimising the fresh resource usage remains as 3. The direct integration scheme cost lesser (2.55 M$/y) compared to the header design because no cost is required for building the water main. It is also because, for direct integration, a single pump is required for a single pipeline connection, i.e. one pump per transfer from source to sink. However, in the header design, one pump is required to transfer water from the source to the header, and another pump to transfer water from the header to the sink. This assumption causes additional cost for the process.

Total Site Headers. For the Total Site water headers design, all the individual sources and sinks are grouped together to form the site Composite Curves. This is to determine the overall freshwater target for the industrial site. Figure C-1 shows the Composite Curves representation for the Total Site. The overall freshwater target for the site is identified as 765.69 t/h. A similar headers design procedure is applied to the Composite Curves. The result shows that at least 3 headers from the water sources are required to fulfil the overall fresh resource target.

Notice that this approach assumes that no internal recycling before the Total Site headers design. The solutions obtained directly from this approach may require an unnecessary header, e.g. source from Plant 1 is sent to the header, and the water from the header is sent back to plant 1. If internal recycling is allowed, the number of headers required for the system is at least 2 (one below the Site Pinch Point and one above the Site Pinch Point).

Using the same data and method from Fadzil et al. (2018), the total freshwater target achieved is 830.46 t/h with two headers. However, their work considers the uneven mixing of the sources in the header, and they assume the headers flow in a certain sequence. They also

fixed the number of headers and the range of the concentration level in the headers prior to performing optimisation or Pinch Analysis.

Table C-1: Results comparison using a different approach for internal water mains design-plant 1 for a single contaminant case. The optimal number of headers exclude freshwater and wastewater headers

	Objectives	Direct integration	Header design			
			Graphical Approach	Optimisation Approach		
				H = 1	H = 2	H = 3	H = 4
Freshwater requirement (t/h)	F_{FWT}	206.7	206.7	302.4	240.6	206.7	206.7
	Cost	206.7	-	302.4	258.8	234.8	221.9
Wastewater requirement (t/h)	F_{FWT}	206.7	206.7	302.4	240.6	206.7	206.7
	Cost	206.7	-	302.4	258.8	234.8	221.9
TAC (M$/y)	Cost	2.55	-	3.72	3.24	2.94	2.80
Optimal No. of headers	F_{FWT}	-	3	1	2	3	3
	Cost	-	-	1	2	3	4

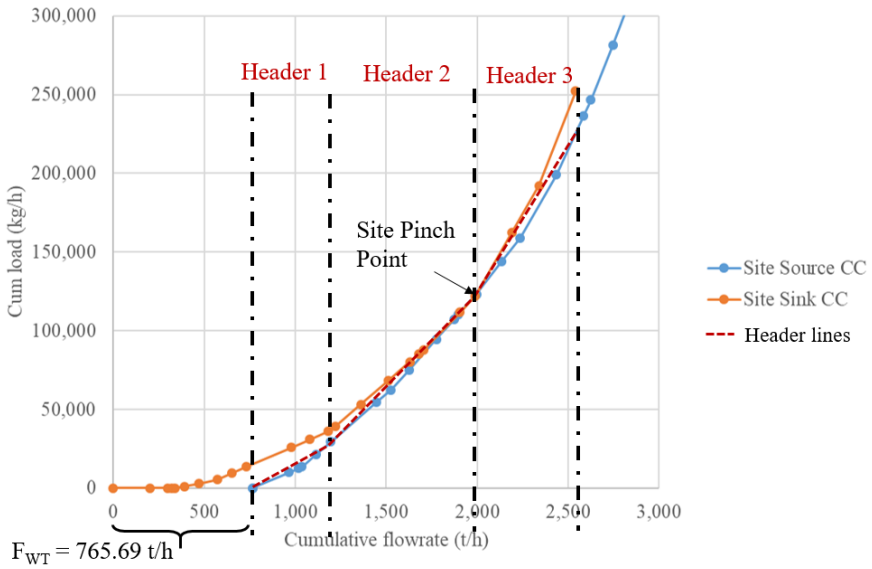

Figure C-1: Total Site water mains design using Composite Curves for a single contaminant case

Table C-2 shows a comparison of the results of each approach. For the mathematical approach, the options for internal source recycling within processes are allowed. Notice that the model with headers only set the internal source recycling flowrates to be zero, i.e. $F_{p,SRi,SKj} = 0$. The optimal number of headers considering just headers design is 3, which is consistent with the solutions obtained using the graphical approach. However, if the internal

recycling option is allowed, the optimum number of headers required is just 2 (exclude freshwater and wastewater headers) to reach the overall freshwater target of 765.96 t/h. If the cost criterion is used, the results show that only a single water header is to be used (adding the freshwater header and wastewater header, the total number of water main is 3) compromised with the additional freshwater requirement. This is due to the capital cost is more expensive than the operating cost. For direct integration, i.e. direct utilising sources between plants, is a more expensive scheme due to the high piping cost.

Table C-2: Results comparison using different approaches for Total Site water mains design- for a single contaminant case. The optimal no. of headers excludes freshwater and wastewater headers

	Objectives	Direct Integration	Header design		
			Graphical Approach	Optimisation Approach	
				Headers only	Internal recycling + Headers
Total Freshwater requirement (t/h)	F_{FWT} Cost	765.96 865.28	765.96 -	765.96 947.35	765.96 834.31
Total Wastewater requirement (t/h)	F_{FWT} Cost	765.96 865.28	765.96 -	765.96 947.35	765.96 834.31
TAC (M$/y)	Cost	72.2	-	16.4	12.9
Total No. of headers	F_{FWT} Cost	- -	≥ 2 -	3 1	2 1

C2: Multiple Contaminants

Internal Process Headers. If the cost is considered as the criterion, it indicates that only 1 header yields the solution with the optimum cost, 9.64 M$/y (see the column with H=1) compared to other header design options. It is due to the capital cost is more expensive than the freshwater and wastewater cost. The optimal TAC increases as the specification of the headers (H) is larger. However, the optimum no. of headers for the objective of minimising the fresh resource usage remains as 3. The direct integration scheme cost more (11.1 M$/y) compared to the header design because the distance between plants is higher than the distance from each plant to the site headers. In the direct integration scheme with optimal TAC, the freshwater flow is 1,019.14 t/h, while the freshwater flow for header design with optimal TAC is 1,020.39 t/h. This is due to the capital cost due to piping, water mains, and pumps cost more than the freshwater and wastewater cost. Table C-3 shows the results comparison.

Total Site Headers. *Table C-4* shows a comparison of the results of each approach. The overall fresh resource is identified as 2,075.05 t/h, using both the graphical approach or the mathematical approach for the direct integration scheme. For the mathematical approach, the options for internal source recycling within processes are allowed. Notice that the model with headers only set the internal source recycling flowrates to be zero, i.e. $F_{p,SRi,SKj} = 0$. It is

interesting to note that the optimal number of headers considering just headers design is 5 with freshwater target 2,074.23 t/h by setting freshwater as the objective. This is due to the computation difficulty due to the MINLP formulation for piping and pumps. However, if the internal recycling option is allowed, the optimum number of header required is just 2 to reach the overall freshwater target of 2,074.05 t/h. If the cost criterion is used, the results show that only a single water header is to be used, compromised with additional freshwater requirement (2,091.39 t/h). This is due to the capital cost is more expensive than the operating cost. For direct integration, i.e. direct utilising sources between plants, is a more expensive scheme due to the high piping cost with long distance between plants.

Table C-3: Results comparison using a different approach for internal water mains design-plant 2 for multiple contaminants case. The optimal no. of headers excludes freshwater and wastewater headers

	Objectives	Direct integration	Header design				
			Graphical Approach	Optimisation Approach			
				H = 1	H = 2	H = 3	H = 4
Freshwater requirement (t/h)	F_{FWT}	1,018.50	1,018.50	1,020.02	1,018.50	1,018.50	1,018.50
	Cost	1,019.14	-	1,020.39	1,020.56	1,019.01	1,040.21
Wastewater requirement (t/h)	F_{FWT}	248.50	248.50	250.02	248.50	248.50	248.50
	Cost	249.14	-	250.39	250.56	249.01	270.21
TAC (M$/y)	Cost	11.1	-	9.64	9.93	10.4	12.3
Optimal No. of headers	F_{FWT}	-	3	1	2	2	2
	Cost	-	-	1	2	3	4

Table C-4: Results comparison using a different approach for Total Site water mains design-for multiple contaminant case. The optimal no. of headers excludes freshwater and wastewater headers

	Objectives	Direct Integration	Header design		
			Graphical Approach	Optimisation Approach	
				Headers only	Internal recycling + Headers
Total Freshwater requirement (t/h)	F_{FWT}	2,074.05	2,074.05	2,074.23	2,074.05
	Cost	2,096.68	-	2,127.29	2,091.39
Total Wastewater requirement (t/h)	F_{FWT}	486.05	486.05	486.23	486.05
	Cost	508.68	-	539.28	503.40
TAC (M$/y)	Cost	34.4	-	20.7	20.0
Total No. of headers	F_{FWT}	-	3	5	2
	Cost	-	-	1	1

D: Modified Minmax Core method for Chapter 5

The modified minmax core method follows the same concept as presented in Section 5.2.2, and the constraints are similar to Eqs(5-7 to 5-11) in the manuscript. In this case, the 'n' in the Eq(D-2) represents η value of the minmax core (Drechsel and Kimms, 2011), which is to be maximised. However, the total subsidies have to minimised as well. Notice that the scale of 'n' (0-1) is different with the scale of 'subsidise'. A factor is assigned to the 'n' in the objective function. In this work the factor is set as 10^7.

$$Modified\ LeastCore:\ Min\ \sum_{p} Subsidise\ (p) - n * factor \tag{D-1}$$

$$\sum_{p\in S} x\ (p) \geq n * \left(CS^{sub}(S) + \sum_{p\in S} Subsidise\ (p) \right)\ \forall S \in N \tag{D-2}$$

$$\sum_{p\in N} x\ (p) = CS^{sub}(S) + \sum_{p\in N} Subsidise\ (p) \quad S = N \tag{D-3}$$

$$\sum_{p} Subsidise\ (p) \leq Budget \tag{D-4}$$

$$Subsidise\ (p) \geq |CS^{sub}(p)|\ \ if\ CS^{sub}(p) < 0, \forall p \in P \tag{D-5}$$

Semi-Super-additivity: $CS^{sub}(\{i\}) - \sum_{p\epsilon ps} Subsidise\ (p) \leq CS^{sub}(S)$

$$S = N, where\ i \in S \tag{D-6}$$

E: Nash Equilibrium derivation for taxation

Table E-1: Payoff table for park authority (G) and all stakeholders/plants

	Stakeholders/Plants (P)		
		Recycle (θ)	No Recycle ($1-\theta$)
Park Authority (G)	Regulation ($\emptyset$)	**G**: $-Cost_{\emptyset} - \sum_p sub(p) + \sum_p Tax(p)$ **P**: $-Cost_{\theta} + \sum_p sub(p) - \sum_p Tax(p)$.	**G**:$-Cost_{\emptyset} + \sum_p Tax_o(p)$ **P**: $-Cost_{\theta_o} - \sum_p Tax_o(p)$
	No Regulation ($1-\emptyset$)	**G**: 0 **P**: $-Cost_{\theta}$	**G**: 0 **P**: $-Cost_{\theta_o}$

Each player (stakeholders/authority) could obtain the payoffs depending on their own selected strategy, and the strategy of other players. The wastewater taxes: $Tax(p)$ after recycling and $Tax_o(p)$ before recycling are calculated as follows.

$$Tax(p) = t\left(\sum_{i\epsilon I} F_{p,SRi,WW} C_{p,SRi}\right), \text{ where t = tax rate/kg of pollutant} \quad \text{(E-1)}$$

$$Tax_o(p) = t\left(\sum_{i\epsilon I} F_{p,SRi,WW_0} C_{p,SRi}\right), where\ t\ =\ tax\ rate/kg\ of\ pollutant \quad \text{(E-2)}$$

The total cost for recycling activities for all stakeholders are $Cost_\theta$, and if they do not implement any recycling, they have to pay the cost $Cost_{\theta_o}$. In most of the case, $Cost_\theta$ is larger than $Cost_{\theta_o}$. In this study, these costs are the TAC calculated from the optimisation. $sub(p)$ represents the subsidies obtained from the authority. The probability of regulation (willingness of regulation) is $\emptyset$ from the authority and the probability of recycling (willingness to recycle) denoted as θ for all plants 'p'.

In a mixed strategy game, the payoffs that can be obtained by both players (assumed all stakeholders combined efforts and counted as one player) can be estimated as follows:

$$Payoff_G = \emptyset\left[\theta\left(-Cost_\emptyset - \sum_p sub(p) + \sum_p Tax(p)\right) + (1-\theta)\left(-Cost_\emptyset + \sum_p Tax_o(p)\right)\right] \quad \text{(E-3)}$$

$$Payoff_P = \theta\left[\emptyset\left(-Cost_\theta + \sum_p sub(p) - \sum_p Tax(p)\right) + (1-\emptyset)(-Cost_\theta)\right] + (1-\theta)\left[\emptyset\left(-Cost_{\theta_o} - \sum_p Tax_o(p)\right) + (1-\emptyset)\left(-Cost_{\theta_o}\right)\right] \quad \text{(E-4)}$$

To obtain the Nash Equilibriums, the payoffs are partially differentiated and set to zero for the derivates, i.e.

$$\frac{\partial Payoff_G}{\partial \emptyset} = 0, \frac{\partial Payoff_P}{\partial \theta} = 0 \quad \text{(E-5)}$$

The equilibrium probabilities can be identified using Eq(E-5), and the final results are presented as follows:

$$\theta = \frac{-Cost_\emptyset + \sum_p Tax_o(p)}{\sum_p Tax_o(p) + \sum_p sub(p) - \sum_p Tax\,(p)} \quad \text{(E-6)}$$

$$\emptyset = \frac{Cost_{\theta} - Cost_{\theta_o} - \sum_p sub(p) + \sum_p Tax\,(p)}{\sum_p Tax_o(p)} \quad \text{(E-7)}$$

F: Linearised formulation for non-linear functions for Chapter 7

F1: Regression models of LMTD and UA

Linearisation of LMTD and UA are done by using a regressed equations- see details in Chin et al. (2020b). The regressed models estimates the LMTD and UA with close to 99 % accuracy. The regression parameters are case specifics. Eqs F-1 to F-11 show the formulation for LMTD and UA estimation, for HEN retrofit model P1.

$$Q_{k,p} \leq CPC_i RLC_{i,j,p} + M\left(2 - B^C_{i,j,k,p} - B^H_{ii,ji,k,p}\right) \quad \text{(F-1)}$$

$$Q_{k,p} \geq CPC_i RLC_{i,j,p} - M\left(2 - B^C_{i,j,k,p} - B^H_{ii,ji,k,p}\right) \quad \text{(F-2)}$$

$$LMTD_{k,p} = \lambda_1\left(XXH_{k,p} - XXC_{k,p}\right) + \lambda_2\left(XXH_{k,p} + XXHL_{k,p} - XXC_{k,p} - XXCL_{(k,p)}\right) + \lambda_3 \quad \text{(F-3)}$$

$$UA_{k,p} = \alpha_1 LMTD_{k,p} + \alpha_2 Q_{k,p} + \alpha_3 \quad \text{(F-4)}$$

$$XXH_{k,p} \leq RXH_{ii,jj,p} + \left(1 - B^H_{ii,jj,k,p}\right)M \quad \text{(F-5)}$$

$$XXH_{k,p} \geq RXH_{ii,jj,p} - \left(1 - B^H_{ii,jj,k,p}\right)M \quad \text{(F-6)}$$

$$XXHL_{k,p} \leq RLH_{ii,jj,p} + \left(1 - B^H_{ii,jj,k,p}\right)M \quad \text{(F-6)}$$

$$XXHL_{k,p} \geq RLH_{ii,jj,p} - \left(1 - B^H_{ii,jj,k,p}\right)M \quad \text{(F-7)}$$

$$XXC_{k,p} \leq RXC_{i,j,p} + \left(1 - B^C_{i,j,k,p}\right)M \quad \text{(F-8)}$$

$$XXC_{k,p} \geq RXC_{i,j,p} - \left(1 - B^C_{i,j,k,p}\right)M \quad \text{(F-9)}$$

$$XXCL_{k,p} \leq RLC_{i,j,p} + \left(1 - B^C_{i,j,k,p}\right)M \quad \text{(F-10)}$$

$$XXCL_{k,p} \geq RLC_{i,j,p} - \left(1 - B^C_{i,j,k,p}\right)M \quad \text{(F-11)}$$

F2 Selling and dead size of exchangers ($As_{k,p}$ and $Ad_{k,p}$)

Eqs 7-8 and 7-9 show the non-linear formulation of exchangers' selling size and dead size (scrapping). The formulations below linearise the equations, adapted from Butun et al. (2019).

For selling size:

$$As_{k,p} = \begin{cases} A^{init}_{k,p}\, xs_{k,p} & \forall k \in K,\ \forall p \in P \text{ and } p = 1 \\ Ae_{k,p-1}\, xs_{k,p}\,, & \forall k \in K,\ \forall p \in P \text{ and } p \neq 1 \end{cases} \quad \text{(7-8)}$$

$$As_{k,p} = A^{init}_{k,p} xs_{k,p} \quad \forall k \in K, \forall p \in P \text{ and } p = 1 \quad \text{(F-12)}$$

$$As_{k,p} \leq Ae_{k,p-1} xs_{k,p} \quad \forall k \in K, \forall p \in P \text{ and } p \neq 1 \quad \text{(F-13)}$$

$$As_{k,p} \leq xs_{k,p} M \quad \forall k \in K, \forall p \in P \text{ and } p \neq 1 \quad \text{(F-14)}$$

$$As_{k,p} \geq Ae_{k,p-1} - \left(1 - xs_{k,p}\right)M \quad \forall k \in K, \forall p \in P \; and \; p \neq 1 \tag{F-15}$$

For dead size:

$$Ad_{k,p} = \begin{cases} A_{k,p}^{init}\, xd_{k,p} & \forall k \in K,\ \forall p \in P \; and \; p = 1 \\ Ae_{k,p-1}\, xd_{k,p}\,, & \forall k \in K,\ \forall p \in P \; and \; p \neq 1 \end{cases} \tag{7-9}$$

$$Ad_{k,p} = A_{k,p}^{init} xd_{k,p} \quad \forall k \in K, \forall p \in P \; and \; p = 1 \tag{F-16}$$

$$Ad_{k,p} \leq Ae_{k,p-1} xd_{k,p} \quad \forall k \in K, \forall p \in P \; and \; p \neq 1 \tag{F-17}$$

$$Ad_{k,p} \leq xd_{k,p} M \quad \forall k \in K, \forall p \in P \; and \; p \neq 1 \tag{F-18}$$

$$Ad_{k,p} \geq Ae_{k,p-1} - \left(1 - xd_{k,p}\right)M \quad \forall k \in K, \forall p \in P \; and \; p \neq 1 \tag{F-19}$$

F3 Maximum of sold values, $Cs_{k,p}$

Eq 7-29 depict the selling price of the heat exchanger is the maximum of sold value and the salvage value of the heat exchanger, as shown: To linearise this expression, another two binary variables: nsal and nsel are needed to indicate which value is chosen. Eqs F-20 to F-22 show the linear formulation of the maximum function, adapted from Butun et al. (2019).

$$Cs_{k,p} = \max\left(Csv_{k,p}, xs_{k,p} Csal_k\right) \; \forall k \in K, \forall p \in P \tag{7-29}$$

$$xs_{k,p} Csal_k \leq Cs_{k,p} \leq xs_{k,p} Csal_k + (1 - zsal_{k,p})M \tag{F-20}$$

$$Csv_{k,p} \leq Cs_{k,p} \leq Csv_{k,p} + (1 - zsel_{k,p})M \tag{F-21}$$

$$zsal_{k,p} + zsel_{k,p} = 1 \tag{F-22}$$

F4 Approximation of mean residual life (MRL)

Eq 7-32 shows the formula to compute the MRL of heat exchangers. Since it involves integration from 0 to infinity, a Gauss-Lauguerre quadrature is used, with method shown below:

$$MRL_k(t) = \frac{\left(\int_0^\infty R_k(g+t)dg\right)}{R_k(t)} = \int_0^\infty \frac{e^g e^{-g} R_k(g+t)}{R_k(t)} dg = \int_0^\infty e^{-g} N_k(g) dg \approx \sum_{n=1}^{N} w_n N_{k,n}(g_n) \tag{F-23}$$

$$N_{k,n}(g) = \frac{e^g R_k(g+t)}{R_k(t)} \tag{F-24}$$

$$R_k(t) = e^{-\left(\frac{t}{n_k}\right)^{B_k}} \tag{F-25}$$

Where N represents the N-point quadrature, w_n is the weight parameters, g_n is the parameter replacing the integral, n_k and B_k represent the shape and scale parameters of Weibull reliability function of exchanger 'k'. In this work, a 3-point quadrature is used since it estimates the MRL with close to 95 % accuracy. Table below shows the parameters for 3-points quadrature using Gauss-Lauguerre method. One just need to use the approximation in

Eq A23 to calculate the MRL of exchanger ‘k’ at any period ‘p’, which avoids the intimidating integration.

Table F1: Parameters for Gauss-Lauguerre quadrature

n	g_n	w_n
1	0.415775	0.711093
2	2.29428	0.278518
3	6.28995	0.0103893

F5 Taylor expansion for linear approximations

Formulations below show the linear approximations for heat transfer parameters presented in Chin et al. (2020b) and MRL

$$Ue_{k,p} = \frac{1}{RUe_{k,p}} \approx \left(\frac{1}{RUeo_{k,p}}\right) - \left(\frac{1}{RUeo_{k,p}}\right)^{-2}\left(RUe_{k,p} - RUeo_{k,p}\right) \quad \text{(F-26)}$$

$$(UA)_{k,p} = Ae_{k,p}Ue_{k,p} \approx \left(Aeo_{k,p}Ueo_{k,p}\right) + Aeo_{k,p}\left(Ue_{k,p} - Ueo_{k,p}\right) + Ueo_{k,p}(Ae_{k,p} - Aeo_{k,p}) \quad \text{(F-27)}$$

$$MRL_{k,p} = \sum_{n=1}^{N} w_n e^{g_n} e^{-\left(\frac{im_{k,p}+p}{n_k}\right)^{b_k}+\left(\frac{im_{k,p}}{n_k}\right)^{b_k}} \approx MRLo_{k,p} + \frac{b_k}{n_k^{b_k}}\left(-\left(imo_{k,p}+p\right)^{b_k-1} + \left(imo_{k,p}\right)^{b_k-1}\right) MRLo_{k,p}\left(im_{k,p} - imo_{k,p}\right) \quad \text{(F-28)}$$

$$MRLo_{k,p} = \sum_{n=1}^{N} w_n e^{g_n} e^{-\left(\frac{imo_{k,p}+p}{n_k}\right)^{b_k}+\left(\frac{imo_{k,p}}{n_k}\right)^{b_k}} \quad \text{(F-29)}$$

Where $RUeo_{k,p}$, $Ueo_{k,p}$, $Aeo_{k,p}$, $MRLo_{k,p}$ and $imo_{k,p}$ are some initial values for reciprocal heat transfer coefficients, heat transfer coefficients, exchangers area, mean residual life (MRL) and time for MRL.

Selected Publication List

i. **Chin HH**, Varbanov PS, Liew PY, Klemeš JJ, 2021. Pinch-based targeting methodology for multi-contaminant material recycle/reuse. Chemical Engineering Science, 230, 116129 **[IF = 4.311] [CiteScore = 7.3]**

ii. **Chin HH**, Varbanov PS, Liew PY, Klemeš JJ, 2021. Extension of Pinch Analysis to Targeting and Synthesis of Multi-Contaminant Material Recycle and Reuse Networks. Chemical Engineering Science **(R2 Under Review) [IF = 4.311] [CiteScore = 7.3]**

iii. **Chin HH**, Varbanov PS, Liew PY, Klemeš JJ, 2021. Enhanced Cascade Table Analysis to target and design multi-constraint resource conservation networks. Computers & Chemical Engineering, 148, 107262. **[IF = 3.845] [CiteScore = 7.0]**

iv. **Chin HH**, Xuexiu Jia, Varbanov PS, Klemeš JJ, Liu Z-Y, 2021. Internal and Total Site Water Networks Design with Water Mains Using Pinch-Based and Optimisation Approaches. ACS Sustainable Chemistry & Engineering, 9(19), 6639-6658. **[IF = 8.198] [CiteScore = 12]**

v. **Chin HH**, Varbanov PS, Klemeš JJ, Wan-Alwi SR, 2021. Total Site Material Recycling Network Design and Headers Targeting Framework with Minimal Cross-Plant Source Transfer. Computers & Chemical Engineering, 151, 107364. **[IF = 3.845] [CiteScore = 7.0]**

vi. **Chin HH**, Varbanov PS, Klemeš JJ, Wan-Alwi SR**,** 2021. Industrial Site Water Exchange Network Synthesis Considering Multiple Qualities and Water Headers. Journal of Cleaner Production **(Under Review) [IF = 9.297] [CiteScore = 13.1]**

vii. **Chin HH**, Varbanov PS, Klemeš JJ, Bandyopadhyay S, 2021. Subsidised Water Symbiosis of Eco-Industrial Parks: A Multi-Stage Cooperative Game Theory Approach. Computers & Chemical Engineering **(R1 Under Review) [IF = 3.845] [CiteScore = 7.0]**

viii. **Chin HH**, Varbanov PS, Klemeš JJ, Tan R.R., Benjamin MFD, 2020. Asset Maintenance Optimisation Approaches in the Chemical and Process Industries - A Review. Chemical Engineering Research and Design, 164, 162-194. **[IF = 3.739] [CiteScore = 6.3]**

ix. **Chin HH,** Wang B, Varbanov PS, Klemeš JJ, Zeng M, Wang QW, 2020. Long-term Investment and Maintenance Planning for Heat Exchanger Network Retrofit. Applied Energy, 279, 115713. **[IF = 9.746] [CiteScore = 17.6]**

x. Fan YV, **Chin HH**, Klemeš JJ, Varbanov PS, Liu X, 2020. Optimisation and process design tools for cleaner production. Journal of Cleaner Production, 247, 119181. [**IF = 9.297] [CiteScore = 13.1]**

xi. Klemeš JJ, Varbanov PS, Ocłoń P, **Chin HH**, 2020. Towards Efficient and Clean Process Integration: Utilisation of Renewable Resources and Energy-Saving Technologies. Energies, 12(21), 4092 **[IF=3.004] [CiteScore: 4.7]**

xii. Klemeš JJ, Wang, QW, Varbanov PS, Zeng M, **Chin HH**, Lal NS, Li N, Wang B, Wang XC, Walmsley TG, 2020. Heat transfer enhancement, intensification and optimisation in heat exchanger network retrofit and operation. Renewable and Sustainable Energy Reviews, 120, 109644 **[IF=14.982] [CiteScore: 30.5]**

List of Presentations at International Conferences

i. **Chin HH**, Wang B, Varbanov PS, Klemeš JJ, Markov Decision Process to Optimise Long-term Asset Maintenance and Technologies Investment in Chemical Industry, European Symposium on Computer Aided Process Engineering, Istanbul, 6-9 June 2021 (Poster Online)

ii. **Chin HH**, Wang B, Varbanov PS, Klemeš JJ, Long-Term Process and Asset Optimisation:A Case Study for Heat Exchanger Network Retrofit, Modern Power Systems and Units (MPSU):V International Scientific and Technical Conference, Cracow, Poland, 19-21 May 2021 (Online)

iii. **Chin HH,** Jia XX, Varbanov PS, Klemeš JJ, Wan-Alwi SR, Targeting Flowrates and Concentrations in Internal or Total Site Water Mains for Single Contaminant, The 15th International Conference on Chemical and Process Engineering (ICheaP 15), 23-26 May 2021 (Online)

iv. **Chin HH,** Jia XX, Varbanov PS, Klemeš JJ, Wan-Alwi SR, Fair Profit Allocation Between Plants in Total Site Water Integration- Game Theory Approach, The III International Scientific Conference on "Sustainable and Efficient Use of Energy, Water and Natural Resources (SEWAN), 19-21 April 2021, Saint-Petersburg, Russia (Online)

v. **Chin HH**, Liew PY, Varbanov PS, Klemeš JJ, Pinch Approach for Targeting in Multi-Contaminant Material Recycle/Reuse Network, The 23rd Conference of Process Integration, Modelling and Optimisation for Energy Saving and Pollution Reduction (PRES'20), 17-21 August 2020 (online).

vi. **Chin HH**, Wang B, Varbanov PS, Klemeš JJ, Long-Term Process and Asset Optimisation: A Case Study for Heat Exchanger Network Retrofit, The 4th SEE Sustainable Development of Energy Water and Environment Systems (SDEWES) Conference, 2020 (SEE SDEWES 2020), Sarajevo, Bosnia and Herzegovina, 28 June-2 July 2020 (online).

vii. **Chin HH**, Varbanov PV, Klemeš JJ, Short Term Maintenance Tasks Scheduling with Pinch Methodology, The 5th International Conference on Low Carbon Asia & Beyond – ICLCA 2019 jointly held with The 4th International Conference on Chemical Engineering, Food and Biotechnology- ICCFB 2019, Ho Chi Minh City, Vietnam, 15-17 Oct, 2019

viii. **Chin HH,** Varbanov PS, Klemeš JJ, Lam HL, Application of pinch analysis to opportunistic maintenance management, The 22nd Conference on Process Integration, Modelling and Optimisation for Energy Saving and Pollution Reduction, 2019 (PRES'19), Crete, Greece, 20-23 Oct, 2019

ix. **Chin HH**, Klemeš JJ, Varbanov PS, P-graph Methodology for Utility Targeting in Non-Isothermal Heat-Integrated Water Networks, The 14th Conference on Sustainable Development of Energy, Water and Environment Systems (SDEWES) Dubrovnik, Croatia, 1-6 Oct, 2019